

THE MULTIFUNCTIONAL ENZYMOLOGY OF PAGP

NEW ROLES FOR PAGP IN THE BACTERIAL OUTER MEMBRANE
STRESS RESPONSE

By CHARNEAL L. DIXON, B.A. (Hons.)

A Thesis Submitted to the School of Graduate Studies in Partial Fulfilment of the
Requirement for the Degree Doctor of Philosophy

McMaster University © Copyright by Charneal L. Dixon September 2018

DOCTOR OF PHILOSOPHY (2018)
(Biochemistry and Biomedical Sciences)

McMaster University
Hamilton, Ontario

TITLE: New Roles for PagP in the Bacterial Outer
Membrane Stress Response

AUTHOR: Charneal L. Dixon (B.A.) Wesleyan College

SUPERVISOR: Dr. Russell Bishop

NUMBER OF PAGES: xxiii, 243

Abstract

The ability of Gram-negative bacteria to modulate outer membrane (OM) composition in response to stressful environments is essential for their survival and replication within host tissues. The OM enzyme PagP catalyzes the transfer of palmitate from a glycerophospholipid to lipid A. Lipid A is the endotoxic portion of LPS responsible for transmembrane signalling to initiate the immune response. Palmitoylation of lipid A can either attenuate or stimulate the immune response depending on where the palmitate chain is attached to a specific lipid A molecule. Here we report that the *Escherichia coli* PagP homolog is a multifunctional enzyme, which displays two distinct active sites exposed on either side of the bacterial OM. *E. coli* PagP converts phosphatidylglycerol (PG) to palmitoyl-PG (PPG) using the same cell surface active site involved in the palmitoylation of lipid A. PPG is then serially degraded to *bis*(monoacylglycerol)phosphate (BMP) and either lyso-PG or lyso-BMP by a novel lipase active site located in PagP on the periplasmic side of the OM. The periplasmic lipase active site can be inactivated with the Y87F amino acid substitution. BMP is a novel glycerophosphoglycerol (GPG) that has not previously been reported in bacterial lipid metabolism. Not all PagP homologs have this ability to remodel GPGs. We have identified a divergent lipid A palmitoyltransferase in *Pseudomonas aeruginosa* that does not palmitoylate PG. The *P. aeruginosa* homolog also has different lipid A regiospecificity, adding palmitate on the opposite glucosamine at

the 3'-position compared to the 2-position of the proximal sugar observed for the *E. coli* homolog. We have determined that *P. aeruginosa* PagP is representative of a distinct clade of PagP evolved to fulfill different functions. Although this minor clade is inclusive of homologs that lack obvious sequence similarity with the major clade enterobacterial PagP, we have identified conserved catalytic and structural elements within the minor clade that contribute to our growing understanding of homologous PagP structure/function relationships. A comparative analysis of all available sequences of minor clade PagP homologs has revealed invariant His, Ser, and Tyr residues that are necessary for catalysis. Additionally, a 4-amino acid conserved signature indel or CSI is unique to bacteria clustered phylogenetically within the γ -subclass of Proteobacteria.

Acknowledgements

I would like to thank all the people who contributed in some way to the work described in this thesis. First and foremost, I would like to thank my supervisor, Dr. Russell Bishop, for accepting me into his group. This has been a period of intense learning for me, not only in the scientific arena, but also on a personal level. Thank you for giving me intellectual freedom in my work, supporting my attendance at various conferences, engaging me in new ideas, and demanding a higher standard of work in all my endeavours. I would also like to thank past and present committee members, Dr. Junop Murray, Dr. Alba Guarné, Dr. Lori Burrows and Dr. Leslie MacNeil - each of whom has uniquely contributed to the success of this project.

Every result in this thesis was accomplished with the help and support of fellow lab-mates and collaborators. Emily DeHaas joined the group as an undergraduate research student in 2015. She and I worked together on the palmitoyl-PG and *H. elongata* PagP projects during the last year of my graduate studies, and without her efforts my job would undoubtedly have been more arduous. I greatly benefited from her relentless work ethic and her willingness to start our growth experiments at 4am. I was very fortunate to work with Dr. José Carlos Bozelli, a post-doctoral fellow in Dr. Richard Epanand's lab. While we were unsuccessful in our efforts to reconstitute the *P. aeruginosa* PagP homolog into liposomes, he was an extremely reliable source of practical scientific knowledge,

including the quantification of inorganic phosphate. I would also like to thank Dr. Ryan Lamers, a post-doctoral fellow in the Burrow's group, who patiently taught me his methods for evaluating antimicrobial susceptibility of *P. aeruginosa*. I am also indebted to Dr. Teresa Garrett of Vassar College for her identification and quantification of glycerophospholipids by mass spectrometry. We exchanged communications several times over the course of three years during which we made significant headway in elucidating the functional significance of PPG in the *E. coli* outer membrane. She also tutored me by phone during the preparation of this thesis. Her contributions to the subject were invaluable.

I would like to thank the various members of the Bishop lab with whom I had the opportunity to work and have not already mentioned: Matthew Sapiano, Daniel Zangari, Laxman Panday, Sanchia Miller and Liset Maldonado-Alvarez. They provided a friendly and cooperative atmosphere at work. We were not only able to support each other by deliberating over our problems and findings, but also by talking about things other than the research. I would be remiss if I did not especially thank Sanchia Miller for acting as a sounding board for my experiments and for being my friend and a welcome distraction from the lab.

Finally, I would like to thank my family for their incredible love and support - my husband, mother and brother. This project required stamina and I often found it difficult to be present in moments away from the lab. I would like to thank my husband - Ainsley Dacres, for sharing me with the lab, for picking up the slack at

home, for always showing an interest in my project and for eagerly celebrating my academic accomplishments. My mother, Valrie Dixon, from whom I inherited my stamina, thank you for each time you held my child and allowed to me teleconference, send an email, meet with Russell or simply rest. And last, but not least, my brother Ryan Dixon - for being proof of life outside the lab. Thank you.

For Dixon D. Z. Dacres, my other labour of love.

“You can start late, look different, be uncertain, and still succeed.”
- Misty Copeland

Table of Contents

Abstract	iii
Acknowledgements	v
Dedication	viii
List of Figures	xvi
List of Tables	xx
List of Abbreviations and Symbols	xxi
Declaration of Academic Achievement	xxiii
Chapter 1 - Introduction	1
1.1 Structural Overview of the Gram-negative Cell Envelope.....	1
1.1.1 Inner membrane.....	1
1.1.2 Periplasmic space.....	1
1.1.3 Outer membrane.....	3
1.2 The Outer Membrane Permeability Barrier.....	4
1.2.1 LPS structure.....	4
1.2.2 The Raetz pathway.....	7
1.2.3 Assembly and transport of LPS to the OM	10
1.2.4 Regulation of lipid A modifications.....	12
1.3 The OM Stress Response.....	16
1.4 Biosynthesis and Function of Glycerophospholipids.....	17
1.3.1 Phosphatidic acid.....	22

1.3.2	Cardiolipin.....	22
1.3.3	Palmitoyl-phosphatidylglycerol.....	23
1.3.3.1	<i>Bis</i> (monoacylglycero)phosphate.....	24
1.5	PagP.....	26
1.5.1	Enzymology in the OM.....	26
1.5.2	Role in signal transduction.....	34
1.5.3	PagP in Gram-negative bacteria.....	35
1.5.3.1	<i>P. aeruginosa</i> PagP.....	37
1.6	Thesis Statement.....	40

Chapter 2 - Identification of Novel Glycerophosphoglycerol

	Glycerophospholipid Derivatives in <i>Escherichia coli</i>.....	41
2.1	Author's Preface.....	42
2.2	Abstract.....	43
2.3	Introduction.....	44
2.4	Materials and Methods.....	47
2.4.1	Reagents.....	47
2.4.2	Bacterial strains and growth conditions.....	48
2.4.3	Cloning, expression and purification of PagP.....	50
2.4.4	<i>In vitro</i> palmitoyltransferase reaction.....	51
2.4.5	Determination of phospholipid concentration.....	52

2.4.6 Construction of a quadruple mutant lacking <i>cls</i> and <i>pagP</i> genes...	53
2.4.7 Extraction of lipids from ³² P-radiolabelled cells.....	56
2.4.8 Lipid A mild acid hydrolysis.....	57
2.4.9 MS of lipids.....	58
2.5 Results.....	59
2.5.1 Purified PagP remodels PPG to BMP <i>in vitro</i>	59
2.5.2 PagP-mediated metabolism of BMP to monoacylated phosphoglycerolphosphates.....	67
2.5.3 PPG accumulates in membranes of EDTA-treated <i>E. coli</i>	68
2.5.4 PPG is produced in the same active site that also palmitoylates lipid A.....	70
2.5.5 Identifying a substrate for the PagP periplasmic hydrolase motif....	74
2.6 Discussion.....	77
2.7 Acknowledgements.....	84

Chapter 3 - A Divergent *Pseudomonas aeruginosa* Palmitoyltransferase

Essential for Cystic Fibrosis-Specific Lipid A	85
3.1 Author's preface	86
3.2 Abstract	87
3.3 Introduction.....	88

3.4 Materials and Methods.....	91
3.4.1 Bacterial strains and growth conditions.....	91
3.4.2 Recombinant DNA techniques.....	91
3.4.3 Lipid A extraction.....	93
3.4.4 MALDI-TOF MS analysis.....	94
3.4.5 LPS extraction for GC.....	94
3.4.6 Phylogenetic tree analysis.....	95
3.4.7 <i>P. aeruginosa</i> PagP structure and palmitate docking simulation....	95
3.4.8 <i>P. aeruginosa</i> PagP enzymology.....	95
3.4.9 Cytokine stimulation assay.....	99
3.4.10 Susceptibility assays.....	100
3.5 Results.....	101
3.5.1 Screening for the <i>P. aeruginosa</i> lipid A palmitoyltransferase gene, <i>pagP</i>	101
3.5.2 Matrix-assisted laser desorption ionization-time of flight (MALDI- TOF lipid A analysis reveals loss of palmitoyltransferase activity in strains with mutations in <i>Pa1343</i>	102
3.5.3 Gas chromatography (GC) analysis of lipid A confirms PA1343 is necessary for addition of palmitate.....	105
3.5.4 Sequence analysis of the <i>P. aeruginosa pagP</i> gene and protein indicates PaPagP is unique among PagP enzymes.....	107

3.5.5 <i>P. aeruginosa</i> PagP purification and detergent dependence of its enzymatic activity.....	110
3.5.6 Regiospecificity of lipid A palmitoylation by PaPagP.....	112
3.5.7 His35 is necessary for PaPagP palmitoyltransferase activity.....	115
3.5.8 <i>P. aeruginosa</i> PagP structural model and hydrocarbon ruler.....	116
3.5.9 <i>P. aeruginosa</i> PagP confers resistance to C18G, but does not influence resistance to polymyxins.....	117
3.5.10 Palmitoylation of <i>P. aeruginosa</i> lipid A increases IL-8 production.....	120
3.6 Discussion.....	123
3.6 Acknowledgements.....	128
3.7 Supplementary Information.....	129

Chapter 4 - Conserved structural elements that govern folding, stability and catalysis of PagP in <i>Halomonas elongata</i>.....	133
4.1 Author's preface.....	134
4.2 Abstract.....	135
4.3 Introduction.....	137
4.4 Materials and Methods.....	144
4.4.1 Bacterial strains and growth conditions.....	144

4.4.2	Sequence alignment and phylogenetic analysis.....	144
4.4.3	Recombinant DNA techniques.....	145
4.4.4	Expression and Purification of HePagP.....	151
4.4.5	Protein refolding and detergent exchange.....	153
4.4.6	TEV cleavage.....	154
4.4.7	SDS/PAGE and Western Blot Analysis.....	155
4.4.8	Far-UV CD.....	156
4.4.9	Mass spectrometry analysis.....	156
4.4.10	<i>In vitro</i> palmitoyltransferase assay.....	157
4.4.11	<i>In vitro</i> phospholipase assay.....	158
4.4.12	OM palmitoyltransferase activity assay.....	159
4.5	Results.....	160
4.5.1	Sequence analysis of minor clade PagP homologs.....	160
4.5.2	Site directed mutagenesis <i>in vitro</i> and in <i>in vivo</i>	163
4.5.3	β -barrel domain and α -helical motif of PagP is conserved in <i>H.elongata</i> homolog.....	166
4.5.4	<i>HELO_4100</i> is the gene encoding PagP in <i>H. elongata</i>	168
4.5.5	Enzymology of minor clade PagP homologs.....	173
4.5.6	The 4-amino acid CSI of HePagP is dispensable for folding, but critical for catalysis.....	176

4.5.7 <i>N</i> -terminal motif of HePagP is critical for β -barrel thermal stability and catalytic activity.....	183
4.6 Discussion.....	185
4.7 Acknowledgements.....	191
Chapter 5 - Conclusion	192
5.1 PagP-catalyzed expansion of glycerophosphoglycerol glycerophospholipids	192
5.2 The elusive <i>P. aeruginosa</i> PagP.....	195
5.3 PagP structure-function relationships.....	198
References	201

List of Figures

Figure 1.1. A schematic representation of <i>E. coli</i> K-12 cell envelope.....	2
Figure 1.2. A schematic representation of <i>E. coli</i> K12 lipopolysaccharide.....	5
Figure 1.3. The Raetz pathway for Kdo ₂ -lipid A biosynthesis in <i>E. coli</i> K-12...	8
Figure 1.4. A schematic representation of LPS translocation.....	11
Figure 1.5. Covalent modifications of Kdo ₂ -lipid A in <i>E. coli</i> K-12 and <i>S. enterica</i>	14
Figure 1.6. Chemical structures of the most abundant glycerophospholipids in <i>E. coli</i>	18
Figure 1.7. Pathway for biosynthesis of the most abundant glycerophospholipids in <i>E. coli</i>	20
Figure 1.8. Structural organization of <i>E. coli</i> PagP (PDB: 3GP6).....	25
Figure 1.9. Chemical representation of palmitoylation of <i>E. coli</i> Kdo ₂ -lipid A..	27
Figure 1.10. Chemical representation of palmitoylation of phosphatidylglycerol.....	29
Figure 1.11. Proposed catalytic mechanism of <i>E. coli</i> PagP	32
Figure 1.12. Structural organization of PagP's putative periplasmic active site.....	33
Figure 1.13. Phylogenetic analysis of major clade PagP homologs.....	36
Figure 1.14. Phylogenetic analysis of minor clade PagP homologs.....	38

Figure 2.1. Glycerophosphoglycerols are characterized by the presence of a second glycerol unit as part of the head group.....	46
Figure 2.2. Refolding and spectroscopic analysis of PagP and active site mutants.....	61
Figure 2.3. TLC analysis of glycerophosphoglycerol production by purified PagP <i>in vitro</i>	62
Figure 2.4 Lipid A palmitoylation is induced <i>in vivo</i> by exposure of cells to EDTA and by overexpression of PagP.....	67
Figure 2.5 Structural organization of PagP periplasmic active site.....	69
Figure 2.6 Spectroscopic analysis of refolded PagP variants in SDS/MPD and evaluation of thermal stability.....	71
Figure 2.7 TLC analysis of glycerophosphoglycerol production by purified PagP <i>in vitro</i>	73
Figure 2.8 Negative-ion ESI-MS of PagP's palmitoyltransferase activity assay <i>in vitro</i>	74
Figure 2.9. Stereospecific metabolism of palmitoyl-phosphatidylglycerol.....	76
Figure 2.10. Biochemical schematic of possible rearrangements of glycerophosphoglycerols in <i>E. coli</i>	77
Figure 3.1 <i>Pseudomonas</i> lipid A palmitoylation by PagP.....	108
Figure 3.2 <i>Pal343</i> is required for palmitoylation.....	110
Figure 3.3 GC analysis of total fatty acid content of lipid A isolated from WT.....	112

Figure 3.4 Tree diagram of the palmitoyltransferase enzymes of Gram-negative bacteria and <i>Pseudomonas</i> species generated by using Geneious.....	113
Figure 3.5 Detergent dependence and sensitivity of <i>P. aeruginosa</i> and <i>E. coli</i> PagP.....	115
Figure 3.6 Regiospecificity of phospholipid::lipid A palmitoyltransferase activity.....	117
Figure 3.7 Homology model and hydrocarbon ruler of <i>P. aeruginosa</i> PagP.....	121
Figure 3.8 Palmitoylated lipid A imparts resistance to C18G.....	124
Figure 3.9 THP-1 alveolar macrophages were stimulated with LPS prepared from <i>E. coli</i> , WT, $\Delta pagP$, and $\Delta pagP+Pa1343$ grown under magnesium-limiting conditions for 16 h.....	125
Figure S3.1. PagP enzyme transmembrane prediction of <i>P. aeruginosa</i> , <i>E. coli</i> , and <i>S. Typhimurium</i>	133
Figure 4.1 A bootstrapped maximum-likelihood tree based upon PaPagP.....	154
Figure 4.2 A 4-amino acid indel shared by <i>Halomonas</i> and <i>Pseudomonas</i> PagP homologs.....	175
Figure 4.3 Spectroscopic analysis of refolded <i>P. aeruginosa</i> PagP mutants.....	177
Figure 4.4 Identification of catalytic residues of PaPagP using site-directed mutagenesis.	180
Figure 4.5. I-Tasser Structural alignment of PagP homologs.....	182

Figure 4.6. Surface representation of PagP showing the distribution of charge surface.....	183
Figure 4.7. Spectroscopic analysis of refolded HePagP and evaluation of thermal stability.	185
Figure 4.8. HePagP Hydrocarbon ruler and substrate specificity.....	187
Figure 4.9. Representative TLC autoradiograph showing palmitoylation of phosphatidylglycerol.....	188
Figure 4.10. Effects of CSI on folding, thermal stability and catalysis of HePagP.....	190
Figure 4.11 Lipid IV _A palmitoylation is induced <i>in vivo</i> by overexpression of PagP.....	192
Figure 4.12 Lipid IV _A palmitoylation is induced <i>in vivo</i> by overexpression of PagP.....	193
Figure 4.13. Membrane localization of HePagP _{ΔT2} in induced membranes of <i>E.coli</i> C41(DE3)pLysS transformed with pETΔT2H.....	195
Figure 4.14. Effects of <i>N</i> -terminal motif on folding, thermal stability and catalysis of HePagP.....	197
Figure 5.1 Phosphatidylglycerol binds at the embrasure of PagP.....	214
Figure 5.2. PAO-1 mediated killing of <i>Caenorhabditis elegans</i> used to model virulence.....	217

List of Tables

Table 2.1. <i>E. coli</i> strains used in this study.....	50
Table 2.2. List of Primers used for PCR and Mutagenesis.....	52
Table 2.3. Glycerophosphoglycerol species identified in WJ0124/pPagP.....	64
Table S3.1. Observed masses and proposed compositions for lipid A, by negative-ion MALDI-MS with an <i>m/z</i> scan 1100 to 2200.....	134
Table S3.2: Bacterial strains and plasmids used in this study.....	135
Table S3.3: List of the primers used for the PCR and mutagenesis.....	136
Table 4.1. Bacterial strains and plasmids.....	155
Table 4.2. Protein constructs used in this study.....	160
Table 4.3 Primers used in this study.....	162
Table 4.4. <i>P. aeruginosa</i> PagP mutant specific activities.....	178

List of Abbreviations and Symbols

1-O-OH - 4'-monophosphate
1-O-P - 1,4'-bisphosphate
1-O-PP - 1-pyrophosphate
 α - Alpha
 β - Beta
 γ - Gamma
 δ - Delta
ABC - ATP binding cassette
ACP - Acyl carrier protein
amp - Ampicillin
a.m.u - Atomic mass units
apr - Apramycin
ATP - Adenosine triphosphate
BMP - *Bis*(monoacylglycero)phosphate
C16 - Palmitate
CAMP - Cationic antimicrobial peptides
CD - Circular dichroism
CDP-DAG - Cytidine diphosphate diacylglycerol
CL - Cardiolipin
cls - Cardiolipin synthase
cp - cyclopropane
cpm - Counts per minute
Da - Daltons
DNA - Deoxyribonucleic acid
DPPC - L- α -dipalmitoyl-phosphatidylcholine
EDTA - Ethylenediaminetetraacetic acid
ESI-Q-TOF - Electrospray ionization quadrupole time-of-flight
Far-UV - Far ultraviolet
FRT - Flippase recognition target
G3P - *sn*-glycerol-3-phosphate
GPG - Glycerophosphoglycerol
gen - Gentamicin
HPLC - High performance liquid chromatography
IM - Inner membrane
IPTG - Isopropyl β -D-thiogalactopyranoside
kan - Kanamycin
kDA - Kilodaltons
Kdo - 3-deoxy-D-*manno*-oct-2-ulosonic acid

L-Ara4-N - L-4-aminoarabinose
LB - Luria-Bertani
LBMP - Lyso- *bis*(monoacylglycero)phosphate
LC - Liquid chromatography
LPG - Lyso- phosphatidylglycerol
LPS - Lipopolysaccharide
Lpt - Lipopolysaccharide transport
[M-H]⁻ Negative ion mode
MH⁺ Positive ion mode
MD-2 - Myeloid differentiation factor 2
MPD - 2-methyl-2, 4-pentanediol
MS - Mass spectrometry
MS/MS - Collision-induced dissociation mass spectrometry
OD₆₀₀ - Optical density (600nm)
OM - Outer membrane
OMPLA - Outer membrane phospholipase A₁
P_i - Inorganic phosphate
PA - Phosphatidic acid
PBS - Phosphate buffered saline
PC - Phosphatidylcholine
PCR - Polymerase chain reaction
PDB - Protein data bank
PE - Phosphatidylethanolamine
pEtN - Phosphoethanolamine
PagP - PhoPQ-activated gene P
PG - Phosphatidylglycerol
PLA₂ - Phospholipase A₂
PldB - Lyso-phospholipase L2
PPG - Palmitoyl-phosphatidylglycerol
R_f - Retention factor
SDS-PAGE - Sodium dodecyl sulfate polyacrylamide gel electrophoresis
SEM - Standard error of the mean
sn - Stereospecifically numbered
SOC - Super optimal broth with catabolite repression
TEV - Tobacco etch virus
TLC - Thin layer chromatography
TLR4 - Toll-like receptor 4
T_U - Thermal denaturation
UDP-GlcNAc - UDP-*N*-acetylglucosamine

Declaration of Academic Achievement

The experiments outlined in this thesis were designed, conducted and interpreted by myself and Dr. Russell Bishop unless specified otherwise in the author preface. Liquid chromatography - tandem mass spectrometry was performed by Dr. Teresa Garrett from Vassar College (Chapter 2). The work featured in Chapter 3, reflects a collaborative study between our research group and the laboratory of Dr. Robert Ernst from the University of Maryland. Emily DeHaas and I characterized *H. elongata* PagP described in Chapter 4.

Chapter 1

Introduction

1.1 Structural Overview of the Gram-negative Cell Envelope

The cell envelope of Gram-negative bacteria is a complex, multilayered protective barrier to environmental assaults, the immune system and antibiotics. It consists of two concentric lipid membranes – an inner membrane (IM) and an outer membrane (OM) that delimit an aqueous cellular compartment called the periplasmic space (Silhavy *et al.*, 2010) (Figure 1.1).

1.1.1 Inner Membrane

Like the plasma membrane of eukaryotic cells the bacterial IM is a phospholipid bilayer permeable to lipophilic compounds. An electrochemical proton gradient is maintained across the IM that drives endergonic processes essential to survival.

1.1.2 Periplasmic Space

The periplasm is an aqueous, protein dense matrix between the two bilayer membranes of the Gram-negative cell envelope. The space is occupied by a large variety of macromolecules that are important to the vitality of the changing variety of macromolecules that are important to the vitality of

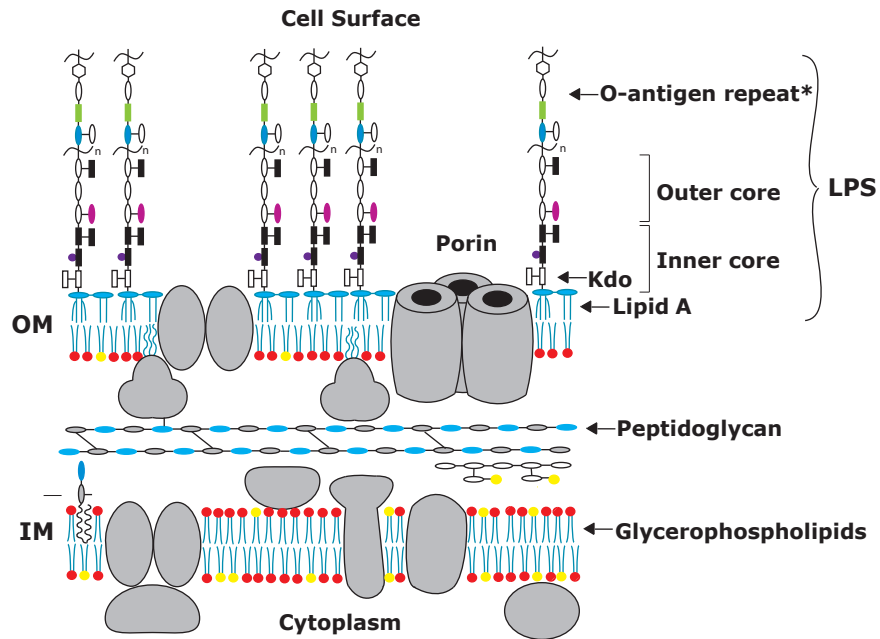


Figure 1.1. A schematic representation of *E. coli* K-12 cell envelope. Adapted from Raetz *et al.*, 2007. The cell envelope in Gram-negative bacteria is characterized by the presence of two lipid bilayers: the outer membrane (OM) and the inner membrane (IM) that are separated by the periplasmic space, which includes a thin layer of peptidoglycan. The OM is an asymmetric lipid bilayer containing mainly lipopolysaccharide (LPS) molecules in the outer leaflet. The inner leaflet of the OM and the symmetrical bilayer of the IM contain glycerophospholipids. *Strains of *E. coli* K-12 do not make O-antigen, unless a mutation in the O-antigen operon is corrected.

the Gram-negative cell (Silhavy *et al.*, 2010). Suspended in the periplasm is a thin layer of peptidoglycan that determines cell shape and provides structural stability to the IM against high osmotic pressure. The OM in *Escherichia coli* is stapled to the underlying peptidoglycan by a lipoprotein called Braun's lipoprotein (Braun, 1975).

1.1.3 Outer Membrane

The OM is the first point of contact with the environment that surrounds the bacterial cell. It is a distinguishing feature of Gram-negative bacteria; Gram-positive bacteria lack this structure. Importantly, the OM is an unusual phospholipid bilayer characterized by a distinct asymmetry of lipids between the inner and outer leaflets. The inner leaflet of the OM mainly consists of glycerol-based phospholipids, whereas the outer leaflet is dominated by lipopolysaccharides (LPS) (Raetz *et al.*, 2007). Similar to most membranes, the hydrophobic nature of the OM prevents the passage of large polar molecules. The low fluidity of the LPS hydrocarbon domain and strong lateral electrostatic interactions between neighboring LPS phosphate groups and divalent cations also prevents small hydrophobic molecules from entering the cell (Nikaido, 2003).

1.2 The Outer Membrane Permeability Barrier

E. coli and other enteric bacteria that inhabit the mammalian gut, must have a cellular envelope that effectively excludes detergents like bile salts. This isn't necessarily the case for other Gram-negative bacteria. The effectiveness of the Gram-negative cell envelope as a perimeter defense, at least in the case of enteric bacteria, depends in large part on the unusually low permeability of the OM to hydrophobic solutes. LPS plays a crucial role in barrier function of the OM. Although LPS is present in most Gram-negative bacteria, it is absent from the OM of some bacteria such as *Borrelia burgdorferi* - the causative agent of Lyme disease (Takayama *et al.*, 1987).

1.2.1 LPS Structure

LPS is typically composed of the hydrophobic membrane-anchoring lipid A moiety, interconnecting core-oligosaccharides and O-antigen repeats (Nikaido, 2003)(Figure 1.2). *E. coli* K-12 lipid A is a β -1',6-linked disaccharide of glucosamine acylated at the 2, 3, 2', and 3' positions with *R*-3-hydroxymyristate and phosphorylated at the 1 and 4' positions. The fatty acids linked to the distal sugar residue are further acylated on their hydroxyl groups, producing acyloxyacyl structures (Raetz and Dowhan, 1990). The hydrophobic nature of lipid A allows it to anchor LPS in the OM. Due to its toxic effects in the setting of Gram-negative infections, lipid A is also known as endotoxin. Lipid A is connected to the core domain of LPS by two 3-deoxy-D-manno-

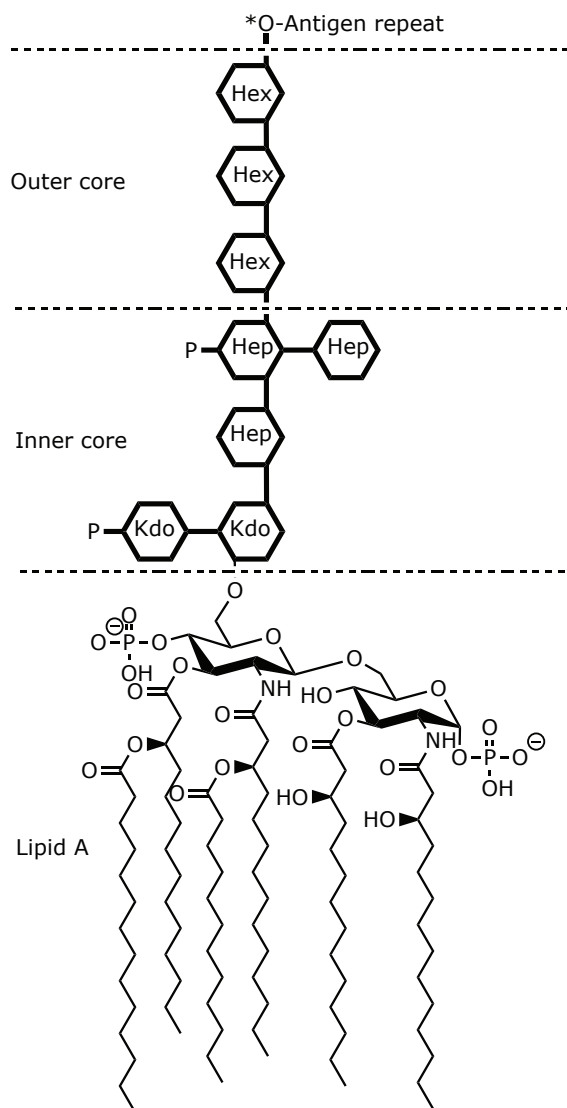


Figure 1.2. A schematic representation of *E. coli* K-12 lipopolysaccharide. Individual LPS molecules may not necessarily contain all of the residues shown. The O-antigen indicated by the asterisk is absent in *E. coli* K12. The LPS molecule typically consists of lipid A and a covalently linked polysaccharide domain that includes an inner and outer core of oligosaccharides, and an O-antigen that may be a long polysaccharide. The acyl chains of the lipid A substructure are largely saturated, and this facilitates tight packing. The nonfluid continuum formed by the LPS molecules is a very effective barrier for hydrophobic molecules. Abbreviations: Kdo, 3-deoxy-D-manno-2-octulosonic acid; Hep, Heptose; Hex, Hexose.

oct-2-ulosonic acid (Kdo) sugars through a labile ketosidic linkage that is susceptible to mild acid hydrolysis. Kdo₂-lipid A usually represents the minimal substructure required for growth of Gram-negative bacteria. This is extended by a few heptose residues, some of which are phosphorylated. The outermost part of the core consists mostly of hexoses. Although *E. coli* K-12 cannot synthesize the O-antigen chain because of an insertion mutation (Stevenson *et al.*, 1994) and thus produces a phenotypically rough strain, most wild-type strains of *Enterobacteriaceae* synthesize this outermost structure of LPS, which often consists of repeating oligosaccharide units; more than 180 unique O-antigenic polysaccharide structures have been reported in *E. coli* alone (Orskov *et al.*, 1977; Stenutz *et al.*, 2006).

The characteristic phosphate groups and acidic sugars in the LPS molecule confer a net negative charge on the bacterial cell surface that is strongly stabilized by divalent cations, mainly Mg²⁺ (Coughlin *et al.*, 1983). This dependence on Mg²⁺ renders the bacterial cell susceptible to cationic antimicrobial peptides (CAMP) (Epan and Epan, 2011). CAMPs are amphipathic molecules with a net positive charge. Their electrostatic interaction with the negatively charged LPS serves to increase the permeability of the OM by displacing some of the Mg²⁺ and destabilizing the strong lateral interactions between LPS. The reduced dielectric constant in the vicinity of the membrane interface strips water molecules away from the peptide bonds and induces secondary structure formation in CAMPs. The resulting amphipathic distribution

of polar and hydrophobic residues in CAMPs facilitates their translocation through the hydrocarbon milieu by a non-porin pathway, termed the self-promoted uptake pathway (Hancock *et al.*, 1995). CAMPs interact with and effectively permeabilize the IM by puncturing holes in the phospholipid bilayer (Bechinger and Lohner, 2006). The resulting openings in the bilayer lead to depolarization of the IM, effectively killing the cell. Alternatively, some CAMPs inhibit specific intracellular target to exert their effects on the bacterial cell.

1.2.2 The Raetz Pathway

Kdo₂-lipid A biosynthesis enzymes are conserved in virtually all Gram-negative bacteria. The biosynthesis of Kdo₂-lipid A is best characterized in *E. coli* (Raetz *et al.*, 2007) (Figure 1.3). There are nine enzymes involved in this constitutive pathway and all have a requirement for cytosolic substrates. LpxA, LpxC, and LpxD are soluble proteins, whereas LpxB and LpxH are peripheral membrane proteins and LpxK, KdtA, LpxL, and LpxM are integral IM proteins (Raetz *et al.*, 2007).

The process begins with the fatty acylation of UDP-*N*-acetylglucosamine (UDP-GlcNAc). LpxA, a cytosolic acyltransferase, transfers *R*-3-hydroxymyristate from acyl carrier protein (ACP) to the 3-OH of UDP-GlcNAc (Raetz and Roderick, 1995). *E. coli* LpxA possesses a selective hydrocarbon ruler, incorporating the *R*-3-hydroxymyristate chain two orders of magnitude

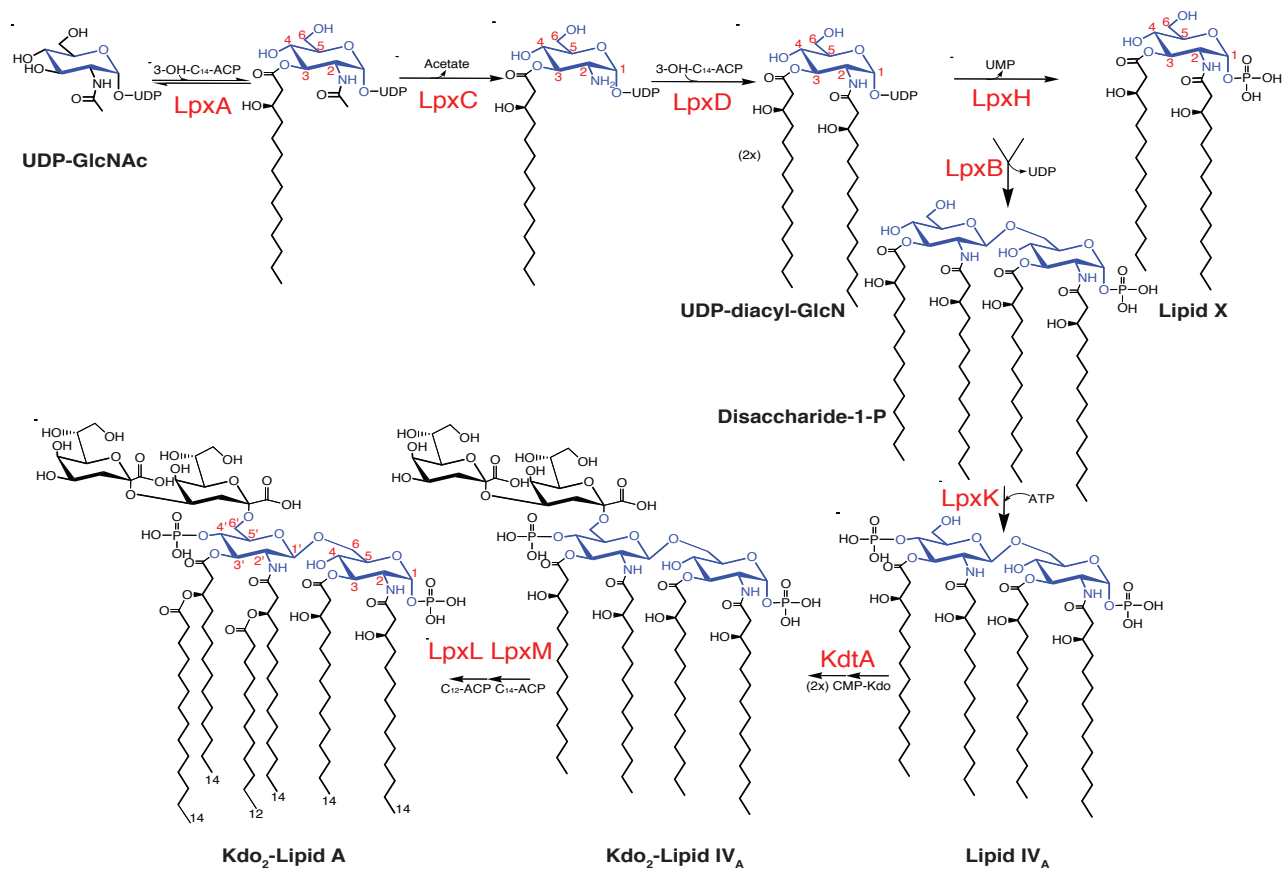


Figure 1.3. The Raetz Pathway for Kdo₂-lipid A Biosynthesis in *E. coli* K-12. Adapted from Raetz *et al.*, 2007. The glucosamine disaccharide backbone of lipid A is shown in blue. The enzymes involved in each step are shown in red. The red numbers specify the glucosamine ring positions of lipid A and its precursors. The black numbers indicate the predominant fatty acid chain lengths found in *E. coli* lipid A. Abbreviations: GlcN, *N*-acetylglucosamine; UDP, Uridine diphosphate; UMP, Uridine monophosphate; ACP, acyl carrier protein.

faster than C12 or C16 hydroxyacyl chains (Wyckoff *et al.*, 1998). Unlike the thermodynamically unfavorable acylation of UDP-GlcNAc (Anderson *et al.*, 1993), the subsequent deacetylation by the Zn^{2+} dependent LpxC is non-reversible and is the first committed step in lipid A biogenesis (Sorensen *et al.*, 1996). Following deacetylation, a second *N*-linked *R*-3-hydroxymyristate derived from ACP is incorporated by LpxD to generate UDP-2,3-diacylglucosamine (Kelly *et al.*, 1993). The pyrophosphate linkage of UDP-2,3-diacylglucosamine is cleaved by LpxH - a highly selective pyrophosphatase that catalyzes an attack of the α -phosphorus of the UDP moiety to form lipid X (2,3-diacylGlcN-1-phosphate) and UMP (Babinski *et al.*, 2002). Next, a disaccharide synthase, LpxB, transfers the 2,3-diacylglucosamine portion of another UDP-2,3-diacylglucosamine molecule to position 6 of lipid X generating the β -1',6 linkage characteristic of all lipid A molecules (Crowell *et al.*, 1986).

The last four steps of the pathway are catalyzed by the integral IM proteins. LpxK, the 4'-kinase, employs ATP to phosphorylate the 4' end of the disaccharide-1-phosphate generated by LpxB to form lipid IV_A (Garrett *et al.*, 1997). Lipid IV_A is a clinically relevant precursor molecule that is an antagonist of inflammation through the toll-like receptor 4 (TLR4) myeloid differentiation factor 2 (MD-2) pathway in human cells, but agonistic in mouse cells (Golenbock *et al.*, 1991). Next, two Kdo sugars are incorporated by KdtA (Clementz and Raetz, 1991) from CMP-Kdo, a labile nucleotide sugar. This

enables the final steps of the pathway as LpxL and LpxM require the Kdo₂-lipid IV_A disaccharide as a substrate for their activity. LpxL and -M transfer lauroyl and myristoyl residues from ACP to the distal glucosamine unit of Kdo₂-lipid IV_A, respectively, resulting in the formation of acyloxyacyl structures (Clementz and Raetz, 1991).

1.2.3 Assembly and Transport of LPS to the OM

Core oligosaccharides and O-antigens are also synthesized in the cytoplasm upon lipid anchors tethered to the inner leaflet on the IM. While the composition and structure of the OM facilitates its unique barrier function, this barrier also introduces challenges for the transport of bacterial components that are produced inside the cell. LPS is delivered by the transenvelope LPS transport (Lpt) complex (Figure 1.4). There are seven essential Lpt proteins and recent structural studies (Dong *et al.*, 2014; Dong *et al.*, 2017; Luo *et al.*, 2017; Qiao *et al.*, 2014) have provided a possible model of how these enzymes work together to directly facilitate translocation of LPS. Lipid A and the covalently linked polysaccharide core are mainly assembled by biosynthetic enzymes in the cytoplasm or at the cytoplasmic face of the IM, and flipped to the periplasmic side by the ATP binding cassette (ABC) transporter MsbA (Doerrler *et al.*, 2004; Ho *et al.*, 2018; Mi *et al.*, 2017; Zhou *et al.*, 1998). Here, O-antigen is ligated to the lipid A-core polysaccharide complex by O-antigen ligase WaaL (Whitfield, 2006), following its independent synthesis in the cytoplasm and

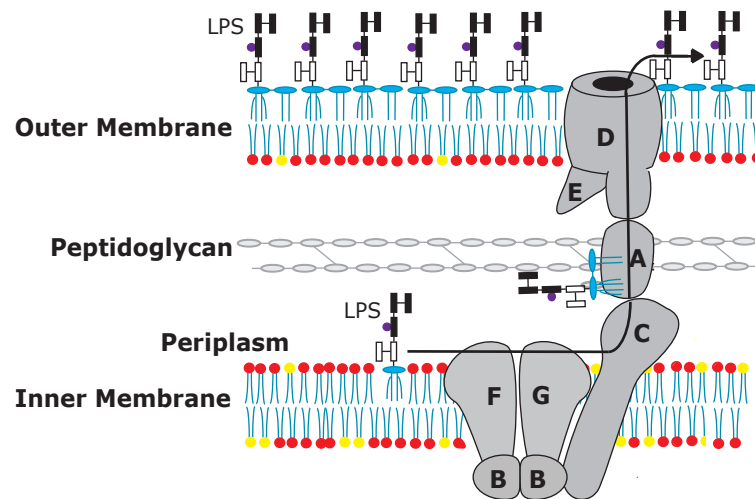


Figure 1.4. A Schematic Representation of LPS Translocation. Lipopolysaccharide (LPS) comprises a lipid A membrane anchor, a core sugar unit and a terminal O-sugar chain. LPS is assembled in the cytoplasm and exported to the external leaflet of the inner membrane. Seven LPS transport (Lpt) proteins (LptA-G) then transport it from the inner to the outer membrane.

transport to the periplasmic space. The subsequent extraction of LPS from the IM, translocation across the periplasmic compartment and assembly at the OM is accomplished with the aid of the Lpt proteins. The ABC transporter complex, LptB₂FG, extracts LPS from the IM and ushers it across the aqueous periplasmic compartment along a protein filament made up of LptC and LptA (Whitfield and Trent, 2014). Finally, a complex between the OM barrel protein LptD and the OM lipoprotein LptE receives LPS from LptA and inserts it into the outer leaflet of the OM (Okuda *et al.*, 2016).

1.2.4 Regulation of Lipid A Modifications

Unlike lipid A biosynthesis enzymes, most lipid A modification enzymes are located either on the periplasmic surface of the IM or in the OM, and vary from organism to organism. Lipid A is subject to several covalent modifications during its transit from the outer surface of the IM to the OM. Accordingly, lipid A modification enzymes are excellent reporters for the translocation of nascent LPS from its initial site of biosynthesis on the cytoplasmic surface of the IM to the outer surface of the OM (Raetz *et al.*, 2007; Sherman *et al.*, 2018). Although not required for growth, these modification enzymes modulate virulence of some Gram-negative pathogens.

In many instances, the lipid A modification systems are induced or repressed by environmental stimuli, such as Mg²⁺ concentrations, or the presence of CAMPs (Bader *et al.*, 2005; Groisman, 2001). The two component

PhoP/PhoQ signal transduction pathway found in most Gram-negative bacteria responds to external stimuli encountered during infection. PhoQ is a membrane-bound sensory kinase that is maintained in a repressed state in the presence of high concentrations of divalent cations (Garcia Vescovi *et al.*, 1996; Groisman, 2001). Divalent cations, like Mg^{2+} , associate with residues located in the sensory domain of PhoQ. CAMPs compete with Mg^{2+} for these binding sites and trigger a signaling cascade that results in the phosphorylation of the response regulator, PhoP. PhoP controls the expression of many genes that are involved in Mg^{2+} transport and in lipid A modification.

Lipid A modifications can be classified into two major classes: modulation of lipid A electrostatic charge and modification of acylation patterns. Figure 1.5 outlines some of these modifications in *E. coli* and *Salmonella enterica*. In order to minimize the electrostatic interaction of CAMPs with the negatively charged LPS, bacteria can reduce the negative charge of the OM by adding phosphoethanolamine (pEtN) and/or L-4-aminoarabinose (L-Ara4-N) to lipid A. Mg^{2+} is an environmental trigger for the cation sensing PhoP/PhoQ two-component system. Under PhoP/PhoQ control EptA (Anandan *et al.*, 2017) adds pEtN to the phosphate at position 1, and ArnT (Petrou *et al.*, 2016) adds L-Ara4-N to the phosphate at the 4' position. The cellular pool of phosphatidylethanolamine (PE) serves as the substrate source for the EptA modification. When L-Ara4-N is not available, EptA may add a second pEtN to the 4' position. This modulation of negative charges on the

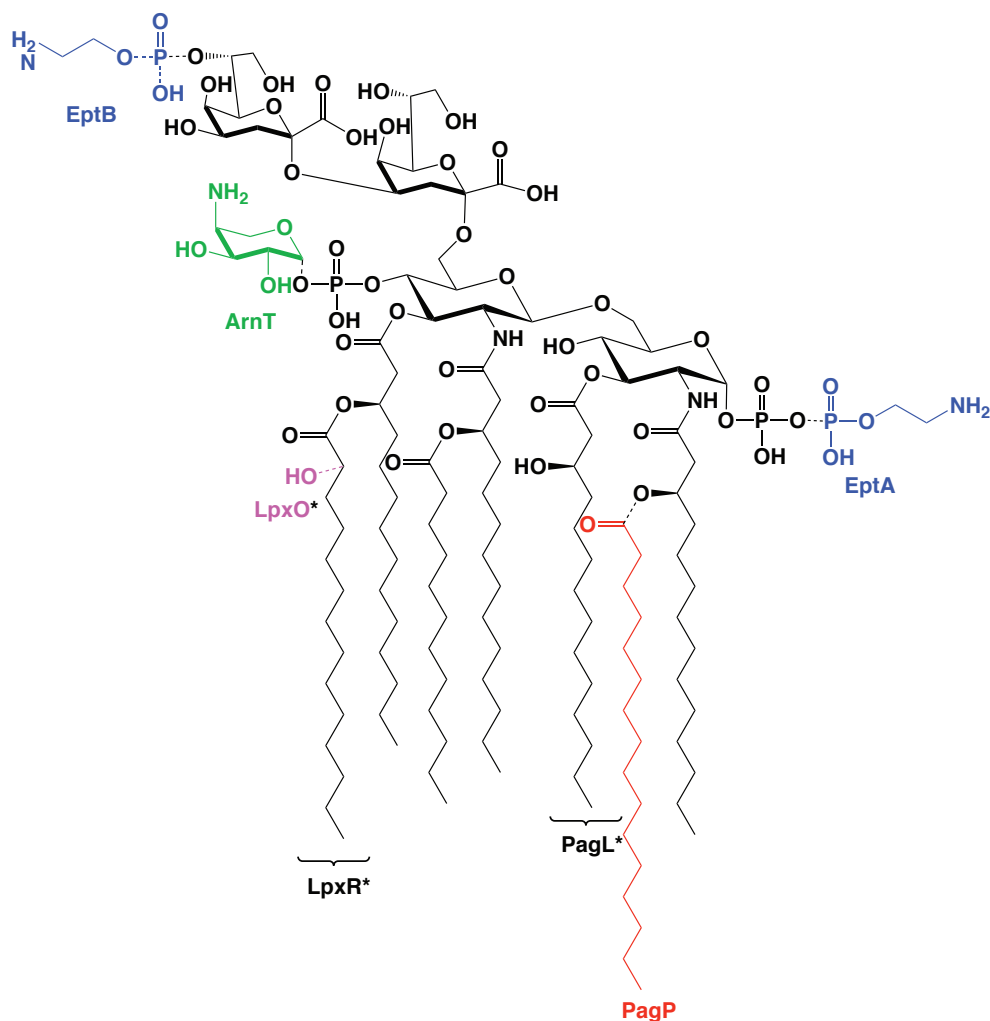


Figure 1.5. Covalent Modifications of Kdo2-Lipid A in *E. coli* K-12 and *S. enterica*. Adapted from Raetz *et al.*, 2007. Enzymes not found in *E. coli* K-12 are indicated by an asterisk. pEtN (blue) and L-Ara4-N (green) groups are added to the 1 and 4' positions of lipid A by EptA and ArnT, respectively. pEtN is also added to the Kdo disaccharide by EptB. PagP is responsible for adding a palmitate (red) to lipid A, while PagL and LpxR act as deacylases. The LpxO modification enzyme (magenta) is not found *E. coli* K-12. Transfer of the *Salmonella* genes encoding this enzyme to *E. coli* results in the expected lipid A modifications. Abbreviations: pEtN, phosphoethanolamine; L-Ara4-N, L-4-aminoarabinose.

bacterial surface is associated with resistance to polymyxin B in *E. coli* and *S. enterica* (Tran *et al.*, 2005)

Other PhoP/PhoQ regulated proteins include PagP. PagP, a transacylase, incorporates a palmitate at the 2-position of lipid A under low Mg^{2+} conditions (Bishop, 2005). LpxO, PagL and LpxR are not under PhoP/PhoQ control. PagL, a deacylase, removes the acyl chain at the 3-position of lipid A (Trent *et al.*, 2001). LpxO catalyzes the formation of the *S*-2-hydroxymyristate moiety, which results in an increase in hydrogen bonding between adjacent lipid A moieties and decreases the penetration of organic molecules that could harm the bacterium (Gibbons *et al.*, 2000; Gibbons *et al.*, 2008). Like PagL, LpxR is an OM deacylase; it catalyzes the cleavage of the 3'-acyloxyacyl linkage of lipid A (Reynolds *et al.*, 2006). To date, only lipid A modification by acylation is known to influence leukocyte CAMP production by modulating the inflammatory response triggered through the TLR4-MD-2 signal transduction pathway (Hajjar *et al.*, 2002).

Another two component system, PmrA/PmrB, functions as a regulator downstream of the PhoP/PhoQ system. PmrA/PmrB can be activated independently by Fe^{3+} or in low pH - PmrD can connect PhoP/PhoQ to PmrA/PmrB in *Salmonella*, but not in *E. coli*. The modification of lipid A with pEtN and L-Ara4-N is primarily controlled by the PmrA/PmrB regulatory system (Gunn *et al.*, 1998; Lee *et al.*, 2004), and PhoPQ when it is engaged by

PmrD (Fu *et al.*, 2007). The Evg system works upstream of PhoP/PhoQ in *E. coli* (Eguchi *et al.*, 2004).

1.3 The OM Stress Response

In their coevolution with the immune system, Gram-negative bacteria have acquired several strategies to arm themselves with a coordinated response to the environment inside the host organism. These include signaling networks, like PhoP/PhoQ that regulate lipid A modification enzymes. They are also armed with a number of envelope stress response systems that sense defects or damage and restore homeostasis. Examples include the Cpx two-component system that responds to misfolded periplasmic and IM proteins (Vogt *et al.*, 2014), and the σ^E response that mediates the bacterial response to OM stress caused by unassembled OM proteins (Barchinger and Ades, 2013) and intermediates of LPS transport and assembly (Lima *et al.*, 2013).

The presence of unfolded OM proteins in the periplasm is the most thoroughly characterized signal for σ^E activation. Following stress, OM proteins accumulate in the periplasm and their C-terminal residues bind to the periplasmic domain of the IM serine protease DegS (Ades *et al.*, 1999). These residues are typically inaccessible in a properly folded OM protein and DegS remains inactive. DegS activation triggers two consecutive proteolytic cleavage steps of the IM protein RseA, releasing σ^E to activate gene expression and RseB. However, the periplasmic protein RseB negatively regulates σ^E activation

by binding RseA and preventing cleavage of DegS, so a signal that inhibits RseB is also required. Recent *in vitro* studies indicate that the acyl chains of lipid A bind RseB and are the signal that displaces it from RseA (Lima *et al.*, 2013). *In vivo*, mutations that either reduce lipid A acylation or truncate the LPS core polysaccharides induce the σ^E response (Lima *et al.*, 2013). Accordingly, the activation of σ^E is two pronged, involving both sensing the OM proteins to activate DegS, and periplasmic LPS to displace RseB from RseA.

1.4 Biosynthesis and Function of Phospholipids

Like lipid A, phospholipids are synthesized at the cytoplasmic face of the IM. At present, it remains unclear how phospholipids reach the OM. There are four known phospholipid transport systems in *E. coli*; the PbgA system is specialized in the export of CL (Dalebroux *et al.*, 2015), while MlaD appears to be adapted for the uptake of PE and PG (Ekiert *et al.*, 2017). Two additional MlaD homologues PqiAB and YebT share some overlapping phenotypes with MlaD, but they are distinctly different and remain to be fully characterized functionally (Isom *et al.*, 2017)

The biosynthesis and functions of phospholipids is best characterized in *E. coli* (Raetz and Dowhan, 1990; Sohlenkamp and Geiger, 2016). *E. coli* membranes are composed of three major phospholipids; its predominant lipids are the zwitterionic phosphatidylethanolamine (PE), and the acidic phosphatidylglycerol(PG) and cardiolipin (CL) (Figure 1.6). The relative

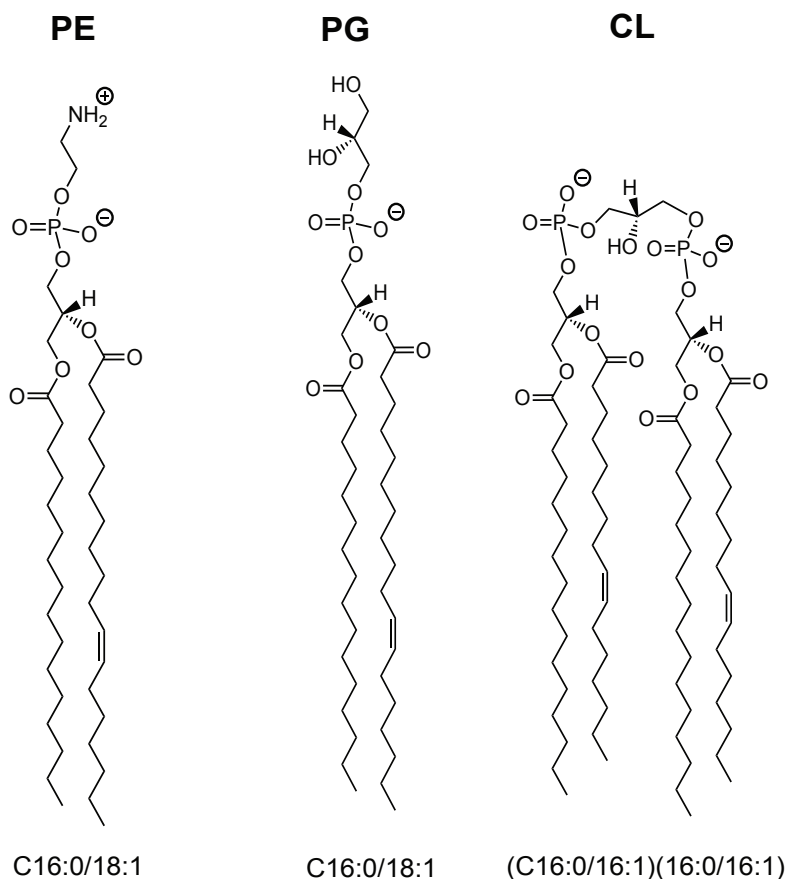


Figure 1.6. Chemical structures of the most abundant glycerophospholipids in *E. coli*. *E. coli* membranes consist of ~75% phosphatidylethanolamine (PE), ~20% phosphatidylglycerol (PG), and ~5% cardiolipin (CL) (Raetz and Dowhan, 1990). Glycerophospholipids are amphipathic molecules, consisting of two hydrophobic fatty acid chains linked to a phosphate-containing hydrophilic head group.

abundances of each of these phospholipid species are similar in the IM and OM (PE, ~75%; PG, ~20%; CL, ~5%) (Cronan, 2003; Raetz and Dowhan, 1990)

Although these phospholipids have different chemical properties due to their head groups, they are synthesized from the same precursor molecule - phosphatidic acid (PA) (Figure 1.7). PA is synthesized in two distinct acyltransferase reactions from *sn*-glycerol-3-phosphate (G3P). Both reactions use thioesters of acyl-ACP as the acyl donors. CdsA is the IM protein responsible for the conversion of PA to the central metabolite cytidine diphosphate diacylglycerol (CDP-DAG). This is the last step before commitment to either the zwitterionic or anionic phospholipid biosynthesis pathway.

In the zwitterionic pathway, phosphatidylserine synthase (Pss) condenses serine with CDP-DAG, producing the anionic lipid PS. PS is then decarboxylated by phosphatidylserine decarboxylase (Psd) forming the zwitterionic lipid PE. Phosphatidylglycerol-phosphate synthase (PgsA) catalyzes the condensation of G3P with CDP-DAG leading to the formation of phosphatidylglycerol-phosphate (Miyazaki *et al.*, 1985), which is the first step in the synthesis of the anionic membrane lipids PG and CL. PGP is dephosphorylated in *E. coli* by any one of three phosphatases - PgpA, PgpB or PgpC, to form PG (Lu *et al.*, 2011). The CL synthases ClsA and Club can synthesize CL by condensation of two PG molecules, but only the ClsA gene

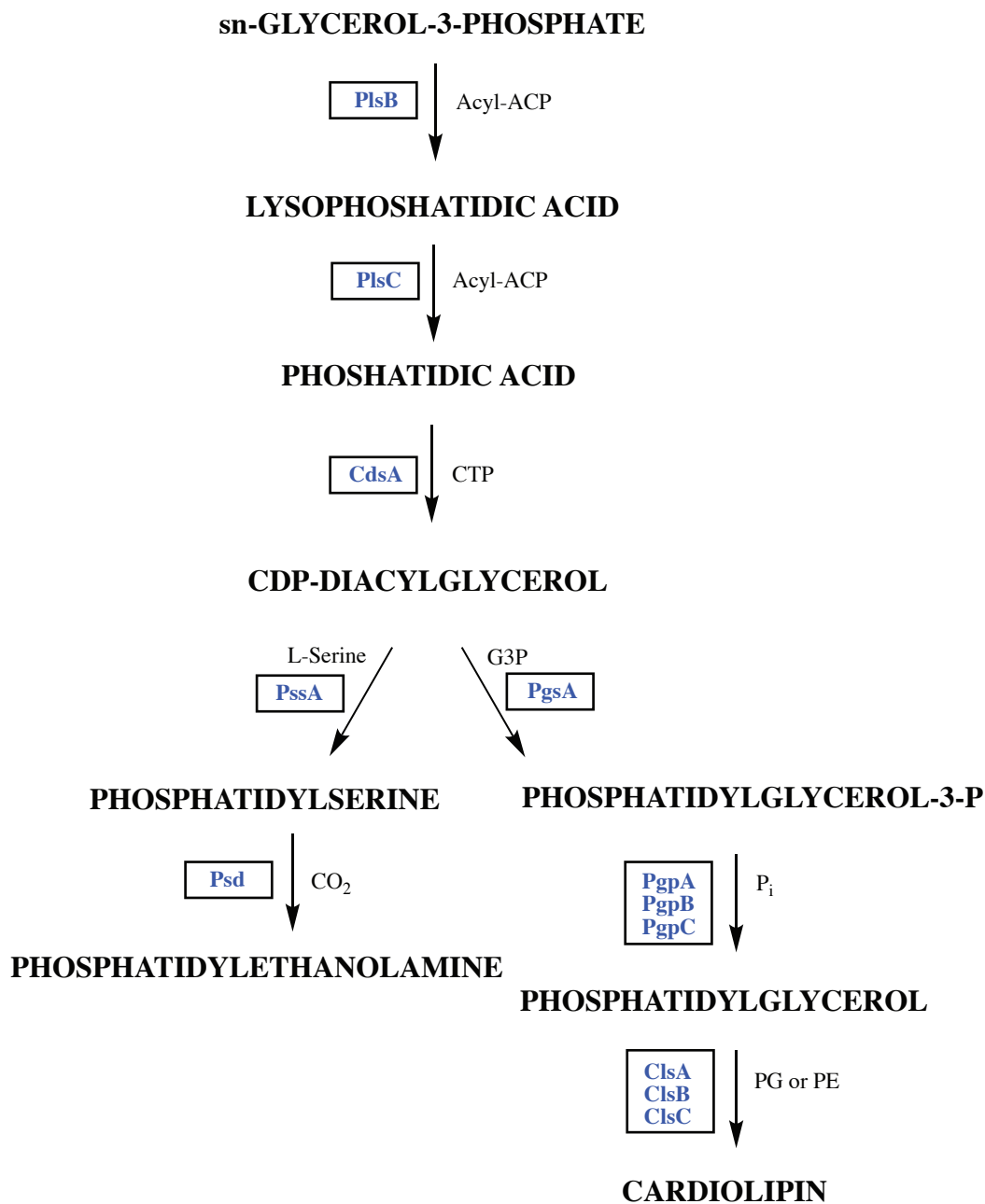


Figure 1.7. Pathway for biosynthesis of the most abundant glycerophospholipids in *E. coli*. The enzymes involved in each step are shown in blue next to the arrow that signifies the step at which they act. Abbreviations: ACP, acyl carrier protein; CTP, cytidine triphosphate; G3P, glycerol-3-phosphate; Pi, inorganic phosphate; PG, phosphatidylglycerol; PE, phosphatidylethanolamine.

appears to be expressed significantly in cells (Guo and Tropp, 2000). A third CL synthase ClsC, can synthesize CL by condensation of PG with PE (Tan *et al.*, 2012).

Based on their collective physical properties, phospholipids are believed to help maintain the permeability barrier of membranes as well as provide a supporting matrix for membrane proteins. PG has the greatest tendency to spontaneously form bilayers because of its requisite cylindrical shape (head group and hydrophobic domain of similar diameter), whereas the cone-shaped PE has a strong tendency to induce negative membrane curvature because lateral pressure becomes greater in the hydrophobic region compared to the membrane interface (Bishop, 2014). A striking feature of CL is the small cross section of its head group relative to the cross section of its four acyl chains. In the presence of divalent cations, CL and PA are conical and function along with PE in inducing negative membrane curvature (Bishop, 2014; Bogdanov *et al.*, 2014; Dowhan, 1997).

The chemical diversity of phospholipids implies that phospholipids have functions other than maintenance of membrane physical state. The regulated increase in lipids like PA (Sutterlin *et al.*, 2014) has recently been demonstrated to help provide resistance to certain antibiotics. PA is not the only phospholipid that accumulates in the OM under conditions that shore up the permeability barrier against antibiotics. It has recently been reported that CL and palmitoyl-phosphatidylglycerol (PPG) accumulate in the *Salmonella* OM under conditions

of PhoP/PhoQ activation, which are known to increase cell resistance to CAMPs (Dalebroux *et al.*, 2014).

1.4.1 Phosphatidic acid

Phosphatidic acid is a minor membrane constituent, comprising only about 0.2% of the total phospholipid in *E. coli*. This is consistent with its role as an intermediate of phospholipid biosynthesis since it is rapidly converted to CDP-DAG. PA can accumulate to 5% or more (Ganong *et al.*, 1980), mostly at the expense of PG and CL, in *cdsA* mutants, the essential gene encoding the enzyme responsible for the conversion of PA to CDP-DAG. OM permeability defects associated with *lptD* mutants can be suppressed by partial loss of function mutations in *cdsA* (Sutterlin *et al.*, 2014). The increased levels of PA in *E. coli*, even in wild-type cells, serves to defend the bacteria against vancomycin (Sutterlin *et al.*, 2014) and erythromycin (Ganong and Raetz, 1982).

1.4.2 Cardiolipin

CL is an acidic tetra-acylated phospholipid. Its dimeric structure and chirally distinct phosphates (Garrett *et al.*, 2007) make it unique amongst the phospholipids found in bacterial and mitochondrial membranes. Despite the growing number of studies on CL, its physiological role in bacteria remains unclear. The redundancy of biosynthetic enzymes in *E. coli* suggests that it plays an important role in cell physiology. However, elucidating the precise role of

CL is complicated by findings that *E. coli* is able to survive the simultaneous disruption of all three CL synthase genes (Tan *et al.*, 2012), suggesting that cardiolipin is non-essential. These mutants have no obvious phenotype except that cells grow at a slower rate and to a lower density than the corresponding wild-type cells. CL accumulates during the stationary phase in *E. coli* (Cronan, 1968; Hiraoka *et al.*, 1993). PhoP/PhoQ activation dramatically increases the amount of CL in the *Salmonella* OM and resistance to CAMPs (Dalebroux *et al.*, 2014); increased trafficking of CL to the OM is necessary for survival of the organism within host tissues (Dalebroux *et al.*, 2015). Still it remains unclear how CL mediates barrier function.

1.4.3 Palmitoyl-phosphatidylglycerol

In addition to the major phospholipids, low level (~0.1% total) lipids are formed when an additional acyl chain is added to the headgroup of PG or lyso-PG to form acyl-PG (Kobayashi *et al.*, 1980) and *bis*(monoacylglycero)phosphate (BMP), respectively. Two enzymes that affect headgroup-acylated phospholipids levels in *E. coli* are the IM transacylase, lyso-phospholipase L2 (PldB) (Hsu *et al.*, 1991) and the OM lipid A modification enzyme, PagP (Dalebroux *et al.*, 2014). Although acyl-PG is present in both bilayers, the OM appears to be enriched with a palmitoylated-PG (PPG) species, while the IM carries C14:0, C14:1, 16:0 or 16:1 at the sn-3' position (Dalebroux *et al.*, 2014).

Synthesis of OM PPG molecules is regulated by the PhoPQ system. In contrast, IM acyl-PG species showed minimal specific variation in PhoP-null mutants relative to wild-type and PhoPQ-activated bacteria (Dalebroux *et al.*, 2014). The number of PPG molecules is estimated to be similar to that of palmitoylated lipid A molecules. Like CL, the functional significance of the regulated increase of PPG is unknown.

1.4.3.1 *Bis*(monoacylglycero)phosphate

BMP is a structural isomer of PG (Garrett, 2017) and a minor component of animal tissues (Hullin-Matsuda *et al.*, 2009). There is good evidence that BMP is synthesized from phosphatidylglycerol in the endosomal system (Chevallier *et al.*, 2008; Hullin-Matsuda *et al.*, 2007). The unique stereochemical configuration of BMP found in the late endosomes of eukaryotic cells (Brotherus *et al.*, 1974) is believed to depend on an enzyme that inverts the configuration of the PG substrate, but this enzyme remains to be identified (Thornburg *et al.*, 1991). BMPs unique stereochemistry also makes it resistant to most phospholipases. There is one unconfirmed reports of BMP in some alkalophilic strains of *Bacillus* species (Nishihara *et al.*, 1982). If confirmed, this would be the first exception to the rule that BMP is strictly of mammalian origin and not present in prokaryotes, yeasts and higher plants.

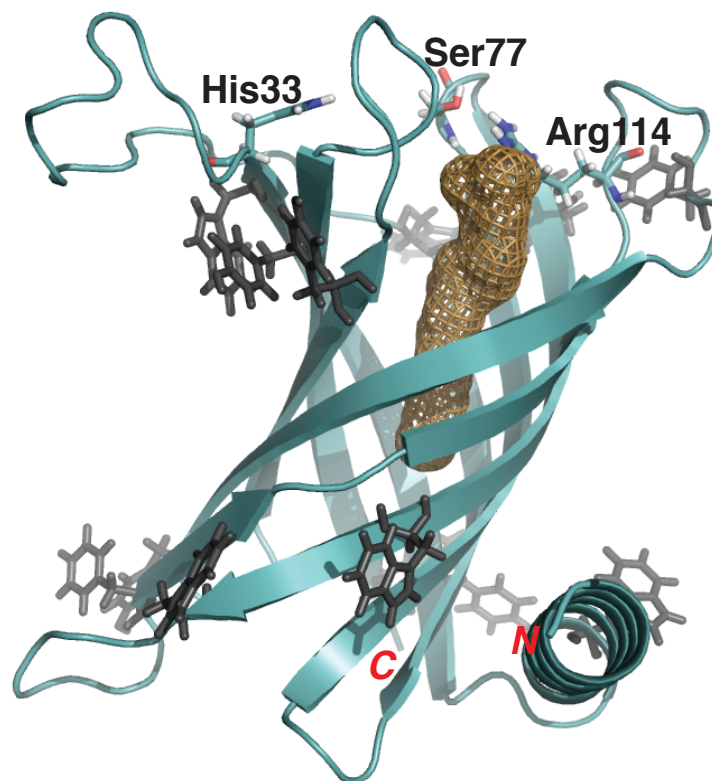


Figure 1.8. Structural organization of *E. coli* PagP (pdb: 3GP6). Ribbon diagram of *E. coli* PagP (cyan) with a molecule of SDS bound in the hydrocarbon ruler. The coordinates for the L1 loop are provided by Chris Neale and Régis Pomes at the University of Toronto. The aromatic belt residues are depicted as black sticks. *E. coli* PagP catalysis depends on invariant His, Ser, and Arg residues on the extracellular face, labelled in black. The *N* and *C* termini of the enzyme are labelled in red.

1.5 PagP

PagP functions to modify the structure of lipid A with a palmitate chain (Bishop *et al.*, 2000). Of the many enzymes involved in lipid A modification, PagP is the only known enzyme that is located in the OM. The *pagP* gene was first identified in a *Salmonella* mutant that exhibited a deficiency in lipid A palmitoylation and a hypersensitivity to CAMPs (Guo *et al.*, 1998). The structure of the *E. coli* homologue has been solved by both solution nuclear magnetic resonance (NMR) spectroscopy (Hwang *et al.*, 2004; Hwang *et al.*, 2002) and X-ray crystallography (Ahn *et al.*, 2004; Cuesta-Seijo *et al.*, 2010) to reveal an eight stranded antiparallel β -barrel preceded by a short amphipathic α -helix at the *N*-terminus (Figure 1.8). PagP sits with its barrel axis tilted by roughly 25° with respect to the membrane normal and its active site residues are exposed on the cell's exterior surface. The tilted position of PagP is inferred from the alignments of aromatic residues with the membrane interface (Ahn *et al.*, 2004; Schulz, 2002). An interior hydrophobic pocket in the outer leaflet-exposed half of the molecule functions as a hydrocarbon ruler that allows the enzyme to distinguish palmitate from other acyl chains found in phospholipids.

1.5.1 Enzymology in the OM

PagP remains dormant in the OM when its phospholipid donor is restricted to the inner leaflet. However, when OM lipid asymmetry is perturbed,

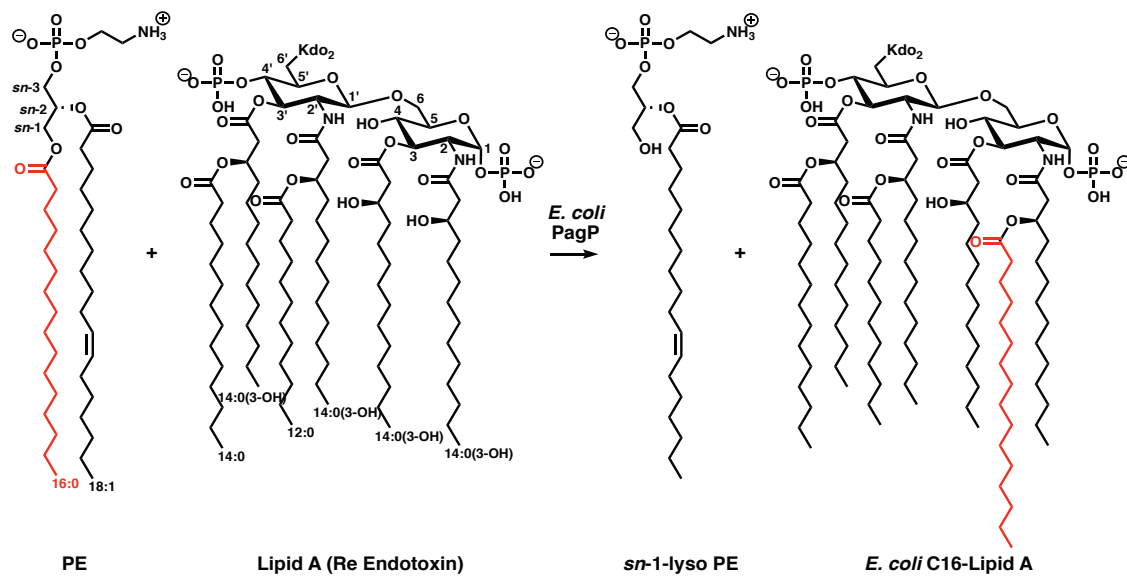


Figure 1.9. Chemical representation of palmitoylation of *E. coli* Kdo₂-lipid A. PagP catalyzes the transfer of palmitate from the *sn*-1 position of a glycerophospholipid to the R-3 hydroxymyristate group at the 2-position of lipid A, generating a hepta-acylated lipid A and *sn*-1 lyso-phosphatidylethanolamine. Abbreviations: PE, phosphatidylethanolamine.

such as might occur in the presence of CAMPs or when divalent cations are limiting, the resulting translocation of substrate lipids to the outer leaflet serves to trigger PagP activity (Jia *et al.*, 2004). In addition to directly activating PagP in the OM, the presence of CAMPs and divalent cation limitation also activate the PhoP/PhoQ virulence signal transduction system in the IM, which is known to activate the transcription of the *pagP* gene (Bader *et al.*, 2005; Bishop, 2005; Guo *et al.*, 1998).

PagP catalyzes the transfer of a palmitate chain from a phospholipid to lipid A (Figure 1.9) (Bishop *et al.*, 2000). The palmitoylation of lipid A by PagP increases the hydrophobicity of lipid A so as to provide resistance to certain CAMPs (Guo *et al.*, 1998). Additionally, lipid A palmitoylation can either attenuate or accentuate the inflammatory response (Hajjar *et al.*, 2002) triggered through the TLR4/MD2 signal transduction pathway (Kawasaki *et al.*, 2004; Park *et al.*, 2009), depending on where the palmitate chain is attached to a particular lipid A molecule.

PagP has both rapid palmitoyltransferase and slow phospholipase activity *in vitro*. However, studies on the OM phospholipase OMPLA indicates it is unlikely that PagP functions as a phospholipase *in vivo* (Hardaway and Buller, 1979). Palmitoylation of non-physiological miscible and acylated alcohols is observed *in vitro*. PagP also incorporates a palmitate into the headgroup of phosphatidylglycerol (Figure 1.10) both *in vivo* and *in vitro*

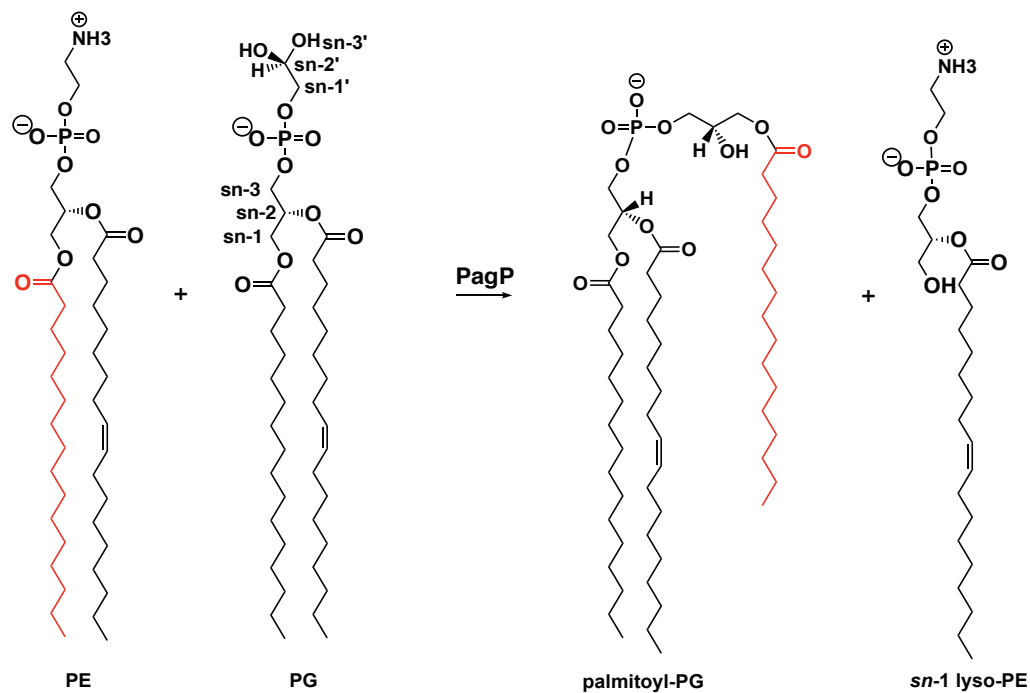


Figure 1.10. Chemical representation of palmitoylation of phosphatidylglycerol. PagP catalyzes the transfer of palmitate from a glycerophospholipid to the *sn*-3' polar headgroup of phosphatidylglycerol (PG) to produce palmitoyl-PG. Abbreviations: PE, phosphatidylethanolamine

(Dalebroux *et al.*, 2014). Palmitoylated lipid A and palmitoylated PG (PPG) were observed in a 1:1 ratio in the *Salmonella* OM. Therefore, the susceptibility of *pagP* mutants to CAMPs, previously attributed solely to palmitoylation of lipid A, might also involve palmitoylation of PG.

A striking enzymological feature of PagP is its ability to distinguish a 16-carbon saturated palmitate chain from a cellular phospholipid pool filled with 14-, 16- and 18-carbon acyl chains (Bishop, 2005). In the phospholipid pool, 16- and 18-carbon acyl chains are predominant at the *sn*-2 position, whereas 14- and 16-carbon acyl chains are most prevalent at the *sn*-1 position. A fundamental question is how does PagP select a palmitate chain when other acyl chains are abundantly present? The β -barrel of PagP is outfitted with an interior hydrophobic pocket known as the hydrocarbon ruler (Ahn *et al.*, 2004; Bishop, 2005; Khan and Bishop, 2009). The phospholipid donor must migrate into the external leaflet before diffusing laterally through the β -barrel wall at a site known as the crenel, (Cuesta-Seijo *et al.*, 2010; Khan and Bishop, 2009) it is here that regiospecificity for the *sn*-1 acyl chain is enforced, with the result that 18-carbon acyl chains esterified to the *sn*-2 position are barred from interrogation by the hydrocarbon ruler. Y147 gates the crenel; the Y147F mutation unlatches the crenel resulting in a loss of regiospecificity and the incorporation of stearate into lipid A (Khan, unpublished data). Substitutions of the G88 residue lining the floor of the hydrocarbon ruler shortens the selected acyl-chain and can convert the enzyme into a myristoyltransferase that functions

both *in vitro* and *in vivo* (Khan *et al.*, 2010a; Khan *et al.*, 2007). Since 14-carbon acyl chains at the *sn*-1 position are effectively excluded by the hydrocarbon ruler, only 16-carbon acyl chains at the *sn*-1 position are incorporated into lipid A. Lipid A binds opposite the crenel at another lateral opening in the β -barrel wall known as the embrasure (Khan and Bishop, 2009).

In principle the binding of the phospholipid and lipid A substrates can occur either by a sequential (ternary complex) or a non-sequential (acyl-enzyme) mechanism. The kinetics of *E. coli* PagP in a detergent micellar assay system confirms the former: both substrates must bind to the enzyme to form a ternary complex prior to catalysis (Bishop, unpublished). Structural details of a PagP:phospholipid:lipid A ternary complex remain to be elucidated, but this structure will likely reveal an ordering of residues in the dynamic cell surface loops and reveal the details of PagP's catalytic mechanism. In the interim, given what we now know about the essential catalytic roles and arrangement of the invariant His33, Ser77 and Arg114 (Bishop, unpublished) in *E. coli* PagP, PagP likely functions through a mechanism similar to that proposed by Liang Tong for the carnitine acyltransferases (Jogl *et al.*, 2004; Jogl and Tong, 2003). In this provisional mechanism, the Arg114 electrostatically stabilizes the polar head group of the phospholipid, leaving His33 and Ser77 to take part in the transesterification reaction depicted in Figure 1.11. His33 acts as a general base and is the key catalyst, while Ser77 functions to stabilize the electric charge on the tetrahedral intermediate.

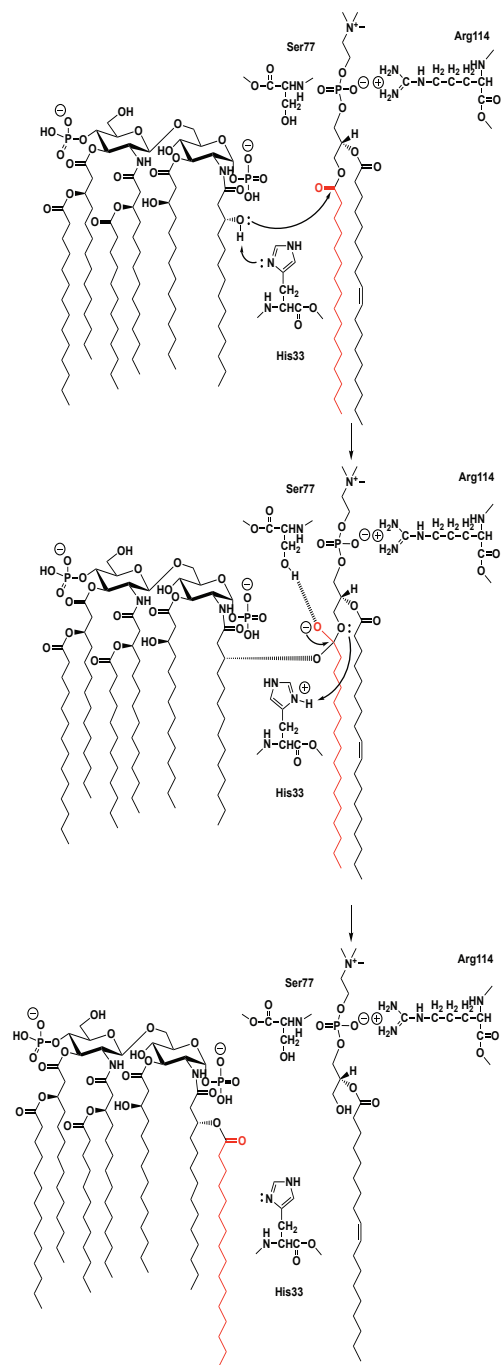


Figure 1.11. Proposed catalytic mechanism of *E. coli* PagP. His33 acts as a general base to abstract a proton from the lipid A 2-OH moiety, activating it for nucleophilic attack on the *sn*-1 carbonyl carbon of the glycerophospholipid palmitate chain. A hydrogen bonding interaction with the γ -OH of Ser77 then stabilizes the oxyanion on the resulting tetrahedral intermediate. His33 acts as a general acid to finally protonate the *sn*-1 OH leaving group to secure the transfer of the palmitate chain from the phospholipid to lipid A.

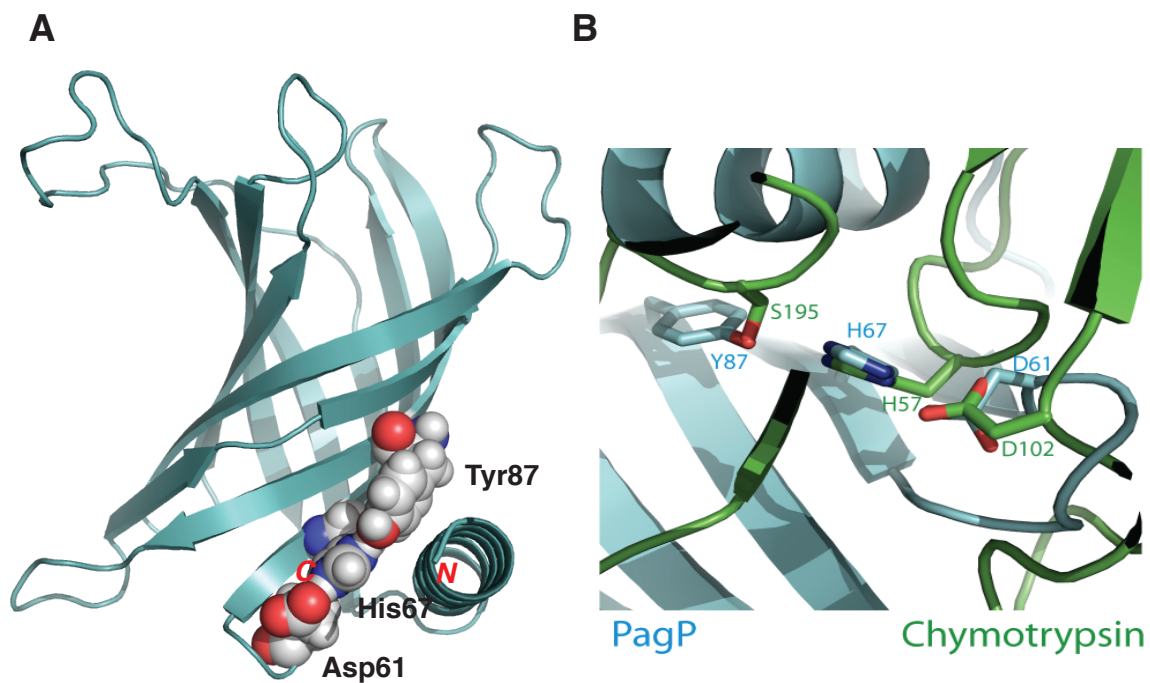


Figure 1.12. Structural organization of PagP's putative periplasmic active site. (A) Ribbon diagram of PagP from *E. coli*. Catalytically significant residues on the periplasmic face are labelled in black, while the *N* and *C* termini of the enzyme are labelled in red. (B) Superposition of PagP's putative periplasmic triad on chymotrypsin's charge relay system.

1.5.2 Role in signal transduction

In addition to lipid A and PG palmitoylation, activation of PagP in *E. coli* can also trigger truncation of the R3 core oligosaccharides in the cytoplasm. In previous studies of an *E. coli* O157:H7 mutant with an OM permeability defect we determined that PagP can exert control on cytoplasmic enzymes of LPS core oligosaccharide biosynthesis that leads to a failure in O-antigen attachment (Smith *et al.*, 2008). In this instance, PagP utilizes both its *N*-terminal amphipathic helix and a putative periplasmic catalytic triad composed of Asp61, His67 and Tyr87 (Figure 1.12). It is particularly interesting that the arrangement of these residues in PagP is nearly superimposable on Chymotrypsin's catalytic triad.

Chymotrypsin is a serine protease with a catalytic triad composed of an Asp, a His and a Ser, with serine's hydroxyl group serving as the nucleophile in the enzyme's active site (Stroud *et al.*, 1972). The Ser-His-Asp motif is one of the most thoroughly characterized catalytic motifs amongst hydrolytic enzymes. Although PagP's putative catalytic triad lacks a serine residue, there is no known biochemical reason that its tyrosine residue could not function in the hydrolysis of amide or ester bonds (Brady *et al.*, 1990).

The biological significance of the R3 truncation is not currently known. However, given the physical separation between the OM and the cytoplasm, PagP most likely functions as a sensory transducer that is activated by a breach in the OM permeability barrier. Efforts to discover the downstream signaling

components that respond to the activated state of PagP have so far been unsuccessful.

1.5.3 PagP in Gram-negative bacteria

PagP has been identified in a narrow group of Gram-negative bacteria, most of which have a pathogenic or intracellular lifestyle (Bishop, 2005). Homologues of PagP can be classified into a major and minor clade. The major clade homologues are distributed between the β and γ subclasses of proteobacteria and includes well known enterobacterial PagP homologs from *Salmonella* and *E. coli*. Figure 1.13 shows a maximum-likelihood tree based on PagP protein sequences. The tree was rooted using sequences of PagP homologs from *Bordetella*. *Legionella* PagP seems to be the link between the divergent *Bordetella* homolog and PagP from the more derived γ -proteobacteria. A gene duplication event is thought to have occurred in some members of the γ -proteobacteria leading to horizontal transfer of plasmids and transposable elements in plant endophytes like *Klebsiella*. The minor clade is characterized by a lack of obvious primary structural similarity with major clade PagP homologs, and has a more diverse distribution that includes the β , γ and δ subclass within the phylum proteobacteria, as well as *Halanaerobium* of the phylum firmicutes (Figure 1.14). Horizontal gene transfer is a pervasive mechanism of diversification that explains seemingly random distributions. Horizontal gene transfer in bacteria occurs through phage transduction,

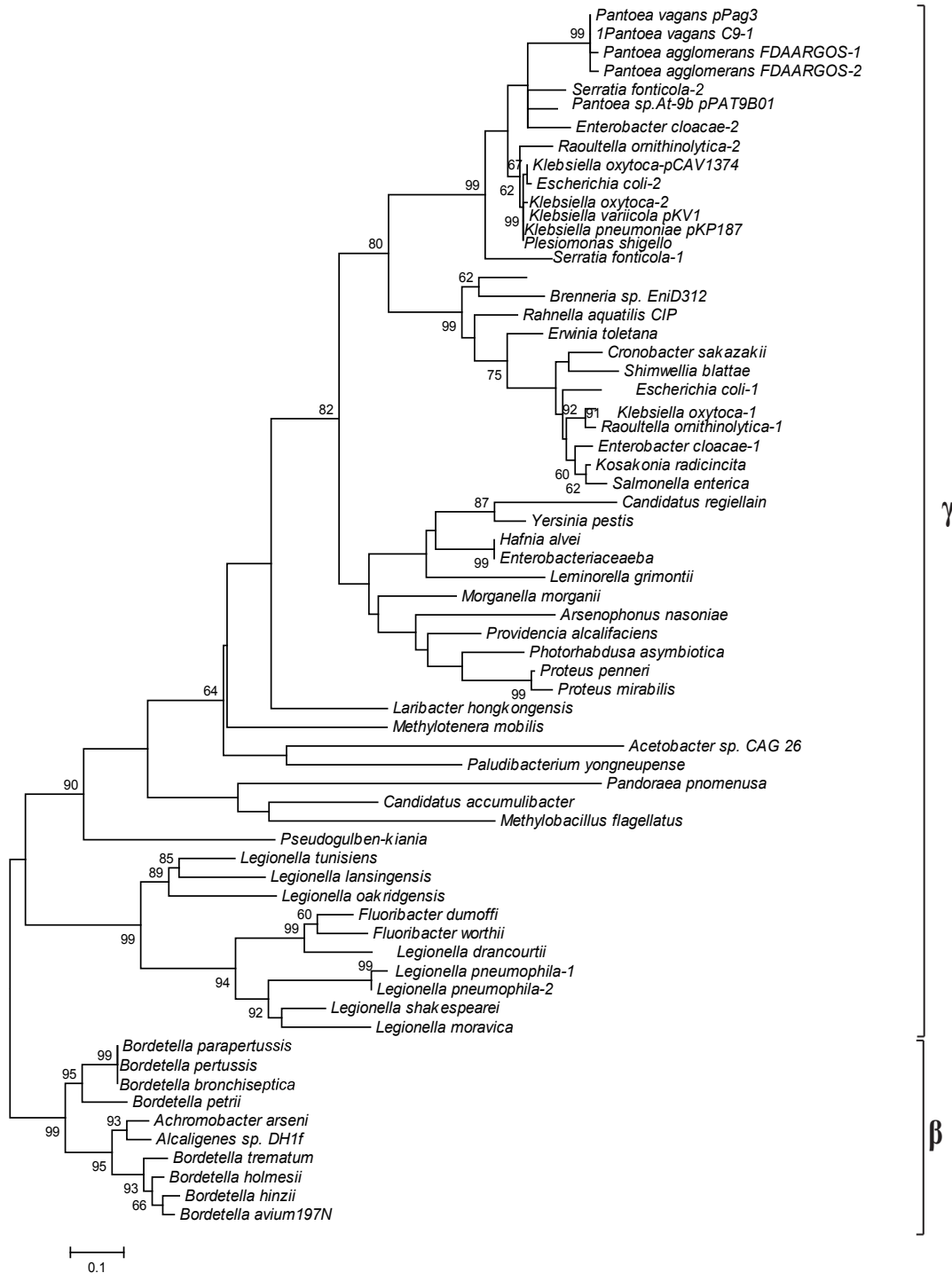


Figure 1.13. Phylogenetic analysis of major clade PagP homologous. Courtesy of Sanchia Miller and Radhey Gupta. Maximum-likelihood phylogenetic tree showing the distribution of PagP homologues from the major clade. The tree was generated by MEGA 6.0 (Tamura *et al.*, 2013) from 65 amino acid sequences aligned with ClustalW. The Neighbour-Joining method was applied to a matrix of pairwise distances and trees were bootstrapped 100 times.

transformation, or conjugation, the latter is particularly important for the spread of antibiotic resistance. However, an alternative perspective would be that a common ancestor of the β -proteobacteria gave rise to both the major and minor clade through vertical descent. To date, only one minor clade homolog, *Pseudomonas aeruginosa* PagP (PaPagP), has been characterized (Thaipisuttikul *et al.*, 2014).

1.5.3.1 *P. aeruginosa* PagP

The PhoP-dependent gene, *pal343* (McPhee *et al.*, 2006), has recently been identified as the gene encoding the *P. aeruginosa* lipid A palmitoyltransferase enzyme (Thaipisuttikul *et al.*, 2014). Despite a lack of obvious primary sequence similarity with known PagP enzymes, the β -barrel tertiary structure with an interior hydrocarbon ruler appears to be conserved; there is no evidence to suggest that PaPagP has an amphipathic α -helix at its *N*-terminus. PaPagP recapitulates much of the enzymology of the well known *E. coli* homolog, including the ability to enzymatically exclude acyl chains shorter or longer than palmitate. However, PaPagP adds palmitate on the opposite glucosamine compared to that of *E. coli* (Thaipisuttikul *et al.*, 2014). Regulated acylation at the 3' position is important for *Pseudomonas* pathogenesis (Ernst *et al.*, 2007; Ernst *et al.*, 1999). *P. aeruginosa*, produces a distinctly pro-inflammatory lipid A that is important for morbidity and mortality in *P. aeruginosa* infections (Ernst *et al.*, 1999). *Pseudomonas* lipid A is a β -(1,6)-



Figure 1.14 A bootstrapped maximum-likelihood tree based upon PaPagP. Courtesy of Sanchia Miller and Radhey Gupta. An unrooted tree showing distribution of PagP homologues based on *P. aeruginosa* PagP homolog. The tree was generated by MEGA 6.0 (Tamura *et al.*, 2013) from 35 amino acid sequences aligned with ClustalW. Includes *Rhodoferax* and *Comamonas* of the β -subclass, *Pseudomonas* and *Halomonas* of γ -subclass, *Geobacter* of the δ -subclass of proteobacteria, as well as *Halanaerobium* of the phylum Firmicutes. Bootstrap percentages are indicated at the branching points.

linked disaccharide of glucosamine substituted with phosphate groups at the 1 and 4' positions. Primary fatty acyl chains include amide-linked R-3-hydroxylaurate at the 2 and 2' positions and ester-linked R-3-hydroxydecanoate at the 3 and 3' positions. Secondary fatty acyl chains include the acyloxyacyl additions of laurate to the 2' position, and of S-2-hydroxylaurate to the 2 position. Deacylation of the R-3-hydroxydecanoate at the 3 position is also seen in the majority of *Pseudomonas* strains. *Pseudomonas* isolated from individuals with CF synthesize lipid A palmitoylated at the 3' position, resulting in a hexa-acylated structure (m/z 1684) (Ernst *et al.*, 2007). *Pseudomonas* lipid A alters host innate immune responses, including increased resistance to some antimicrobial peptides and an elevated pro-inflammatory response, consistent with the synthesis of a hexa-acylated structure preferentially recognized by the TLR4-MD-2 complex (Thaipisuttikul *et al.*, 2014). Previous studies have reported changes in cytokine levels resulting from TLR4 stimulation with palmitoylated lipid A in addition to the effects seen on CAMP resistance. Palmitoylation in other Gram-negative pathogens has been described as imparting antagonistic effects when used to stimulate TLR4 (Loppnow *et al.*, 1986; Tanamoto and Azumi, 2000). However, increased cytokine production resulting in inflammation is not seen with other palmitoylated lipid A, indicating a unique role for this modification in *Pseudomonas* pathogenesis.

1.6 Thesis Statement

The commencement of my PhD coincided with the discovery of novel PagP homologs. During my 6 years of study, I explored the hypothesis that PagP is a multifunctional enzyme. The thesis of my PhD is that *E. coli* PagP is a multifunctional enzyme with two distinct active sites located on opposite sides of the membrane; this enzyme palmitoylates lipid A at position 2 and expands glycerophosphoglycerol phospholipids, whereas PagP homologs from *P. aeruginosa* and *H. elongata* exclusively palmitoylate lipid A at position 3'. I was able to reveal these structure function relationships by comparing the activity of mutant enzymes, both purified *in vitro* and expressed in the bacterial outer membrane. The work included in this thesis can be summarized into three discoveries:

- 1) *E. coli* PagP makes a novel phospholipid *bis*(monoacylglycero)phosphate, which is derived from palmitoyl-phosphatidlyglycerol using a periplasmic active site (Chapter 2).
- 2) *P. aeruginosa* PagP is specific for the 3' position of lipid A and does not palmitoylate PG (Chapter 3).
- 3) *E. coli* PagP and *P. aeruginosa* PagP represent major and minor clades respectively, and display evidence of a shared common ancestor (Chapter 4)

Chapter 2

Identification of Novel Glycerophosphoglycerol Phospholipids in

Escherichia coli

2.1 Author's Preface

Outer membrane (OM) lipid asymmetry is maintained by the Mla pathway, a six-component system that is widespread in Gram-negative bacteria. This chapter reports the discovery of novel glycerophosphoglycerol (GPG) phospholipids and is focused on understanding the role of PagP in OM lipid homeostasis. We report that *E. coli* PagP remodels phosphatidylglycerol (PG) to palmitoyl-PG, *bis*(monoacylglycero)phosphate (BMP) and either lyso-PG or lyso-BMP, both *in vitro* and *in vivo*. I first visualized these GPG derivatives in an *E. coli* cardiolipin deficient strain using autoradiography. The structural identification of these lipids was facilitated using normal phase liquid chromatography coupled with electrospray ionization mass spectrometry performed by Dr. Teresa Garrett. Emily DeHaas (an undergraduate student under my supervision) and I prepared mutant variants of the cell surface and periplasmic active sites, and conducted *in vitro* enzyme assays to elucidate the molecular details of enzymatic synthesis. Russell Bishop and I analyzed the data, prepared the figures and wrote the chapter.

2.2 Abstract

The ability of Gram-negative bacteria to carefully modulate outer membrane (OM) lipid composition in response to environmental stress is essential for their survival and replication within host tissue. Here, lipids of *Escherichia coli* have been analyzed by thin layer chromatography (TLC) and also using normal phase liquid chromatography coupled with electrospray ionization quadrupole time-of-flight mass spectrometry to reveal a distinctive family of glycerophosphoglycerol (GPG) phospholipids of which phosphatidylglycerol (PG) is the cardinal member. The bacterial OM enzyme PagP plays a crucial role in remodeling the OM by transferring a palmitate chain from a phospholipid to the proximal glucosamine unit of lipid A and the polar head group of PG. Using ethylenediaminetetraacetic acid to trigger PagP activity in a subset of *pagP* mutants, we found that PagP palmitoylates PG at its cell surface active site. PPG molecules accumulate in the outer leaflet of the OM, and are presumably flipped to the inner leaflet where PagP possesses a periplasmic active site that functions as a lipase converting PPG to *bis*(monoacylglycero)phosphate (BMP) and either lyso-PG or lyso-BMP.

2.3 Introduction

The cell envelope of *Escherichia coli* and other Gram-negative bacteria consist of an inner membrane (IM) and an outer membrane (OM) (Raetz and Whitfield, 2002). The OM has unique permeability properties because of its asymmetric bilayer architecture, which includes an inner glycerol-based phospholipid monolayer and an outer monolayer of lipopolysaccharides (LPS). The outermost LPS barrier prevents entry of harmful agents such as detergents and antibiotics because LPS phosphate groups are electrostatically bridged by divalent cations (Nikaido, 2003). LPS is subject to various covalent modifications during its translocation between the IM and OM. These modifications directly influence OM permeability and promote resistance to antibiotics (Nikaido, 2003). Recent evidence suggests the involvement of neighboring phospholipids in establishing a barrier crucial to antibiotic resistance and intracellular survival in the host (Dalebroux *et al.*, 2015; Dalebroux *et al.*, 2014; Sutterlin *et al.*, 2014), but this has yet to be elucidated in full molecular detail.

Acyl-phosphatidylglycerol (acyl-PG) is a minor anionic phospholipid that has been reported in animals (Poorthuis and Hostetler, 1975), a lipid-containing bacteriophage (Tsukagoshi *et al.*, 1976) and several bacterial species (Makula *et al.*, 1978; Olsen and Ballou, 1971; Yague *et al.*, 1997). In bacteria, there are two known sources of acyl-PG; the IM lyso-phospholipase L2 (PldB) and the OM palmitoyltransferase (PagP) catalyze the synthesis of acyl-PG by

two distinct biochemical pathways. PldB catalyses the transfer of an acyl group from lyso-phospholipid to PG for formation of acyl-PG (Hsu *et al.*, 1991; Karasawa *et al.*, 1985). The second enzyme, PagP, incorporates a palmitate chain at the *sn*-3' position of the PG head group using a phospholipid as the palmitoyl donor (Dalebroux *et al.*, 2014). PagP is bifunctional and also catalyzes the transfer of palmitate from the *sn*-1 position of a phospholipid to lipid A (Bishop *et al.*, 2000). The two populations of acyl-PG can be readily distinguished because the IM acyl-PG headgroup pool includes a mixture of different acyl chain types, but acyl-PG in the OM is exclusively palmitoylated (Dalebroux *et al.*, 2014).

We analyzed lipids of *E. coli* by applying high-resolution mass spectrometry (MS) coupled to front-end chromatographic separation (Garrett *et al.*, 2007). In *E. coli* the main phospholipids are phosphatidylethanolamine (PE ~75%), phosphatidylglycerol (~20%) and cardiolipin (CL~5%) (Cronan, 2003; Raetz and Dowhan, 1990). We report that PagP can expand the PG pool into a novel group of glycerophosphoglycerol (GPG) phospholipids. GPG phospholipids are characterized by the presence of a second glycerol unit as part of the head group (Figure 2.1). We know that PagP converts PG to palmitoyl-PG (PPG) (Dalebroux *et al.*, 2014), but here we provide molecular details for how this is accomplished. While PPG is reported to accumulate in the bacterial OM, we demonstrate that PPG is not the end product in the *E. coli* OM. Instead, PPG

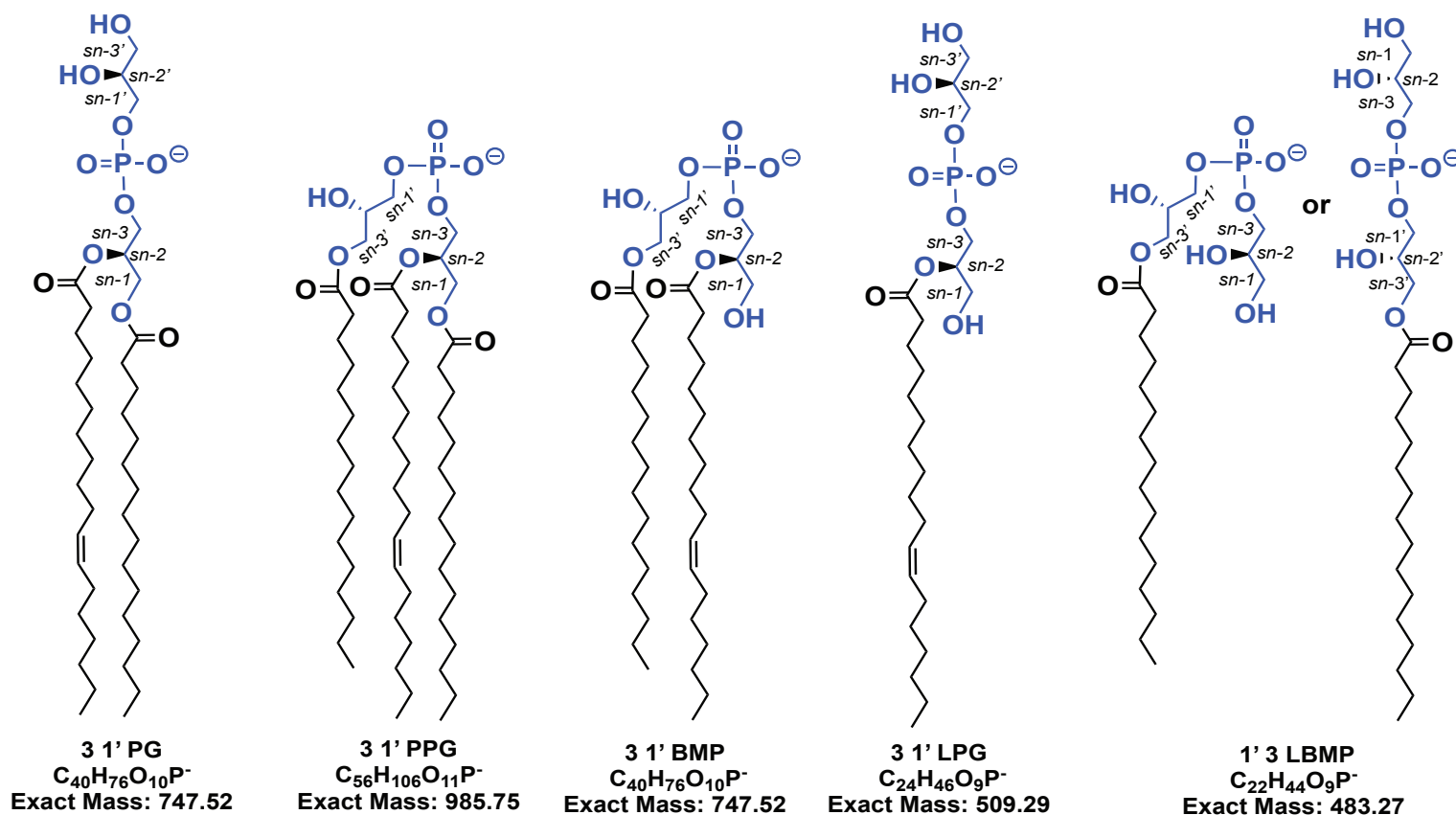


Figure 2.1. Glycerophosphoglycerols are characterized by the presence of a second glycerol unit as part of the head group. Chemical structure of phosphatidylglycerol (PG), palmitoyl-PG (PPG), *bis*(monacylglycerol)phosphate (BMP), lyso-PG (LPG) and lyso-BMP (LBMP) are representative of one of many possible structures in *E. coli*. The glycerophosphoglycerol group is shown in blue. The palmitate chain is esterified to the *sn*-1 or *sn*-3' position, *cis*-vaccenic acid is esterified at *sn*-2.

is serially degraded to *bis*(monoacylglycero)phosphate (BMP) and either lyso-PG (LPG) or lyso-BMP (LBMP) by PagP. This finding is extremely important because BMP and the final monoacylated GPG products represent novel lipid metabolic pathways not previously reported in bacteria. In fact, an enantiomer of BMP is only known to occur in late stage endosomes of eukaryotic cells (Hullin-Matsuda *et al.*, 2007). These novel bacterial GPG derivatives could represent a distinct signaling lipid reflecting different roles of phospholipids in the adaptation to the environment.

2.4 Materials and Methods

2.4.1 Reagents

Tryptone and yeast extract were purchased from Difco. Liquid Luria-Bertani (LB) media was the normal media for growth in all experiments and was made with 10 g of tryptone, 5 g of yeast extract, 10 g of NaCl per L and adjusted to pH 7.0 with 6 N NaOH. Solid LB medium consisted of the liquid broth with 20 g of agar per L. Reagent grade chloroform and methanol were purchased from EMD Millipore. L-(+)-arabinose, isopropyl β -D-thiogalactopyranoside (IPTG), sodium dodecyl sulphate (SDS), 2-methyl-2, 4-pentenediol (MPD), phosphate buffered saline (PBS), acetic acid, 88% formic acid, pyridine and sodium acetate were purchased from Sigma Glass-backed Silica Gel 60 TLC plates were from Merck. L- α -dipalmitoyl-phosphatidylcholine (DPPC), *E. coli* L- α -phosphatidylglycerol (PG) and L- α -phosphatidylethanolamine (PE) were

obtained from Avanti Polar Lipids, Inc. $^{32}\text{P}_i$ 1 mCi (37 MBq) and *sn*-1,2-di-(16:0- ^{14}C)-phosphatidylcholine (^{14}C -DPPC) (370 kBq) were purchased from Perkin Elmer Inc. Taq DNA Polymerase and the Quikchange XL site-directed mutagenesis kit were from Agilent Technologies.

2.4.2 Bacterial strains and growth conditions.

Escherichia coli W3110 is designated as the wild-type (WT) with respect to its phospholipid composition. All strains and plasmids with corresponding genotypes are listed in Table 2.1. *E. coli* strain BKT12 was kindly provided by William Dowhan. Plasmids were provided by Lori Burrows (pBADGr), Joaquin Ortega (pSim6) and Pep Charusanti (pIJ773). Cells were generally cultured in LB at 37°C, shaking at 200 r.p.m, to an OD_{600} = 0.4 to 0.6 after a 1:100 dilution of an overnight starter culture, unless otherwise stated. Cultures were adjusted, when indicated, to a final concentration of 25 mM ethylenediaminetetraacetic acid (EDTA). Following treatment of cells with or without EDTA, cells were harvested by centrifugation at room temperature and washed once with phosphate buffered saline. The pBADGr-derived (*Asikyan et al.*, 2008) plasmids were grown with 0.1% L-(+)-arabinose unless indicated otherwise. When necessary, LB was supplemented with antibiotics at the following concentrations: 100 $\mu\text{g}/\text{mL}$ ampicillin (*amp*), 25 $\mu\text{g}/\text{mL}$ kanamycin (*kan*), 15 $\mu\text{g}/\text{mL}$ gentamicin (*gen*), 100 $\mu\text{g}/\text{mL}$ apramycin (*apr*).

Table 2.1. *E. coli* strains used in this study.

Strains /Plasmids	Description	Source
<i>E. coli</i> strains		
MC1061	F ⁻ , λ, <i>araD139</i> , Δ(<i>ara-leu</i>)7697, Δ(<i>lac</i>)X74, <i>galU</i> , <i>galK</i> , <i>hsdR2</i> (r _K -m _K ⁺), <i>mcrB1</i> , <i>rpsL</i>	Casadaban and Cohen, 1980
WJ0124	MC1061 Δ <i>pagP</i> :: <i>amp</i> ^r	Jia <i>et al.</i> , 2004
W3110	F ⁻ λ <i>rph-1</i> INV(<i>rrnD-rrnE</i>)	Smith <i>et al.</i> , 2008
DIXC03	W3110 Δ <i>clsA</i> , Δ <i>clsB</i> , Δ <i>clsC</i> :: <i>kan</i> ^R , Δ <i>pagP</i> :: <i>apr</i> ^R	Tan <i>et al.</i> , 2012
Plasmids		
pET21a(+)	T7 lac promoter and terminator MCS, C-terminal His-tag Amp ^R	Novagen
pBADGr	pMLBAD backbone with <i>dhfr</i> replaced with <i>aacCI</i> ; arabinose inducible; Gm ^R	Lefebvre and Valvano, 2002; Asikayan <i>et al.</i> , 2008
pIJ773	pBluescript KS(+) containing the apramycin resistance gene and <i>oriT</i> of Plasmid RP4, flanked by FRT sites (Amp ^R)(Apra ^R)	Gust <i>et al.</i> , 2003 Don Court
pSim6	<i>PL</i> ^{-gam-bet-exo} genes under control of C1857 repressor, Amp ^R (Ts)	This study This study
pETCrcAΔS	pET21a(+) with <i>E. coli pagP</i> gene	This study
pETCrcAΔS.S77A	Derivative of pETCrcAΔS with S77A point mutation	This study
pETCrcAΔS.Y87F	Derivative of pETCrcAΔS with Y87F point mutation	This study This study
pPagP	pBadGr with <i>E. coli pagP</i> gene	This study
pS77A	Derivative of pPagP with S77A point mutation	This study
pY87F	Derivative of pPagP with Y87F point mutation	This study
pH67S	Derivative of pPagP with H67S point mutation	This study

2.4.3 Cloning, expression and purification of PagP

To purify PagP in a denatured state, we expressed it without its native signal peptide. The cloning of the *E. coli pagP* gene with a deleted leader sequence was described previously (Hwang *et al.*, 2002). The protein was expressed using IPTG induction in *E. coli* C41(DE3) (Lucigen) transformed with the plasmid pETCrcAΔS - which does not include a poly-histidine tag, or its mutant derivatives that were constructed using the QuikChange protocol. Cells were harvested, resuspended in 10mM Tris-HCl (pH 8.0) and ruptured using a Thermo French Press Cell Disrupter. Insoluble protein was collected by centrifugation and the pellet was washed twice with 2% Triton X-100. The washed inclusion bodies were directly solubilized in 1% SDS, 1M MPD, 10mM Tris-HCl (pH 8.0). The suspension was heated to 100C and the protein was refolded by slow cooling as previously reported (Cuesta-Seijo *et al.*, 2010).

Refolding was quantitative as judged by an SDS-PAGE assay (Michaux *et al.*, 2008). In order to increase the resolution of the folded and unfolded PagP bands on SDS-PAGE, we used 18% (w/v) polyacrylamide gels that were polymerized with high amounts of initiator. For every 10 ml of 0.375 M Tris-HCl (pH 8.8), 18% acrylamide 0.1% SDS resolving gel solution, we added 0.25 ml of 10% (w/v) ammonium persulfate and 0.025 ml of N, N, N', N' - tetramethylethylenediamine. In this system, folded PagP migrates more slowly than unfolded PagP. Circular dichroism confirmed that the refolded protein was

predominantly β sheet and exhibited a characteristic exciton couplet at 232 nm (Khan *et al.*, 2007) indicating the correct formation of the hydrocarbon ruler.

2.4.4 *In vitro* palmitoyltransferase reaction

The protocol for palmitoyltransferase *in vitro* reactions was adapted from assays described by (Cuesta-Seijo *et al.*, 2010). PagP was assayed in a volume of 25 μ L with *sn*-1,2-di-(16:0- 14 C)-PtdCho to achieve a final concentration 20 μ M (4,000 cpm/ μ L). DPPC, PG or Kdo₂-lipid A were added to a final concentration of 100 μ M. The lipids were dried under N₂ (g) and dissolved in 22.5 μ L of reaction buffer containing 0.1 M Tris-HCl (pH 8.0), 10 mM EDTA, and 0.25% n-dodecyl β -D-maltoside (DDM). Reactions were started by addition of 2.5 μ L of PagP(1 μ g/mL). The PLA₂ control (4 mU/ μ L) was incubated with 10 mM CaCl₂ in place of EDTA. Reactions were incubated at 30 °C for 4 h and terminated by adding 12.5 μ L to 22.5 μ L of chloroform, methanol (1:1 v/v); 5 μ L of the lower organic phase provided 10,000 cpm for spotting onto a TLC plate. The TLC plates were developed for 150 minutes in solvent C (chloroform, methanol, water 65:25:4, v/v) solvent system in a sealed glass tank. The plates were then exposed overnight to a PhosphorImager screen and developed the next day with a Molecular Dynamics Typhoon 9200 PhosphorImager.

For palmitoyltransferase reactions with unlabeled lipids, PagP was assayed in a volume of 1mL and the reactants were scaled forty times. The

reaction was terminated by converting to a two phase Bligh-Dyer mixture.

800 μ L of the lower phase was collected and dried under nitrogen.

2.4.5 Determination of phospholipid concentration

PPG was isolated from the palmitoyltransferase reaction was quantified by measuring the amount of inorganic phosphate released after digestion. The dried lipid extract was re-dissolved in 200 μ l of chloroform and methanol (4:1, v/v) and 20 μ l aliquots were added to three acid washed Pyrex test tubes. A 1 mM standard phosphate solution was prepared from reagent grade KH_2PO_4 . From this solution a standard series was prepared using volumes of 0, 25, 50, 75, 100, 150, 200 and 400 μ l. A 10 % w/v solution of magnesium nitrate was prepared by dissolving 10 g of $\text{Mg}(\text{NO}_3)_2 \cdot 6\text{H}_2\text{O}$ in 100 ml of 95 % ethanol. 30 μ l of magnesium nitrate solution was added to the samples and standards and was taken to dryness by shaking each tube in flame. The tubes were cooled at room temperature before adding 300 μ l of 0.5 N HCl to hydrolyze any pyrophosphate that might have been formed. Pyrophosphate breaks down about 5%, so that this method is not very satisfactory for determining inorganic phosphate if labile phosphate esters are present in large excess. The tubes were capped with marble and boiled in a hot water bath for 15 minutes. The samples were allowed to cool and then incubated with 700 μ l of a mixture of one part 10 % Ascorbic acid and six parts 0.42 % ammonium molybdate in 1N H_2SO_4 for 10 minutes at 60°C. The absorbance at 820nm of each standard was measured in

triplicate used to generate a calibration curve. The absorbance of the standards was also measured and the calibration curve was used to determine the unknown concentration of PPG. The concentration of PPG was reported as an average of the triplicate.

2.4.6 Construction of a quadruple mutant lacking *cls* and *pagP* genes

Genetic material was amplified by polymerase chain reaction (PCR) with Taq DNA Polymerase following the manufacturer's protocols. Primers were synthesized by Integrated DNA Technology. Colony PCR was used to screen for appropriate colonies, and then the PCR products were sequenced at the Farncombe Sequencing Facility at McMaster University. Plasmid transformations were accomplished using electroporation. All genomic gene deletions and plasmid constructs were verified by PCR and DNA sequencing.

BKT12 mutant with multiple chromosomal deletions of *cls* genes were derived from the Keio single deletion collection (Baba *et al.*, 2006; Tan *et al.*, 2012). To generate the quadruple mutant DIXC03 ($\Delta pagP$, $\Delta clsA$, $\Delta clsB$, $\Delta clsC$), a *pagP* knockout was made in the BKT12 background using the pIJ773 plasmid (Gust *et al.*, 2003) as the template to amplify the apramycin resistance

Table 2.2. List of Primers used for PCR and Mutagenesis

Primer name	Sequence
For deleting <i>pagP</i>	
pagPFwd	AGCTTTGCTATGCTAGTAGTAGATTTTTGATAAATGTTTTATGGT CACAAATGAGCAAAGGGGATGATAAGTTTATC
pagPRev	CCGCTCGCCAGTCGATTGGCTGATGGATGCGCTTTCAGTTTTGA GACAAATGAAGTTTTAGTAACTTCTTTAA
For verifying knockout	
apr_IntF	CAGGCAGAGCAGATCATCTCTGT
apr_IntR	CAGAGATGATCTGCTCTGCCTG
pagP_IntF	CTAACGCAGATGAGTGGATGAC
pagP_IntR	CGGTGAATCCCAGACCTAAATG
For point mutations	
S77AFwd	TTCCCATTTGTTCCACGCGTCCTTAAATGCCATGG
S77ARev	CCATTGGCATTTAAGGACGCGTGGAACAAATGGGAA
Y87FFwd	GGAACCGATTGCCGATTCCGGATGGGAAAGT
Y87FRev	ACTTTCCCATCCGAATCCGGCAATCGGTTC
H67AFwd	GGCCATGGCATAACAGACCACTCCAATTACCTTTTTCATCC
H67ARev	GGATGAAAAAGGTAATTGGAGTGGTCTGTATGCCATGGCC
H67SFwd	GGCCATGGCATAACAGACCACTCCAATTACCTTTTTCATCC
H67SRev	GGATGAAAAAGGTAATTGGAGTGGTCTGTATGCCATGGCC
For sequencing point mutations	
pBADFwd	ATGCCATAGCATTTTTATCC (For pBADGr plasmids with <i>E. coli</i> araBAD promoter)
pBADRev	GATTTAATCTGTATCAGG (For pBADGr plasmids with <i>E. coli</i> araBAD promoter)
T7	TAATACGACTCACTATAGGG (For pET21 plasmids with T7 promoter)
T7term	GCTAGTTATTGCTCAGCGG (FOR pET21 plasmids with T7 terminator)

gene (*aac(3)IV*) and the temperature sensitive pSim6 previously described (Datta *et al.*, 2008). Plasmid pSim6 contains the same λ -Red system that is used to construct knockouts in *E. coli* and is used to facilitate homologous recombination between the knockout cassette and the target locus in the chromosome.

To construct the knockouts, pSim6 was first introduced into BKT12 using electroporation. Single colonies were generally inoculated from plates into 5 ml of LB media and grown at 37 °C overnight to stationary phase. A 1% inoculum was then subcultured into fresh medium and allowed to resume growth at 37 °C. When the culture reached an optical density at 600 nm (OD_{600}) of 0.4 to 0.6, the cells were centrifuged at 2400 *g* for 20 minutes and washed twice with ice-cold 10% glycerol. Cells were resuspended in the residual glycerol solution after the final wash. A 50 μ l aliquot of the dense suspension was then mixed with 100 to 200 ng of plasmid DNA and electroporated at 2500 mV. SOC medium was added immediately after electroporation. The sample was then incubated for 1 h at 37 °C on a rotary platform shaker at 200 r.p.m and then spread onto LB plates containing ampicillin.

The knockout cassette consisted of three distinct regions: the *aac(3)IV* gene that confers apramycin resistance, FRT sites that flanked *aac(3)IV*, and 50 bp regions at each end that were homologous to the chromosomal region to be deleted. We constructed this cassette by ordering PCR primers that contained the 50 bp homologous regions on the 5' end of each primer and consensus sites

used to amplify *aac(3)IV* and the flanking FRT sites from plasmid pIJ773 on the 3' ends. The design of primers followed that used by Hirotada Mori for construction of the Keio deletion library i.e. the reverse primer retains 21 bp at the end of the gene to minimize polar effects on downstream genes. PCR amplification using pIJ773 as the template was then used to make the cassette. The cassette was electroporated into recombination-competent BKT12 bearing pSim6 - 200 to 500 ng of the knockout cassette was used for electroporation, and after transformation, cells were plated on LB agar plates containing apramycin and incubated overnight at 37 °C. PCR was used to screen for recombinants with the correct insertion of the knockout cassette.

2.4.7 Extraction of lipids from ³²P- radiolabelled cells.

Total lipids were extracted from cells using the Bligh and Dyer method (Bligh and Dyer, 1959). An overnight culture grown at 37 °C was diluted 100-fold into 5 ml of LB broth containing appropriate antibiotics and 5 µCi/ml ³²Pi and was allowed to grow at 37 °C for 3 h, unless indicated otherwise. The ³²P-labeled cells were grown to OD₆₀₀ of ~0.4 and harvested. The final cell pellet from the growth of *E. coli* was resuspended in 0.8 mL of PBS and transferred to a glass culture tube. Methanol and chloroform were added to the cell suspension to generate a single phase Bligh-Dyer mixture (methanol/chloroform/PBS; 2:1:0.8 v/v/v). After a 1 h incubation at room temperature, the mixture was centrifuged. The lipid A is covalently attached to the LPS in the insoluble pellet.

The supernatant containing phospholipids was transferred to a clean tube and phase separation was induced using a two phase Bligh-Dyer mixture (methanol/chloroform/PBS; 2:2:1.8 v/v/v) by the addition of 1 mL chloroform and 1 mL PBS. The mixture was centrifuged to resolve the phases, and the lower phase was transferred to a clean glass tube and dried under a stream of nitrogen. The dried lipid samples were stored at -20°C. Non-radioactive dried lipid films were also extracted for analysis by normal phase normal-phase liquid chromatography electrospray ionization mass spectrometry (LC-ESI-Q-TOF) and Collision-induced dissociation mass spectrometry (MS/MS) as described previously (Bulat and Garrett, 2011).

The dried lipids were re-dissolved in chloroform and methanol (4:1, v/v). The ^{32}P -labeled lipids were spotted onto a TLC plate (20,000 cpm/lane), which was developed in the solvent A (chloroform, methanol, acetic acid 65:25:5, v/v) or solvent B (chloroform, pyridine, 88% formic acid, water 50:50:16:5, v/v) as specified. After drying, the plates were exposed to a PhosphorImager Screen overnight and developed the next day with a Molecular Dynamics Typhoon 9200 PhosphorImager.

2.4.8 Lipid A mild acid hydrolysis

Analysis of lipid A released by mild acid hydrolysis from ^{32}P -labeled cells was adapted from (Zhou *et al.*, 1998). Typically, 5 ml of LB broth cultures were labeled with 5 $\mu\text{Ci/ml}$ $^{32}\text{P}_i$. The ^{32}P -labeled cells were harvested by

centrifugation and washed once with 5 ml of PBS. The pellet was resuspended in 0.8 ml of PBS and converted into a single-phase Bligh/Dyer mixture by adding 2 ml of methanol and 1 ml of chloroform. After 10 min of incubation at room temperature, the insoluble material was collected by centrifugation in a clinical centrifuge. The pellet was washed once with 5 ml of a fresh single-phase Bligh/Dyer mixture. This pellet was then dispersed in 1.8 ml of 12.5 mM sodium acetate, pH 4.5, containing 1% SDS, with sonic irradiation in a bath apparatus. The mixture was incubated at 100 °C for 30 min to cleave the ketosidic linkage between Kdo and the distal glucosamine sugar of lipid A. After cooling, the boiled mixture was converted to a two-phase Bligh/Dyer mixture by adding 2 ml of chloroform and 2 ml of methanol. Phases were separated and the lower phase material was collected and washed once with 4 ml of the upper phase derived from a fresh neutral two-phase Bligh/Dyer mixture. The lower phase lipid A sample was collected and dried under a stream of nitrogen gas. The lipid A sample was dissolved in 100µl of chloroform/methanol (4:1, v/v), and a 5000 cpm portion of the sample was applied to the origin of a Silica Gel 60 TLC plate. TLC was conducted in a developing tank in the solvent system C. The plate was dried and visualized with a PhosphorImager.

2.4.9 MS of *Lipids*

The products of the *in vitro* reactions were re-suspended in 100µl of chloroform, methanol (2:1, v/v) and analyzed using LC-ESI-Q-TOF mass

spectrometry as described previously (Garrett *et al.*, 2007). The HPLC effluent (0.4 ml/min) from normal-phase chromatography on a Zorbax Rx-SIL column was analyzed using an Agilent 6520 quadrupole time-of-flight mass spectrometer in the negative-ion mode. Mass spectra were obtained scanning from 100 to 2000 at 1 spectra per second with the following instrument parameters: fragmentor voltage -175 V, drying gas temperature -325 °C, drying gas flow -11 l/min, nebulizer pressure -45 psig, capillary voltage -4000V. Data were collected in profile mode with the instrument set to 3200 mass range under high resolution conditions at 2 GHz data acquisition rate. The instrument was calibrated using Agilent ESI- L low concentration tuning mix and under normal operating conditions the resolution of the instrument was ~15,000. The mass accuracy of the instrument was between 1 and 5 ppm; therefore, measured masses are given to three decimal places. Data acquisition and analysis was performed using Agilent MassHunter Workstation Acquisition Software and Agilent MassHunter Workstation Qualitative Analysis Software (Agilent Technologies, Santa Clara, CA), respectively. Exact masses of lipid species were obtained using PerkinElmer ChemBioDraw Ultra, version 16.0.1.4.

2.5 Results

2.5.1 Purified PagP remodels PPG to BMP *in vitro*.

Wild-type PagP, and the Y87F and S77A mutants were expressed into inclusion bodies (Hwang *et al.*, 2002), purified (Khan *et al.*, 2007) and refolded

(Cuesta-Seijo *et al.*, 2010) as previously described. PagP and its mutants were refolded as judged by a gel shift assay (Michaux *et al.*, 2008) and the presence of a positive exciton band in the circular dichroism (CD) spectra at 232 nm (Khan *et al.*, 2007) (Figure 2.2). It has previously been demonstrated that purified *Salmonella* PagP can palmitoylate the *sn*-3'-OH moiety of PG *in vitro* (Dalebroux *et al.*, 2014). We were able to reproduce this for *E. coli* PagP using assay conditions similar to those described by Dalebroux *et al.* (2014).

Figure 2.3 shows the autoradiograph of *in vitro* assays when purified PagP and its mutants were incubated with the labeled palmitate donor dipalmitoyl-1-¹⁴C-DPPC, and an unlabeled acceptor. ¹⁴C-DPPC is digested with phospholipase A₂ (PLA₂) as a positive control for PagP's phospholipase activity. In the absence of an acceptor, PagP is known to exhibit slow phospholipase activity that results in an accumulation of palmitic acid. When lipid A is present, some of the palmitic acid is transferred to it, producing C16-lipid A. When PG is the acceptor, a number of distinct products are apparent in this assay. In order to determine the identity of the products, reactions with unlabeled lipid substrates were extracted and analyzed using LC-ESI-Q-TOF MS in the negative mode. When PG is the acceptor, the [M-H]⁻ ions of acyl-PG species are enriched (Figure 2.4A). The most abundant ion *m/z* 985.754 corresponds by exact mass to 50:1 (total number of carbons in the acyl chains: to total number of unsaturations) PPG, with palmitate esterified to the *sn*-1 and *sn*-3' positions,

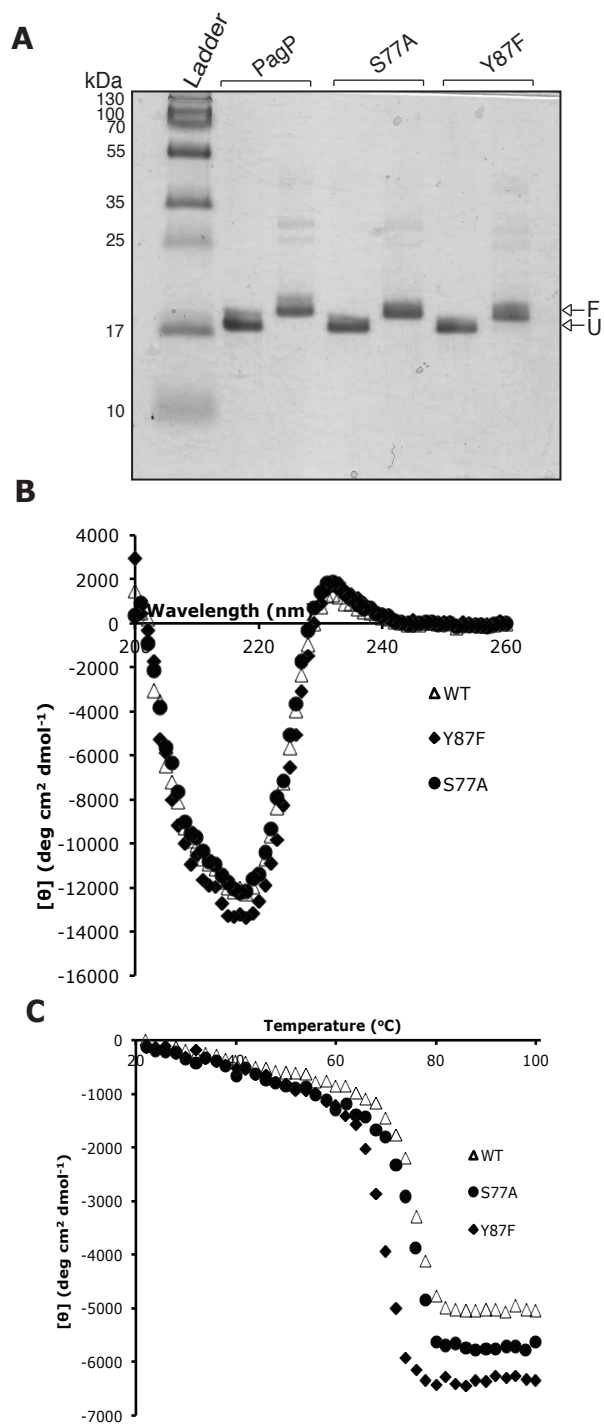


Figure 2.2 Refolding and spectroscopic analysis of PagP and active site mutants. A) Wildtype PagP and the S77A and Y87F mutants were refolded in SDS-MPD and evaluated by SDS-PAGE. B) PagP, S77A and Y87F were further analyzed by circular dichroism (CD) spectroscopy C) and the thermal unfolding profiles were obtained by following the loss of the peak ellipticity at 232nm.

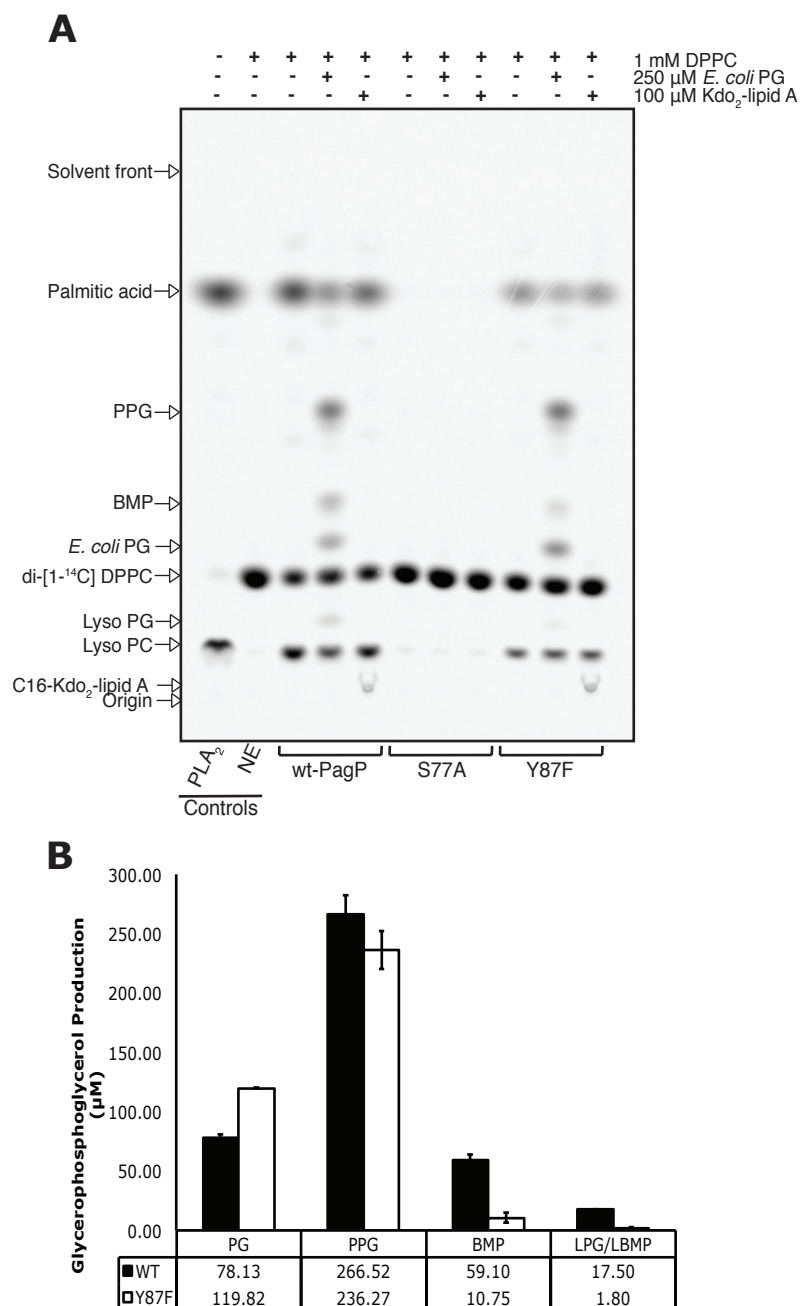


Figure 2.3 TLC analysis of glycerophosphoglycerol production by purified PagP *in vitro*. A) Representative TLC of the phospholipase reaction supplemented with PG or lipid A. Incubation with commercial phospholipase A₂ (PLA₂) reveals the location of free palmitic acid and lyso-PC. Cold phosphatidylglycerol (PG) becomes radioactive as a result of a phospholipid transacylase reaction, where PG is first converted to lyso-PG by phospholipase activity and then reacylated using ¹⁴C-DPPC to regenerate labelled PG. Additional species observed include palmitoyl-PG (PPG), *bis*(monacylglycerol)phosphate (BMP), and lyso-PG. Solvent system: chloroform, methanol, water (CHCl₃:CH₃OH:dH₂O (65:25:4 v/v) B) Quantification of glycerophosphoglycerols produced.

and *cis*-vaccenic acid esterified to the *sn*-2 position. Upon collision induced dissociation (MS/MS), the $[M-H]^-$ ions of m/z 985.754 give a product ion spectra containing predominant $[M-H-255.231]^-$ ions arising from the loss of palmitate from the *sn*-1 and *sn*-3' positions (Figure 2.5A). If palmitate is removed from the *sn*-3' position in the glycerol headgroup or the *sn*-1 in the glycerol backbone of PPG (m/z 985.754) negative product ions of m/z 747.525 are formed (Figure 2.4B). These negative ions correspond to PG and its stereoisomer *bis*(monoacylglycerol)phosphate (BMP). PG and BMP are indistinguishable by mass when they have the same number of carbons and saturations. However, each lipid metabolite can be confirmed using MS/MS and/or comparison to retention time and MS behavior of synthetic standards. The product ions resulting from the loss of the phosphoglycerol headgroup of PG or the acylphosphoglycerol of BMP are distinct (Figure 2.5B). When the catalytically inactive S77A mutant was assayed the results are comparable to the no enzyme standard. Unexpected, the Y87F mutant produced the same products as the wild-type enzyme, but with less BMP (Figure 2.3B). There are two probable pathways for BMP formation: PagP hydrolyses one of the acyl chains esterified in the glycerol backbone of PPG or PagP adds an acyl chain to the glycerol headgroup of LPG. We investigated the former by incubating purified PagP with ^{14}C -PPG and its diether analog (Figure 2.6 A and B). When PagP was incubated with ^{14}C -PPG, we observed the formation of BMP and palmitic acid (Figure 2.6 C and D). As suspected, PPG can be used as a palmitate donor

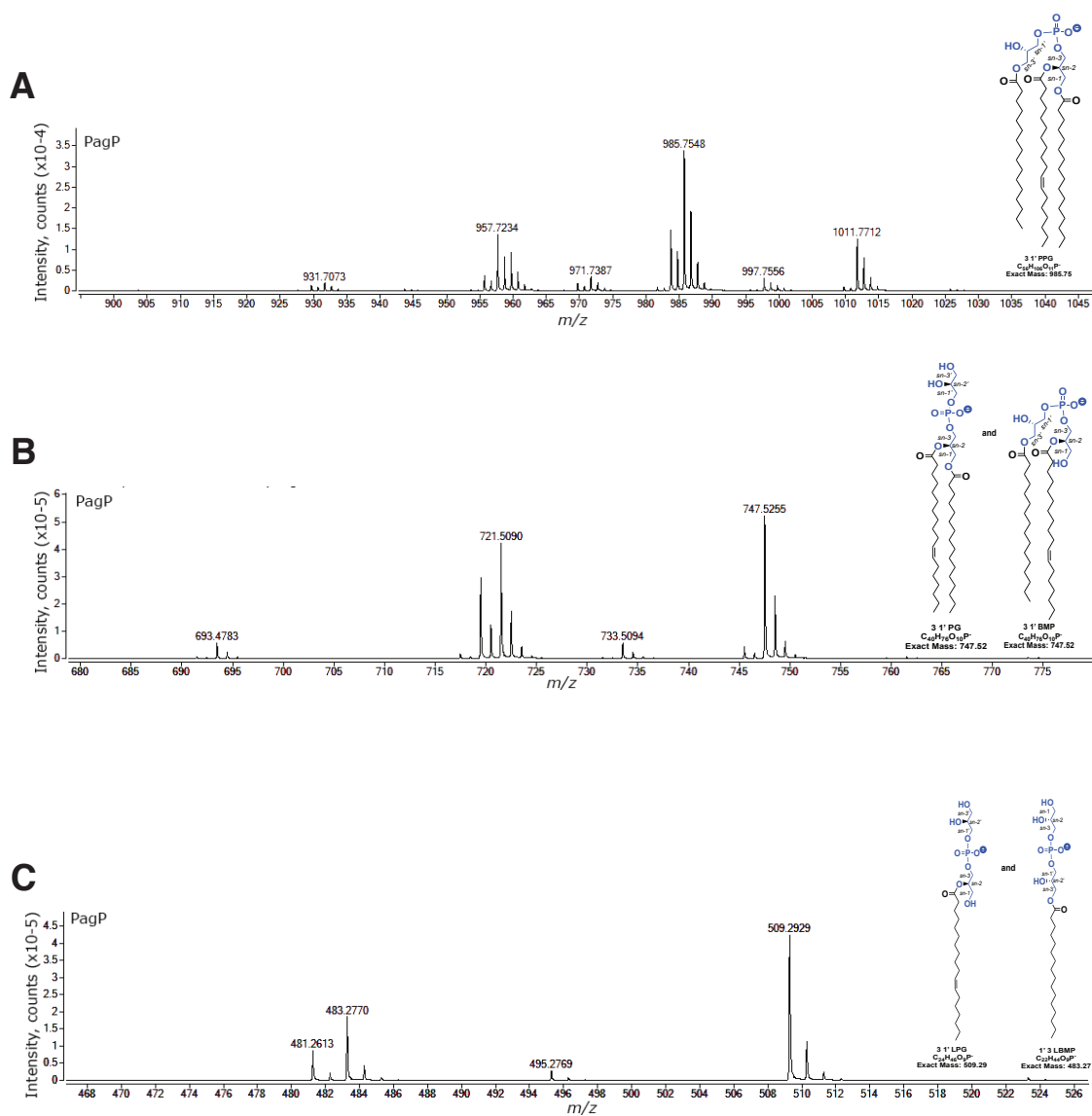


Figure 2.4. Negative-ion ESI-MS of the lipid extract from PagP *in vitro* activity assay.

Wild-type PagP was incubated with 1 mM dipalmitoyl-phosphatidylcholine (DPPC) and 1 mM *E. coli* phosphatidylglycerol (PG) (Figure 2.3, lane 4). A) Negative-ion ESI-MS from 875-1015 a.m.u range and chemical representation of PPG (m/z 985.75). B) Negative-ion ESI-MS from m/z 680-760 and chemical representation of *bis*(monoacylglycerol)phosphate (BMP) and PG (m/z 747.52). C) Negative-ion ESI-MS from m/z 460-520 of the reaction mixture and chemical representation of 16:0 LBMP (m/z 483.27) and 18:1 LPG (m/z 509.29).

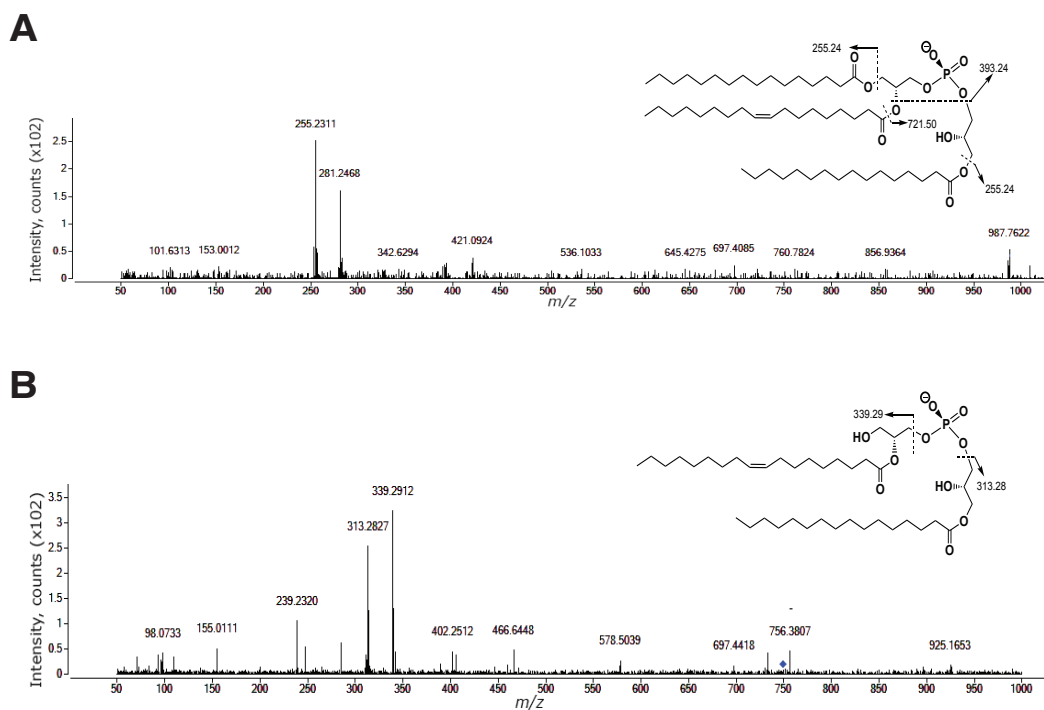


Figure 2.5. Collision induced dissociation product ion spectra of PPG and BMP.
 A) Negative ion MS/MS of palmitoyl-phosphatidylglycerol (PPG) with *m/z* 985.75. [M-H]⁻ ions of *m/z* 255 arising from loss of palmitate from the *sn*-1 and *sn*-3' positions.
 B) [M-H]⁻ ions of *m/z* 313 arising from loss of acylphosphoglycerol of *bis* (monoacylglycero)phosphate (BMP).

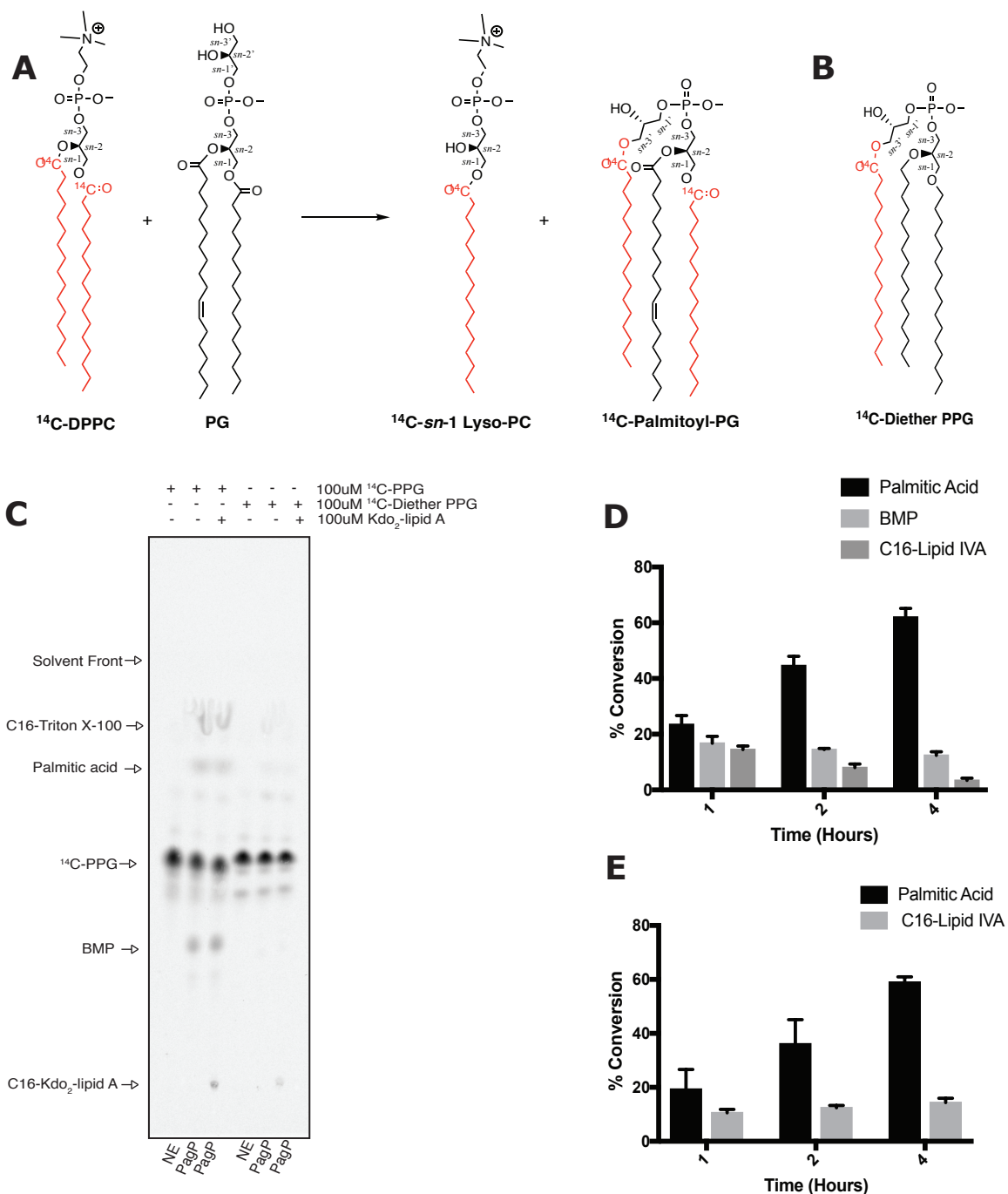


Figure 2.6. Stereospecific metabolism of palmitoyl-phosphatidylglycerol. A) Chemical representation of the biosynthesis of ¹⁴C radiolabelled palmitoyl-phosphatidylglycerol (PPG) *in vitro*. B) Diether PPG only has a hydrolyzable acyl-chain at the *sn*-3' position of the head group glycerol moiety. C) A representative TLC autoradiograph showing degradation of PPG to form BMP (Rf = 0.506). The formation of BMP must involve the removal of an acyl-chain from position *sn*-1 or *sn*-2 of the proximal glycerol moiety. D & E) Percentage conversion of PPG and diether-PPG to palmitic acid, respectively.

for lipid A palmitoylation. BMP did not accumulate when PagP was incubated with the *sn*-1, *sn*-2 diether analog of PPG. However, palmitic acid is produced from the hydrolysis of palmitate esterified at position *sn*-3' of the head group glycerol moiety (Figure 2.6 C & E). The results of this *in vitro* assay suggest that PagP reduces PPG to BMP by catalyzing the specific hydrolysis of one of the acyl chains esterified at the *sn*-1 or *sn*-2 position of PPG (Figure 2.6).

2.5.2 PagP-mediated metabolism of BMP to monoacylated phosphoglycerolphosphates

The negative ions at *m/z* 483.277 and 509.29 were also enriched (Figure 2.4C). The *m/z* 509.29 ion corresponds by exact mass and MS/MS to LPG (18:1) with *cis*-vaccenic acid esterified in the glycerol backbone. This is consistent with PagP utilizing PG as a donor for the palmitoyltransferase reaction by transferring palmitate esterified at the *sn*-1 position. The *m/z* 483.277 ion also corresponds to LPG (16:0) with palmitic acid in the glycerol backbone. Another likely explanation for the occurrence of this negative ion is the hydrolysis of one of the acyl chains esterified to BMP to produce LBMP (reverse LPG).

2.5.3 PPG accumulates in the membranes of EDTA-treated *Escherichia coli*.

The treatment of *E. coli* cultures with millimolar amounts of EDTA rapidly induces palmitoylation of lipid A by specifically activating the OM enzyme PagP (Jia *et al.*, 2004). A *pagP* mutant *E. coli* WJ0124 (MC1061 $\Delta pagP$) and its isogenic parent MC1061, carrying a *pagP* expression plasmid, were labelled with ^{32}P orthophosphate, cultured and induced with arabinose to over-express PagP under control of the pBAD promoter. Cells were briefly treated with EDTA to activate PagP. Equal counts of phospholipids extracted by single phase Bligh-Dyer, were resolved on silica gel 60 TLC plates using solvent system A and exposed to a PhosphoImager. The spot corresponding to PG is significantly diminished when cells over-expressing PagP are treated with EDTA compared with the lipid extracts from cells carrying the empty plasmid. This is consistent with PG being consumed to produce PPG when PagP is activated. Also expected was the accumulation of lysophospholipids as a byproduct of phospholipids being utilized as acyl donors for the palmitoyltransferase activity of PagP. A leading spot corresponding to PPG, with an R_f value higher than the major phospholipids PE, PG and CL also accumulates when PagP is over-expressed (Figure 2.7A).

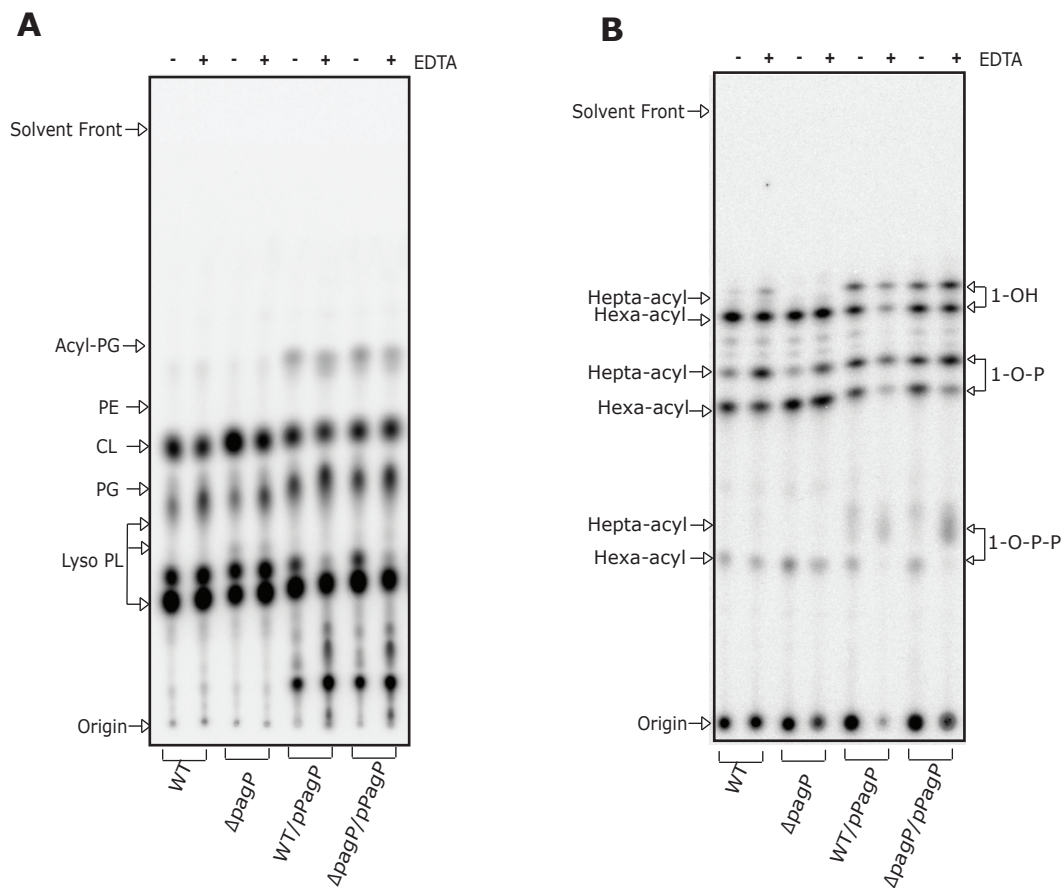


Figure 2.7 PPG accumulates in *E. coli* cells induced to overexpress PagP.

Thin layer chromatograms showing A) Phospholipids isolated from ^{32}P radiolabelled *E. coli* wildtype (MC1061) and ΔpagP (WJ0124) transformed with empty pBADGr or pPagP were resolved using CHCl_3 , MeOH, acetic acid (65:25:5 v/v) and B) Lipid A was labeled with ^{32}P and isolated from cells by mild acid hydrolysis. The lipid A isolates were separated by TLC using CHCl_3 , Pyridine, 88% Formic acid, dH_2O (50:50:16:5 v/v). The three species of lipid A that were identified previously by mass spectrometry (Zhou *et al.*, 1999) are indicated to the right of the figure and include the lipid A 1,4'-bisphosphate (1-O-P), the 1-pyrophosphate (1-O-P-P), and the 4'-monophosphate (1-OH). The hexa- and hepta-acylated derivatives of each lipid A species are indicated to the right of the chromatogram.

2.5.4 PPG is produced in the same active site that also palmitoylates lipid A

In the course of investigating the palmitoylation of PG, we also observed a notable increase in intensity of the spot corresponding to CL. To investigate this further we prepared a *pagP* knockout in a CL deficient strain called DIXC03. Again, cells were labeled with ^{32}P and treated with 25mM of EDTA to promote accumulation of PPG *in vivo*. When PagP was over-expressed in DIXC03, we observed the accumulation of an unknown lipid with an R_f value nearly identical to CL (Figure 2.8A, lane 3), in addition to the leading spot corresponding to the acyl-PG. Dalebroux *et al.* (2014) previously reported that moderate PhoQ activity prompted modest yet reproducible increases in CL by TLC, prompting us to consider the possibility that PagP could also function as a cardiolipin synthase (*cls*). However, lipids extracted from cells and analyzed with one-dimensional TLC and ESI-MS showed no detectable CL. The unknown lipid was identified as BMP based on its combination of retention time and m/z ratio.

We also generated two active site mutations to determine if PagP converts PG to PPG using the same cell surface active site involved in palmitoylation of lipid A. Mutations of S77 and Y87 were each cloned into the arabinose inducible pBADGr vector and transformed into DIXC03. The cell surface active site was inactivated with a S77A amino acid substitution; this mutant no longer produces hepta-acylated lipid A (Figure 2.8B).

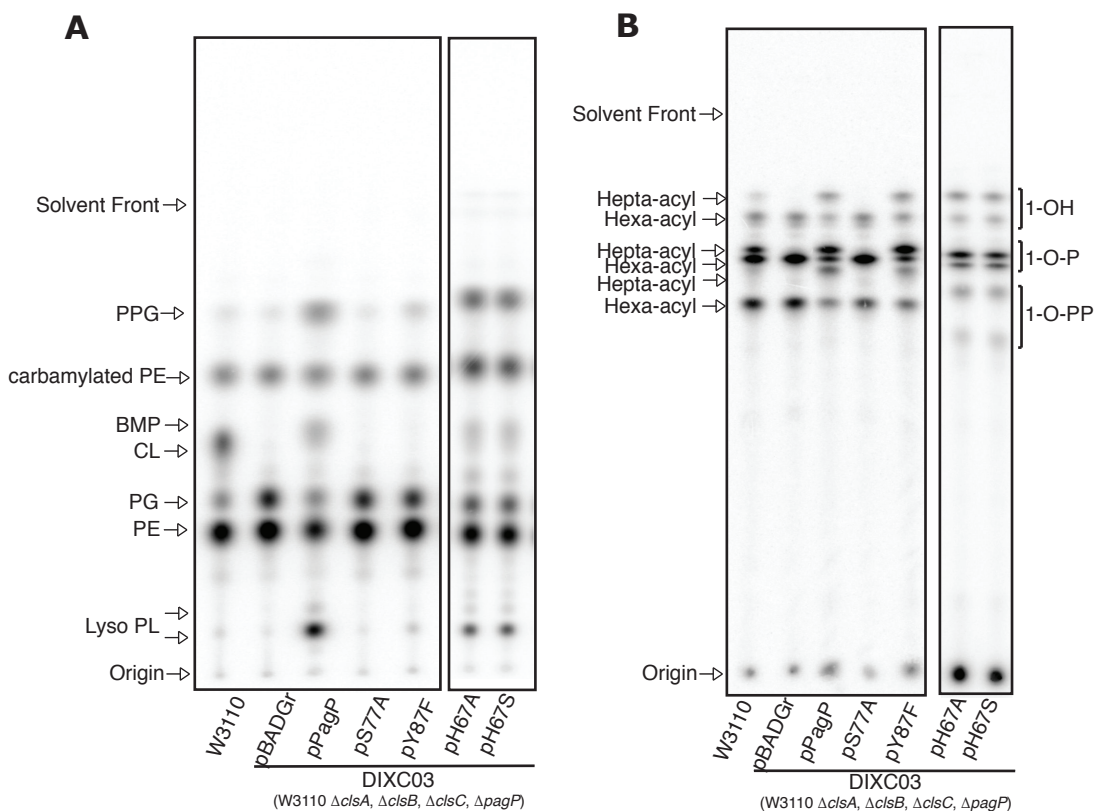


Figure 2.8. BMP accumulates in *E. coli* cells induced to overexpress PagP. Glycerophospholipids isolated from the cardiolipin deficient and *pagP* mutant strain DIXC03 (Δ pagP, Δ clsA, Δ clsB, Δ clsC) and its isogenic parent W3110. Thin layer chromatogram showing A) phospholipid composition profiles for *E. coli* DIXC03 over-expressing PagP and two of its active site mutants (S77A and Y87F). The S77A mutation in the cell surface active site does not accumulate PPG. In the Y87F mutant, residual PPG is evident, but BMP and LPG are absent. The H67A/S mutants have glycerophospholipid profiles similar to wild type enzyme. B) Lipid A proliferates for *E. coli* DIXC03 over expressing PagP and its active site mutants.

Table 2.3. Glycerophosphoglycerol species identified in WJ0124/pPagP

GPG molecular species	Molecular Formula [M-H] ⁺	Exact Mass [M-H] ⁺	Observed Mass [M-H] ⁺
PG			
28:1	C ₃₄ H ₆₄ O ₁₀ P ⁻	663.4243	663.432
28:0	C ₃₄ H ₆₆ O ₁₀ P ⁻	665.4399	665.445
30:1	C ₃₆ H ₆₈ O ₁₀ P ⁻	691.4556	691.459
30:0	C ₃₆ H ₇₀ O ₁₀ P ⁻	693.4712	693.475
31:1	C ₃₇ H ₇₀ O ₁₀ P ⁻	705.4712	705.472
32:2	C ₃₈ H ₇₀ O ₁₀ P ⁻	717.4712	717.475
32:1	C ₃₈ H ₇₂ O ₁₀ P ⁻	719.4869	719.491
33:2	C ₃₉ H ₇₂ O ₁₀ P ⁻	731.4869	731.491
33:1	C ₃₉ H ₇₄ O ₁₀ P ⁻	733.5025	733.506
34:2	C ₄₀ H ₇₄ O ₁₀ P ⁻	745.5025	745.506
34:1	C ₄₀ H ₇₆ O ₁₀ P ⁻	747.5182	747.519
35:2	C ₄₁ H ₇₆ O ₁₀ P ⁻	759.5182	759.51
35:1	C ₄₁ H ₇₈ O ₁₀ P ⁻	761.5338	761.530
36:2	C ₄₂ H ₇₈ O ₁₀ P ⁻	773.5338	773.538
37:2	C ₄₃ H ₈₀ O ₁₀ P ⁻	787.5495	787.524
Acyl PG			
42:0	C ₄₈ H ₉₂ O ₁₁ P ⁻	875.6383	875.645
44:2	C ₅₀ H ₉₂ O ₁₁ P ⁻	899.6383	899
44:1	C ₅₀ H ₉₄ O ₁₁ P ⁻	901.6539	901.653
46:2	C ₅₂ H ₉₆ O ₁₁ P ⁻	927.6696	927.673
46:1	C ₅₂ H ₉₈ O ₁₁ P ⁻	929.6852	929.684
48:2	C ₅₄ H ₁₀₀ O ₁₁ P ⁻	955.7009	955.698
48:1	C ₅₄ H ₁₀₂ O ₁₁ P ⁻	957.7165	957.718
48:0	C ₅₄ H ₁₀₄ O ₁₁ P ⁻	959.7322	959.7
49:2	C ₅₅ H ₁₀₂ O ₁₁ P ⁻	969.7165	969.721

Table 2.3 continues on next page

49:1	$C_{55}H_{104}O_{11}P^-$	971.7322	971.731
50:3	$C_{56}H_{102}O_{11}P^-$	981.7265	981.724
50:2	$C_{56}H_{104}O_{11}P^-$	983.7322	983.737
50:1	$C_{56}H_{106}O_{11}P^-$	985.7478	985.750
51:2	$C_{57}H_{106}O_{11}P^-$	997.7478	997.750
51:1	$C_{57}H_{108}O_{11}P^-$	999.7635	999.751
52:3	$C_{58}H_{106}O_{11}P^-$	1009.7478	1009.744
52:2	$C_{58}H_{108}O_{11}P^-$	1011.7635	1011.772
BMP			
30:1	$C_{36}H_{68}O_{10}P^-$	691.4556	691.469
30:0	$C_{36}H_{70}O_{10}P^-$	693.4712	693.459
32:2	$C_{38}H_{70}O_{10}P^-$	717.4712	717.471
32:1	$C_{38}H_{72}O_{10}P^-$	719.4869	719.492
32:0	$C_{38}H_{74}O_{10}P^-$	721.5025	721.506
33:2	$C_{39}H_{72}O_{10}P^-$	731.4869	731.494
33:1	$C_{39}H_{74}O_{10}P^-$	733.5125	733.512
34:2	$C_{40}H_{74}O_{10}P^-$	745.5025	745.508
34:1	$C_{40}H_{76}O_{10}P^-$	747.5182	747.519
36:2	$C_{42}H_{78}O_{10}P^-$	773.5338	773.542
LPG			
16:1	$C_{22}H_{42}O_9P^-$	481.2572	481.2593
16:0	$C_{22}H_{44}O_9P^-$	483.2728	483.2746
17cp	$C_{23}H_{42}O_9P^-$	495.2728	495.2733
18:1	$C_{24}H_{46}O_9P^-$	509.2885	509.2910
19cp	$C_{25}H_{48}O_9P^-$	523.3041	523.2996

*GPG species are denoted by the total number of carbons in the acyl chains:total number of unsaturations in the acyl chains. Abbreviations: cp, cyclopropane.

When compared to cells over-expressing wild-type PagP, the intensity of the leading spot corresponding to acyl-PG, was reduced to background levels in the S77A mutant (Figure 2.8A, lane 4). This suggests that PagP utilizes the same cell surface active site to palmitoylate lipid A and PG. The second mutation, a Y87F substitution, inactivates the putative periplasmic triad. Cells over-expressing the Y87F mutant continued to produce PPG and hepta-acylated lipid A. BMP was notably absent in both of these mutant constructs.

Negative-ion electrospray ionization mass spectrometry (ESI-MS) was performed on the phospholipid isolates from the cells treated with EDTA (Figure 2.9 and 2.10). The $[M-H]^-$ ions of each GPG phospholipid are reported in Table 2.3. The predominant $[M-H]^-$ ions in the 875-1015 a.m.u. range at m/z 875.639, 901.660, 926.726, 940.739, 957.720, 971.734, 985.750 and 1011.766 correspond by exact mass to the m/z expected for acyl-PG. The product ion spectrum of the ion at m/z 985.750 from the cellular phospholipid extract was identical to that seen for lipids produced in the *in vitro* assay (Figure 2.5A).

2.5.5 Identifying a substrate for the PagP periplasmic hydrolase motif.

In order to identify BMP, standard high performance liquid chromatography (HPLC) was used to separate the lipid extracts from DIXC03 cells over-expressing PagP prior to infusion into the MS (Figure 2.10) as

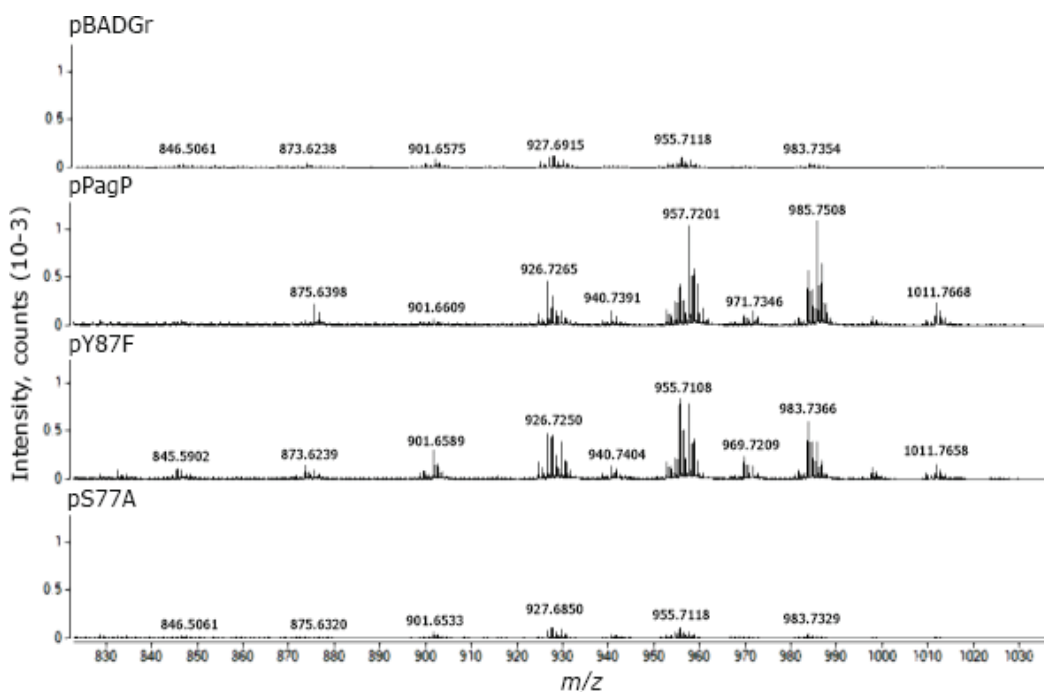


Figure 2.9. PPG accumulates in cell expressing PagP and the Y87F mutant, but not S77A. Negative-ion electrospray ionization mass spectrometry (ESI-MS) from m/z 830 to 1030 of the phospholipid analytes eluting at 8 minutes. The major $[M-H]^-$ ions correspond to acyl-PG molecular species as shown in Table 2.3. Phospholipids were isolated from *E. coli* WJ0124 transformed with pBADGr carrying PagP, the S77A or Y87F. The lipid extracts were separated by HPLC and analyzed by ESI-MS.

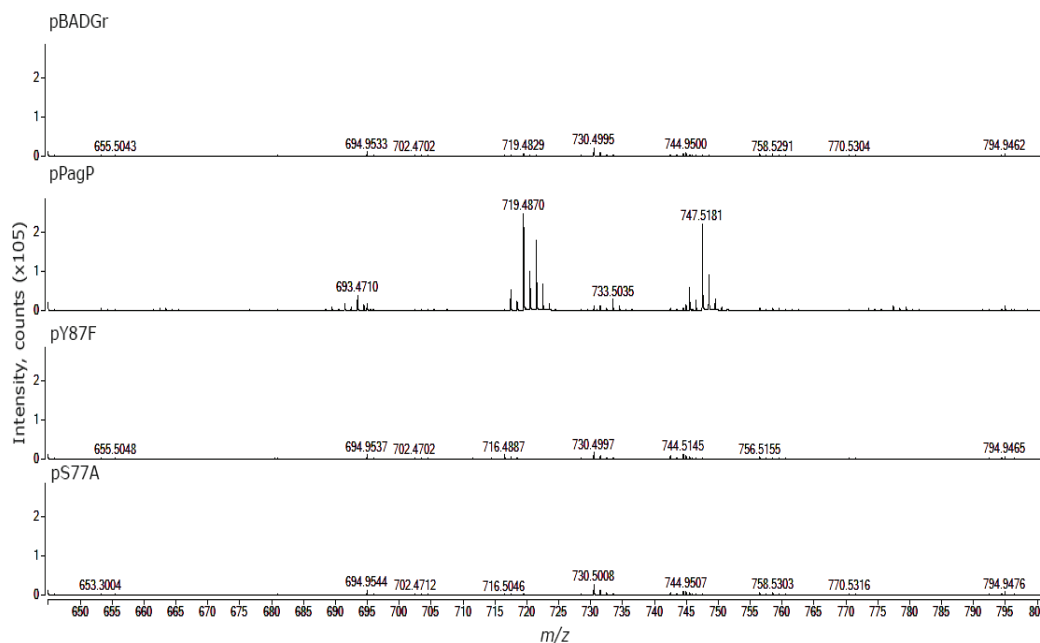


Figure 2.10. BMP accumulates in cells expressing PagP, but not the S77A or Y87F mutants. Negative-ion electrospray ionization mass spectrometry (ESI-MS) from m/z 650 to 800 of the phospholipid analytes eluting at 18 minutes. The major $[M-H]^-$ ions correspond to BMP molecular species as shown in Table 2.3. Phospholipids were isolated from *E. coli* WJ0124 transformed with pBADGr carrying PagP, the S77A or Y87F. The lipid extracts were separated by HPLC and analyzed by ESI-MS.

described previously (Garrett *et al.*, 2007). BMP elutes at 18 minutes, two minutes earlier than PG (Figure 2.11). The absence of accumulated BMP in cells over-expressing the active site mutants is revealing. The implication is that PPG instead of accumulating indefinitely in *E. coli*, is being converted to BMP by PagP. More specifically, PagP may function as a lipase and Y87 is somehow necessary for the conversion of PPG to BMP. The stereochemical configuration of the BMP formed in the experiments described above is not known. BMP formed from PPG is expected to retain the original 3-*sn*-glycerophospho-1'-*sn*-glycerol configuration (Figure 2.12).

We also investigated the role of H67 of the putative periplasmic triad by preparing serine and alanine substitution (Figure 2.8). The lipid profiles of both these mutants were unremarkably similar to wild-type PagP, suggesting that that H67 was not important for hydrolysis of PPG to produce BMP.

2.6 Discussion

High-resolution MS coupled to front-end chromatographic separation was used to identify PagP-catalyzed expansion of glycerophosphoglycerol phospholipids in *E. coli* OMs. It has previously been shown that PagP catalyzes the palmitoylation of PG to produce PPG (Dalebroux *et al.*, 2014). Here we report, for the first time, that PagP displays limited phospholipase activity for GPG phospholipids. PagP serially hydrolyzes PPG to BMP and LBMP as part of a novel lipid metabolic pathway. Moreover, we

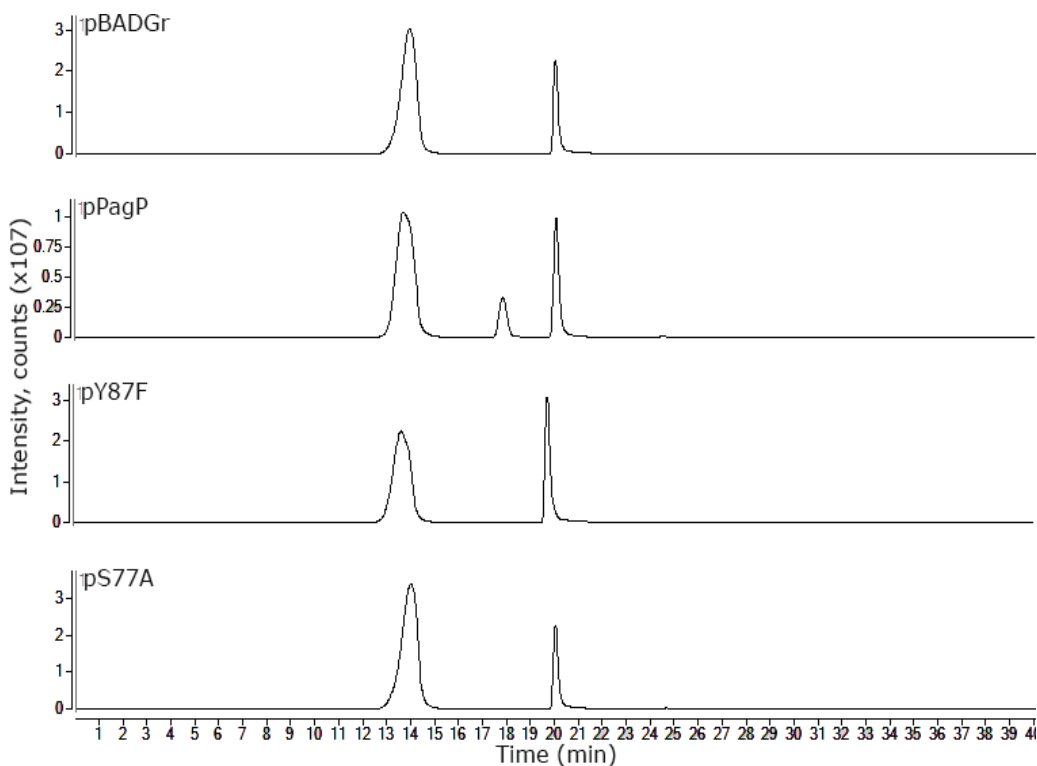


Figure 2.3 BMP and PG elute at different times by HPLC. LC chromatogram showing retention times for BMP and PG. The peaks at 18' and 20' correspond to BMP and PG, respectively. The peak at 14' is a reference peak and not relevant. Phospholipids were isolated from *E. coli* WJ0124 transformed with pBADGr carrying PagP, the S77A or Y87F. The lipid extracts were separated by HPLC prior to Negative-ion electrospray ionization mass spectrometry (ESI-MS) analysis (Figure 2.10)

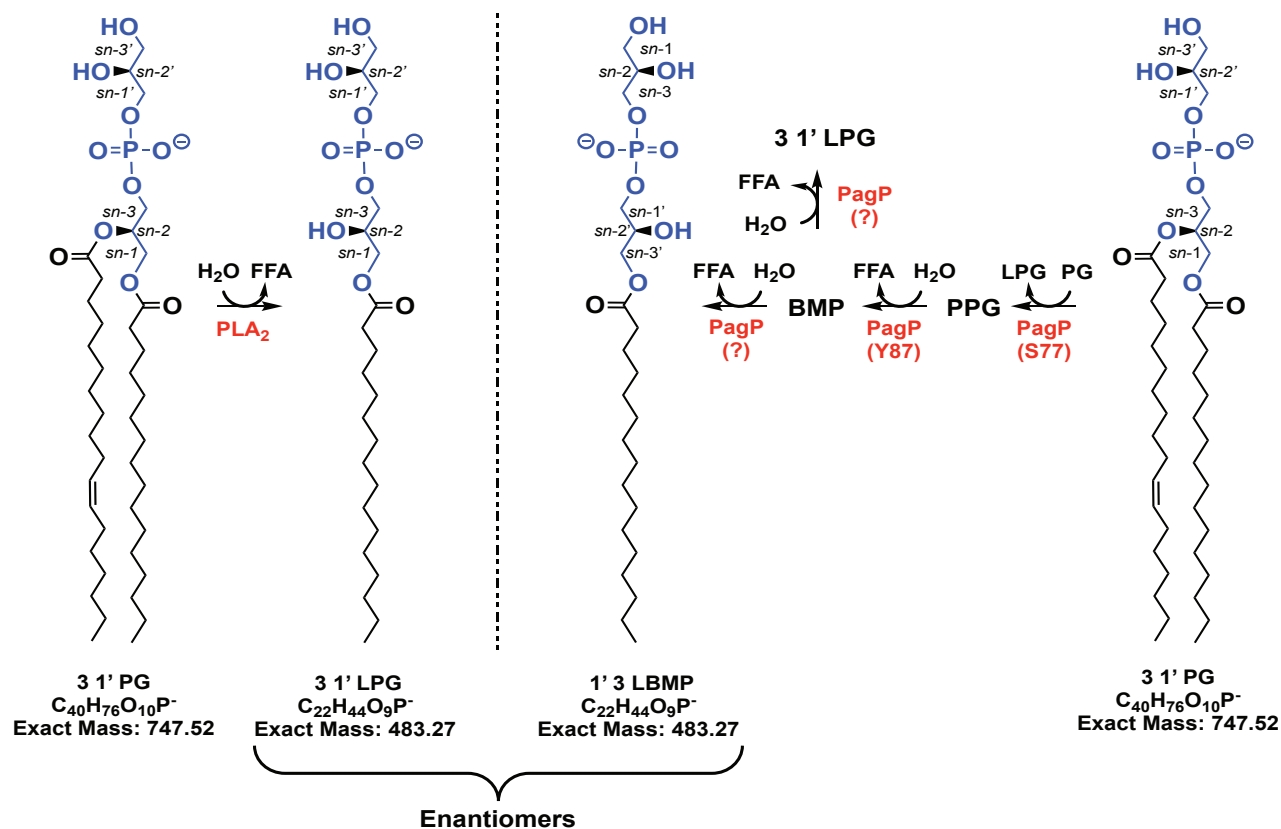


Figure 2.12. Proposed mechanism for expansion of glycerophosphoglycerols in *E. coli*. The first step (right to left), PagP removes the palmitate from position *sn*-1 of PG and transfers it to the *sn*-3' position of the head group glycerol moiety of another PG molecule to produce palmitoyl-PG (PPG) at the cell surface active site. The cell surface active site can be inactivated with a S77A amino acid substitution. In the second step, PagP function as a lipase and removes the palmitate at the *sn*-1 position of PPG to produce BMP. This is believed to occur in the inner leaflet of the outer membrane as Y87 is necessary for the conversion of PPG to BMP. The third step may lead to the formation of the stereospecific LBMP, which is the enantiomer of the LPG produced when a phospholipase A₂ (PLA₂) removes the fatty acid from position *sn*-1 of PG. The production of the stereospecific LBMP has yet to be adequately described but must involve removal of *cis*-vaccinate from position *sn*-2 of BMP.

identify PagP as a multifunctional enzyme with distinctly different active sites displayed on opposite sides of the outer membrane.

The over-expression of PagP in *E. coli* membranes promotes the accumulation of PPG; this occurs at the expense of PG. PG is found in almost all bacterial genera, representing 20-25% of the phospholipids in most Gram-negative bacteria (Cronan, 2003). It is estimated that ~31% of the total OM PG is palmitoylated at *sn*-3' during PhoP/PhoQ activation (Dalebroux *et al.*, 2014). We induced PagP expression in a PhoP/PhoQ-independent manner by cloning *pagP* into a plasmid vector under control of the arabinose inducible pBAD promoter. We observed an accumulation of acyl-PG and a depletion of PG. The severity of the depletion is likely the result of over-expressing PagP.

Importantly, there are two populations of acyl-PG. The IM acyltransferase PldB, synthesizes a triacylated product with a mixture of different acyl chain types at *sn*-3' (Hsu *et al.*, 1991) whereas the PagP product is exclusively palmitoylated (Dalebroux *et al.*, 2014). PagP is normally a latent enzyme, but it can be directly activated in the OM by lipid redistribution associated with the addition of millimolar EDTA to the cell culture (Jia *et al.*, 2004). Unlike PagP, PldB does not appear to be activated by EDTA as the intensity of the leading spot in the *pagP* mutant background did not vary with the addition of the chelator. The synthesis of acyl-PG by PldB thus appears to be independent of EDTA treatment. As such, despite co-migrating, the two

populations can be readily distinguished by the very specific method used to activate PagP. On this basis, we did not separate the inner and outer membranes.

The presence of BMP in the lipid extracts was not immediately apparent to us because BMP is a structural isomer of PG - both molecules have the exact same molecular formula. Even with high resolution MS, it is not possible to distinguish between diacylglycerophosphate molecules such as PG and BMP isoforms when the acyl chains total the same number of carbons and unsaturations (Garrett, 2017). The presence of BMP was also obscured by CL. BMP co-migrates with CL during TLC due to similar physical properties. The presence of BMP is immediately apparent by TLC in cardiolipin-deficient cells.

Gram-negative bacteria possess a highly conserved OM phospholipase A (OMPLA) that hydrolyzes ectopic phospholipids within the outer leaflet of the OM to maintain bilayer asymmetry (Malinverni and Silhavy, 2009). It has been argued that due to the broad specificity of OMPLA, it is unlikely that PagP functions as a phospholipase *in vivo* (Hardaway and Buller, 1979), although PagP exhibits slow phospholipase activity in the absence of a lipid A acceptor and various alcohols can substitute as acyl acceptors for lipid A *in vitro* (Khan and Bishop, 2009). Our data strongly suggests that PagP functions as a phospholipase and hydrolyzes PPG to BMP in the OM. TLC and MS indicate that palmitoylation of PG occurs on the cell surface and requires the same active site residue involved in the transesterification of lipid A. Cells that do not produce PPG do not accumulate BMP. We were unable to identify BMP in the

eluent during normal phase chromatography and the product ions generated from MS/MS of the ion at m/z 747.52 are consistent with PG. Our data further indicates that lipolysis of PPG occurs on the opposite facing periplasmic active site. The Y87F substitution prevents the release of BMP, despite the accumulation of PPG.

The periplasmic motif of PagP's crystal structure resembles the catalytic triad of the proteolytic enzyme chymotrypsin; the main difference is that the nucleophilic S195 in chymotrypsin is replaced by Y87 (Figure 2.5B), but geometric differences in the orientation of the imidazole and the carboxylate functional groups are also apparent. The putative periplasmic active site residues are organized like a catalytic triad and might enhance the nucleophilic character of Y87. No catalytic triad has ever been described to replace the nucleophilic serine with a tyrosine in a proteolytic enzyme; however we suspect in PagP that this novel catalytic triad functions instead as a lipase. If the motif that we have identified functions as a triad, we should be able to disrupt the charge relay by removing the imidazole of histidine, which acts as a general base. To test this hypothesis, we prepared a serine and alanine substitution of H67. Neither of these mutations affected the accumulation of BMP. While we have identified a substrate for the periplasmic motif, and it does appear to function as a hydrolase, it does not function as a triad.

BMP is highly enriched in eukaryotic lysosomes and endosomes. Eukaryotic BMP exhibits an unusual $sn1:sn1'$ structure different from the

sn3:sn1' configuration of its precursor, PG (Hullin-Matsuda *et al.*, 2009). The stereochemical configuration of the BMP formed in the experiments described above is not known. BMP formed from PPG might retain the original 3-*sn*-glycerophospho-1'-*sn*-glycerol configuration or it could give rise to a mixture of *sn3:sn1'*, *sn3:sn3'* or *sn1:sn1'*. There is precedent for inversion of the glycerol stereochemistry by the biosynthetic enzymes involved in BMP formation (Thornburg *et al.*, 1991).

While we were able to control the expansion of PPG into BMP, the results with the S77A mutant indicate that purified *E. coli* PagP palmitoylates PG to form PPG using the same active site involved in palmitoylation of lipid A. Naturally we are intrigued by the observation that certain residues critical for catalysis *in vivo*, are dispensable for activity *in vitro*. The reduced level of BMP in the Y87F mutant is consistent with the complete loss of BMP seen when this mutant was expressed in cells. To account for the residual BMP produced by Y87F *in vitro*, we propose that the cell surface active site can metabolize PPG to PG or BMP in the detergent micellar environment, but not in the restrictive lamellar phospholipid bilayer. If PPG is rapidly flipped to the inner leaflet of the OM after it first emerges in the external leaflet, then it would be able to avoid processing to BMP at the cell surface active site, thus expelling the dependence of Y87F *in vivo*. Our detergent-based assays do in fact suggest that the cell surface active can metabolize PPG to PG by transferring palmitate from the *sn*-3'-OH moiety of PPG to lipid A (Figure 2.9C). This may be important for

clearance of accumulated PPG and maintaining cellular lipid homeostasis. We also can't rule out the possibility that Y87 may be critical for flipase activity; without the restrictions imposed by the lamellar OM, Y87 is perhaps made redundant in the micellar environment.

PagP plays a crucial role in remodeling the OM by transferring a palmitate chain from a phospholipid to lipid A and PG during PhoPQ-regulated OM barrier remodeling (Bishop *et al.*, 2000; Dalebroux *et al.*, 2014). PagP is also activated by OM damage, which suggest the enzyme can function as a part of an acute OM stress response system. BMP and LBMP may be important intermediates of the lipolysis of PPG and could function as second messengers for lipid mediated signal transduction. In order to fully understand the functional significance of BMP, including the mechanism of biosynthesis in the cell, it is important to first determine the exact structure, including the stereochemistry.

2.7 Acknowledgement

We thank members of the Bishop laboratory and Dr. Teresa Garrett for helpful discussions and critical reading of this manuscript. We would also like to thank Dr. José Carlos Bozelli Junior for assistance with inorganic phosphate assays. This work was supported by CIHR Operating Grant MOP-84329.

Chapter 3

A divergent *Pseudomonas aeruginosa* palmitoyltransferase essential for cystic fibrosis-specific lipid A

Adapted from Molecular Microbiology, Vol. 91, Iyarit Thaipisuttikul, Lauren E. Hittle, Ramesh Chandra, Daniel Zangari, Charneal L. Dixon, Teresa A. Garrett, David A. Rasko, Nandini Dasgupta, Samuel M. Moskowitz, Lars Malmström, David R. Goodlett, Samuel I. Miller, Russell E. Bishop and Robert K. Ernst, A divergent *Pseudomonas aeruginosa* palmitoyltransferase essential for cystic fibrosis-specific lipid A, 158-174, Copyright 2014, with permission from John Wiley & Sons Ltd.

3.1 Author's preface

Prior to beginning my graduate studies, Dr. Robert Ernst (University of Maryland) identified the PhoP-dependent gene, *Pa1343*, as a candidate gene for phospholipid:lipid A palmitoyltransferase activity in *Pseudomonas aeruginosa*. The work presented in this chapter is focused on the identification and characterization of the elusive *P. aeruginosa* PagP enzyme. Under the auspice of Dr. Russell Bishop, Daniel Zangari (a summer student) and I expressed and purified PaPagP by adapting a preexisting procedure that is used for enterobacterial PagP. We also developed an *in vitro* assay using lipid IV_A, which made it possible for us to determine that the *Pseudomonas* PagP adds palmitate on the opposite glucosamine compared to that of *E. coli*. MALDI-TOF MS was used by Dr. Teresa Garrett to analyze the lipid products of the *in vitro* assay. The phylogenetic study (Figure 3.4), susceptibility assays (Figure 3.8) and cytokine stimulation (Figure 3.9) were performed by members of the Ernst Lab.

3.2 Abstract

Strains of *Pseudomonas aeruginosa* isolated from the airways of cystic fibrosis patients constitutively add palmitate to lipid A, the membrane anchor of lipopolysaccharide. The PhoPQ-regulated enzyme PagP is responsible for the transfer of palmitate from outer membrane phospholipids to lipid A. This enzyme has previously been identified in many pathogenic Gram-negative bacteria, but in *P. aeruginosa* had remained elusive, despite abundant evidence that its lipid A contains palmitate. Using a combined genetic and biochemical approach, we identified *Pa1343* as the *P. aeruginosa* gene encoding PagP. Although Pa1343 lacks obvious primary structural similarity with known PagP enzymes, the β -barrel tertiary structure with an interior hydrocarbon ruler appears to be conserved. *P. aeruginosa* PagP (PaPagP) transfers palmitate to the 3' position of lipid A, in contrast to the 2 position seen with the enterobacterial PagP. Palmitoylated *P. aeruginosa* lipid A alters host innate immune responses, including increased resistance to some antimicrobial peptides and an elevated pro-inflammatory response, consistent with the synthesis of a hexa-acylated structure preferentially recognized by the TLR4/MD2 complex. Palmitoylation commonly confers resistance to cationic antimicrobial peptides; however, increased cytokine production resulting in inflammation is not seen with other palmitoylated lipid A variants, indicating a unique role for this modification in *P. aeruginosa* pathogenesis.

3.3 Introduction

Gram-negative bacteria have double membranes; an inner membrane composed of a phospholipid bilayer partitioning the cytoplasm from the periplasm, and a complex outer membrane with an inner leaflet composed of phospholipids and an outer leaflet dominated by lipopolysaccharide (LPS). This structuring of membranes allows the bacteria to rely on the outer membrane to defend against environmental stressors and host derived factors through alterations in the composition of porin/proteins, lipids, and LPS (Needham and Trent, 2013; Nikaido and Vaara, 1985; Raetz *et al.*, 2007).

Lipopolysaccharide can be divided into three major constituents: O-antigen projecting from the cell surface, a conserved core oligosaccharide, and lipid A, which anchors LPS to the bacterial outer membrane. O-antigen is a polysaccharide with repeating oligosaccharide units of variable length and among the first bacterial cellular components to come into contact with the host upon infection; as such, it is critical for evading host defences, including phagocytosis and activated complement (Dasgupta *et al.*, 1994). The core oligosaccharide is composed of non-repeating sugar moieties linking O-antigen to lipid A. Core modifications contribute to the release of bacterial toxins (Horstman *et al.*, 2004), as well as porin incorporation within the membrane (Diedrich *et al.*, 1990). The hydrophobic portion of LPS, lipid A, plays a distinct role in innate immune system signaling and modulation (Curtis *et al.*, 2011;

Fujimoto *et al.*, 2013; Galanos *et al.*, 1985) as well as influencing outer membrane fluidity and permeability (Raetz *et al.*, 2007).

Lipid A remains a focus for study due in large part to its endotoxic properties leading to endotoxemia, localized tissue destruction, and septic shock. While the general structure of lipid A is conserved between Gram-negative bacteria, variations in the acyl chain number (4 to 7) and carbon length (10 to 18) are observed between species (Caroff *et al.*, 2002; Nikaido and Vaara, 1985); such variation contributes to the diversity in virulence seen within bacterial populations (Needham and Trent, 2013; Wilkinson, 1996). The ability to control lipid A variation in response to environmental cues further enhances virulence.

Many Gram-negative bacteria modify their lipid A through palmitoylation (addition of a saturated C16 fatty acid), which has the effect of altering host responses. Palmitoylation results in increased resistance to cationic antimicrobial peptides (CAMPs) (Raetz *et al.*, 2007; Trent, 2004) and alterations in the ability to stimulate innate immunity through toll-like receptor (TLR) 4-mediated responses (Alexander and Rietschel, 2001; Kawasaki *et al.*, 2004; Kong *et al.*, 2011).

The enzyme PagP was first shown to be responsible for palmitoylation of lipid A in enteric bacteria. The *pagP* gene was identified in *Salmonella* (Guo *et al.*, 1998) and its homologue in *Escherichia coli* was later purified from the outer membrane and shown to be a phospholipid::lipid A palmitoyltransferase

enzyme (Bishop, 2005; Bishop *et al.*, 2000). Homologues of PagP are found in *Bordetellae* (Preston *et al.*, 2004), *Yersinia* (Rebeil *et al.*, 2004), and *Legionella* (Robey *et al.*, 2001) and have been implicated in pathogenesis. Unlike most lipid A biosynthetic enzymes that require access to cytosolic substrates, PagP is located in the outer membrane, where it transfers palmitate from the *sn*-1 position of a phospholipid to the 2 position of lipid A (Bishop *et al.*, 2000).

Cystic fibrosis (CF) is the most common lethal autosomal recessive disease of Caucasians. In this disorder, chronic lung infections with *Pseudomonas aeruginosa* are strongly associated with disease progression and premature mortality (Davis *et al.*, 1996; Folkesson *et al.*, 2012). Our previous studies have demonstrated that one of the earliest known *P. aeruginosa* adaptations to the CF lung is the synthesis of a characteristic lipid A structure distinct from lipid A isolated from acute infection (blood, ear, eye and urinary tract), bronchiectasis (non-CF lung infections), or environmental isolates (Ernst *et al.*, 1999). The CF-specific lipid A structure differs from other lipid A species in the constitutive addition of palmitate (Ernst *et al.*, 2007; Ernst *et al.*, 1999; Miller *et al.*, 2011; Moskowitz *et al.*, 2004).

The constitutive expression of palmitoylated lipid A by *P. aeruginosa* isolated from CF patients with chronic lung infections indicates that this modification is critical to adaptation and survival within the CF lung (Moskowitz and Ernst, 2010). Although the enzyme responsible for this CF-specific modification has remained elusive, its characterization will be essential

in understanding *P. aeruginosa* early adaptation to the CF airway. Here, we report the identification of *Pa1343* (<http://www.pseudomonas.com>), a PhoP-dependent gene of unknown function (McPhee *et al.*, 2006), as the gene encoding the palmitoyltransferase enzyme PagP. We hypothesize that PagP dependent palmitoylation of lipid A mediates important adaptations of *P. aeruginosa* to host microenvironments, including increased resistance to antimicrobial peptides and alterations of host innate immune responses.

3.4 Materials and Methods

3.4.1 Bacterial strains and growth conditions

P. aeruginosa and other bacterial strains used during these studies are listed in Table S3.2. *P. aeruginosa* PAO1 strain was used for mutagenesis and subsequently served as the WT control. Bacterial cells for LPS or lipid A analysis were obtained after overnight growth with aeration in N-minimal medium (5 mM KCl, 7.5 mM (NH₄)₂SO₄, 0.5 mM K₂SO₄, 1 mM KH₂PO₄, 0.1 M Tris HCl, 0.1% w/v Casamino acids, 38 mM Glycerol) supplemented with either 1 mM (high or repressing) or 8 μM (low or inducing) MgCl₂, or in LB medium supplemented with 1 mM MgCl₂.

3.4.2 Recombinant DNA techniques

Restriction enzyme digestions, ligations, transformations, and DNA electrophoresis were performed as described by manufacturer's instructions. The

oligonucleotide primers used for DNA sequencing and PCR gene amplification were manufactured by Invitrogen and are listed in Table S3.3. Purification of genomic DNA and plasmids, PCR products, and restriction fragments were performed with the Qiagen kits, according to the manufacturer's instructions. DNA sequencing was performed at the University of Maryland core facility. Plasmids used in these studies are shown in Table S3.2.

We cloned *Pa1343* on pUCP19-USER vector using USER™ Friendly Cloning Kit (New England BioLab Cat. #E5500S). The resulting plasmids were electroporated into *Pseudomonas*. The transformants were then selected by 200 $\mu\text{g ml}^{-1}$ carbenicillin for *Pseudomonas*. The recombinant Pa1343 was expressed by induction with IPTG. For the clean knockout of *Pa1343*, a deleted fragment of *Pa1343* was amplified from genomic DNA by PCR with *Pfu* Turbo DNA polymerase (Invitrogen). The PCR fragment was then cloned in counter-selectable plasmid pEXGWD using Gateway Cloning system (Invitrogen). Briefly, the PCR fragment was first cloned on the Gateway-compatible vector pDONR201 using BP Clonase II (Invitrogen Cat. #11789-020). The resulting product was then introduced into *E. coli* DH5 α cells by heat shock, and the bacterial transformants were selected on plates containing kanamycin (50 $\mu\text{g ml}^{-1}$). The PCR fragment was subsequently introduced into the broad-host-range plasmid pEXGW-D using LR Clonase II (Invitrogen Cat. #11791-020). The plasmid was then introduced into PAO1 or PAK strain derivatives by 10 min electroporation protocol (Choi *et al.*, 2006). The resulting merodiploids were

formed via the integration of suicide plasmid by a single cross-over event. The merodiploid state was then resolved via sucrose selection in the presence of gentamicin, resulting in deletion of the WT gene.

For the generation of point mutations in Pa1343, a full-length *Pa1343* including 1 kb flanking sequence on both sides was amplified and cloned on pEXGW-D as described above. The plasmid then underwent site-directed mutagenesis by using QuikChange® XL Site-Directed Mutagenesis Kit (Stratagene Cat. #200516). The mutated plasmids were then transformed into PAO1 and counter selected as described above. The final genomic point mutations were confirmed by sequencing.

3.4.3 Lipid A extraction

For MS analysis, lipid A was extracted using the Caroff method (El Hamidi *et al.*, 2005). Briefly, bacteria were suspended in isobutyric acid and ammonium hydroxide (1M) solution ratio 5:3 (vol./vol.). The samples were incubated at 100°C for 1 h and centrifuged. The supernatant was collected in new tubes and diluted with equal volume water and lyophilized. The dry pellets were then washed with 100% methanol and finally extracted in chloroform-methanol mixtures.

3.4.4 MALDI-TOF MS analysis

Lipid A structures were assessed by negative-ion MALDI-TOF MS. Lyophilized lipid A was extracted in chloroform/ methanol and then 1 μ l was mixed with 1 μ l of Norharmane MALDI matrix. All MALDI-TOF experiments were performed using a Bruker Autoflex Speed MALDI-TOF mass spectrometer (Bruker Daltonics, Billerica, MA). Each spectrum was an average of 300 shots. ES tuning mix (Aligent, Palo Alto, CA) was used for calibration.

3.4.5 LPS extraction for GC

The rapid extraction of LPS was performed as described previously (Somerville *et al.*, 1996). Briefly, 10 mg bacterial cell pellet was suspended in 500 μ l of toxin free water and the equal amount of 90% phenol and incubated at 70°C for 1 h with constant shaking. The mixture was cooled on ice for 5 min and centrifuged at 9391 g for 10 min. The supernatant was collected in a new glass tube. The collected fraction was washed with diethyl ether two times by centrifugation at 845 g for 5 min. Finally, the lower phase containing LPS was collected and then lyophilized. For the GC, fatty acids were converted into methyl esters by methanolysis (2M HCl in methanol; Alltech, Lexington, KY) of dried LPS at 90°C for 18 h. The mixture was extracted twice with hexane before subjecting to GC using an HP 5890 series II with a 7673 autoinjector. Fatty acid methyl esters (Matreya bacterial acid methyl esters, CP mix no.1114)

and pentadecanoic acid (Sigma, St Louis, MO) were used as standard of a known fatty acid mixture and internal concentration control respectively.

3.4.6 Phylogenetic tree analysis

Phylogenetic tree analysis was done using the Geneious tree builder. The Cost Matrix Blosum62 was used with a Gap open penalty of 10 and a Gap extension penalty of 1. The global alignment was performed with free end gaps. Jukes-Cantor was used as the genetic distance model with the UPGMA tree build method and no out-group.

3.4.7 *P. aeruginosa* PagP structure and palmitate docking simulation

The Pa1343 sequence was uploaded to the I-TASSER (Roy *et al.*, 2010; Zhang, 2008) database which predicts secondary structure and models a 3D structure of the protein. The results of the simulation were visualized in PyMOL (PyMOL, Schrödinger, LLC). Docking simulations were performed using the Autodock/Autodock Vina (Seeliger and de Groot, 2010; Trott and Olson, 2010) plugins for PyMOL.

3.4.8 *P. aeruginosa* PagP enzymology

Plasmid pET21a-Pa1343 was constructed by cloning the 402 bp fragment carrying *Pa1343* without signal sequence from plasmid pUCP19-

Pa1343 into the IPTG-inducible T7-promoter expression vector pET21a(+), which was opened by *XhoI-NdeI* digestion. PCR gene amplification was performed with 5 U of *Taq* polymerase in a volume of 50 μ l of the supplied buffer with 150 ng of pUCP19-Pa1343 as template, 0.2 μ M of the appropriate primers (Forward: 5'-TATACATAT GGCCGACGGCGACTT-3' and Reverse: 5'-TATACTCGA GTCAGAGACGCAGGCCGA-3') and 10 μ M dNTPs. After initial denaturation for 1 min at 94°C, 33 cycles of 30 s at 94°C, 1 min at 53°C and 1.5 min at 72°C were performed, followed by 5 min at 72°C. The *XhoI-NdeI* digested PCR product that was amplified from pUCP19-Pa1343 was cloned into pET21a+ digested with the same enzymes to create plasmid pET21a-Pa1343. All cloned PCR products were subjected to double strand DNA sequencing at the McMaster University MOBIX Lab DNA Sequencing and Oligo Synthesis Facility to confirm the absence of any spurious mutations.

Escherichia coli BL21(DE3) cells were transformed with pET21a-Pa1343 and plated on LB agar plates with 100 μ g ml⁻¹ ampicillin. The plates were incubated at 37°C for 16-20 h and then stored at 4°C. A colony was selected from the plate and added to an overnight culture (10 ml LB with 0.1 mg ml⁻¹ ampicillin). The cultures were incubated for 16-20 h, and then added to a new 1 L culture (LB with 0.1 mg ml⁻¹ ampicillin). Cultures were grown at 37°C with shaking at 200 r.p.m. and induced with 1 mM IPTG at an OD₆₀₀ of 0.4 to 0.6. The cultures continued to grow for another 4 h at 37°C. The cells were centrifuged at 7500 g for 10 min, the LB was poured off, and pellet was stored

at -80°C . The cell pellet was then resuspended in 40 mL 50 mM Tris-HCl (pH 8) and 5 mM EDTA. The cells were then lysed in a Thermo French Press Cell Disrupter and centrifuged at 34 000 g for 20 min at 4°C . The supernatant was poured off and the pellet was resuspended in 24 mL 2% Triton X-100 and 50 mM Tris-HCl (pH 8) and then centrifuged at 34 000 g for 20 min at 4°C . The pellet was resuspended in 32 mL 50 mM Tris-HCl (pH 8) and centrifuged at 7600 g for 20 min at 4°C . The final pellet was resuspended in 20 mL 6 M guanidine-HCl with 50 mM Tris-HCl (pH 8) and centrifuged at 7600 g for 10 min at 4°C . The supernatant was collected and stored at 4°C . Samples were collected at each stage of the isolation and concentrations were determined using the BCA method (Smith *et al.*, 1985). Samples in 6M Guanidine-HCl and 10 mM Tris-HCl (pH 8) were dialysed against 4L water with stirring for 4 h, then the water changed and stirred overnight. The precipitated samples were centrifuged at 7600 g for 15 min and the water was poured off. The pellets were dissolved in 20 ml of 1% SDS, 1 M MPD (Sigma), and 10 mM Tris-HCl (pH 8) (Cuesta-Seijo *et al.*, 2010). The solutions were heated in a boiling water bath for 2 min, and allowed to return to room temp on the bench overnight. The samples were centrifuged at 7600 g for 20 min to remove any remaining precipitate. The liquid samples were collected and stored at 4°C . The concentrations were determined by measuring the absorbance using a molar extinction coefficient (ϵ) of $17210\text{ cm}^{-1}\text{M}^{-1}$.

The palmitoyltransferase *in vitro* assays are adapted from *Cuesta-Seijo et al.* (2010). Phosphatidylcholines and Kdo₂-lipid A were obtained from Avanti Polar Lipids, lipid IV_A was obtained from Peptides International (Louisville, KY), and dipalmitoyl-1-¹⁴C-DPPC was obtained from Perkin-Elmer. Briefly, the reactions were carried out in a final volume of 25 μL, with enough ¹⁴C-DPPC to obtain a final concentration of 20 μM. ¹⁴C-DPPC was dried by leaving the microcentrifuge tubes open to the air for 30 min. Lipid A was dried down under a stream of N₂(g) and dissolved in 22.5 μL reaction buffer [0.25% DDM, 100 mM Tris-HCl (pH 8), and 10 mM EDTA]. The activity buffer with lipid A was added to the microcentrifuge tubes and equilibrated for 30 min. Reactions were started by addition of 2.5 μL of *P. aeruginosa* PagP (25 ng total). As a control, phospholipase A₂ (PLA₂) was added to the first lane, but substituting CaCl₂ for EDTA in the reaction buffer. Reactions were run at 30°C for 1 h, at which point they were stopped by adding 12.5 μL of the reaction to 22.5 μL of 1:1 CHCl₃/MeOH. The bottom layer was then spotted (5 μL) on a silica gel 60 TLC plate. The TLC plates were developed for 2.5 h in CHCl₃:MeOH:H₂O (65:25:4 v/v) solvent system in a sealed glass tank. The plates were then exposed overnight to a PhosphorImager screen and developed the next day with a Molecular Dynamics Typhoon 9200 PhosphorImager. Non-radioactive dried lipid films were resuspended in CHCl₃:CH₃OH, (2:1 v/v) and analyzed by normal phase LC-ESI-Q-TOF and MS/MS as described previously (*Garrett et al.*, 2011).

[³²P]-lipid IV_A was prepared from *E. coli* BKT09 (provided by Pei Zhou, Duke University) (Table S3.2) by mild acid hydrolysis as described (Zhou *et al.*, 1998) followed by extraction from TLC plates. The dried ³²P-labelled lipids were dissolved in 100 μL of CHCl₃/MeOH (4:1 v/v) and spotted onto a TLC plate and developed in the solvent system CHCl₃/ pyridine/88% formic acid/H₂O (50:50:16:5 v/v). After drying, the plate was exposed to an X-ray film to locate the relevant lipid IV_A species. The desired compound was scraped off the plate and the silica chips were extracted with 5 ml of a single phase Bligh/Dyer mixture of CHCl₃ :MeOH:H₂O (1:2:0.8, v/v) at room temperature for 1 h. The suspension was centrifuged and the supernatant was passed through a glass Pasteur pipette fitted with a small glass wool plug. The flow-through was collected and converted into a two-phase Bligh/ Dyer mixture by adding 1.3 mL CHCl₃ and 1.3 ml MeOH, mixed thoroughly and partitioned by centrifugation. The lower phase containing [1,4' ³²P]-lipid IV_A was collected and dried under a stream of nitrogen. Assays were performed with [³²P]-lipid IV_A at ~ 100 cpm μL⁻¹, cold lipid IV_A at 100 μM, and phosphatidylcholines at 1 mM in 0.25% DDM, 100 mM Tris-HCl (pH 8), and 10 mM EDTA as described above.

3.4.9 Cytokine stimulation assay

Ninety-six-well plate (Corning Costar, Acton, MA) was seeded with 200 μL of 8 × 10⁴ cells ml⁻¹ of human monocytic THP-1 cells in Gibco RPMI 1640 (Invitrogen) supplemented with 10% Gibco heat-inactivated fetal bovine serum

(Invitrogen), 100 units ml⁻¹ penicillin/streptomycin and 50 nM vitamin D3 (Sigma, St Louis, MO). The cells were incubated at 37°C in the humid air with 5% CO₂ for 72 h for cells differentiation. For stimulation, purified LPS was resuspended in sterile water and followed by sonication. The LPS was diluted as needed in RPMI medium supplemented with 2% human serum and then added to the cell suspension. After 16 h incubation, the supernatant was harvested for IL-8 level measurement using Human CXCL8/IL-8 DuoSet ELISA kit (R&D systems, Minneapolis, MN Cat#DY208) according to the manufacturer's instruction. The highly purified LPS were extracted for this assay by the phenol-water method of Westphal and Jann was used (Westphal and Jann, 1965).

3.4.10 Susceptibility assays

A CAMP killing assay was used to test mutant strains of PAO1 for resistance to C18G, an α -helical CAMP derived from the COOH-terminus of the human platelet factor IV. Briefly, the overnight culture in N-minimal broth supplemented with 8 μ M MgCl₂ was diluted 1:40 and grown to an OD₆₀₀ of 0.07. Then the culture was further diluted 1:50, and 100 μ L was inoculated into a microtitre plate. The bacterial cultures were challenged with serial dilutions of C18G. After 2 h, the culture was diluted and plated on LB plate for counting the colony forming units (cfu) and calculating survival percentage. All experiments were done in triplicate. Conventional colistin agar dilution and alternative

polymyxin B sulphate plate assays, used to test mutant strains of PAK for resistance to the polymyxins, were performed as described (Miller *et al.*, 2011).

3.5 Results

3.5.1 Screening for the *P. aeruginosa* lipid A

palmitoyltransferase gene, *pagP*

To identify candidate genes with palmitoyltransferase activity, we used a variety of *in silico* analysis strategies including fold and function assignment system (FFAS) profiling, multiple sequence alignments, and transmembrane prediction. Initially, we used FFAS03 (Jaroszewski *et al.*, 2005) to identify genes of interest. For further analysis, profiles were created for all *P. aeruginosa* genes encoding open reading frames shorter than 300 amino acids, as PagP in other bacteria were approximately 160-180 amino acids in length. A profile for the 1THQ structure of *E. coli* PagP crystallized from LDAO was matched against each *P. aeruginosa* protein (e.g. using BLOSUM substitution matrixes), FFAS profiles were then constructed from 1THQ and this profile was searched against the *P. aeruginosa* profiles, generating 23 potential hits. Based on this information, we further identified the putative transmembrane spanning regions of these proteins. Utilizing the multiple sequence alignments algorithm (DAS - <http://www.sbc.su.se/~miklos/DAS/>), a unique pagP profile having the *S. Typhimurium*, and *E. coli* sub-species enzymes as representative examples, produced a pattern with two increases in DAS profile score at either end of the

sequence and three smaller increases in the middle (Fig. S1). Curves are obtained by pairwise comparison of the proteins in the test set in ‘each against the rest’ fashion. Two cut-offs are indicated on the plots, a strict one at 2.2 DAS score, and a loose one at 1.7. The horizontal solid line (strict cut-off) and dashed line (loose cut-off) indicates the number of matching segments and the actual location of the transmembrane segment respectively. Using this information, twenty-three transposon mutants from the University of Washington two-allele transposon mutant library, (<http://www.genome.washington.edu/UWGC/pseudomonas/index.cfm>) were obtained and screened for loss of palmitoyltransferase activity.

3.5.2 Matrix-assisted laser desorption ionization-time of flight (MALDI-TOF) lipid A analysis reveals loss of palmitoyltransferase activity in strains with mutations in *Pal343*

Individual transposon insertion mutants were grown under PhoPQ-activating conditions shown (low magnesium - 8 μ M) and screened by MALDI-TOF mass spectrometry (MS) for lipid A lacking palmitate, as compared with the wild-type (WT) strain, PAO1. A single mutant that contained a transposon insertion in the gene *Pal343* lacked the characteristic ion peak seen upon PagP induction by magnesium limitation. *P. aeruginosa* lipid A is a β -(1',6)-linked glucosamine disaccharide substituted with phosphate groups at the 1 and 4' positions (Figure 3.1). Primary fatty acyl chains include amide-linked R-3-

hydroxylaurate at the 2 and 2' positions and ester-linked *R*-3-hydroxydecanoate at the 3 and 3' positions. Secondary fatty acyl chains include the acyloxyacyl additions of laurate to the 2' position (m/z 1418), and of *S*-2-hydroxylaurate to the 2 position (m/z 1616). Deacylation of the *R*-3-hydroxydecanoate at the 3 position is also seen in the majority of *P. aeruginosa* strains (m/z 1446). *P. aeruginosa* isolated from individuals with CF pulmonary disease synthesize lipid A palmitoylated at the 3' position, resulting in a hexa-acylated structure (m/z 1684) (Ernst *et al.*, 2007). To confirm Pa1343 was the PagP enzyme in *P. aeruginosa*, a clean deletion of the *Pa1343* was constructed using standard allelic exchange techniques (Invitrogen Gateway Technology) and confirmed by sequencing. WT (PAO1), $\Delta pagP$ and $\Delta pagP+Pa1343$ driven off the pUCP19 plasmid were grown in inducing (low magnesium) and non-inducing conditions (high magnesium - 1 mM) followed by lipid A isolation and analysis by MALDI-TOF MS. All strains were able to synthesize the lipid A species corresponding to the major peak m/z 1446 (penta-acylated) and the minor species at m/z 1616 (non-palmitoylated hexa-acylated). Each of these peaks shows a neighbouring peak with a m/z difference of +16, indicating an additional hydroxylation of the laurate at the 2' position. Upon magnesium-limited growth of WT, palmitoylation observed at the 3' hydroxydecanoate of the penta-acylated lipid A results in additional peaks m/z 1684 (one hydroxylaurate) and m/z 1700 (two hydroxylaurates) (Figure 3.2A and B).

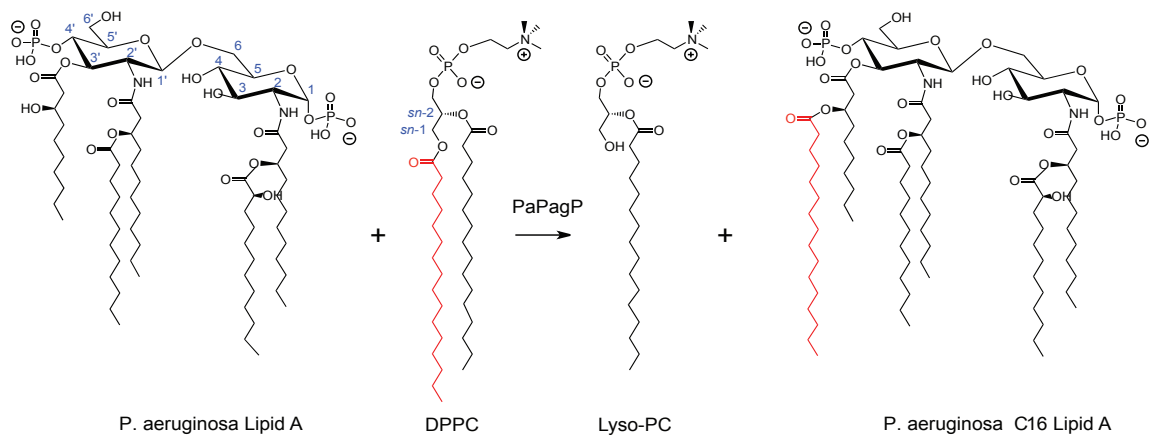


Figure 3.1 *Pseudomonas* lipid A palmitoylation by PagP. Predominant lipid A species isolated from WT under non-inducing conditions. PaPagP transfers palmitate from the *sn*-1 position of a phospholipid to position 3' of lipid A.

The $\Delta pagP$ mutant strain did not show any palmitoylated lipid A species under either inducing or non-inducing conditions (Figure 3.2C and D). Overexpression of *pagP* in the $\Delta pagP+Pal343$ strain resulted in palmitoylated species under both inducing and non-inducing conditions. Additional species *m/z* 1854 and *m/z* 1870 under magnesium limited conditions indicate the retention of the 3-hydroxydecanoate at the 3 position (Figure 3.2E and F) resulting in the synthesis of a hepta-acylated lipid A species. Electrospray ionization (ESI) tandem MS was performed to confirm the addition of palmitate at the 3' position. A summary of all structures and corresponding peaks can be found in Table S3.1.

3.5.3 Gas chromatography (GC) analysis of lipid A confirms *Pal343* is necessary for addition of palmitate

Gas chromatography analysis of lipid A was performed to confirm that *Pal343* is required for the addition of palmitate in *P. aeruginosa*. WT, $\Delta pagP$, and $\Delta pagP+Pal343$ strains were grown in inducing conditions and analyzed by GC with flame ionization detection. Total fatty acids were isolated and quantified against a C15 internal standard. Evaluation of the total fatty acid composition of WT lipid A showed an incorporation of 8% palmitate. No incorporation of palmitate was seen in the $\Delta pagP$ strain, as was indicated by MS results. Palmitoyltransferase activity was restored after complementation of the gene in trans with palmitate making up 11% of the total fatty acids of lipid A

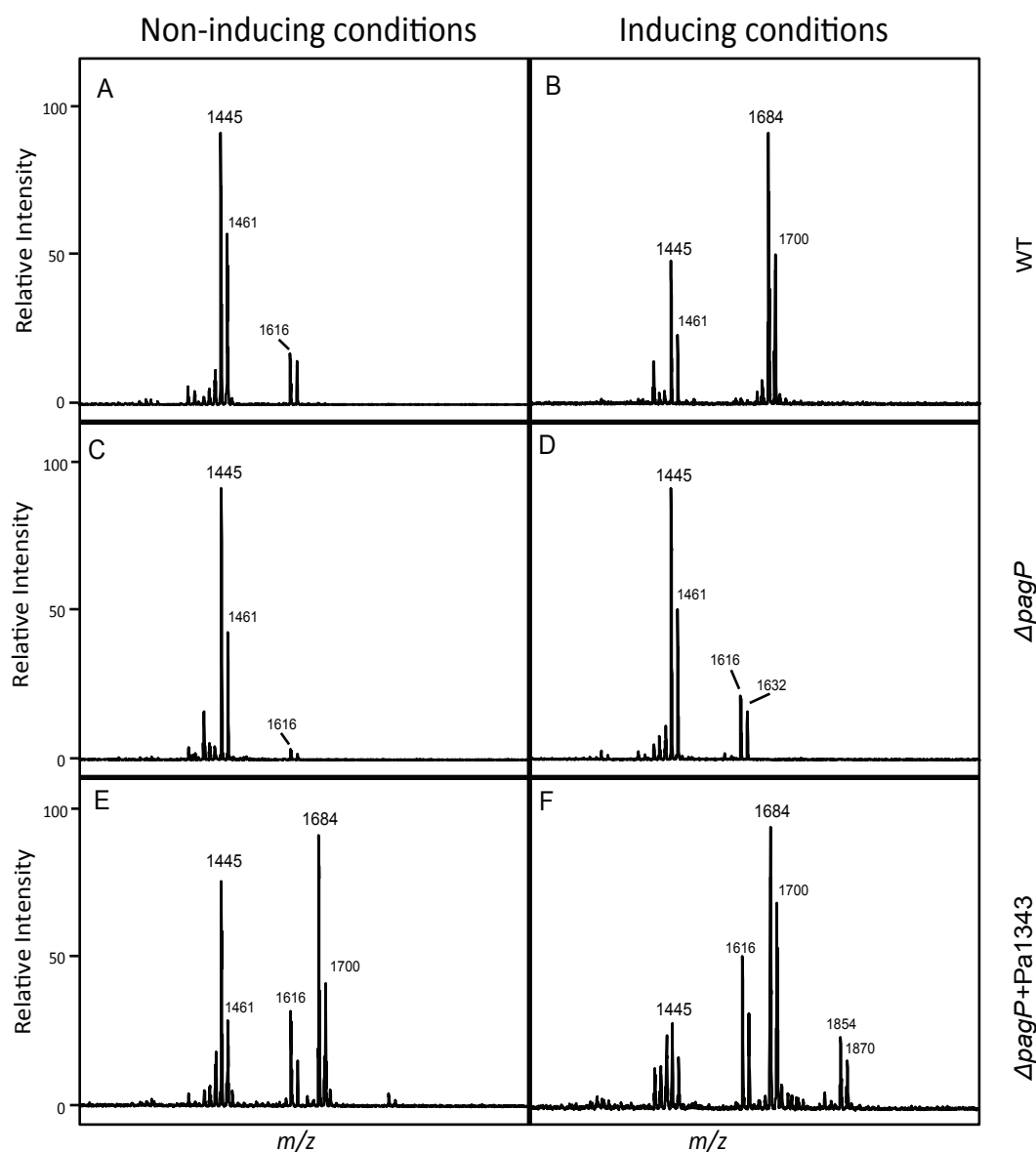


Figure 3.2. Pa1343 is required for palmitoylation. A and B) Lipid A was isolated from WT under inducing and non-inducing conditions. Inducing conditions resulted in hexa-acylated lipid A containing palmitate m/z 1684. C and D) $\Delta pagP$ did not produce palmitoylated lipid A under non-inducing or inducing conditions. E and F) PagP activity was restored in the $\Delta pagP$ +PA1343 strain when grown under both inducing and non-inducing conditions. Peaks present at m/z 1684 and m/z 1854 correspond to the palmitoylated hexa- and hepta-acyl lipid A, respectively.

(Figure 3.3). Taken together the data strongly indicates Pa1343 acts as PagP in *P. aeruginosa*.

3.5.4 Sequence analysis of the *P. aeruginosa* pagP gene and protein indicates *P. aeruginosa* PagP is unique among PagP enzymes

After successful identification of the *P. aeruginosa* pagP gene, a phylogenetic tree was constructed to determine the evolutionary relatedness between *P. aeruginosa* pagP and pagP homologues in other Gram-negative pathogens. These results demonstrate that the pagP sequences from *E. coli*, *Yersinia*, *Salmonella*, and *Bordetella* subspecies, grouped together indicating these pagP genes derived from a common ancestor (Figure 3.4A blue box). In contrast, pagP genes identified in the Pseudomonads clustered loosely together with a separate and distinct cluster containing the *P. aeruginosa* pagP genes (Figure 3.4A red box). This separation indicates *P. aeruginosa* pagP has dramatically diverged to the point of no longer being comparable to the known PagP sequences. A previous structural alignment of PagP enzymes in *E. coli*, *S. Typhimurium*, *Erwinia chrysanthemi*, *Yersinia pestis*, *Photobacterium luminescens*, *Legionella pneumophila*, and *B. pertussis* resulted in strong sequence alignment between all species (Ahn *et al.*, 2004). Alignment of *P. aeruginosa* PagP with *Salmonella* and *E. coli* PagP enzymes showed little indication that these proteins were similar at the protein level (Figure 3.4B). The

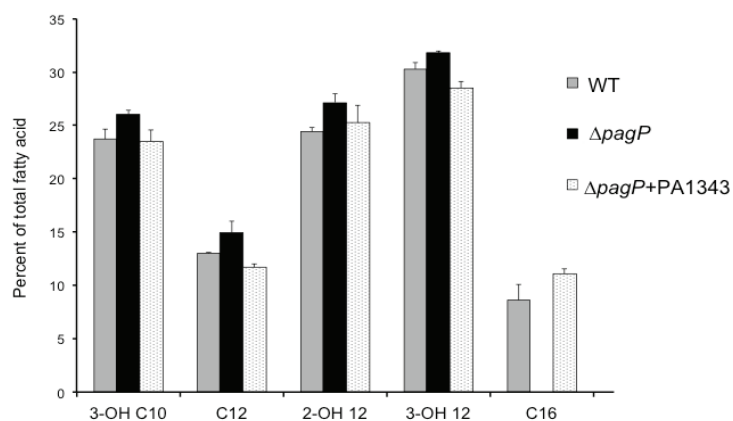


Figure 3.3. GC analysis of total fatty acid content of lipid A isolated from WT (white bars), $\Delta pagP$ (black bars) and $\Delta pagP+Pa1343$ (grey bars). Complete loss of C16 is seen in $\Delta pagP$. C16 incorporation was restored in the complemented strain. Results represent three biological replicates.

E. coli PagP protein aligned with the translated *P. aeruginosa* PagP sequence shows an identity of 24% (BLAST). *P. aeruginosa* PagP aligned with *S. Typhimurium* PagP showed 21% identity, while *E. coli* compared with *Salmonella* resulted in 75% identity (Figure 3.4B).

3.5.5 *P. aeruginosa* PagP purification and detergent dependence of its enzymatic activity

Experimental evidence provides support for the presence in *P. aeruginosa* PagP of a hydrocarbon ruler to incorporate only a C16 fatty acid into *P. aeruginosa* lipid A because the enzyme appears to exclude acyl chains longer and shorter than palmitate, which are abundantly present in the cellular phospholipid pool. Despite the low overall sequence similarity, a procedure for purification and folding of *E. coli* PagP (Cuesta-Seijo *et al.*, 2010) served to produce purified and enzymatically active *P. aeruginosa* PagP (Figure 3.5A). A strikingly similar profile of detergents that either support or inhibit enzymatic activity of *P. aeruginosa* PagP and *E. coli* PagP was observed (Figure 3.5B). Since detergents that effectively mimic the structures of fatty acyl chains are *E. coli* PagP competitive inhibitors, only detergents with bulky substituents that sterically preclude their binding within the hydrocarbon ruler are able to support the lipid A palmitoyltransferase reaction (Khan *et al.*, 2010a; Khan *et al.*, 2010b). As shown in Figure 3.5B, phospholipase activity for both *P. aeruginosa* PagP and *E. coli* PagP is preserved with Triton X-100, DDM, or Cyfos-7

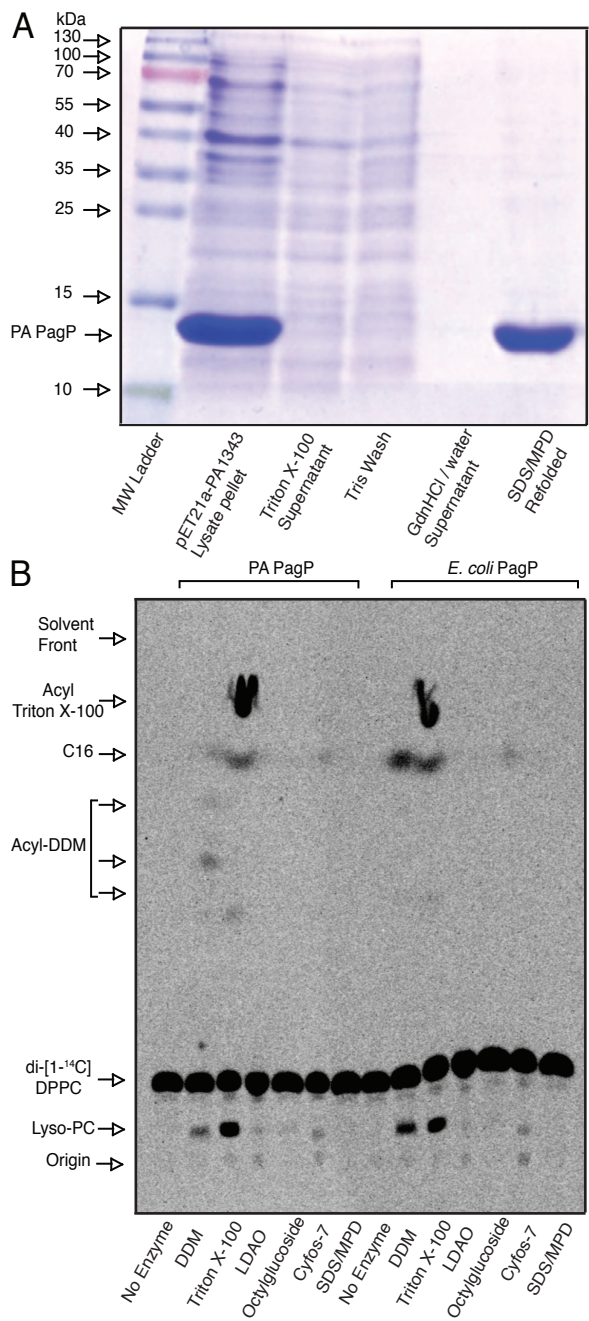


Figure 3.5 Detergent dependence and sensitivity of *P. aeruginosa* and *E. coli* A) SDS-PAGE assessment of PaPagP purification by selective precipitation. Forty microgram of protein from cell lysate pellet and refolded PaPagP samples were resolved with similar volumes of wash material and stained with Coomassie Blue dye. B) Thin layer chromatogram showing phospholipase activity in the absence of lipid A acceptors. Phospholipase activity is associated with production of free palmitate (C16) and Lyso-PC from DPPC in the presence of dodecylmaltoside (DDM), Triton X-100, and Cyfos-7. LDAO (lauryldimethylamine-N-oxide); SDS/MPD (mixture of SDS and 2,4-methyl-2-pentanediol).

in decreasing order of specific activity. In each case, Triton X-100 participates as a substrate in the palmitoyl-transferase reaction. Although DDM is the preferred detergent for *E. coli* PagP because it readily supports activity without participating as a substrate (Khan *et al.*, 2007), trace amounts of DDM appear to be acylated by *P. aeruginosa* PagP. Both enzymes appear to slowly utilize Cyfos-7 as a supporting detergent without it participating as a substrate. LDAO, octylglucoside, and SDS/MPD are all detergent systems that support PagP folding, but without supporting activity due to competitive detergent inhibition. The overall similarity in the detergent-activity relationships strongly supports common structure-function relationships between *P. aeruginosa* PagP and *E. coli* PagP.

3.5.6 Regiospecificity of lipid A palmitoylation by *P.*

aeruginosa PagP

To compare the phospholipid:lipid A palmitoyltransferase activity of *P. aeruginosa* PagP and *E. coli* PagP, we monitored palmitoylation of lipid IV_A and *E. coli* Kdo₂-lipid A (Figure 3.6). Whereas *E. coli* PagP could palmitoylate both substrates, *P. aeruginosa* PagP could only palmitoylate lipid IV_A, consistent with the available regiospecificities for palmitoylation at the 3' position in *P. aeruginosa* PagP and for the 2 position in *E. coli* PagP; both these positions are free in lipid IV_A while only the latter is free in Kdo₂-lipid A. In order to determine the location of the palmitate added to lipid IV_A, the *in vitro*

lipid IV_B and lipid IV_B' products (Figure 3.6B) generated by *E. coli* PagP and *P. aeruginosa* PagP, respectively, were analyzed using liquid chromatography ESI quadrupole TOF (LC-ESI-Q-TOF) MS. The expected product was readily detected in both the negative ([M-H]⁻, *m/z* 1642.076) and positive mode ([M+H]⁺, *m/z* 1644.091), and eluted at ~ 50.5 min. Collision induced dissociation MS (MS/MS) was performed on the [M⁺H⁺]⁺ ion to determine the location of the added palmitate. MS/MS analysis of the [M⁺H⁺]⁺ generated from *E. coli* PagP yielded an oxonium product ion (referred to as the B⁺¹ ion) (Costello and Vath, 1990; Que *et al.*, 2000; Qureshi *et al.*, 1983; Raetz *et al.*, 1985) with a *m/z* of 694.420 consistent with the palmitate being added to an acyl chain of the proximal glucosamine (Figure 3.6C). The ion at *m/z* 596.443 corresponds to the B⁺¹ ion having lost the 1-phosphate. In contrast MS/MS analysis of the [M⁺H⁺]⁺ generated from the *P. aeruginosa* PagP yielded a B⁺¹ ion with a *m/z* of 932.647 consistent with the palmitate being added to an acyl chain of the distal glucosamine (Figure 3.6C). The ion at *m/z* 834.668 corresponds to the B⁺¹ ion having additionally lost the 1-phosphate. In addition, product-ions corresponding to the loss of the palmitate from B⁺¹ (with or without the 1-phosphate) at *m/z* 676.411 and 578.434 respectively are readily detected in the *in vitro* product generated using the *P. aeruginosa* PagP. Taken together, these results verify that the purified *E. coli* and *P. aeruginosa* PagP enzymes palmitoylate lipid IV_A on the proximal and distal glucosamine units, respectively.

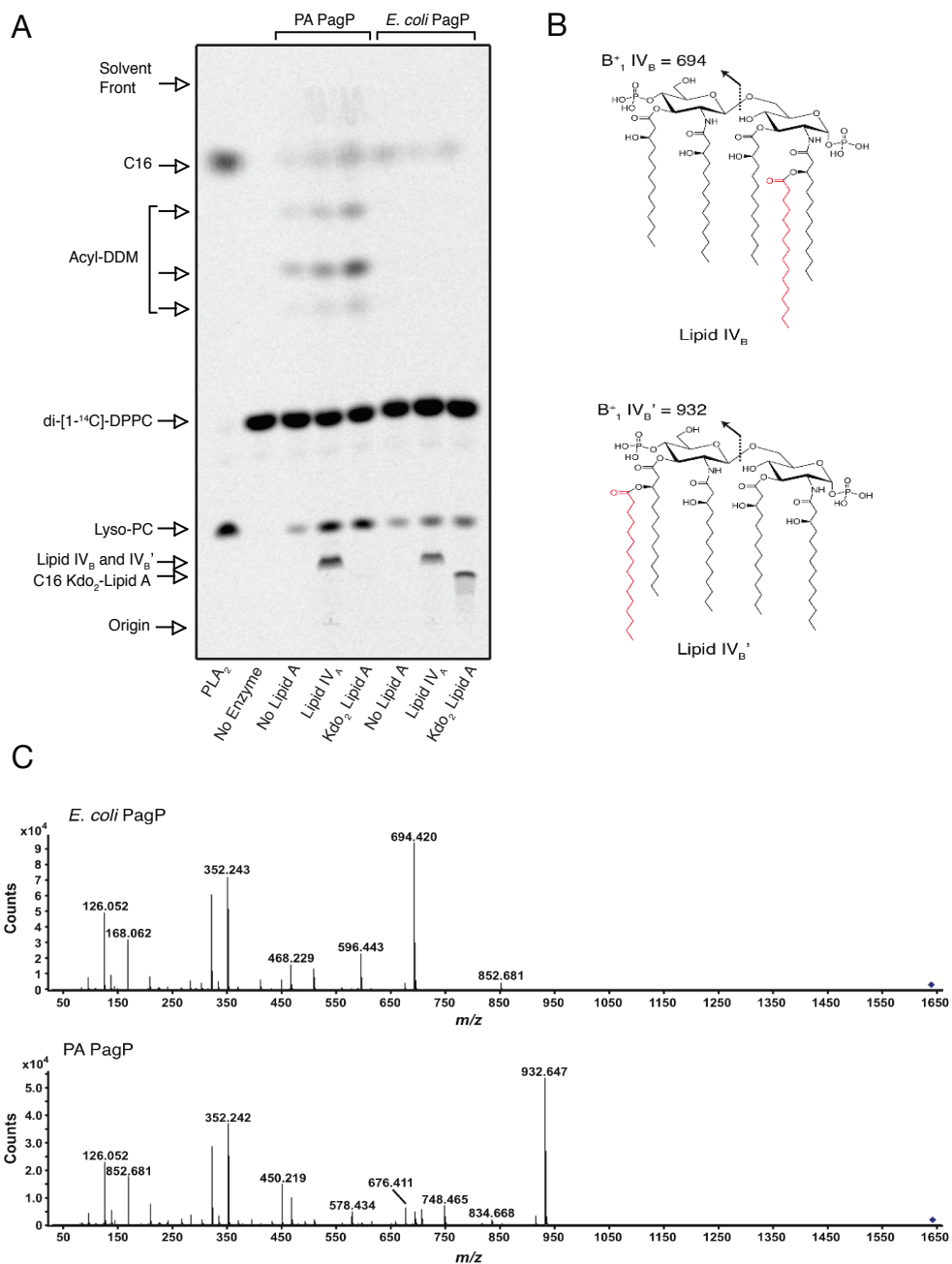


Figure 3.6 Regiospecificity of phospholipid::lipid A palmitoyltransferase activity. A). Thin layer chromatogram as described in Figure 3.5B using DDM, but showing palmitoylation of 100 μ M lipid IV_A and Kdo₂-lipid A to produce lipid IV_B, lipid IV_B'', and C16-Kdo₂-lipid A. B) Structure of lipid IV_B and lipid IV_B''. C) MS/MS performed on the [M+H]⁺ lipid IV_B and lipid IV_B''. *P. aeruginosa* and *E. coli* PagP reveal distinctly different B₁ ions (exact masses 932.6586 and 694.4290 daltons), characteristic of palmitoylation on the distal and proximal lipid A glucosamine units respectively.

3.5.7 His35 is necessary for *P. aeruginosa* PagP

palmitoyltransferase activity

Once the PagP activity and regiospecificity of *P. aeruginosa* PagP had been established, we focused on identifying the amino acid residues critical for activity. His33, Asp76 and Ser77 are highly conserved among characterized PagP enzymes (*E. coli* and *Salmonella*) and are thought to make up the enzymatic catalytic site (Hwang *et al.*, 2002). These residues are seemingly duplicated at residues His42 and His45, Asp84 and Asp86, and Ser85 and Ser87 in *P. aeruginosa* PagP. An additional histidine, His35, was also found in *P. aeruginosa* PagP and may also be important for enzyme function. In order to pinpoint which of the indicated amino acids were critical for activity, each of the sites were mutated to uncharged and hydrophobic amino acids. Mutations were made by introduction of the suicide plasmid pEXGWD resulting in the following amino acid substitutions: H35F, H35N, H42F, H42N, H45F, H45L, H45N, D84A, D84N, S85A, S85G, D86A, D86N, S87A, S87G and DSDS-AGNA (D84A, S85G, D86N, S87A). All mutants were grown under inducing conditions and LPS was prepared for MALDI-TOF analysis (Caroff *et al.*, 1988; El Hamidi *et al.*, 2005). Alterations of His45, Asp84, Asp86, Ser85 or Ser87 alone did not alter protein function as evaluated by the presence of a peak at m/z 1684. Function was retained even after replacement of all four aspartic acid and serine residues. In contrast, mutation of the His35 rendered *P. aeruginosa* PagP non-functional (Table 3.1). Based on this analysis, we demonstrated that

catalytic activity of *P. aeruginosa* PagP is dependent on His35 without the additional residues implicated in *E. coli* PagP function, suggesting that the distinctly different regiospecificities of these two enzymes might affect distinctive arrangements of catalytic residues.

3.5.8 *P. aeruginosa* PagP structural model and hydrocarbon ruler

In order to visualize the *P. aeruginosa* PagP protein structure, its sequence was uploaded to the I-TASSER online protein structure and function predictions tool. This system uses threading, where the sequence and predicted secondary structure of the protein are matched with solved structures in the Protein Data Bank (PDB) library to identify the best templates. The I-TASSER program then splits the sequence into fragments based on the template alignments, which are then reassembled to full-length models. Finally, hydrogen bonding networks are optimized and steric overlaps are removed (Roy *et al.*, 2011). Interestingly, five of the top 10 template structures used by I-TASSER from the PDB were of PagP, and the top template was PagP crystallized in SDS/MPD (Cuesta-Seijo *et al.*, 2010). We then used the Autodock/Autodock Vina (Seeliger and de Groot, 2010; Trott and Olson, 2010) PyMOL plugins, to run a docking simulation with palmitate (Seeliger and de Groot, 2010). The results of the simulation in Figure 3.7A and B show the mesh representation of *P. aeruginosa* PagP with palmitate docked in the interior hydrophobic pocket

reminiscent of the *E. coli* hydrocarbon ruler. Hydrophobic residues on the exterior of the protein are located where they would be embedded in the membrane, while the hydrophilic portions are at the expected solvent-exposed membrane interface regions. The terminal six methylene units of the palmitate chain maintain van der Waals contacts with the *E. coli* hydrocarbon ruler (Khan *et al.*, 2010b) and a similar interaction is apparent in *P. aeruginosa* PagP (Figure 3.7A and B). To validate the presence of a hydrocarbon ruler in *P. aeruginosa* PagP, we prepared [³²P]-lipid IV_A from strain BKT09 (Emptage *et al.*, 2012) for use as an acceptor with non-radioactive phosphatidylcholines of defined acyl chain composition as donors (Figure 3.7C). The results demonstrate that *P. aeruginosa* PagP clearly shares *E. coli* PagP's unique ability to discriminate acyl chains that differ from palmitate by only a single methylene unit (Khan *et al.*, 2010a; Khan *et al.*, 2010b). Based on the *P. aeruginosa* PagP homology model, His35, like His33 in *E. coli* PagP, maps to the cell surface region adjacent to the hydrocarbon ruler.

3.5.9 *P. aeruginosa* PagP confers resistance to C18G, but does not influence resistance to polymyxins

After identification and functional analysis of *P. aeruginosa* PagP was established, we focused on identifying its role within the context of the host innate immune system. Increased lipid A acylation by palmitoylation has been reported to promote resistance to CAMPs, possibly via increase in the outer

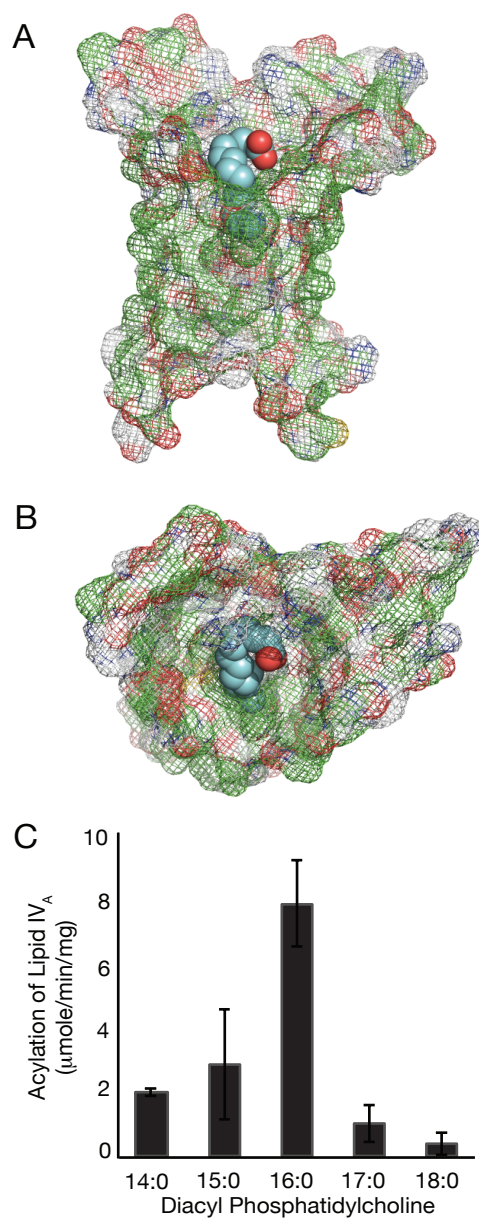


Figure 3.7. Homology model and hydrocarbon ruler of PaPagP. Mesh representations of PaPagP viewed parallel (A) and above (B) the membrane plane with bound palmitate coloured in cyan. Panel (C) shows the specific activity for the conversion by PaPagP of $[^{32}\text{P}]$ -lipid IV_A to lipid IV_B, using symmetrical phosphatidylcholine donors of saturated acyl chain compositions varying from C14 to C18 in methylene unit increments.

membrane permeability barrier and altered lipid packing leading to repulsion of hydrophobic portions on CAMPs (Ernst *et al.*, 2001). Killing assays were performed using C18G, a synthetic α -helical CAMP derived from human platelet factor IV, to determine the role *P. aeruginosa* PagP may play in resistance to CAMPs. WT, $\Delta pagP$, and $\Delta pagP+Pa1343$ strains were grown under magnesium limited conditions to promote palmitoylation and strains were challenged with serial dilutions of C18G followed by plating to assess survival. Colonies were counted and compared with non-treated samples for survival counts. C18G resistance in these backgrounds (WT, $\Delta pagP$, $\Delta pagP+Pa1343$) was dependent of PagP enzymatic activity, because the concentration of peptide at which 50% of bacteria were killed was approximately six times greater for WT and complemented strain (1.8 and 2.0 μgml^{-1} respectively) than for the $\Delta pagP$ null mutant (0.31 $\mu\text{g ml}^{-1}$) (Figure 3.8). In contrast, we did not detect an effect of *pagP* deletion when constitutively polymyxin-resistant *pmrB12* and $\Delta phoQ$ strains (Miller *et al.*, 2011; Moskowitz *et al.*, 2012) were grown under magnesium-replete conditions and tested by conventional colistin agar dilution and alternative polymyxin B sulphate plate assays (Table 3.2). The lack of effect on the *pmrB12* strain phenotype is not surprising, given the demonstrated inhibitory effect of this system on lipid A palmitoylation (Moskowitz *et al.*, 2012). However, the $\Delta phoQ$ strain is known to add palmitate to its lipid A constitutively (Miller *et al.*, 2011), thus the lack of *pagP* deletion effect in this

strain background indicates that lipid A palmitoylation does not influence PhoPQ-dependent polymyxin resistance in *P. aeruginosa*.

3.5.10 Palmitoylation of *P. aeruginosa* lipid A increases IL-8 production

Previous studies have reported changes in cytokine levels resulting from TLR4 stimulation with palmitoylated lipid A in addition to the effects seen on CAMP resistance. Palmitoylation in other Gram-negative pathogens have been described as imparting antagonistic effects when used to stimulate TLR4 (Feist *et al.*, 1989; Loppnow *et al.*, 1986; Tanamoto and Azumi, 2000). We have previously shown that CF-specific lipid A containing palmitate was associated with increased inflammatory responses (Ernst *et al.*, 1999) indicating that this modification is likely involved in progression of airway disease. Activation of TLR4 by LPS upregulates the expression of pro-inflammatory cytokines via the NF κ B pathway. The pro-inflammatory cytokine IL-8 was used as a readout for TLR4 activity. Immune response effects of *P. aeruginosa* PagP activity were tested by isolating LPS from PAO1, Δ *pagP*, and the Δ *pagP*+*Pal343* after growth in PagP inducing conditions followed by stimulation of Vitamin D3 differentiated human-derived monocytic THP-1 cells for 16 h. Supernatants were harvested and tested by ELISA for TLR activation by IL-8 expression using *E. coli* LPS as a positive control. Overall, IL-8 expression by cells

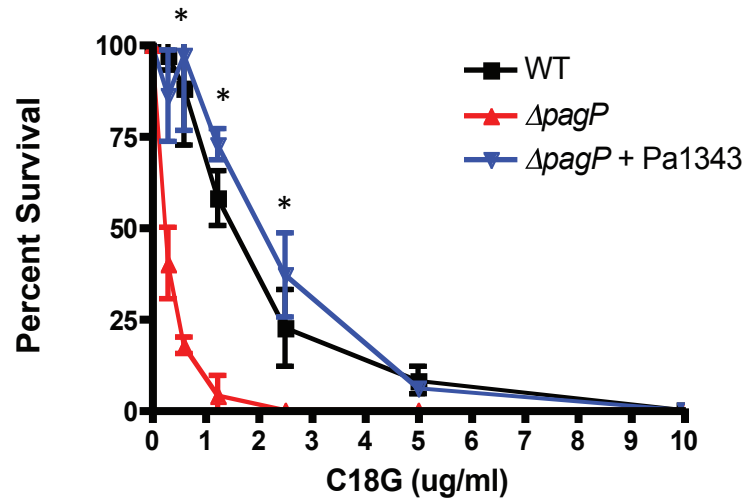


Figure 3.8 Palmitoylated lipid A imparts resistance to C18G. WT, $\Delta pagP$ and $\Delta pagP + Pa1343$ were incubated with increasing amounts of the CAMP C18G and plated to assess susceptibility. Expression of Pa1343 imparted a significant survival advantage against C18G. *P < 0.01.

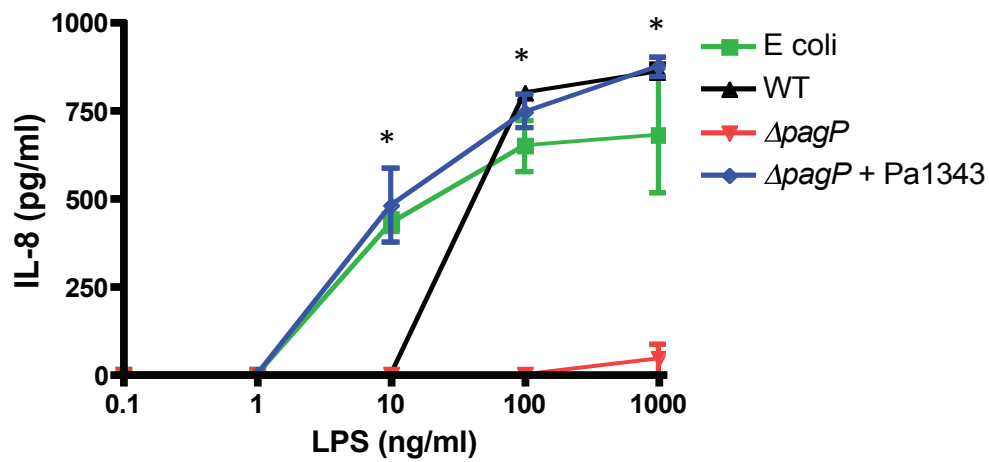


Figure 3.9 Cytokine stimulation assay. THP-1 alveolar macrophages were stimulated with LPS prepared from *E. coli*, WT, $\Delta pagP$, and $\Delta pagP + Pa1343$ grown under magnesium-limiting conditions for 16 h. After incubation supernatants were harvested and used for ELISA measuring IL-8 production. WT and $\Delta pagP + Pa1343$ were able to stimulate significantly higher levels of IL-8 than the $\Delta pagP$ mutant. All experiments were performed in three biological replicates. * $P < 0.01$.

stimulated with $\Delta pagP$ LPS was significantly lower than WT and $\Delta pagP+Pal343$ expressing a functional PagP (Figure 3.9). The complemented strain induced significantly higher levels of IL-8 than WT and $\Delta pagP$ when LPS was added at a concentration of 10 ng ml^{-1} ($P = 0.01$). Both WT and $\Delta pagP+Pal343$ induced significantly higher levels of IL-8 at 100 ng ml^{-1} ($P = 0.001$) and $1 \text{ } \mu\text{g ml}^{-1}$ ($P = 0.0001$) than the deletion strain.

3.6 Discussion

Gram-negative bacteria modify their LPS in response to external stimuli. Within the host, bacteria must defend against fluctuations in pH, temperature, ion limitation, as well as protect against assault by immune cells and toxic reactive products. Addition of palmitate to lipid A by PagP is seen frequently in Gram-negative pathogens in response to host factors. This additional fatty acyl chain aids in resistance to CAMPs, dampens TLR signalling, and contributes to the overall remodelling and stabilization of the membrane. Lipid A isolated from *P. aeruginosa* infecting the CF lung shows constitutive addition of palmitate making identification and characterization of the PagP enzyme in *P. aeruginosa* of particular interest. Understanding the role palmitoylated lipid A plays in this unique infection might help explain long-term *P. aeruginosa* survival and target this modification as a potential treatment to block disease progression.

Upon *in silico* *P. aeruginosa* identification of candidate *pagP* genes, individual transposon insertion mutants representing them were screened for loss of palmitoyltransferase activity by MALDI-TOF MS after induction by magnesium limitation. One mutant, *Pal343*, showed loss of PagP activity. Deletion of this gene resulted in the inability to produce the palmitoylated hexa-acylated lipid A species (m/z 1684) upon growth in inducing conditions. Further analysis of fatty acids isolated from the $\Delta pagP$ mutant lipid A showed no incorporation of palmitate, whereas WT and in trans complemented strains were able to produce hexa-acylated lipid A containing palmitate.

Although *P. aeruginosa* PagP imparts a similar function to that of previously identified PagP enzymes, phylogenetic tree analysis and amino acid sequence alignment showed little similarity to known PagP proteins. This analysis at first indicated *P. aeruginosa* PagP might not have evolved from the common PagP ancestor and was potentially a distinctly different enzyme, albeit one similar both in size and in being targeted for secretion by an *N*-terminal signal peptide. However, most lipid A acylation enzymes possess active sites that are exposed to the cytosol in order to utilize thioester substrates, yet PagP uses a phospholipid as the palmitoyl donor and is uniquely capable of functioning within the outer membrane. If *P. aeruginosa* palmitoylates its lipid A using a phospholipid donor, then it could possess a true homologue of *E. coli* PagP among the pool of small β -barrel proteins in the *P. aeruginosa* outer membrane. This, in fact, appears to be the case, and our finding that purified *P.*

aeruginosa PagP recapitulates the enzymology of *E. coli* PagP is certainly consistent with an orthologous relationship.

What sets *E. coli* PagP apart from all known outer membrane β -barrel structures is its interior hydrophobic pocket lined by a detergent molecule, which demarcates the hydrocarbon ruler for measuring the selected *sn*-1 palmitoyl group within the phospholipid donor (Khan *et al.*, 2010b). The evidence that *P. aeruginosa* PagP and *E. coli* PagP are true homologues comes from the observations that the *P. aeruginosa* PagP homology model recreates a similar interior hydrophobic pocket for binding the terminal 6 methylene units of hydrocarbon chains as does *E. coli* PagP, and that the predicted existence of a hydrocarbon ruler in *P. aeruginosa* PagP could be confirmed by the observed enzymatic exclusion of acyl chains longer or shorter than palmitate. To our knowledge, PagP from *E. coli* and *P. aeruginosa* are the only integral membrane enzymes of lipid metabolism known to possess a hydrocarbon ruler capable of distinguishing acyl chains with methylene unit precision. Additionally, *P. aeruginosa* PagP can be purified as an active enzyme using a procedure that was developed for purification of active *E. coli* PagP, the purified *P. aeruginosa* PagP enzyme displays inhibition by the same detergents that bind within the *E. coli* PagP hydrocarbon ruler, and both enzyme activities depend on the same narrow spectrum of detergents that do not bind within the hydrocarbon ruler. Structural details of a PagP:phospholipid:lipid A ternary complex remain to be elucidated, but this structure will likely reveal an ordering of residues in the

dynamic cell surface loops and evince the details of the PagP catalytic mechanism. Our finding that the organization of catalytic His residues in the cell surface loops is not perfectly conserved likely reflects the distinctly different regiospecificities for palmitoylation of lipid A at the 2 and 3' positions, respectively, in *E. coli* and *P. aeruginosa* PagP. Perhaps these differences, combined with known functional differences between the outer membrane barriers for enterobacteria and the pseudomonads, will eventually explain how these two distinct families of PagP homologues have diverged beyond the level of detection at the amino acid sequence level. Nevertheless, the common elements of surface catalytic His residues flanking a conserved β -barrel interior hydrophobic pocket seem to be rudimentary for enzymatic palmitoylation of lipid A in bacterial outer membranes.

Resistance to CAMPs is an important evasion mechanism for pathogens. Many infections resistant to antibiotics are treated with polymyxins as a last resort. In addition, immune cells, such as neutrophils, release CAMPs to aid in bacterial clearance. Palmitate addition leads to resistance to these CAMPs in *E. coli* and *Salmonella*. Susceptibility experiments carried out here using *P. aeruginosa* expressing palmitoylated lipid A showed protection was limited to the α -helical peptide C18G, while resistance to polymyxins, typically mediated by lipid A phosphate modification, did not change. This limited resistance pattern indicates protection against these peptides is not the primary function of palmitoylation, leading our focus to other means of immune modulation.

P. aeruginosa lipid A isolated from patients with CF has been shown previously to produce a pro-inflammatory response. Here we were able to show modification of lipid A by *P. aeruginosa* PagP contributes to this pro-inflammatory property. Multiple factors influence agonistic properties of lipid A including terminal phosphorylation, chain length and position, unsaturation and overall acylation quantity of the lipid A molecule. These factors play a key role in optimal binding of MD2-TLR4-LPS leading to dimerization and downstream immune signalling. TLR4 antagonists, while able to bind to the complex, are not capable of inducing dimerization events. Strong agonists typically have fatty acid chains of 12 and 14 carbons in length, *P. aeruginosa* lipid A is comprised of fatty acids of 10 and 12 carbon chains contributing to a suboptimal fit within the MD2 binding pocket. Addition of the longer palmitoyl chain to *P. aeruginosa* lipidA may alter binding by seating the molecule higher in the pocket exposing regions of lipid A necessary for MD2/TLR4 dimerization. Additionally, the change from a penta-acylated to hexa-acylated lipid A is ideal for shifting of the glucosamine backbone necessary for phosphate interaction with the positively charged residues on TLR4 (Park *et al.*, 2009).

Modifications to lipid A resulting in a pro-inflammatory molecule may be advantageous within the CF lung where an influx of immune cells can provide nutrients and growth factors but are not able to clear infection. Inflammation increases the trafficking of cells, such as neutrophils to sites of infection leading to bacterial clearance. Within the CF lung, responding immune

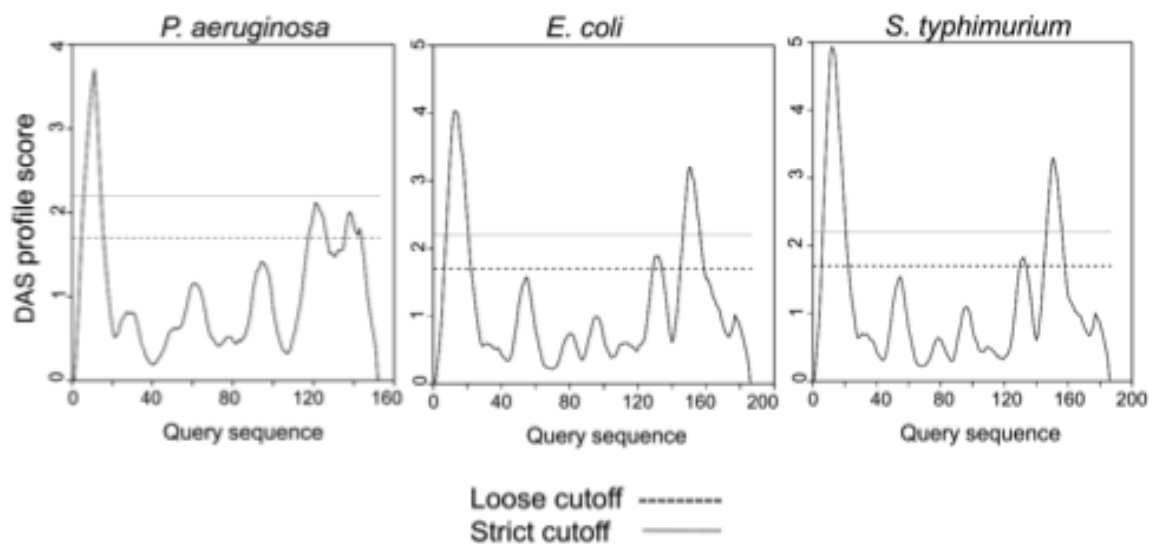
cells have a decreased ability to penetrate into the host mucus layer and clear bacteria. Additionally, *P. aeruginosa* evades neutrophils through release of secreted factors leading to cell death. Increasing inflammation and thus increasing cellular trafficking leads to lysis of trapped neutrophils and release of cellular contents containing nutrients into the mucus layer depositing elements necessary for growth and survival within this unique environment.

The ability of *P. aeruginosa* to adapt to and persist within the CF lung depends on tight control of lipidA modifications in response to environmental conditions. The detailed understanding of the *P. aeruginosa* PagP enzyme that has been gained through these studies will support the development of novel strategies for combating a pathogen with emerging resistance to many treatment options. Modulation of this enzyme may help control levels of inflammation that already contribute to disease progression as well as disrupting a mechanism for metabolite acquisition critical to survival within the CF lung environment.

3.6 Acknowledgements

This study was supported by the Canadian Institutes of Health Research operating grant MOP-125979 (REB), the National Science Foundation-Major Research Instrumentation Award 1029659 (TAG) and the National Institutes of Health grants R01AI067653 (SMM), RO1AI030479 (SIM), and R01AI047938 (RKE).

3.7 Supplementary Tables and Figures



Supplementary Figure S3.1. PagP enzyme transmembrane prediction of *P.*

aeruginosa, *E. coli*, and *S. Typhimurium*, by using server DAS

(<http://www.sbc.su.se/~miklos/DAS/>). The horizontal scale depicts the relative

amino acid number, and vertical scale represents DAS profile score. The

horizontal solid line (strict cutoff) and dashed line (loose cutoff) indicates the

number of matching segments and actual location of the transmembrane

segment respectively.

SUPPLEMENTAL TABLE 1

Experimental <i>m/z</i>	C-3'	C-2'	C-3	C-2	Phosphate configuration
1168	C10(3-OH)	C12(3-OH):C12	H	C12(3-OH)	Monophosphate
1184	C10(3-OH)	C12(3-OH)	H	C12(3-OH):C12(2-OH)	Monophosphate
1196	H	C12(3-OH):C12	H	C12(3-OH):C12(2-OH)	Monophosphate
1212	H	C12(3-OH):C12(2-OH)	H	C12(3-OH):C12(2-OH)	Monophosphate
1248	C10(3-OH)	C12(3-OH):C12	H	C12(3-OH)	Diphosphate
1264	C10(3-OH)	C12(3-OH)	H	C12(3-OH):C12(2-OH)	Diphosphate
1276	H	C12(3-OH):C12	H	C12(3-OH):C12(2-OH)	Diphosphate
1366	C10(3-OH)	C12(3-OH):C12	H	C12(3-OH):C12(2-OH)	Monophosphate
1382	C10(3-OH)	C12(3-OH):C12(2-OH)	H	C12(3-OH):C12(2-OH)	Monophosphate
1446	C10(3-OH)	C12(3-OH):C12	H	C12(3-OH):C12(2-OH)	Diphosphate
1462	C10(3-OH)	C12(3-OH):C12(2-OH)	H	C12(3-OH):C12(2-OH)	Diphosphate
1536	C10(3-OH)	C12(3-OH):C12	C10(3-OH)	C12(3-OH):C12(2-OH)	Monophosphate
1552	C10(3-OH)	C12(3-OH):C12(2-OH)	C10(3-OH)	C12(3-OH):C12(2-OH)	Monophosphate
1604	C10(3-OH)C16	C12(3-OH):C12	H	C12(3-OH):C12(2-OH)	Monophosphate
1616	C10(3-OH)	C12(3-OH):C12	C10(3-OH)	C12(3-OH):C12(2-OH)	Diphosphate
1632	C10(3-OH)	C12(3-OH):C12(2-OH)	C10(3-OH)	C12(3-OH):C12(2-OH)	Diphosphate
1684	C10(3-OH)C16	C12(3-OH):C12	H	C12(3-OH):C12(2-OH)	Diphosphate
1700	C10(3-OH)C16	C12(3-OH):C12(2-OH)	H	C12(3-OH):C12(2-OH)	Diphosphate
1854	C10(3-OH)C16	C12(3-OH):C12	C10(3-OH)	C12(3-OH):C12(2-OH)	Diphosphate

Supplementary Table S3.1. Observed masses and proposed compositions for lipid A, by negative-ion MALDI-MS with an *m/z* scan 1100 to 2200. Only assignable peaks with unambiguous exact masses and charge states are listed.

SUPPLEMENTAL TABLE 2		
Strain or plasmid	Description	Source
Strains		
<i>Pseudomonas aeruginosa</i>		
PAO1	Wild-type laboratory-adapted strain	S. Lory, Harvard
PAO1+PA1343	Wild-type PAO1 expressing PA1343 in trans	This study
$\Delta pagP$	PAO1 derivative with PA1343 deleted	This study
$\Delta pagP$ +PA1343	PAO1 deletion of PA1343, complemented	This study
H35F:: <i>pagP</i>	35 th histidine of PA1343 changed to phenylalanine	This study
H35N:: <i>pagP</i>	35 th histidine of PA1343 changed to asparagine	This study
H42F:: <i>pagP</i>	42 th histidine of PA1343 changed to phenylalanine	This study
H42N:: <i>pagP</i>	42 th histidine of PA1343 changed to asparagine	This study
H45F:: <i>pagP</i>	45 th histidine of PA1343 changed to phenylalanine	This study
H45L:: <i>pagP</i>	45 th histidine of PA1343 changed to leucine	This study
H45N:: <i>pagP</i>	45 th histidine of PA1343 changed to asparagine	This study
D84A:: <i>pagP</i>	84 th aspartic acid of PA1343 changed to alanine	This study
D84N:: <i>pagP</i>	84 th aspartic acid of PA1343 changed to asparagine	This study
S85A:: <i>pagP</i>	85 th serine of PA1343 changed to alanine	This study
S85G:: <i>pagP</i>	85 th serine of PA1343 changed to glycine	This study
D86A:: <i>pagP</i>	86 th aspartic acid of PA1343 changed to alanine	This study
D86N:: <i>pagP</i>	86 th aspartic acid of PA1343 changed to asparagine	This study
S87A:: <i>pagP</i>	87 th serine of PA1343 changed to alanine	This study
S87G:: <i>pagP</i>	87 th serine of PA1343 changed to glycine	This study
DSDS-AGNA:: <i>pagP</i>	84, 85, 86 and 87 aspartic acid and serine of PA1343 changed to alanine, glycine, asparagine and alanine respectively	This study
PAK		
PAK <i>pmrB12</i>	Wild-type laboratory-adapted strain	S. Lory, Harvard
PAK <i>pmrB12</i>	Pm-resistant PAK derivative with <i>pmrB12</i> allele	S. M. Moskowitz, Mass General Hospital
PA <i>pmrB12</i> $\Delta pagP$	PAK <i>pmrB12</i> derivative with PA1343 deleted	This study
PAK $\Delta phoQ$	Pm-resistant PAK derivative with <i>phoQ</i> deleted	S. I. Miller, University of Washington
PAK $\Delta phoQ$ $\Delta pagP$	PAK derivative with <i>phoQ</i> and PA1343 deleted	This study
<i>E. coli</i> BW25113	Wild-type strain for BKT09	Pei Zhou, Duke University
<i>E. coli</i> BKT09	<i>E. coli</i> BW25113 $\Delta pagP$, $\Delta lpxP$, $\Delta lpxM$, $\Delta lpxL$::Kan	B. K. Tan, Duke University
Plasmids		
pUCP19-USER	A hybrid plasmid between pNEB206A (New England Biolab) and pUCP19: Car'	A. Hinz, University of Washington
pPA1343	pUCP19-USER containing PA1343: Car'	This study
pDONR 201	Gateway cloning vector Kan'	Invitrogen
pEXGWD	Suicide vector in <i>P. aeruginosa</i> ; sacB, Gen'	Invitrogen
pET21a-PA1343	PA1343 expression vector	This study

Supplementary Table S3.2: Bacterial strains and plasmids used in this study.

SUPPLEMENTAL TABLE 3

Primer name	Sequence
For cloning PA1343	
PA1343_USER_fp	GGAGACAUGTCACGCTTTCCTTCCTTC
PA1343_USER_rp	GGGAAAGUGGGAGTCTCCTGTGCGAGTGA
pUCP19-PA1343_fp	TATACATATGGCCGACGGCGACTT
pUCP19-PA1343_rp	TATACTCGAGTCAGAGACGCAGGCCGA
For deleting PA1343	
PA1343-1	GGGACAAGTTTGTACAAAAAAGCAGGCTCCGGAGATGATGTTTCATGCC
PA1343-2	CCCGTTCCTGGCCTCAGAGACGCAGGGATCCGAGATAGCGCATGGGACTCCAGGC
PA1343-3	GCCTGGAGTCCCCATGCGCTATCTCGGATCCCTGCGTCTCTGAGGCCAGGAACGGG
PA1343-4	GGGACCACCTTTGTACAAGAAAGCTGGGTGGTATCCTCTGAATGACGG
For point-mutagenesis	
H35F_fp	AGCGTCTACACCCGGTTTTTCAACCCGGACCCCT
H35F_rv	AGGGTCCGGGTTGAAAAACCGGGTGTAGACGCT
H35N_fp	AGCGTCTACACCCGGAATTTCAACCCGGACCCCT
H35N_rv	AGGGTCCGGGTTGAAATTCGGGTTAGACGCT
H42F_fp	AACCCGGACCCCTGAATTCACAATCACCAGGAC
H42F_rv	GTCCTGGTGATTGTTGAATTCAGGGTCCGGGTT
H42N_fp	AACCCGGACCCCTGAAAACAACAATCACCAGGAC
H42N_rv	GTCCTGGTGATTGTTGTTTTTCAGGGTCCGGGTT
H45F_fp	CCTGAACACAACAATTTCCAGGACCTGCTCGGC
H45F_rv	GCCGAGCAGGTCCTGGAAATGTTGTGTTTCAGG
H45L_fp	CCTGAACACAACAATCTCCAGGACCTGCTCGGC
H45L_rv	GCCGAGCAGGTCCTGGAGATTGTTGTGTTTCAGG
H45N_fp	CCTGAACACAACAATAACCAGGACCTGCTCGGC
H45N_rv	GCCGAGCAGGTCCTGGTTATTGTTGTGTTTCAGG
DB4A_fp	CCTGGGCAAGCGTTTTCCGCGTACAGCTACCCGG
DB4A_rv	CCGGGTAGCTGTCACTGGCGAAACGCTTGCCGAGG
DB4N_fp	CCTGGGCAAGCGTTTTCAACAGTACAGCTACCCGG
DB4N_rv	CCGGGTAGCTGTCACTGTTGAAACGCTTGCCGAGG
S85A_fp	GGGCAAGCGTTTTCGACGCTGACAGCTACCCGGTCT
S85A_rv	AGACCGGGTAGCTGTGACGCTCGAAACGCTTGCCC
S85G_fp	GGGCAAGCGTTTTCGACGCTGACAGCTACCCGGTCT
S85G_rv	AGACCGGGTAGCTGTACCCGTCGAAACGCTTGCCC
DB6A_fp	CAAGCGTTTTCGACAGTCCAGCTACCCGGTCTACC
DB6A_rv	GGTAGACCGGGTAGCTGGCACTGTGCGAAACGCTTG
DB6N_fp	CAAGCGTTTTCGACAGTAAACAGCTACCCGGTCTACC
DB6N_rv	GGTAGACCGGGTAGCTGTTACTGTGCGAAACGCTTG
S87A_fp	CGTTTCGACAGTGACGCCTACCCGGTCTACCTG
S87A_rv	CAGGTAGACCGGGTAGGCGTCACTGTGCGAAACG
S87G_fp	CGTTTCGACAGTGACGGCTACCCGGTCTACCTG
S87G_rv	CAGGTAGACCGGGTAGCCGCTCACTGTGCGAAACG
DB4A-S85G_fp	CCTGGGCAAGCGTTTTCCGCGTACAGCTACCCGGTCT
DB4A-S85G_rv	GACCGGGTAGCTGTACCCGGCGAAACGCTTGCCGAGG
DB6N-S87A_fp	CAAGCGTTTTCGACAGTAAACAGCTACCCGGTCTACC
DB6N-S87A_rv	CAGGTAGACCGGGTAGGCGTACTGTGCGAAACGCTTG
DB4A-S85G-DB6N-S87A_fp	CCTGGGCAAGCGTTTTCCGCGTAAACAGCTACCCGGTCTACCTG
DB4A-S85G-DB6N-S87A_rv	CAGGTAGACCGGGTAGGCGTACCCGGCGAAACGCTTGCCGAGG
For sequencing	
PA1343 seq-1	GAGCTCGTCAGCGACGAC
PA1343 seq-2	GGTTTTCTGACGGTTCGTTTC
PA1343 seq-3	GTGGAACCGCTGACGATT

Supplementary Table S3.3: List of the primers used for the PCR and mutagenesis.

Chapter 4

Structure-function relationships among a minor clade of PagP homologs

4.1 Author's Preface

Prior to beginning my graduate work, the gene encoding the *Pseudomonas aeruginosa* lipid A palmitoyltransferase (PaPagP) had been identified in the laboratory of Dr. Robert K. Ernst at the University of Maryland. As part of a collaborative study with the Ernst laboratory, we purified PaPagP and characterized it as a divergent homolog with conserved structural and functional features despite a lack of primary amino acid sequence similarity with the well-characterized enterobacterial PagP. We asked new questions, such as “what is the phylogenetic relationship between PaPagP and the enterobacterial PagP?” and “do other divergent homologs like PaPagP exist?” The work described in this chapter addresses these questions and contributes to our growing understanding of PagP structure-function relationships. Emily DeHaas, an undergraduate research student under my supervision, characterized the *Halomonas elongata* PagP homolog during her undergraduate thesis. We worked in partnership, cloning, expressing and purifying the constructs described in this study. I performed the *in vitro* assays and supervised the ³²P experiments. The conserved signature indel was identified by Dr. Radhey Gupta. I prepared the multiple sequence alignments, homology models and electrostatic potential analysis. Russell Bishop and I analyzed the data, prepared the figures and wrote the manuscript.

4.2 Abstract

The outer membrane (OM) enzyme PagP modifies the lipid A component of lipopolysaccharide with a palmitoyl group; this modification has been implicated in resistance to host immune defenses. There are two clades of PagP, the major clade and the minor clade, which have evolved to fulfill distinct functions in different groups of bacteria. The minor clade, exemplified by *Pseudomonas aeruginosa* PagP (PaPagP), includes homologs that lack obvious primary structural similarity with the major clade PagP homologs from enterobacteria. A comparative analysis of all available sequences of minor clade PagP homologs has revealed invariant His, Ser, and Tyr residues that are necessary for catalysis. Additionally, a 4-amino acid conserved signature indel or CSI is unique to bacteria clustered phylogenetically within the γ -subclass of Proteobacteria. The 4-amino acid CSI is specific to *Halomonas* and is located in the periplasmic turn T2 of *H. elongata* PagP (HePagP), where it is essential for palmitoyltransferase activity *in vitro* and in the bacterial OM. The 4-amino acid insert can be superimposed on the T2 turn of *E. coli* PagP (EcPagP), but in PaPagP the T2 turn is significantly contracted. Mutational expansion of the T2 turn in PaPagP does not affect palmitoyltransferase activity in the bacterial OM. HePagP is also predicted to have an extension at the *N*-terminus, reminiscent of the amphipathic α -helix of EcPagP. Thermal denaturation experiments point to a crucial role for the *N*-terminal extension in modulating β -barrel stability. The

structural and functional similarities between EcPagP and HePagP indicate that the major and minor PagP clades are derived from a common ancestor.

4.3 Introduction

Homologous proteins are descended from a common ancestor and usually possess conserved elements of sequence and structure, which can be used to infer evolutionary relationships. A high incidence of amino acid sequence identity can imply homology, but some homologous proteins can exhibit undetectable amino acid sequence identity (Murzin, 1998). In these instances, an alignment of 3-dimensional structures can be useful in deducing homology (Cheng *et al.*, 2005; Dietmann and Holm, 2001), as even distantly related proteins tend to maintain similar structural folds (Chothia and Lesk, 1986; Hilbert *et al.*, 1993). We have previously reported the identification and characterization of a divergent homolog of the bacterial outer membrane (OM) enzyme PagP in *Pseudomonas aeruginosa* (PaPagP), sharing no detectable amino acid sequence identity with the well-known enterobacterial PagP homologs (Thaipisuttikul *et al.*, 2014).

The solved NMR and x-ray structures of *Escherichia coli* PagP (EcPagP) revealed an 8-strand anti-parallel β -barrel preceded by an *N*-terminal amphipathic α -helix (Ahn *et al.*, 2004; Cuesta-Seijo *et al.*, 2010; Hwang *et al.*, 2004; Hwang *et al.*, 2002). A hallmark of PagP that sets it apart from all known OM β -barrel structures is its interior hydrophobic lipid acyl chain-binding pocket, known as the hydrocarbon ruler, which measures the selected *sn*-1 palmitoyl group donated by a phospholipid during the enzymatic palmitoylation of lipid A (Ahn *et al.*, 2004; Bishop, 2005; Khan *et al.*, 2007). Lipid A is the

endotoxic portion of lipopolysaccharide (LPS) responsible for triggering the innate immune response to infections. Palmitoylation of lipid A has been shown to provide resistance to certain cationic antimicrobial peptides or CAMPs (Guo *et al.*, 1998) and to attenuate the inflammatory response signaled through the host toll-like receptor-4 (TLR4) and myeloid differentiation factor-2 (MD-2) signal transduction pathway (Hajjar *et al.*, 2002; Kawasaki *et al.*, 2004; Park *et al.*, 2009). EcPagP palmitoylates lipid A on the proximal glucosamine unit to attenuate inflammation, but PaPagP instead adds palmitate to the distal glucosamine unit to stimulate inflammation (Thaipisuttikul *et al.*, 2014). We propose that two clades of PagP evolved to fulfill distinct functions in these different groups of Gram-negative bacteria.

Here we describe the minor clade of PagP homologs, which includes PaPagP and members distributed among three of the five known classes of Proteobacteria, as well as members from *Halanaerobium* of the phylum Firmicutes (Figure 4.1). Minor clade PagP members from the γ -Proteobacteria include opportunistic pathogens such as *Pseudomonas* and *Halomonas*, while members from the δ - and β -Proteobacteria, including *Geobacter* and *Rhodospirillum rubrum*, respectively, live freely in the environment and have the metabolic potential to enzymatically reduce iron (Kim *et al.*, 2012). With the exception of PaPagP all of the minor clade homologs are hypothetical proteins of unknown function. Based on homology modeling the β -barrel tertiary structure with an interior hydrocarbon ruler is conserved in PaPagP (Thaipisuttikul *et al.*, 2014).

We now identify and characterize the PagP homolog from *Halomonas elongata* (HePagP). With the comparative analysis of two full-length sequences of PagP from *H. elongata* and *P. aeruginosa* we describe new catalytic and structural elements, and discuss their evolutionary significance.

EcPagP catalysis depends on invariant His, Ser, and Arg residues, but only the catalytic His residue has been previously identified in PaPagP (Thaipisuttikul *et al.*, 2014). We now identify the corresponding Ser residue, and conclude that minor clade PagP homologs depend on an additional invariant Tyr residue instead of an Arg residue. The first of the structural elements in HePagP is a 4-amino acid conserved signature indel or CSI, which corresponds to the surface-exposed periplasmic T2 turn of EcPagP. A CSI is a molecular marker within a protein amino acid sequence alignment where an insertion or deletion serves to demarcate phylogenetic relationships. A CSI is typically flanked by conserved sequences and is usually present in cell-surface loops of a protein (Gupta, 1998). The second structural element is an *N*-terminal extension in HePagP, which corresponds to the post-assembly clamp of EcPagP (Huysmans *et al.*, 2010). The *N*-terminal amphipathic α -helix of EcPagP is not strictly conserved in the minor clade, but a functionally analogous sequence is uniquely present among the PagP homologs from the halomonads. This study provides important insights into the evolution of structure-function relationship among the bacterial family of OM PagP enzymes.

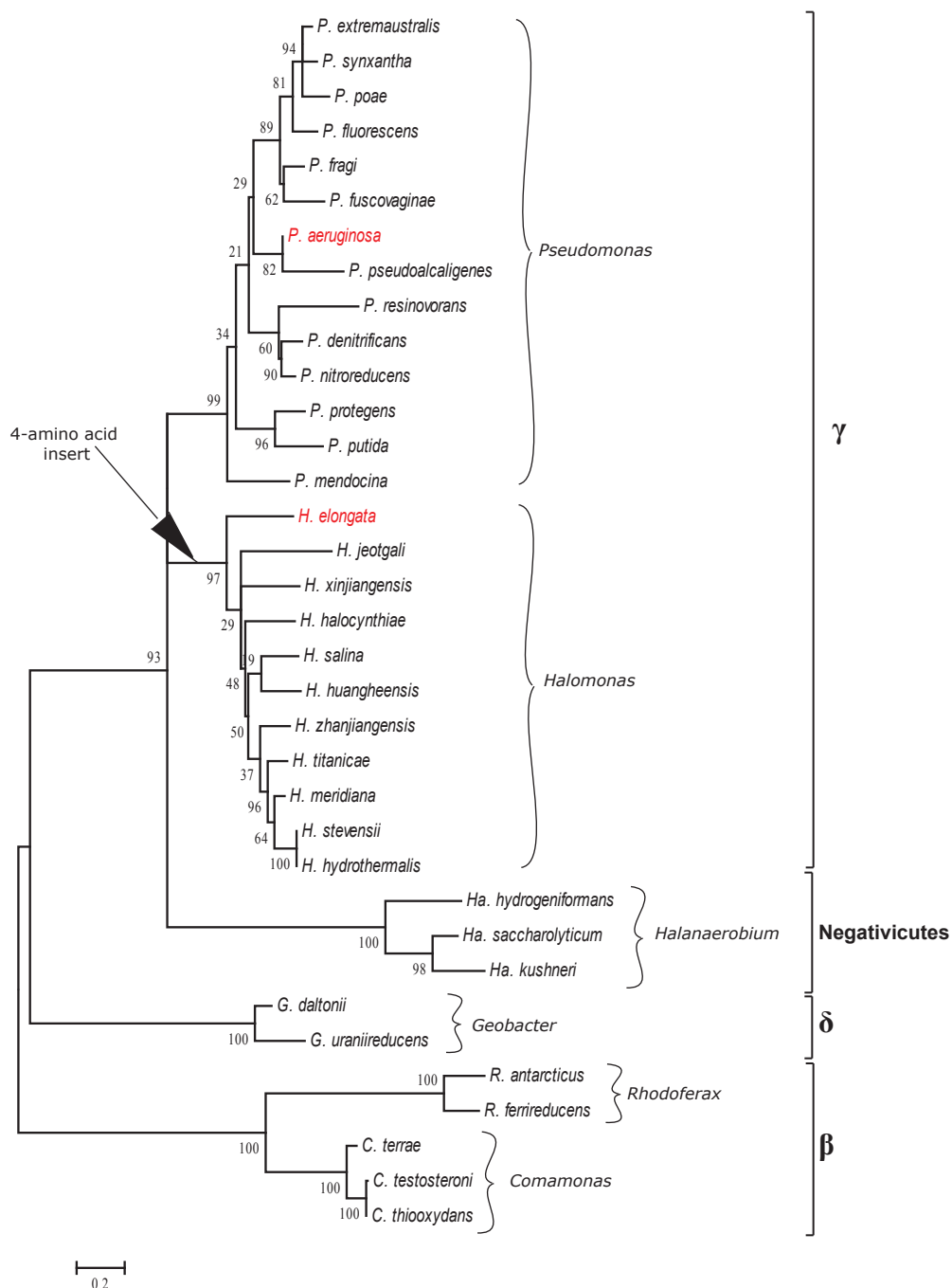


Figure 4.1 A bootstrapped maximum-likelihood tree based upon PaPagP. Courtesy of Sanchia Miller and Radhey Gupta. An unrooted tree showing distribution of PagP homologues based on *P. aeruginosa* PagP (PaPagP) homolog. Includes *Rhodofera* and *Comamonas* of the β subclass, *Pseudomonas* and *Halomonas* of γ -subclass, *Geobacter* of the δ subclass of proteobacteria, as well as *Halanaerobium* of the phylum Firmicutes. All of the species containing the 4-amino acid insert are indicated by the arrow. Bootstrap percentages are indicated at the branching points.

Table 4.1. Bacterial strains and plasmids

Bacterial Strains	Description	Source
<i>E. coli</i> strains		
BKT09	BW25113 $\Delta pagP$, $\Delta lpxP$, $\Delta lpxM$, $\Delta lpxL::kan^R$	Emptage <i>et al.</i> , 2012
WJ0124	MC1061 $\Delta pagP::amp^r$	Jia <i>et al.</i> , 2004
<i>E. coli</i> C41(DE3)	F ⁻ <i>ompT hsdS_B</i> (r _B ⁻ m _B ⁻) <i>gal dcm</i> (DE3)	Lucigen
<i>E. coli</i> C41(DE3)pLysS	F ⁻ <i>ompT hsdS_B</i> (r _B ⁻ m _B ⁻) <i>gal dcm</i> (DE3) pLysS (CmR)	Lucigen
XL-1 Blue	<i>recA1 endA1 gyrA96 thi-1 hsdR17 supE44 relA1 lac</i> [F' <i>proAB lacI^q ZΔM15 Tn10</i> (Tet ^r)].	Agilent
<i>P. aeruginosa</i> strains		
MB5919 $\Delta pagP$	MB5919 (<i>P. aeruginosa</i> PAO1) harbouring $\Delta pagP$	Balibar and Grabowicz, 2016
Plasmids		
pET21a(+)	IPTG-inducible T7 RNA polymerase-promoter expression vector (amp ^R)	Novagen
pBADGr	L-arabinose inducible pBAD promoter expression vector (gen ^R); pMLBAD backbone with <i>dhfr</i> replaced with <i>aacCI</i>	Asikayan <i>et al.</i> , 2008; Lefebre and Valvano, 2002
pETHeloHΔS	462 bp <i>NdeI-XhoI</i> PCR product carrying <i>HELO_4100</i> cloned into pET21a+ with C-terminal His6 tag, no signal peptide.	This study
pETΔT2HΔS	Derivative of pETHeloHΔS with <i>H. elongata</i> PagPΔ83-86	This study
pETΔNTHΔS	Derivative of pETHeloHΔS with <i>H. elongata</i> PagPΔ1-20	This study
pETEcNTHΔS	Derivative of pETHeloHΔS with <i>H. elongata</i> PagPΔ1-20 substituted with NADEWMTTFRENIAQTWQQ	This study
pETHeloH	555 bp <i>NdeI-XhoI</i> PCR product carrying <i>HELO_4100</i> cloned into pET21a+ with C-terminal His6 tag, with <i>E. coli</i> signal peptide	This study
pETΔT2H	Derivative of pETHeloH with <i>H. elongata</i> PagPΔ83-86	This study

<i>Table 4.1 continues on next page</i>		
pBADHePagP	561 bp <i>Ecol-HindIII</i> PCR product carrying <i>HELO_4100</i> cloned into pBADGr with C-terminal His6 tag	This study
pBADdT2	Derivative of pBADdT2 with <i>H. elongata</i> PagP Δ 84-87	This study
pET-Pa1343	402 bp <i>NdeI-XhoI</i> PCR product carrying <i>pa1343</i> cloned into pET21a+, no signal peptide.	Thaipisuttikul <i>et al.</i> , 2014
pET-PaH17A	Derivative of pET-Pa1343 with H17A point mutation	This study
pET-PaN25A	Derivative of pET-Pa1343 with N25A point mutation	This study
pET-PaN26A	Derivative of pET-Pa1343 with N26A point mutation	This study
pET-PaN50A	Derivative of pET-Pa1343 with N50A point mutation	This study
pET-PaS51A	Derivative of pET-Pa1343 with S51A point mutation	This study
pET-PaQ54A	Derivative of pET-Pa1343 with Q54A point mutation	This study
pET-PaY84A	Derivative of pET-Pa1343 with Y84A point mutation	This study
pET-PaY88A	Derivative of pET-Pa1343 with Y88A point mutation	This study
pET-PaD90A	Derivative of pET-Pa1343 with D90A point mutation	This study
pET-PaK91A	Derivative of pET-Pa1343 with K91A point mutation	This study
pET-PaN95A	Derivative of pET-Pa1343 with N95A point mutation	This study
pBAD-Pa1343	477 bp <i>Ecol-HindIII</i> PCR product carrying <i>HELO_4100</i> cloned into pBADGr with <i>E. coli</i> signal peptide	This study
pBADT2	Derivative of pBAD-Pa1343 with D66_S67insLWHF	This study
pBAD-PaH17A	Derivative of pBAD-Pa1343 with H17A point mutation	This study
pBAD-PaN25A	Derivative of pBAD-Pa1343 with N25A point mutation	This study
pBAD-PaN26A	Derivative of pBAD-Pa1343 with N26A point mutation	This study

<i>Table 4.1 continues on next page</i>		
pBAD-PaN50A	Derivative of pBAD-Pa1343 with N50A point mutation	This study
pBAD-PaS51A	Derivative of pBAD-Pa1343 with S51A point mutation	This study
pBAD-PaQ54A	Derivative of pBAD-Pa1343 with Q54A point mutation	This study
pBAD-PaY84A	Derivative of pBAD-Pa1343 with Y84A point mutation	This study
pBAD-PaY88A	Derivative of pBAD-Pa1343 with Y88A point mutation	This study
pBAD-PaD90A	Derivative of pBAD-Pa1343 with D90A point mutation	This study
pBAD-PaK91A	Derivative of pBAD-Pa1343 with K91A point mutation	This study
pBAD-PaN95A	Derivative of pBAD-Pa1343 with N95A point mutation	This study

4.4 Material and Methods

4.4.1 Bacterial strains and growth conditions

Bacterial strains used during these studies are listed in Table 4.1. *E. coli* BKT09 (Emptage *et al.*, 2012) and *P. aeruginosa* MB5919 Δ *pagP* (Balibar and Grabowicz, 2016) were grown according to established procedures. Briefly, strains were grown in Luria-Bertani (LB) medium. Unless otherwise stated antibiotics were used when appropriate with the following concentrations: 25 μ g/mL kanamycin (kan), 50 μ g/mL gentamicin (gen), 100 μ g/mL ampicillin (amp).

4.4.2 Sequence alignment and phylogenetic analysis

A Blastp search was carried out on the Pa1343 sequence from *Pseudomonas aeruginosa* (Genbank ID No. 880995) and sequences of 35 homologs from diverse bacteria were retrieved. A multiple sequence alignment of these proteins was created using the ClustalW 2.1 program (Larkin *et al.*, 2007). A maximum-likelihood phylogenetic tree based on 100 bootstrap replicates of the sequence alignment for PagP homologs was constructed using MEGA 6 (Tamura *et al.*, 2013) as previously described (Naushad *et al.*, 2014). Visual examination of the multiple sequence alignment revealed a 4-amino acid CSI unique to bacteria clustered phylogenetically within the γ -subclass of proteobacteria. The *pa1343* and *HELO_4100* gene products are hereafter referred to as PagP. The sequence of the putative *H. elongata pagP* gene was

retrieved from the Genbank database (*HELO_4100*; Genbank ID No. CBV43984.1). The amino sequence was uploaded to the I-TASSER database (Roy *et al.*, 2010; Zhang, 2008), which predicts secondary structure and provides a 3-dimensional model structure of the protein. HePagP was visualized using the PyMOL Molecular Graphics System (Delano Scientific, San Carlos, CA, USA) and the electrostatic surface potential distribution was calculated using the adaptive Poisson-Boltzman solver plug-in with the scale set from -5 kcal/mol to +5 kcal/mol.

4.4.3 Recombinant DNA techniques

The bacterial genes used in these studies were synthesized by Integrated DNA Technology-GeneArt, unless otherwise indicated. The chimeric protein constructs in this study are shown in Table 4.2. All oligonucleotide primers (Invitrogen) used in our mutagenesis and cloning procedures are identified in Table 4.4. Restriction enzyme digestions, ligations, mutagenesis, transformations, and DNA electrophoresis were performed as described by manufacturer instructions. Quikchange XL site-directed mutagenesis kit was from Agilent Technologies. DNA sequencing was performed at the Farncombe Sequencing Facility at McMaster University.

Plasmid pBADHePagP was constructed by subcloning the 561bp *EcoRI-HindIII* fragment carrying *HELO_4100* with the gene encoding the

Table 4.2. Protein constructs used in this study

Proteins constructs and extinction coefficients, ϵ_{280}	Amino acid sequence
Protein expression in outer membranes	
HePagP _{WT} (29450 M ⁻¹ cm ⁻¹)	<u>MNVSKYVAIFS</u> <u>FVIQLISVGKVFA</u> <u>TPVHANPPALS</u> <u>SLDWPPKLE</u> <u>LDHTLVQTS</u> <u>LYTRHFNP</u> <u>DPEHTNHQELIGLEFHTPDDWL</u> <u>AGGAHFQNSFAQDTFYLYVGRQFP</u> <u>LWHF</u> <u>AHDTTLRAKLT</u> <u>AGLLHGYRGEYRDKIPFNHLETAPAALPSIGIRWKRVEGD</u> <u>LIVFGAAGL</u> <u>MITAGLRF</u> <u>HHHHHHH</u>
HePagP _{ΔT2} (23950 M ⁻¹ cm ⁻¹)	<u>MNVSKYVAIFS</u> <u>FVIQLISVGKVFA</u> <u>TPVHANPPALS</u> <u>SLDWPPKLE</u> <u>LDHTLVQTS</u> <u>LYTRHFNP</u> <u>DPEHTNHQELIGLEFHTPDDWL</u> <u>AGGAHFQNSFAQDTFYLYVGRQFPAHDTTLRAKLTAGLLH</u> <u>GYRGEYRDKIPFNHLETAPAALPSIGIRWKRVEGD</u> <u>LIVFGAAGL</u> <u>MITAGLRF</u> <u>LEHHHHHHH</u>
PaPagP _{WT} (18910 M ⁻¹ cm ⁻¹)	<u>MNVSKYVAIFS</u> <u>FVIQLISVGKVFA</u> <u>ADDGDFWYLQTSVYTR</u> <u>HFNP</u> <u>DPEHNNHQDLLGLEYNRADGVL</u> <u>AGGATFNSFSQRSN</u> <u>YAYLGKRFD</u> <u>SDSYPVYLKLTGGLLQGYRGEYRDKIPLNRF</u> <u>GVAPAI</u> <u>PSVGVRF</u> <u>GPLGSELVLLGNSAAMINLGLRLL</u> <u>EH</u> <u>HHHH</u>
PaPagP _{InsT2} (24410 M ⁻¹ cm ⁻¹)	<u>MNVSKYVAIFS</u> <u>FVIQLISVGKVFA</u> <u>ADDGDFWYLQTSVYTR</u> <u>HFNP</u> <u>DPEHNNHQDLLGLEYNRADGVL</u> <u>AGGATFNSFSQRSN</u> <u>YAYLGKRFD</u> <u>LWHF</u> <u>SDSYPVYLKLTGGLLQGYRGEYRDKIP</u> <u>LNRF</u> <u>GVAPAI</u> <u>PSVGVRF</u> <u>GPLGSELVLLGNSAAMINLGLRLL</u> <u>E</u> <u>HHHHHHH</u>
Protein expression in inclusion bodies	
HePagP _{TEV} (29450 M ⁻¹ cm ⁻¹)*	<u>M</u> <u>HHHHHHH</u> <u>ENLYFQ</u> <u>↓G</u> <u>TPVHANPPALS</u> <u>SLDWPPKLE</u> <u>LDHTLVQTS</u> <u>LYTRHFNP</u> <u>DPEHTNHQELIGLEFHTPDDWLAGGAHFQ</u> <u>NSFAQDTFYLYVGRQFP</u> <u>LWHF</u> <u>AHDTTLRAKLTAGLLHGYRGEYRDKIPFNHLETAPAALPSIGIRWKRVEGD</u> <u>LIVFGAAGL</u> <u>MITAGLRF</u>
HePagP _{WT} (29450 M ⁻¹ cm ⁻¹)	<u>M</u> <u>TPVHANPPALS</u> <u>SLDWPPKLE</u> <u>LDHTLVQTS</u> <u>LYTRHFNP</u> <u>DPEHTNHQELIGLEFHTPDDWLAGGAHFQNSFAQDTFYLYVGRQ</u> <u>F</u> <u>L</u> <u>WHF</u> <u>AHDTTLRAKLTAGLLHGYRGEYRDKIPFNHLETA</u> <u>PAALPSIGIRWKRVEGD</u> <u>LIVFGAAGL</u> <u>MITAGLRF</u> <u>LE</u> <u>HHHHHHH</u> <u>H</u>
HePagP _{ΔT2} (23950 M ⁻¹ cm ⁻¹)	<u>M</u> <u>TPVHANPPALS</u> <u>SLDWPPKLE</u> <u>LDHTLVQTS</u> <u>LYTRHFNP</u> <u>DPEHTNHQELIGLEFHTPDDWLAGGAHFQNSFAQDTFYLYVGRQ</u> <u>F</u> <u>PAHDTTLRAKLTAGLLHGYRGEYRDKIPFNHLETAPAALP</u> <u>SIGIRWKRVEGD</u> <u>LIVFGAAGL</u> <u>MITAGLRF</u> <u>LE</u> <u>HHHHHHH</u>

Table 4.2 continued

HePagP _{ΔNT} (23950 M ⁻¹ cm ⁻¹)	M <u>A</u> D HTLVQTSLYTRHFNPDP E HTNHQELIGLEFHTPDDWL AGGAHFQNSFAQDTFYLYVGRQF L W H F AHDTTLRAKLT AGLLHGYRGEYRDKIPFNHLETAPAALPSIGIRWKRVEGDLI VFGAAGLMITAGLRF L E H H H H H H H
HePagP _{EcNT} (34950 M ⁻¹ cm ⁻¹)	M N A D E W M T T F R E N I V Q T W Q Q L DHTLVQTSLYTRHFNPDP EHTNHQELIGLEFHTPDDWLAGGAHFQNSFAQDTFYLYVG RQF L W H F AHDTTLRAKLTAGLLHGYRGEYRDKIPFNHLE TAPAALPSIGIRWKRVEGDIVFGAAGLMITAGLRF L E H
PaPagP _{WT} (34950 M ⁻¹ cm ⁻¹)	M A D D GDFWYLQTSVYTRHFNPDP E HNNHQDLLGLEYNRA DGVLAGGATFNSFSQRSNYAYLGKRFDSYSPVYLKLTGG LLQGYRGEYRDKIPLNRFVAPAIIPSVGVRFGLGSELVLL GNSAAMINLGLRL L E H

Proteins expressed in the bacterial outer membranes include the native signal peptide of *E. coli* PagP (underlined). The N-terminal α -helix and extension are shown in red. The T2 indel is shown in blue. Residues added by *Nde*I and *Xho*I restriction sites are shown in green. Poly-histidine tag (6X-His) and TEV cleavage sequence are in bold. Estimated extinction coefficients are in units of M⁻¹ cm⁻¹, at 280 nm measured in water.

Table 4.4 Primers used in this study

Primer	Sequence
For point mutations	
prH17AF	5'GCGTCTACACCCGGGCTTTCAACCCGGACC3'
prH17AR	5'GGTCCGGGTTGAAAGCCCGGGTGTAGACGC3'
prN25AF	5'CCCGGACCCTGAACACGCCAA TCACCAGGACCTG3'
prN25AR	5'CAGGTCTTGGTGA TTGGCGTGTTCAGGGTCCGGG3'
prN26AF	5'GGACCCTGAACACAACGCTCACCAGGACCTGCTC3'
prN26AR	5'GAGCAGGTCCTGGTGAGCGTTGTGTTTCAGGGTCC3'
prS51AF	5'GACCTTCCGCAACGCGTTCAGCCAGCG3'
prS51AR	5'CGCTGGCTGAACGCGTTGCGGAAGGTC3'
prQ54AF	5'CGCAACTCGTTCAGCGCGCGCTCCAACACTACGC3'
prQ54AR	5'GCGTAGTTGGAGCGCGCGCTGAACGAGTTGCG3'
prY84AF	5'GCCTGTTGCAGGGCGCTCGCGGCGAATAACC3'
prY84AR	5'GGTATTCGCCGCGAGCGCCCTGCAACAGGC3'
prD90AF	5'GGCGAATACCGCGCCAAGATCCCGCTG3'
prD90AR	5'CAGCGGGATCTTGGCGCGGTATTCGCC3'
prK91AF	5'CGGTTTCAGCGGGATCGCGTCGCGGTATTCGCC3'
prK91AR	5'GGCGAATACCGCGACGCGATCCCGCTGAACCG3'
prN95AF	5'ACAAGATCCCGCTGGCCCGCTTCGGCGTCG3'
prN95AR	5'CGACGCCGAAGCGGGCCAGCGGGATCTTGT3'
For CSI mutations	
prdT2Fwd	5'GGCAGGCAGTTTCCCGCTCATGACACGACG3' (For deleting indel in HePagP)
prdT2Rev	5'CGTCGTGTCATGAGCGGGAAACTGCCTGCC3'(For deleting indel in HePagP)
prT2Fwd	5'GGCAAGCGTTTCGACCTGTGGCACTTCAGTGACAGCTACCCGGTCTACCTG3' (For inserting indel in PaPagP)
prT2Rev	5'CGGGATGAGCTTCAGGTAGACCGGGTAGCTGTCACTGAAGTGCCACAGGTCGAA3' (For inserting indel in PaPagP)
<i>Table 4.4 continues on next page</i>	

For sequencing mutations	
pBADFwd	ATGCCATAGCATTTTTATCC (For pBADGr plasmids with <i>E. coli</i> araBAD promoter)
pBADRev	GATTTAATCTGTATCAGG (For pBADGr plasmids with <i>E. coli</i> araBAD promoter)
T7	TAATACGACTCACTATAGGG (For pET21 plasmids with T7 promoter)
T7term	GCTAGTTATTGCTCAGCGG (FOR pET21 plasmids with T7 terminator)

native signal peptide of *E. coli* PagP fused on the 5' end and a C-terminal 6X-His tag, into the arabinose-inducible vector pBADGr (Asikyan *et al.*, 2008). Plasmid pBADGr is a derivative of pMLBAD (Lefebvre and Valvano, 2002) in which a gentamicin resistance cassette has been inserted into the trimethoprim resistance gene *dhfr*II. The product was propagated in XL-1 blue cells isolated and sequenced using primers pBAD primers. Successful subcloning into pBADGr vector using the *Eco*RI and *Hind*III restriction sites was verified by antibiotic selection, screening on an agarose gel and DNA sequencing using the pBADFwd and pBADRev primers. The T2 mutant, HePagP Δ T2, was prepared using site-directed mutagenesis by deleting the amino acids LWHF (HePagP Δ 84-87) corresponding to the indel.

To express HePagP_{TEV} with a cleavable *N*-terminal poly-histidine (6X-His) tag in cytoplasmic inclusion bodies, Tobacco etch virus (TEV) cleavage sequence (Glu-Asn-Leu-Tyr-Phe-Gln↓Gly), followed by *HELO_4100* excluding its signal sequence (Δ S), was cloned into the pET21a+ plasmid (Novagen) using restriction enzymes *Nde*I, which adds a Met residue to the mature *N*-terminal end of the protein, and *Xho*I. A stop codon at the end of the *HELO_4100* gene sequence was included to prevent translation through the vector C-terminal 6X-His tag. The C-terminal 6X-His tag fusion plasmids pETHeloH Δ S, pETecNTH Δ S, pET Δ NTH Δ S, pET Δ T2H Δ S, pET Δ T2H were constructed similarly except that the stop codon was excluded to allow translation through the *Xho*I site, which adds Leu and Glu followed by the 6X-His tag from the

vector. The resulting plasmids were sequenced from the T7 promoter and/or terminator.

The 477bp *EcoRI-HindIII* fragment, inclusive of *pa1343* and the *N*-terminally fused native signal peptide of EcPagP were cloned into pBADGr to construct pBAD-Pa1343. pBADT2, which includes an insertion mutation of the Leu, Trp, His, Phe between Asp66 and Ser67 was derived from pBAD-Pa1343. Construction of the pETPa1343 plasmid has been described elsewhere (Thaipisuttikul *et al.*, 2014). The point mutations of His17, Asn25, Asn26, Asp50, Ser51, Gln54, Tyr84, Tyr88, Asp90, Lys91 to Ala were derived from both pETPa1343 and pBAD-Pa1343. All cloned constructs were subjected to double strand DNA sequencing at the Farncombe Sequencing Facility at McMaster University to confirm the absence of any spurious mutations.

4.4.4 Expression and Purification of HePagP

To purify HePagP in a denatured state, we expressed it without its native signal peptide in *E. coli* C41(DE3) transformed with the plasmid pETHeloHΔS or its mutant derivatives according to methods adapted from (Bishop *et al.*, 2000; Khan *et al.*, 2007). Briefly, bacteria were cultured in 1 L of LB medium supplemented with ampicillin and grown to an optical density at 600 nm (OD₆₀₀) of 0.4 to 0.6 and then induced with 1 mM isopropyl β-D-thiogalactopyranoside (IPTG) for 4 h. The cells were harvested, resuspended in 20 mL of 50 mM Tris-HCl (pH 8.0) and 5.0 mM EDTA, and passed through a large French pressure

cell at 10 000 psi. The insoluble material was recovered by centrifugation in a Beckman MLA-80 rotor at 27 000 rpm and 4 °C for 20 min using an Optima MAX-E ultracentrifuge. The pellets were washed in 20 mL of 50 mM Tris-HCl (pH 8.0) and 2% Triton X-100 followed by 20 mL of 50 mM Tris-HCl (pH 8.0) and then solubilized in 10 mL of 50 mM Tris-HCl (pH 8.0) and 6 M Gdn-HCl. Supernatants were collected after centrifugation. The crude sample was loaded onto a 5mL bed of His-bind resin (Novagen) that was charged with 50 mM NiSO₄ and equilibrated with 5 column volumes of 10 mM Tris-HCl (pH 8.0), 250 mM NaCl, 6 M Gdn-HCl, and 5 mM imidazole. The sample was washed with 10 column volumes of the equilibration buffer and eluted with 250 mM imidazole. Column fractions were assessed for purity using SDS-PAGE. The purest fractions were pooled and dialyzed twice against 4 L of water, yielding a white precipitate.

To express the C-terminal 6X-His tagged PagP in membranes (Bishop *et al.*, 2000), a single colony of *E. coli* C41(DE3)pLysS transformed with pETHeloH was inoculated into 10 mL of medium, grown to an OD₆₀₀ = 0.7, and then added directly to 1 L of fresh medium. The culture was then grown to OD₆₀₀ = 0.5 before induction with 1 mM IPTG for 4 h. Cells were harvested, washed once with PBS and lysed as described in the preceding section. Debris was removed by centrifugation in a Beckman MLA-80 rotor at 80 000 rpm and 4 °C for 30 min using an Optima MAX-E ultracentrifuge. The membrane pellet was washed with 5 mL of PBS by resuspending it using syringes equipped

serially with 18, 21 and 25 guage needles. The washed membrane was then resuspended in the same manner using 2 mL of 10 mM Tris-HCl (pH 8.0), 1 mM MgSO₄, 0.1% *n*-dodecyl- β -D-maltopyranoside (DDM). The volume was adjusted to 4 mL with the same buffer prior to centrifugation at 80 000 rpm. This procedure was repeated with the same buffer containing 0.2, 0.4, 0.5, 1.0% DDM, followed by a final resuspension with 10 mM Tris-HCl (pH 8.0) containing 10 mM EDTA and 1.0% DDM. The supernatant from the 0.4 and 0.5% DDM solubilization was adjusted to 250 mM NaCl and 5 mM imidazole. It was loaded onto a 1.4 ml bed of charged His-bind resin that had been prepared according to the manufacturer's instructions (Novagen) in a 0.8 x 4 cm open Poly-Prep chromatography column (Bio-Rad), pre-equilibrated with three column volumes of 10 mM Tris-HCl (pH 8.0), 250 mM NaCl, 0.1% DDM containing 5 mM imidazole. After the sample flowed through the column, the resin was washed with 10 column volumes of the pre-equilibration buffer and then eluted with serial 1 mL of pre-equilibration buffer containing 250 mM imidazole. The membrane fractions were subject to sodium dodecyl sulfate polyacrylamide gel electrophoresis (SDS/PAGE) and western blot analysis.

4.4.5 Protein refolding and detergent exchange

Following purification, the precipitated protein was dissolved in 5 mL of 6 M Gdn-HCl, 50 mM Tris-HCL (pH 8.0). The concentration was determined by using an estimated extinction coefficient, ϵ_{280} (Table 4.2). The denatured

solution was diluted dropwise into a 10-fold excess of 0.5% lauryldimethylamine-*N*-oxide (LDAO), 50 mM Tris-HCl (pH 8.0) (Hwang *et al.*, 2002) and stirred overnight at 4°C. The folded proteins were exchanged into DDM and concentrated using Ni²⁺ affinity chromatography. The column was charged as previously described and equilibrated with 3 column volumes of 0.1% LDAO, 100 mM Tris-HCl (pH 8.0), 250 mM NaCl, 5 mM imidazole. The protein was applied to the column and washed with 10 column volumes of equilibration buffer containing 0.2% DDM instead of LDAO and eluted by adjusting the buffer to include 200 mM imidazole. The protein solution was dialyzed against 0.2% DDM, 100 mM Tris-HCl (pH 8.0) overnight to remove salts. Total protein concentration was determined by bicinchoninic acid assay (BCA) (Smith *et al.*, 1985) and folding was assessed by far-ultraviolet circular dichroism (far-UV CD) spectroscopy as previously described (Khan *et al.*, 2007).

4.4.6 TEV cleavage.

AcTEV™ Protease (Thermo Fisher Scientific) was used to cleave the 6X-His tag fused at the *N*-terminus of HePagP_{TEV}. AcTEV Protease specifically recognizes a seven-amino acid sequence (Glu-Asn-Leu-Tyr-Phe-Gln-Gly, cleaving between Gln and Gly). The acTEV protease (300U) was incubated with 0.6 mg of HePagP_{TEV} in 0.1% DDM, 0.5 mM EDTA and 1 mM DTT at room

temperature for 24 h. Cleavage was verified by 15% SDS-PAGE and stained with Coomassie Blue dye as previously described (Khan and Bishop, 2009).

4.4.7 SDS/PAGE and Western Blot Analysis

Protein purity was quantitative as judged by SDS-PAGE and stained with Coomassie Blue dye as previously described (Khan and Bishop, 2009). 16% w/v polyacrylamide gels were prepared. For every 10 ml of 1.5 M Tris-HCl (pH 8.8), 16% acrylamide 0.1% SDS resolving gel solution, we added 0.1 ml of 10% (w/v) ammonium persulfate and 0.01 ml of N, N, N', N' - tetramethylethylenediamine.

Fractions collected during membrane isolation and protein purification were also subject to western blot analysis. Trichloroacetic acid (TCA) precipitated samples were resolved on 13% w/v polyacrylamide gels. The gels were rinsed with water and transferred onto Polyvinylidene difluoride membranes using the iBlot2 dry blotting system at 20 V for 1 min, 23 V for 4 mins and 25 V for 2 mins. The membrane was transferred to a dark container to keep light sensitive reagents protected. The membrane was rinsed once with 1X PBS, covered completely with 10 mL of blocking buffer (3% BSA, 1% goat serum in 1X PBS, 0.1% Tween) and incubated for 1 h at room temperature with gentle shaking. The blocking buffer was adjusted with 5 μ L of mouse anti-his antibody and incubated for an additional hour at room temperature with gentle shaking. The blocking buffer was discarded and the membrane washed 5 times

for 5 minutes each with 1X PBS, 0.1% Tween. A 1 in 2000 dilution of the second antibody, Alexa-Fluor 790 goat anti-mouse antibody, in 0.1% Tween, 0.1% SDS and 1X PBS, was applied to the washed membrane for another hour long incubation. The secondary antibody buffer was discarded and the membrane washed as described above then visualized at 700 and 800nm with the LI-COR Odyssey® Infrared Imaging System.

4.4.8 Far-UV CD

Protein samples analyzed by far-UV CD were maintained at a concentration 0.3 mg/mL in 0.2% DDM, 10 mM Tris-HCl (pH 8.0) unless otherwise stated (Khan *et al.*, 2007). A cuvette with a path length of 1 mm was used with an Aviv 215 spectrophotometer, which was linked to a Merlin Series M25 Peltier device for temperature control. For each sample, three accumulations were averaged at a data pitch of 1 nm and a scanning speed of 10 nm/min. The temperature was maintained at 25°C, and data sets were obtained from 200 to 260 nm. Thermal unfolding (T_U) profiles were obtained by heating the samples from 20 to 100°C at 218 nm with a temperature slope of 2°C/min and a response time of 16 seconds.

4.4.9 Mass spectrometry analysis

Protein samples precipitated from water prior to detergent folding were analyzed at the McMaster Regional Centre of Mass Spectrometry (MRCMS).

The wet pellets were dissolved in a solution of 1% formic acid and acetonitrile (1:1 v/v) just prior to electrospray ionization mass spectrometry (ESI-MS). The sample concentration was maintained at 1 ng/ μ L and the sample injected directly onto an Agilent G1696 TOF Mass Spectrometer. The data were acquired using an Agilent MassHunter Workstation, version A.02.01 (B730), and analyzed using Agilent MassHunter Workstation Software Qualitative Analysis (Version B.02.00, Build 2.0.197.0), and the spectra were deconvoluted using the maximum entropy in BioConfirm Software.

4.4.10 *In vitro* palmitoyltransferase assay

The *in vitro* palmitoyltransferase assays are adapted from those described previously (Cuesta-Seijo *et al.*, 2010). L- α -dipalmitoyl-phosphatidylcholine (DPPC) was obtained from Avanti Polar Lipids and lipid IV_A was obtained from Peptides International (Louisville, KY). Radiolabeled *sn*-1,2-di-(16:0-1-¹⁴C)-phosphatidylcholine (¹⁴C-DPPC) (370kBq) was obtained from Perkin-Elmer Inc. Briefly, the reactions were carried out in a final volume of 25 μ L with sufficient ¹⁴C-DPPC to obtain a radiochemical concentration of 20 μ M; this was diluted to 1 mM by adding sufficient unlabeled DPPC. Lipids were dried under a stream of N₂(g) and dissolved in 22.5 μ L of reaction buffer containing 0.25% DDM, 0.1 M Tris-HCl (pH 8.0), 10 mM EDTA. The reaction mixture was equilibrated for 30 min prior to starting by the addition of 2.5 μ L of

enzyme (375 ng total). Phospholipase A₂ (PLA₂) (4 milliunits/μL) was also assayed as a positive control, with 10 mM CaCl₂ in place of EDTA in the reaction buffer. Reactions were run at 30°C for a total of 6 h. A 5 μL (20000 cpm) aliquot of the reaction mixture was spotted onto a silica gel 60 (Merck) TLC plate at 2, 4 and 6 h. The TLC plates were developed for ~3 h in a chloroform, methanol and water (65:25:4, v/v) solvent system equilibrated in a sealed glass tank. The plates were then exposed overnight to a PhosphorImager screen and developed the next day with a Molecular Dynamics Typhoon 9200 PhosphorImager.

4.4.11 *In vitro* phospholipase assay

Phospholipase assays were conducted using DPPC in a volume of 25 μL to achieve a final concentration of 1 mM. Trace amounts of ¹⁴C-DPPC was added to achieve a radiochemical concentration of 20 μM. Lipids were dried under a stream of N₂(g) and dissolved in 22.5 μL of reaction buffer (0.25% DDM, 100 mM Tris-HCl (pH 8.0), and 10 mM EDTA). The reactions were started with the addition of 2.5 μL of enzyme to give 15 μg/mL in the assay conducted at 30°C. Reactions were terminated by spotting 5 μL (20000 cpm) of the reaction mixture onto a silica gel 60 TLC plate. The experiment was conducted for 6 h with the reaction being spotted at 2, 4 and 6 h. The TLC plates were developed in a chloroform, methanol and water (65:25:4, v/v) solvent system. The plates were exposed overnight to a PhosphorImager screen and

developed the following day with a Molecular Dynamics Typhoon 9200 PhosphorImager.

4.4.12 OM palmitoyltransferase activity assay

Plasmids pBADHePagP and pBADdT2 were electroporated into *E. coli* BKT09 (Table 4.1). Total lipids from these cells were extracted using a single-phase Bligh/Dyer mixture (Bligh and Dyer, 1959). Analysis of lipid IV_A released by mild acid hydrolysis from ³²P-labeled cells was adapted from (Jia *et al.*, 2004; Zhou *et al.*, 1998). Typically, an overnight culture grown at 37 °C was diluted 100-fold into 5mL of LB broth containing appropriate antibiotics and 5 µCi/mL ³²P_i and was grown to OD₆₀₀ of ~0.4, after which the culture was adjusted to include 25 mM of EDTA. Cells were allowed to grow for an additional 5 mins prior to harvesting in a clinical centrifuge. The cell pellet was resuspended in 0.8 mL of PBS and transferred to a Teflon-lined capped glass tube. Methanol and chloroform were added to the cell suspension to generate a single-phase Bligh/Dyer mixture (methanol/chloroform/PBS; 2:1:0.8 v/v/v). After a 1 h incubation at room temperature, the mixture was centrifuged and the insoluble material was washed once with 5 ml of a fresh single-phase Bligh/Dyer mixture. The wet pellet was dispersed in 1.8 mL of 12.5 mM sodium acetate, pH 4.5, containing 1% SDS, with sonic irradiation in a bath apparatus. The mixture was incubated at 100 °C for 30 min. After cooling, the boiled mixture was converted to a two-phase Bligh/Dyer mixture by adding 2 mL of

chloroform and 2 mL of methanol. Partitioning was made by centrifugation, and the lower phase material was collected and washed once with 4mL of the upper phase derived from a fresh neutral two-phase Bligh/Dyer mixture. The lower phase was collected and dried under a stream of N₂ gas. The lipid sample was dissolved in 100 µL of chloroform/methanol (4:1, v/v), and a 5000 cpm portion of the sample was applied to the origin of a Silica Gel 60 TLC plate. The plate was resolved in a sealed tank that was previously equilibrated for ~ 4 h with solvent system chloroform, pyridine, 88% formic acid, water (50:50:16:5 v/v). The plates were dried and exposed to a PhosphorImager screen overnight before developing the next day with a Molecular Dynamics Typhoon 9200 PhosphorImager.

4.5 Results

4.5.1 Sequence analysis of minor clade PagP homologs

HePagP was identified using a variety of *in silico* analyses including Basic Local Alignment Search Tool (BLAST; (Altschul *et al.*, 1990), multiple sequence alignments (Larkin *et al.*, 2007), and phylogenetic tree analysis (Tamura *et al.*, 2013). Initially, we used PaPagP (Thaipisuttikul *et al.*, 2014) as the query sequence in a BLAST search to identify homologous genes of interest. Our search revealed that several species of Gram-negative bacteria encode amino acid sequences homologous to PaPagP. These homologs were distributed between *Rhodoferrax* of the β -subclass, *Pseudomonas* and *Halomonas* of the γ -

subclass, and *Geobacter* of the δ -subclass of Proteobacteria, as well as *Halanaerobium* of the phylum Firmicutes. A maximum-likelihood phylogenetic tree was constructed from these homologous sequences (Figure 4.1). In this tree, *Pseudomonas* and *Halomonas* PagP homologs branched distinctly from proteobacterial PagP homologs, and from the *Halanaerobium* PagP homologs. We further investigated the phylogenetic relationship between HePagP and PaPagP by preparing a separate multiple sequence alignment (Figure 4.2). PagP homologs from the pseudomonads have a deletion corresponding to an invariant 4-amino acid insertion in the halomonad PagP homologs having the consensus sequence LWQP.

We recently demonstrated that the catalytic activity of PaPagP is dependent on H17 (H35 with signal peptide included) (Thaipisuttikul *et al.*, 2014). We identified 10 other residues with putative catalytic activity based on secondary structure prediction models and a separate multiple sequence alignment of PaPagP with homologous proteins from pseudomonads. There are a total of forty-eight conserved residues, nineteen of which map to the surface of PaPagP. Excluding those recently investigated (Thaipisuttikul *et al.*, 2014), there are seventeen remaining. Of these, only the polar residues (N25, N26, N50, S51, Q54, Y84, Y88, D90, K91, N95) are likely candidates for a role in catalysis. Of note, there is only one conserved serine, S51, mapping to the surface of PaPagP. PaPagP has no conserved arginine residues.

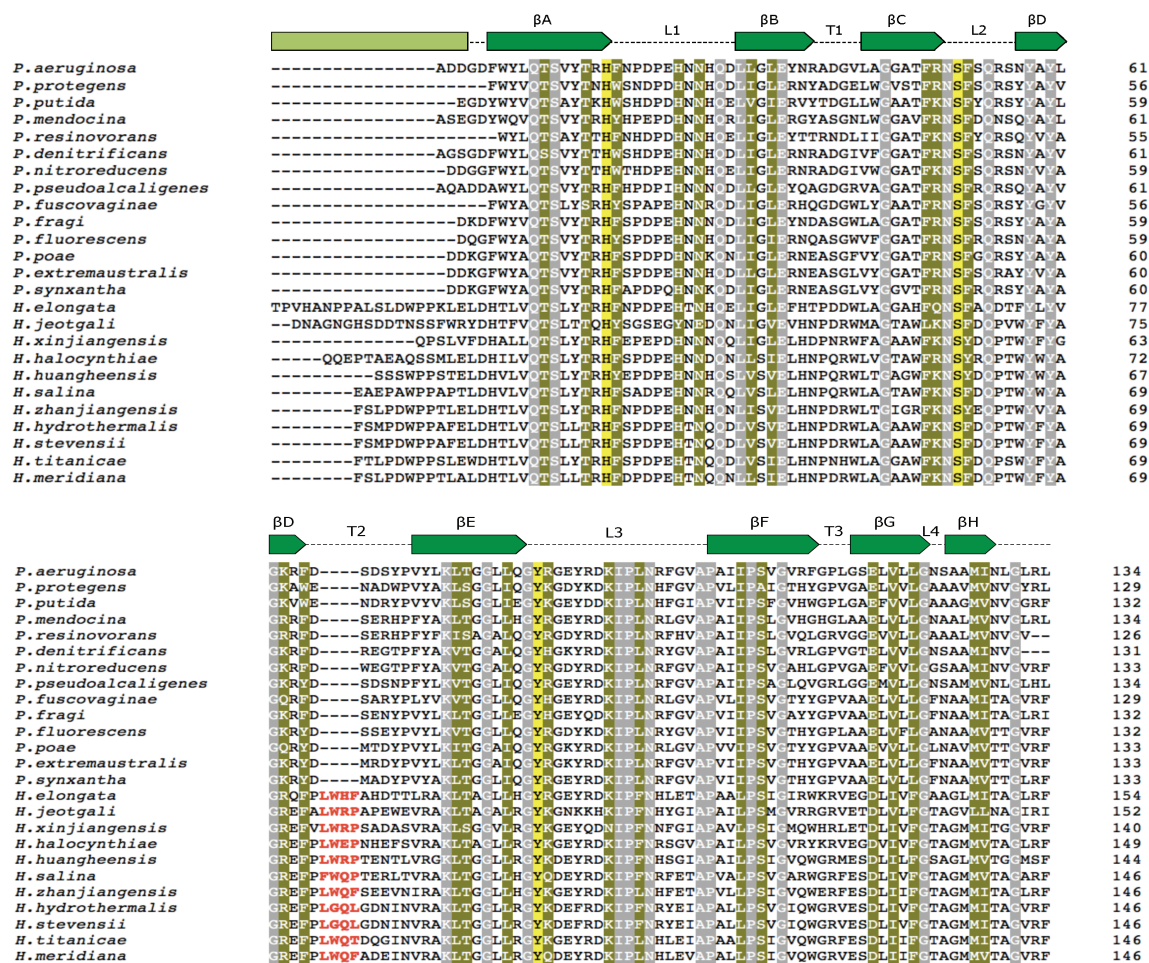


Figure 4.2 A 4-amino acid indel shared by *Halomonas* and *Pseudomonas* PagP homologs. Multiple sequence alignment of PagP showing a 4-amino acid CSI (red) that is uniquely shared by *Pseudomonas* and *Halomonas*. The alignment was constructed after removal of signal peptides predicted by SIGNALP (Peterson *et al.*, 2011). The His, Ser and Tyr, residues shown to be essential for catalysis by site-directed mutagenesis, are highlighted in yellow. Absolutely conserved residues are highlighted in gray, and highly conserved residues are highlighted in green.

4.5.2 Site directed mutagenesis *in vitro* and *in vivo*

To assess the possibility that an all-together different catalytic mechanism than that proposed for EcPagP might be at work, all ten invariant residues mapping to PaPagP's surface were replaced by mutagenesis. The mass of each mutant protein was determined by ESI-MS and compared to the calculated theoretical mass. CD spectroscopy was used to evaluate folding, and the mutants were assayed for activity *in vitro* using the lipid A precursor – lipid IV_A, as the palmitoyl acceptor (Thaipisuttikul *et al.*, 2014). H17A, N26A, S51A, Q54A, Y84A and N95A mutations display a far-UV spectral signature (Figure 4.3) nearly superimposable with that of wild-type PaPagP indicating similarly folded structures. The CD spectra for N25A and D90A were significantly distorted with negative ellipticity maxima near 208 nm and 222 nm, rather than a 218 nm maximum characteristic of n→π* transition derived from peptide bonds in a largely β-sheet conformation (Saxena and Wetlaufer, 1971). Despite this, D90A continues to function as a phospholipase *in vitro*, with a 4-fold reduction in palmitoyltransferase activity. N25A has only residual palmitoyltransferase activity, and a 10-fold decrease in phospholipase activity. We observed a similar trend for Q54A, even though the enzyme's fold is estimated to be the same as wildtype. The N26A mutation affects activity in a manner similar to the N25A, except that the secondary structure of the enzyme is not significantly affected by the substitution to alanine. Y84A has only residual palmitoyltransferase and phospholipase activity, while the Y88A, K91A

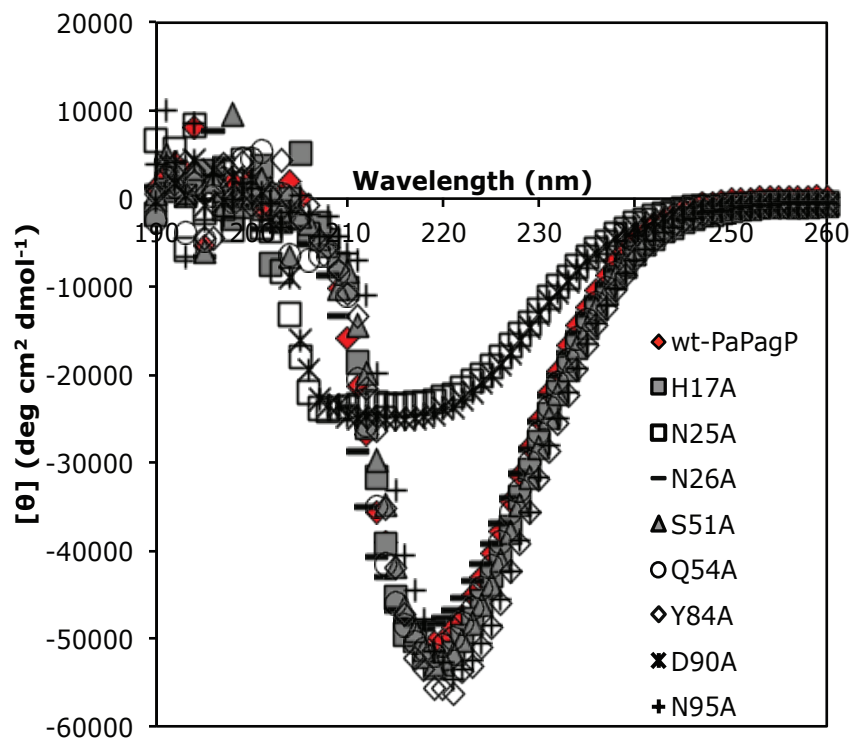


Figure 4.3 Spectroscopic analysis of refolded *P. aeruginosa* PagP mutants. PaPagP and its mutants were refolded in SDS/MPD, diluted in DDM and analyzed by far-UV CD spectroscopy. The mutants H17A, N26A, S51A, Q54A, Y84A, N95 and wild type PaPagP have nearly superimposable CD spectra indicating similarly folded structures. N25A and D90A lack the β -barrel signatures characteristic of PagP.

Table 4.4. *P. aeruginosa* PagP mutant specific activities

Mutant	Palmitoyltransferase (20 μ M [14 C]-DPPC) + 1 mM DPPC+ 100 μ M lipid IV _A	Phospholipase (20 μ M [14 C]-DPPC)
Wildtype	201 \pm 39.4	222.7 \pm 1.28
H17A	Not Detected	Not Detected
N25A	1.8 \pm 2.19	25.9
N26A	3.6 \pm 0.53	42.3
S51A	Not Detected	Not Detected
Q54A	97.8 \pm 13.98	253.3
Y84A	0.4 \pm 9.14	17.2
Y88A	211.1 \pm 2.8	198.9
D90A	179.3 \pm 20.4	51.4
K91A	202.4 \pm 11.2	211.2
N95A	152.6 \pm 51.1	225.3

and N95A mutations did not significantly affect activity. H17A and S51A are inactive in our detergent-based *in vitro* assays. The mutants were expressed with the native signal peptide of PaPagP, under control of the arabinose-inducible promoter pBAD, and activity was triggered by EDTA, in the membranes of a *P. aeruginosa* *Pa1343* deletion strain to assess activity *in vivo*. H17, S51, and Y84 are the only residues, that when substituted to alanine proved to be critical for catalysis *in vivo* (Figure 4.4).

4.5.3 β -barrel domain and α -helical motif of PagP is conserved in *H. elongata* homolog

PaPagP is not predicted to have an amphipathic α -helix at its *N*-terminus, although the β -barrel tertiary structure with an interior hydrocarbon ruler is conserved (Thaipisuttikul *et al.*, 2014). PaPagP consists of 134 residues and shares ~70% amino acid sequence similarity with HePagP, which is 154 residues in length with most of its differences being restricted to the first 20 residues at the *N*-terminus. We suspected that the observed difference in length might be due to the presence of an extension at the *N*-terminus of HePagP. To test this hypothesis the I-TASSER protein structure prediction protocol (Zhang, 2008) was used to construct a homology model of HePagP based on the 3-dimensional structure of *E. coli* PagP (PDB 3GP6). We used four secondary structure prediction protocols: JPRED (Drozdetskiy *et al.*, 2015), SCRATCH

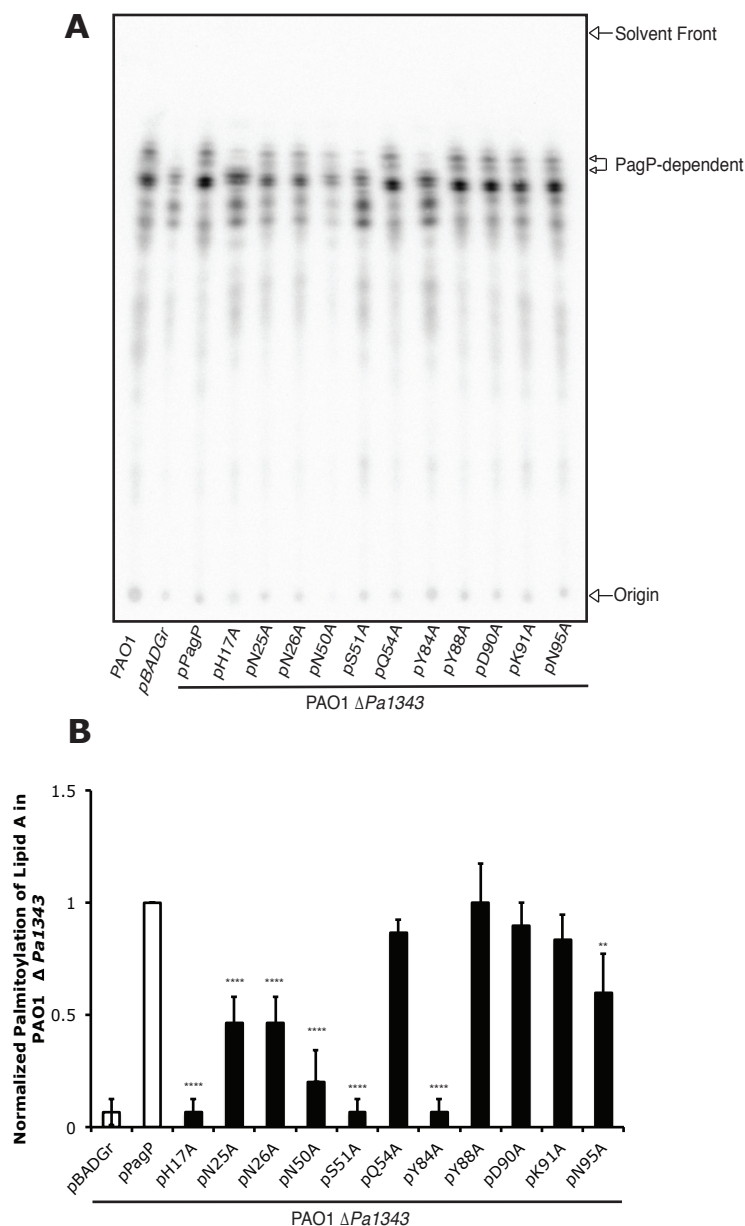


Figure 4.4 Identification of catalytic residues of PaPagP using site directed mutagenesis. Mutations in *P. aeruginosa* PagP result in cells deficient in palmitoylated lipid A. Total lipids were extracted from stationary phase cultures of PAO1 Δ Pa1343 transformed with empty pBADGr vector, PagP or mutant enzyme. The derivative strains were grown in LB and radiolabeled with 32 P. All cultures were treated with 25 mM EDTA for 15 min before sample collection as previously reported (Balibar and Grabowicz, 2016). Samples were developed by TLC and visualized using a phosphor screen. The two major PagP-dependent lipid A species are marked with arrows. A) Representative TLC of lipid A species with and without palmitoyl group B) Production of PagP dependent lipid A species normalized to wild-type. Dunnett's multiple comparison test was used to compare each mutant to wild-type. N=3, **** p< 0.0001; **p, 0.002

(Cheng *et al.*, 2005), PREDICTPROTEIN (Rost *et al.*, 2004), and I-TASSER (Zhang, 2008), to estimate the secondary structure of the first 20 amino acid residues in HePagP. The general consensus of all of the predictions indicates that the *N*-terminal extension is at least partially random and does not contain any α -helical secondary structure due to two pairs of tandem proline residues. Only SCRATCH suggests that there could be some β -structure dispersed within the *N*-terminal extension of HePagP. We also determined from the homology model that the 4-amino acid CSI corresponds to the periplasmic turn T2 observed in *E. coli* PagP (EcPagP); this 4 amino acid insertion is predominantly hydrophobic and sits adjacent to a positively charged surface pore, not observed on the periplasmic face of either EcPagP or PaPagP (Figure 4.5 and Figure 4.6).

4.5.4 *HELO_4100* is the gene encoding PagP in *H. elongata*

In order to confirm that *HELO_4100* encodes the *H. elongata* lipid A palmitoyltransferase, the gene product was expressed with a cleavable 6X-His tag fused to the amino terminus with a TEV cleavage sequence. HePagP was purified under denaturing conditions and we estimate that the fusion protein was ~95% pure at the time of refolding (Figure 4.7A) After refolding in LDAO, the protein was exchanged into 0.2% DDM to facilitate proteolytic cleavage. This was necessary as LDAO inhibits TEV protease activity (Lundback *et al.*, 2008). The cleavage reaction was monitored using SDS-PAGE, and >85% cleavage

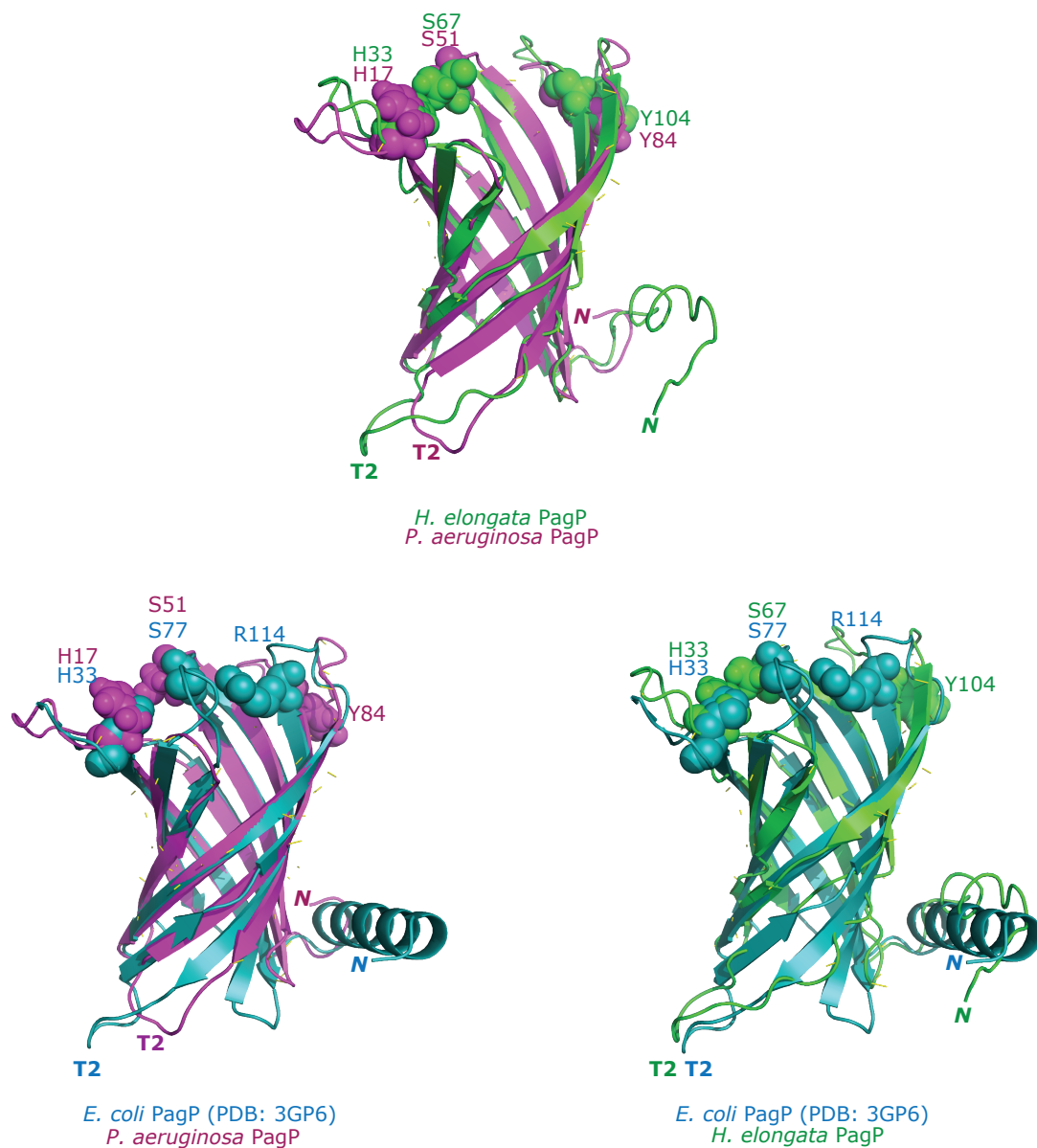


Figure 4.5. I-Tasser Structural alignment of PagP homologs. The homology models of *H. elongata* PagP (green) and *P. aeruginosa* PagP (magenta) are aligned with respect to the solved structure of *E. coli* PagP (cyan). The catalytic triad of these enzymes is shown as spheres. The N-terminus (N) and second periplasmic turn (T2) for each enzyme are labeled.

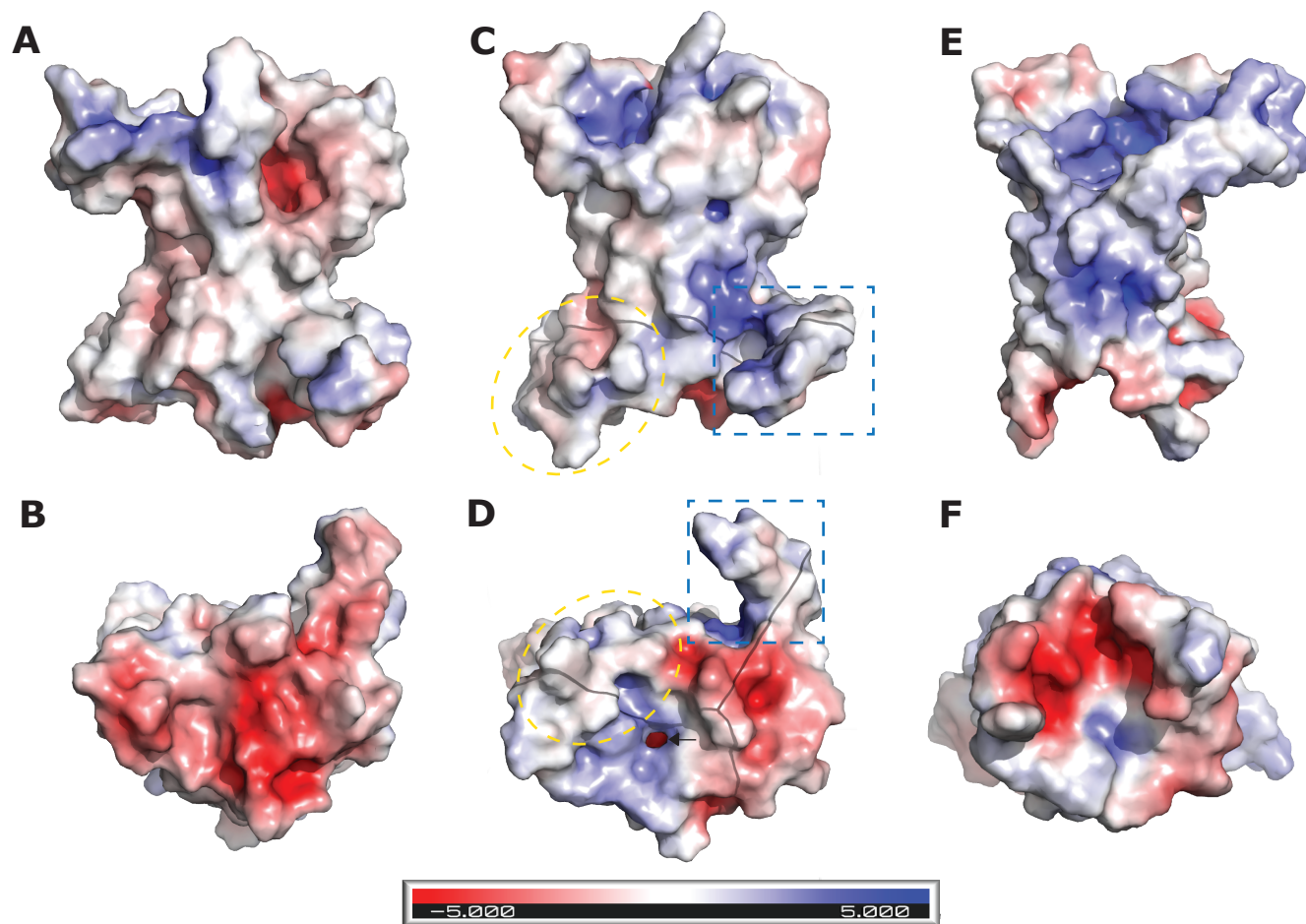


Figure 4.6. Surface representation of PagP showing the distribution of charge surface. Electrostatic surface potential representations for *E. coli* PagP (A & B), *H. elongata* PagP (C & D) and *P. aeruginosa* PagP (E & F). The location of the region formed by the 4-amino acid CSI in *H. elongata* is indicated by the yellow dash circle and the region formed by the *N*-terminal extension is indicated by blue dash box. The positively charged surface is shown in blue whereas negatively charged surface is shown in red. The views on the bottom shows PagP charge distribution after 90° rotation revealing a positively charged pore (arrow) in *H. elongata* PagP. The Electrostatic Potential surface distribution was calculated in PyMOL using the adaptive Poisson–Boltzman solver plug-in. PyMOL Molecular Graphics System, Delano Scientific, USA, version 2.1.1.

was accomplished after 24 h (Figure 4.7B). An attempt was made to purify the protein using gravity flow, nickel affinity chromatography, however the cleaved 6X-His fragment had a low affinity for the Ni^{2+} column and eluted with the cleaved protein. CD was used to estimate secondary structure and folding of the protein before and after the tag was removed. All CD spectra (Figure 4.7C) displayed a negative ellipticity maximum at 218 nm that is characteristic of a largely β -sheet conformation (Saxena and Wetlaufer, 1971). This observation is consistent with the β -barrel structure of PagP. We also followed loss of the negative ellipticity maximum at 218 nm in thermal unfolding experiments to evaluate the stability of the enzyme. HePagP was unfolded irreversibly in these experiments and precipitated after incubation at 105°C (Figure 4.7D). The fusion protein is considerably more stable in 0.2% DDM than in 0.1% LDAO, since the thermal unfolding temperature (T_U) increased by more than 10°C, and the non-cooperative unfolding behaviour became cooperative unfolding behaviour after the fusion protein was exchanged in DDM. Once the His-tag was cleaved by TEV in DDM, the cooperative unfolding increased to 95°C.

The cleavage reaction was applied to a charged Ni^{2+} column to remove the His-tagged TEV fragments. The His-tagged TEV fragments, did not bind well sufficiently to the column to allow purification of HePagP. Due to the challenges we encountered with purifying the enzyme, we discontinued this construct and opted for a C-terminally His- tagged construct that displays similar CD and thermal stability to the untagged impure sample just shown.

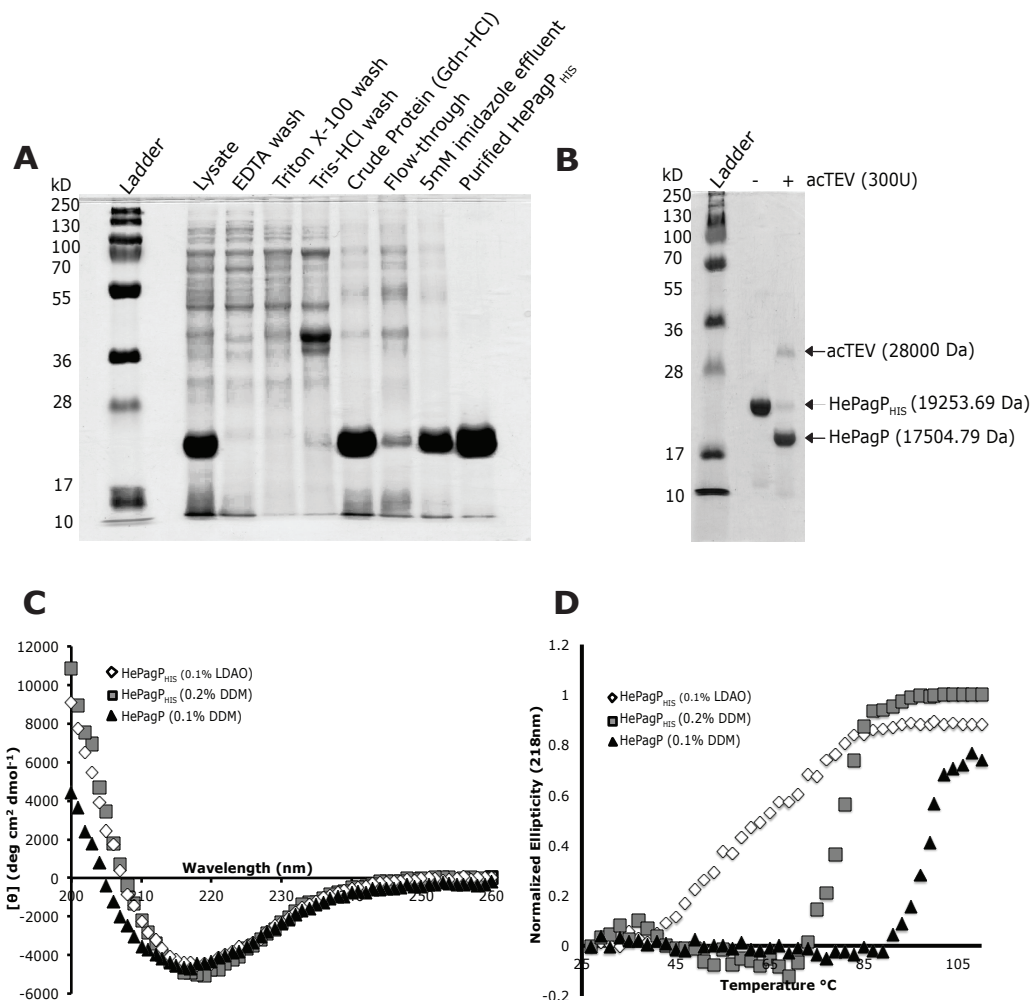


Figure 4.7. Spectroscopic analysis of refolded HePagP and evaluation of thermal stability. HePagP^{TEV} was expressed with a cleavable N-terminal poly-histidine (6X-His) tag in cytoplasmic inclusion bodies in C41(DE3) cells. The fusion protein was purified by selective precipitation and A) Forty microgram of total protein from each wash was resolved with SDS-PAGE. B) Polyhistidine tag of refolded HePagP in 1% DDM was cleaved with 300U of TEV. C) Far-UV CD spectra of refolded HePagP before and after removal of N-terminal polyhistidine tag. D) Thermal unfolding profiles of HePagP assessed by following the loss of the negative ellipticity maximum at 218 nm observed in panel C.

4.5.5 Enzymology of minor clade PagP homologs.

Experimental evidence suggests the presence of a hydrocarbon ruler in HePagP because the enzyme excludes acyl chains longer and shorter than palmitate (Figure 4.8A). Additionally, as shown in Figure 4.8B, only DDM with its bulky substituents that sterically preclude detergent binding within the hydrocarbon ruler, was able to support the lipid A palmitoyltransferase reaction (Khan *et al.*, 2010a; Khan *et al.*, 2010b; Thaipisuttikul *et al.*, 2014). Detergents like LDAO and DPC that mimic the structures of fatty acyl chains are competitive inhibitors of PagP.

To compare the phospholipid:lipid A palmitoyltransferase activity of HePagP and EcPagP, we monitored palmitoylation of lipid IV_A and *E. coli* Kdo₂-lipid A (Figure 4.8D). Whereas *E. coli* PagP could palmitoylate both substrates, HePagP could only palmitoylate lipid IV_A, consistent with the available regiospecificities for palmitoylation at the 3' position in HePagP and for the 2 position in EcPagP; both these positions are free in lipid IV_A while only the latter is free in Kdo₂-lipid A.

We also investigated the ability of HePagP and PaPagP to palmitoylate the *sn*-3'-OH moiety of PG, using assay conditions similar to those described by Dalebroux *et al.* (2014). Figure 4.8C and Figure 4.9 shows the autoradiograph of *in vitro* assays when purified HePagP, PaPagP and EcPagP were incubated with

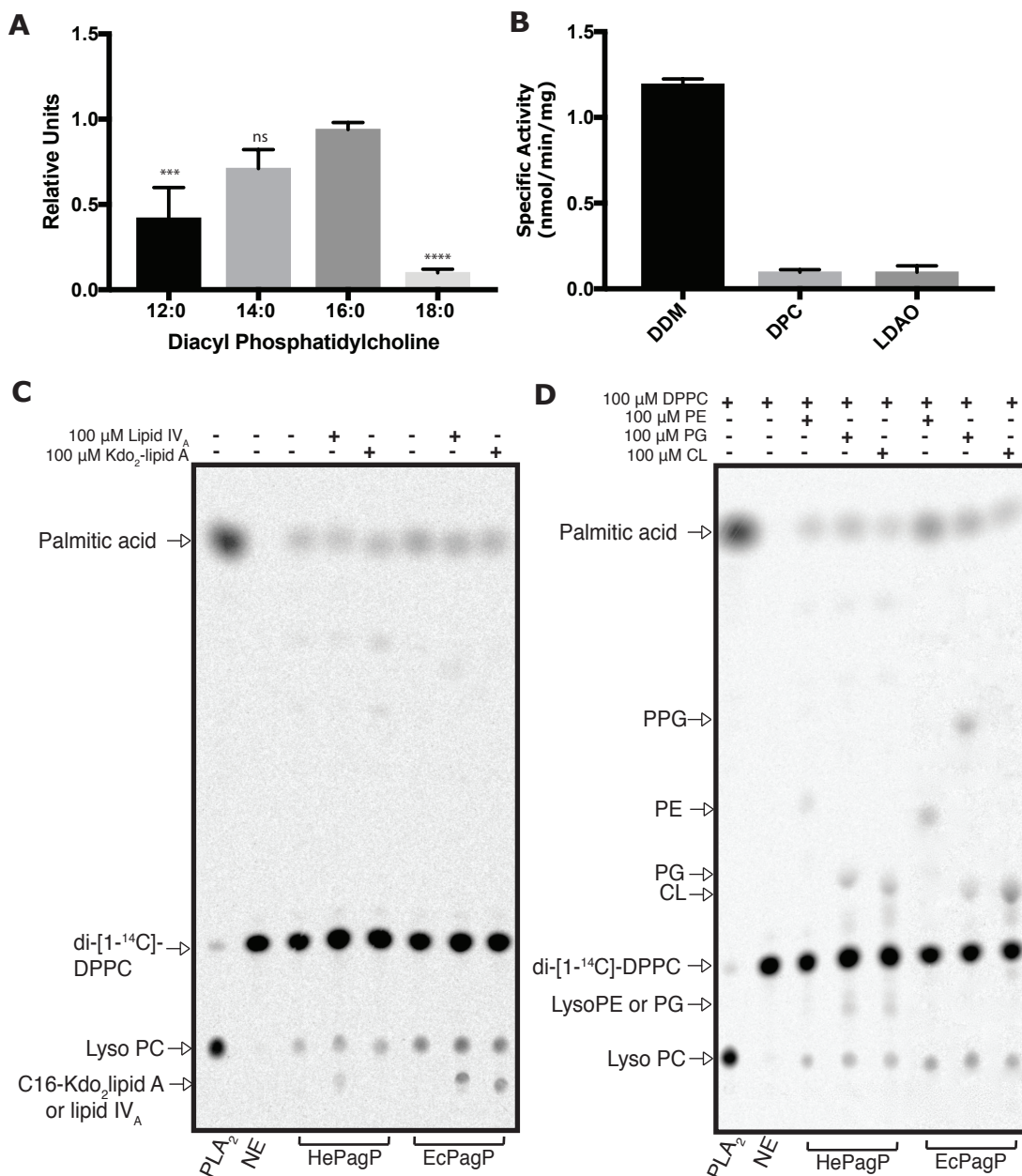


Figure 4.8. HePagP Hydrocarbon ruler and substrate specificity. A) Specific activity for the conversion by PaPagP of [³²P]-lipid IV_A to lipid IV_B using symmetrical phosphatidylcholine donors of saturated acyl chain compositions varying from C12 to C18 in ethylene unit increments. B) Phospholipase activity in the absence of lipid A acceptors. Phospholipase activity is associated with production of free palmitate (C16) and Lyso-PC from DPPC in the presence of dodecyl-maltoside (DDM). C) Thin layer chromatogram showing palmitoylation of lipid IV_A and Kdo₂-lipid A to produce lipid IV_B and C16-Kdo₂-lipid A. D) Thin layer chromatogram showing palmitoylation of phosphatidylglycerol (PG) by EcPagP to produce palmitoyl-PG (PPG). Dunnett's multiple comparison test was used to compare each mutant to wild-type. N=3, **** p< 0.0001; ***p, 0.001. Abbreviations: phosphatidylethanolamine (PE); cardiolipin (CL) Fos-choline-12 (DPC); LDAO (lauryldimethylamine-N-oxide).

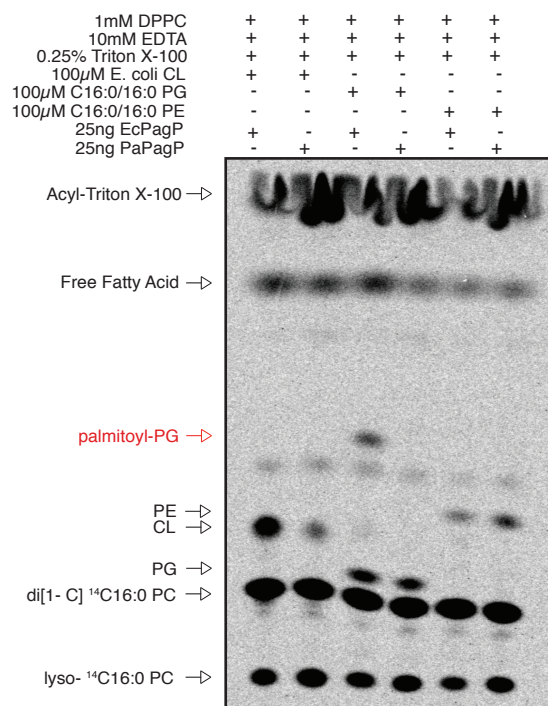


Figure 4.9. Representative TLC autoradiograph showing palmitoylation of phosphatidylglycerol. *P. aeruginosa* PagP (PaPagP) does not transfer palmitate to phosphatidylglycerol (PG) *in vitro*. *E. coli* can transfer palmitate to the *sn*-3'-OH moiety of PG to produce PPG, but does not transpalmitoylate the head group of phosphatidylethanolamine (PE) or cardiolipin (CL).

the labeled palmitate donor dipalmitoyl-1-¹⁴C-DPPC, and an unlabeled phospholipid. In the absence of an acceptor, PagP is known to exhibit slow phospholipase activity that results in an accumulation of palmitic acid and a corresponding lysophospholipid. Subsequent phospholipid::lysophospholipid transacylation can allow ¹⁴C-labeled palmitate to exchange into non-radioactive phospholipids. Finally, when a suitable acceptor is present, as in the case of phosphatidylglycerol (PG), *E. coli* PagP is able to transfer some of that palmitic acid to PG to produce palmitoyl-PG. Neither HePagP nor PagP were able to do this in our detergent based assays.

4.5.6 The 4-amino acid CSI of HePagP is dispensable for folding, but critical for catalysis.

CSI's in conserved regions of proteins can identify functionally important structural elements (Gupta, 1998). To examine the significance of the CSI in the T2 turn, we prepared a mutant with the indel removed (HePagP_{ΔT2}) and compared its secondary structure to wild-type (HePagP_{WT}). HePagP and its T2 mutant were successfully refolded in LDAO and DDM detergents. CD spectra were nearly superimposable indicating similarly folded structures. (Figure 4.10A). We also followed loss of the negative ellipticity maximum at

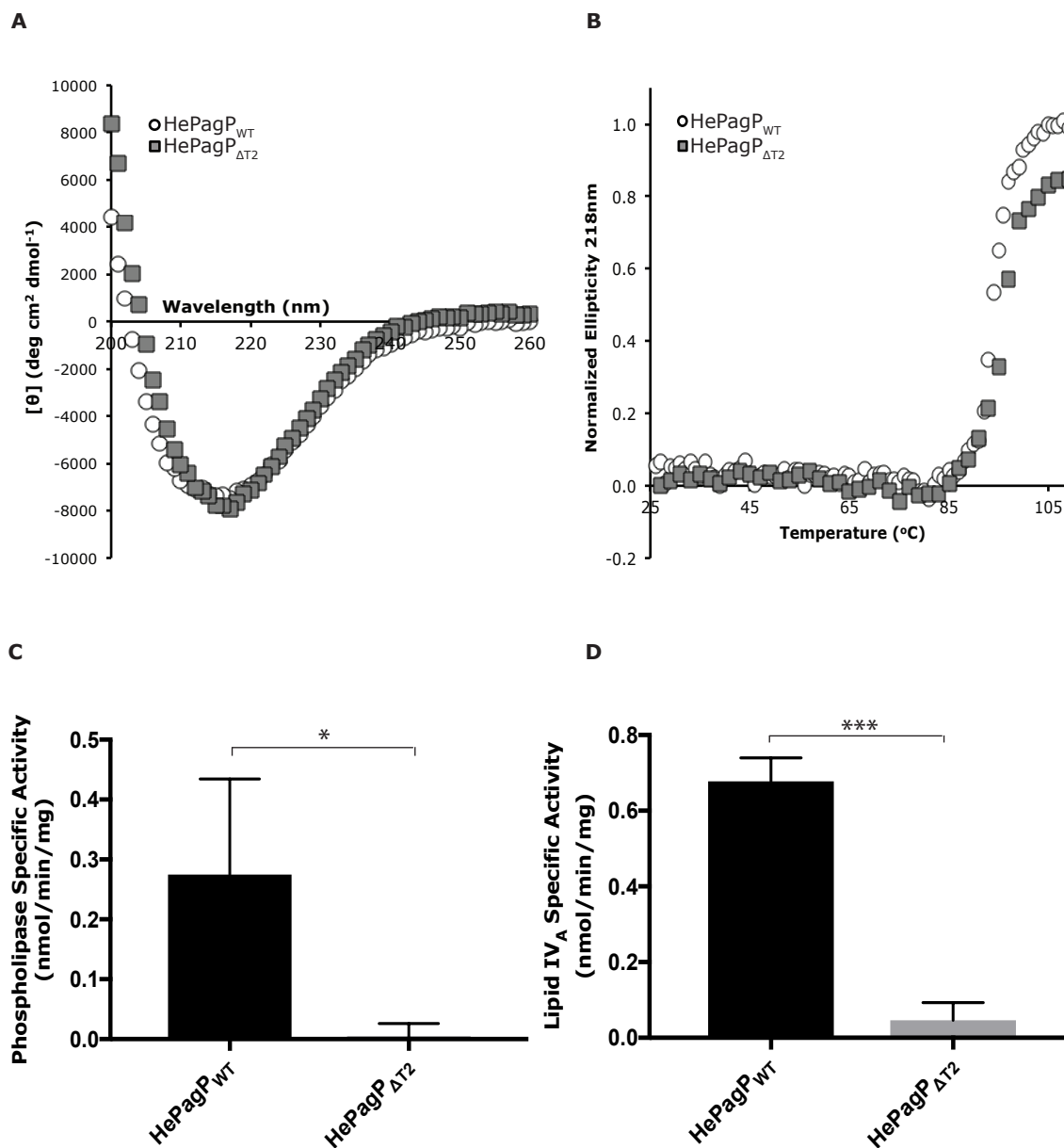


Figure 4.10. Effects of CSI on folding, thermal stability and catalysis of HePagP.

HePagP and HePagP_{ΔT2} were expressed with a C-terminal His-tag in cytoplasmic inclusion bodies in C41(DE3) cells and folded in 0.2% DDM. A) Far-UV CD spectroscopic analysis of refolded HePagP and HePagP_{ΔT2}. B) Thermal unfolding profiles of refolded protein assessed by following the loss of the negative ellipticity maximum at 218 nm observed in panel A. (C and D) Phospholipid:lipid A palmitoyltransferase and phospholipase activity measured for HePagP and T2 mutant. Specific activity for the phospholipase reaction is shown in panel C and that for the palmitoyltransferase reaction in panel D. Error bars represent the mean \pm the SEM. *p < 0.05, ***p < 0.0001

218 nm in thermal unfolding experiments to evaluate the stability of the T2 mutant. Both proteins share a similar T_U near 95°C (Figure 4.10B)

While the loss of the T2 indel did not appear to affect secondary structure or protein stability, we observed effects on enzyme activity. PagP phospholipase activity can be monitored through the hydrolysis of ^{14}C -DPPC, while PagP palmitoyltransferase activity can be monitored through the ^{14}C -palmitoylation of the lipid A precursor lipid IV_A . Refolded HePagP and its T2 mutant were incubated with radiolabeled ^{14}C -DPPC, with and without lipid IV_A . The specific activity of HePagP appears to be 1000-fold higher than that of the T2 mutant for the phospholipase reaction (Figure 4.10C), but this activity was comparable to the no enzyme control and represents the limit of detection. The specific activity for the palmitoyltransferase reaction of HePagP was nearly 15-fold greater than that of the T2 mutant (Figure 4.10D).

We also studied the palmitoylation profiles of HePagP, HePagP $_{\Delta\text{T}2}$, PaPagP and PaPagP $_{\text{InsT}2}$ in the OM of three cell types (Table 4.1): *E. coli* BKT09 (Emptage *et al.*, 2012), which expresses a tetra-acylated lipid A that lacks any acyloxyacyl structures, *E. coli* WJ0124 (Jia *et al.*, 2004), which produces a hexa-acylated lipid A that lacks any acyloxyacyl structures at the 2 and 3 positions, and *P. aeruginosa* MB5919 (Balibar and Grabowicz, 2016), which produces a penta-acylated lipid A that lacks any acyloxyacyl structures at the 3' position. Growth of these cells in ^{32}P -orthophosphate followed by mild acid hydrolysis of the isolated LPS releases ^{32}P -lipid A and ^{32}P -lipid IV_A

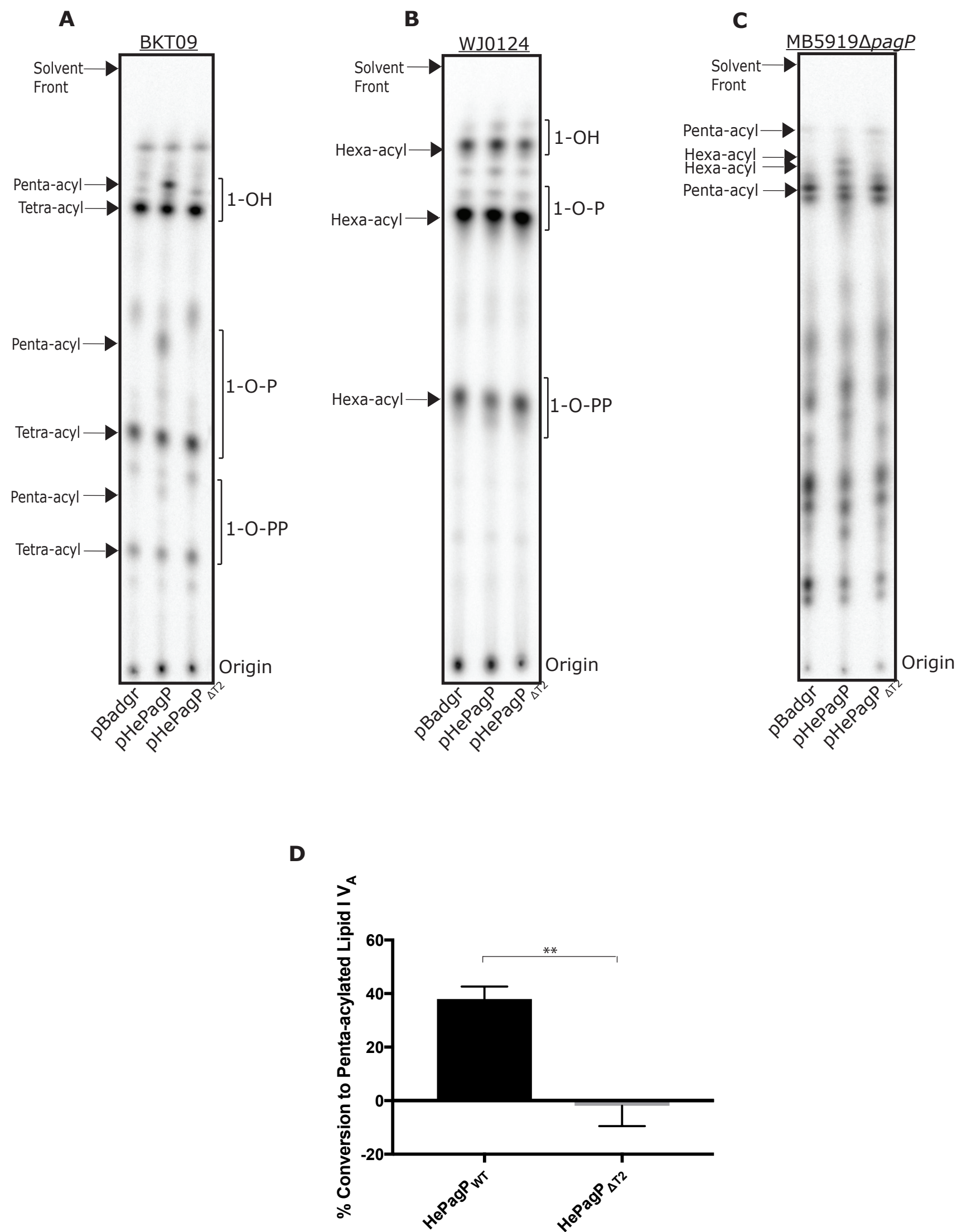


Figure 4.11 Lipid IV_A palmitoylation is induced *in vivo* by overexpression of PagP. Cells were labeled with ³²P and Lipid A or Lipid IV_A isolated by mild acid hydrolysis. (A) The lipid isolates were separated by TLC using solvent system B and visualized with a PhosphorImager. Three lipid species are indicated to the right of the figure and include 1,4'-bisphosphate (1-O-P), 1-pyrophosphate (1-O-P-P), and the 4'-monophosphate (1-OH) Lipid IV_A. The tetra- and penta-acylated derivatives of each Lipid IV_A species are indicated to the left of the figure. HePagP Δ T2 does not produce a penta-acylated lipid species. (B) Chemical representation of 4'-monophosphate Lipid IV_A (C) Approximately 40% of tetraacylated (1-OH) significantly converted to penta-acylated (1-OH) Lipid IV_A. Error bars represent the mean \pm the standard deviation of triplicates. **p,0.001

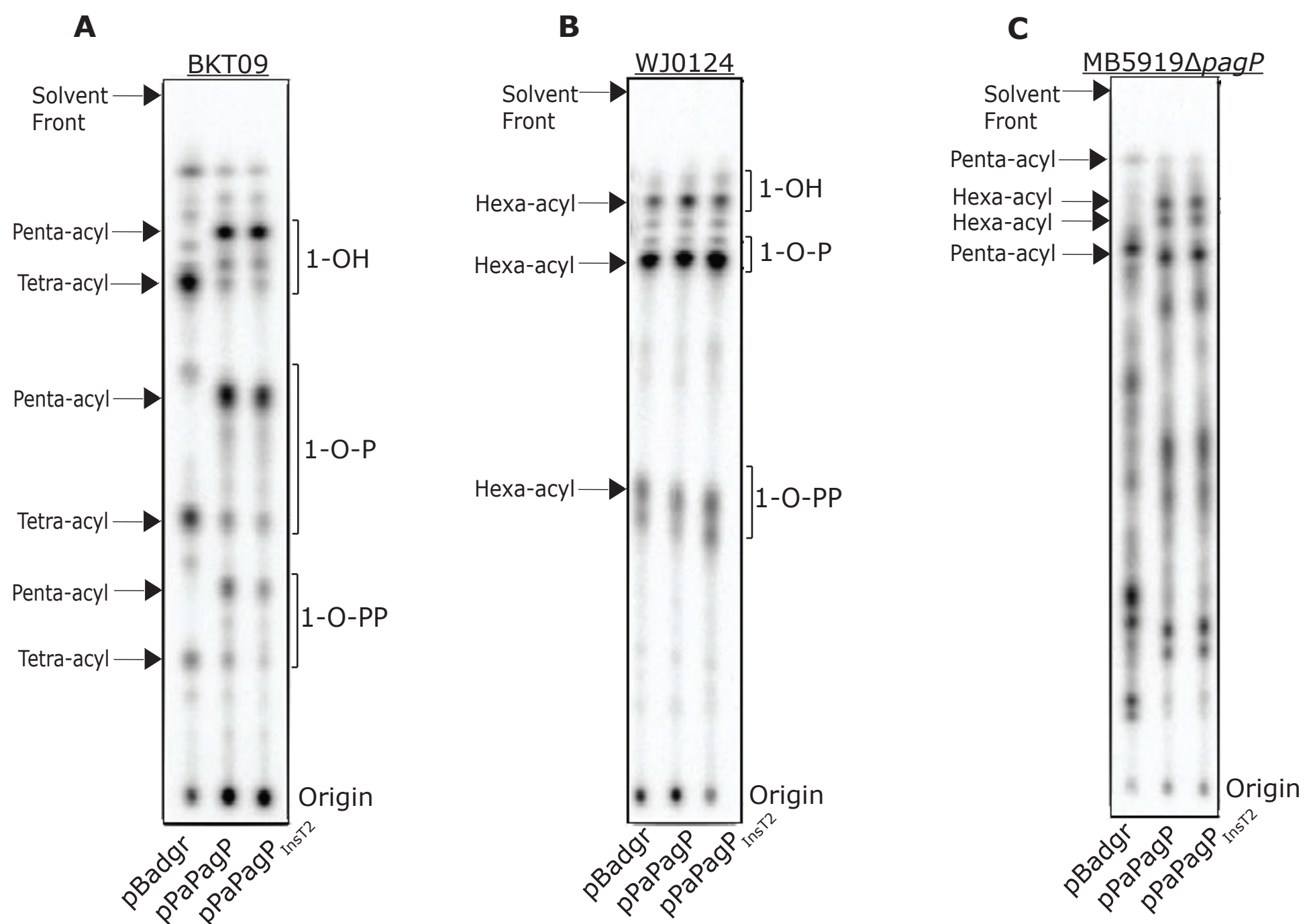


Figure 4.12 Lipid IV_A palmitoylation is induced *in vivo* by overexpression of PagP. Cells were labeled with ³²P and Lipid A or Lipid IV_A isolated by mild acid hydrolysis. (A) The lipid isolates were separated by TLC using solvent system B and visualized with a PhosphorImager. Three lipid species are indicated to the right of the figure and include 1,4'-bisphosphate (1-O-P), 1-pyrophosphate (1-O-P-P), and the 4'-monophosphate (1-OH) Lipid IV_A. The tetra- and penta-acylated derivatives of each Lipid IV_A species are indicated to the left of the figure. PaPagP_{InsT2} does not produce a penta-acylated lipid species. (B) Chemical representation of 4'-monophosphate Lipid IV_A. (C) Approximately 40% of tetraacylated (1-OH) significantly converted to penta-acylated (1-OH) Lipid IV_A. Error bars represent the mean ± the standard deviation of triplicates. **p,0.001

with varying acylation. HePagP and HePagP Δ T2 were overexpressed *in vivo* with native signal peptides from the arabinose inducible pBAD promoter and activity was triggered in membranes by brief treatment with EDTA as previously described (Jia *et al.*, 2004). The lipid IV_A and lipid A migrate in TLC as three separate species depending on the phosphorylation status of the anomeric carbon, but these species are converted to faster-migrating species upon palmitoylation by PagP (Figure 4.11). Insertion of the CSI in PaPagP is not important for palmitoyltransferase activity in the OM because we observed the formation of a faster migrating species in all cells expressing PaPagP and PaPagP_{InsT2} (Figure 4.12). We did not observe the formation of hepta-acylated lipid A species in *E. coli* WJ0124 cells, which suggest that HePagP was unable to use the available 2 and 3 position of the lipid A species produced in these cells (Figure 4.11). HePagP could use the available 3' position in *P. aeruginosa* MB5919 and *E. coli* BKT09. None of the cells carrying the HePagP Δ T2 mutant produced a faster migrating lipid A species, which suggests that it is either enzymatically inactive in membranes or that it fails to be expressed and assembled in these cells.

Due to the modest expression of the pBADGr system described above, we wanted to increase protein production to see if we could detect HePagP Δ T2 assembly in membranes. We used the IPTG-inducible pET21a⁺ system to

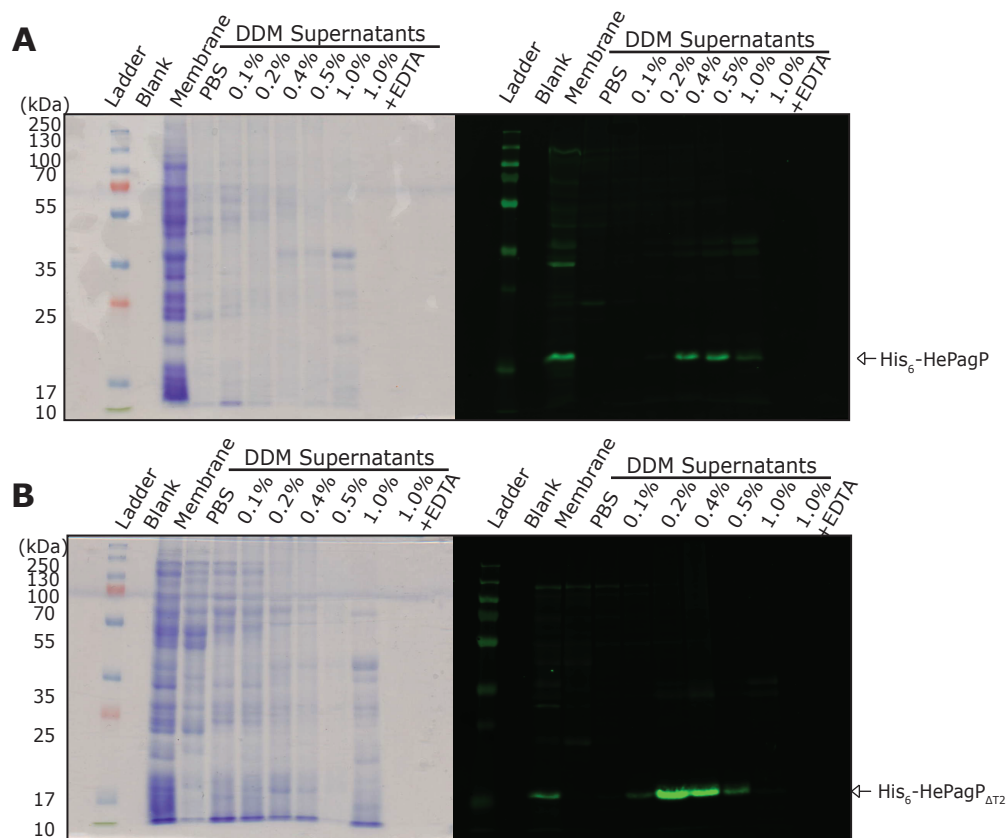


Figure 4.13. Expression and membrane localization of HePagP and HePagP_{ΔT2} in *E. coli* C41(DE3)pLysS. To express C-terminally His-tagged HePagP and HePagP_{ΔT2} a single colony of C41(DE3)pLysS transformed with pETHeloH or pETΔT2H was inoculated into 10mL of LB and grown overnight. The overnight culture was used as a 1% inoculum for 1L of LB. The culture was grown to OD₆₀₀ = 0.4-0.6 before induction with 1mM IPTG for 4H. Cells were harvested and membranes were prepared from cell lysates. The membrane fraction was serially washed with PBS using 18, 21 and 25 gauge syringes. The supernatant was collected by centrifugation. The membranes were resuspended in the same manner using 10mM Tris-HCL pH 8.0 containing 0.1, 0.2, 0.4, 0.5, 1.0% DDM, followed by a final resuspension with 10mM Tris-HCL pH 8 containing 10mM EDTA and 1.0% DDM. Samples were analyzed by SDS-PAGE on 15% polyacrylamide gels followed by Coomassie blue staining or transferred onto polyvinylidene difluoride membranes probed with an anti-His antibody. A) HePagP B) HePagP_{ΔT2}.

express the His-tagged HePagP_{ΔT2} in membranes of *E. coli* C41(DE3) pLysS cells for detection by immunoblotting. Our results confirm that HePagP_{ΔT2} can be over-expressed to the same extent as wild-type and detected in membranes (Figure 4.13), and we presume that it is also expressed and assembled to a lesser extent in *E. coli* BKT09 using the pBADGr system. We conclude that HePagP_{ΔT2} is capable of being expressed and assembled in membranes, but it is enzymatically inactive both in membranes (Figure 4.11) and when refolded *in vitro* (Figure 4.10).

4.5.7 *N*-terminal motif of HePagP is critical for β-barrel thermal stability and catalytic activity

To investigate the role of the *N*-terminal extension in HePagP, we deleted it in HePagP_{ΔNT} and also replaced it with the amphipathic α-helix from *E. coli* PagP in HePagP_{EcNT}. Far-UV CD was used to assess folding of the chimeras, and thermal unfolding profiles were obtained by following the loss of the negative ellipticity maximum at 218nm (Figure 4.14). Both chimeras display spectra similar to HePagP (Figure 4.14A), which is very stable with a T_U near 95°C (Figure 4.14B). Removal of the *N*-terminal extension reduces the T_U by 20°C, but substitution with the *E. coli* amphipathic α-helix restores the T_U to 95°C. The different plateaus reached for the unfolded proteins (Figure 4.14B) indicate the relative amounts of intermolecular β-structure formed in the denatured state, which compensates for the loss of intramolecular β-structure

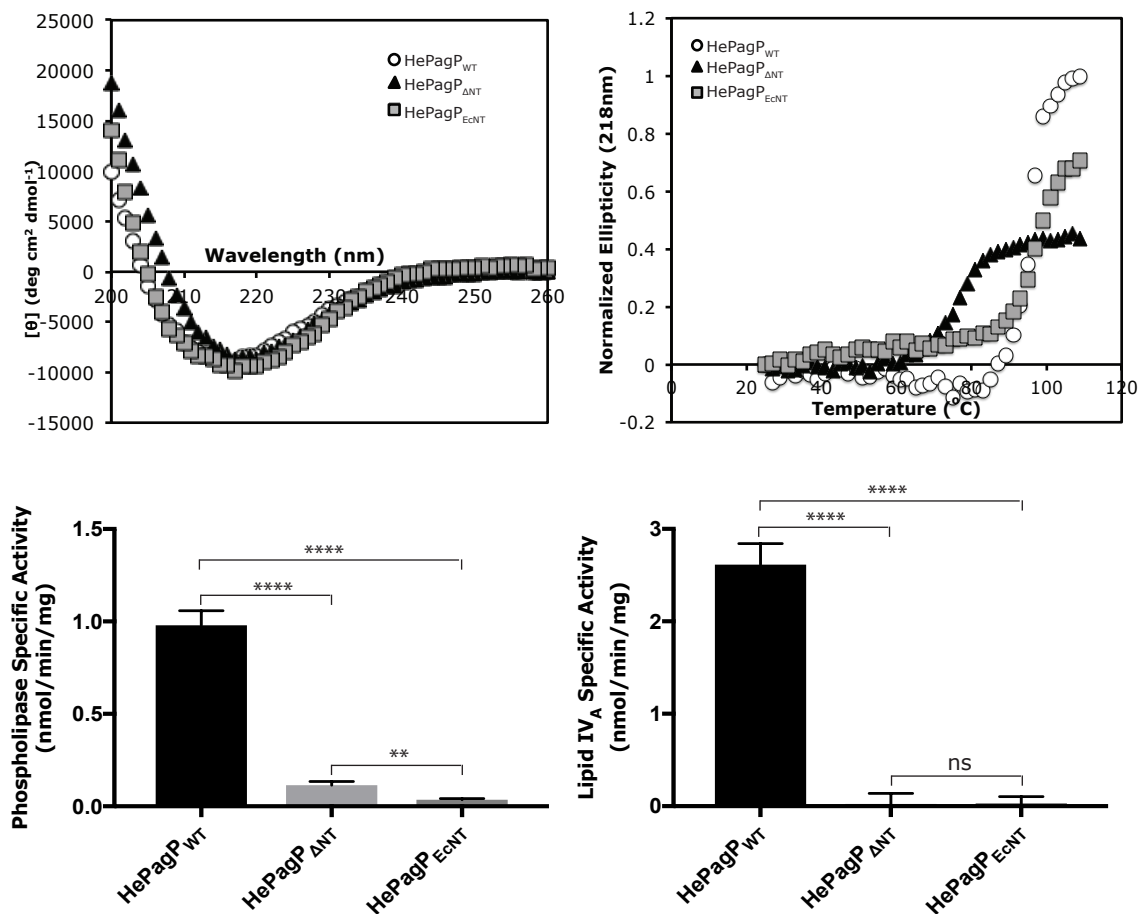


Figure 4.14. Effects of *N*-terminal motif on folding, thermal stability and catalysis of HePagP. A) Far-UV CD spectra of refolded HePagP chimeras. B) Thermal unfolding profiles of refolded protein assessed by following the loss of the negative ellipticity maximum at 218 nm observed in panel A. (C and D) Phospholipid:lipid A palmitoyltransferase and phospholipase activity measured for HePagP chimeras. Specific activity for the phospholipase reaction is shown in panel C and that for the palmitoyltransferase reaction in panel D. Error bars represent the mean \pm SEM of triplicates. ** $p < 0.002$, **** $p < 0.0001$. Abbreviations: ns, not significant.

during β -barrel unfolding because both of these forms of β -structure contribute negative ellipticity at 218 nm (Khan *et al.*, 2007). More importantly, our findings are consistent with the previous functional assignment of the *N*-terminal amphipathic α -helix in *E. coli* PagP as a post-assembly clamp (Huysmans *et al.*, 2010; Iyer and Mahalakshmi, 2016), and the *N*-terminal extension in HePagP might fulfill a similar stabilizing role. Interestingly, HePagP shows enzyme activity that is significantly higher than both chimeras in our detergent based assays (Figure 4.14). In order to optimize secretion into membranes of *E. coli* we expressed HePagP and HePagP $_{\Delta NT}$ by including the signal peptide that is native to *E. coli* PagP. SignalP (Petersen *et al.*, 2011) was used to confirm that cleavable signal sequences were present in the encoded chimeric proteins. However, we were unable to confirm the expression in membranes as we did for HePagP $_{\Delta T2}$ (data not shown). We conclude that chimeric signal peptide cleavage and/or targeting to the OM was limiting for these constructs.

4.6 Discussion

Like PaPagP, HePagP has diverged beyond detection at the level of amino acid sequence similarity from the major clade PagP homologs, and yet it can be purified under denaturing conditions using a procedure developed for enterobacterial PagP (Thaipisuttikul *et al.*, 2014). HePagP is remarkably stable with a T_U of 95°C, making it the most thermally stable PagP homolog identified

to date. However, HePagP is also one of the least active PagP homologs, at least when we employ enterobacterial phospholipids and lipid A precursors as substrates, which suggests that HePagP might be adapted to recognize lipid structural features that are unique to the halomonads. Alternatively, it has recently been demonstrated with *Salmonella* and *E. coli* PagP homologs that the thermodynamic cost of high stability can be offset by reduced catalytic activity (Iyer and Mahalakshmi, 2015, 2016). This activity–stability trade-off can be influenced by factors secluded from the catalytic region. Perhaps the 4-amino acid CSI in the T2 turn of HePagP can partly explain its high stability and low enzymatic activity.

The CSI is located in turn T2 on the periplasmic face of the enzyme away from the putative catalytic residues of the extracellular facing loops, as well as the hydrophobic phospholipid binding site. The location of this CSI is not unusual as indels occur most often in loops and turns flanked by conserved sequences (Gupta, 1998; Pascarella and Argos, 1992). Indels in these locations are less likely to disrupt folding than indels in the core of the protein. Importantly, the deletion of the CSI in HePagP produced an inactive protein that folded normally both *in vitro* and *in vivo*. The CSI does not appear to have a functional role in PaPagP as we were unable to detect any changes in the palmitoyltransferase activity in membranes expressing PaPagP_{InsT2}. The genetic changes represented by CSIs have been shown to be essential for the group of organisms in which they are found (Gupta *et al.*, 2017). The CSI clearly

supports a catalytically competent state of the β -barrel scaffold in HePagP. The CSI in HePagP also suggests that a common ancestor of the minor clade shares features of the enterobacterial PagP homologs. Interestingly, a 2-amino acid insertion is also present at the same position in some major clade PagP homologs (Chapter 5). We can't exclude the possibility that the functional role played by this CSI in the minor clade of PagP is also fulfilled by insertions of different lengths in the same position for members of the major clade of PagP. A commonality of indels associated with functional attributes in the same protein from various species can indicate that the proteins are derived from a common ancestor (Gupta, 1998; Gupta *et al.*, 2017).

Another structural element that differs between PaPagP and HePagP is the *N*-terminal extension. HePagP is predicted to have an *N*-terminal extension reminiscent of the amphipathic α -helix found in *E. coli* PagP, whereas PaPagP and other minor clade homologs are not predicted to have this extension. HePagP is unique among minor clade homologs because its structure is intermediate between other minor clade homologs like PaPagP and major clade homologs like EcPagP (Figure 4.5). The *N*-terminal α -helix of *E. coli* PagP has been shown to function as a post-assembly clamp that stabilizes the protein in liposomes (Huysmans *et al.*, 2010; Iyer and Mahalakshmi, 2016). The *N*-terminal extension in HePagP may function in a similar capacity by stabilizing the enzyme as removal of the *N*-terminal extension destabilized the enzyme, as significantly reduced the activity of the enzyme in our detergent assays. This

difference in activity likely reflects a perturbation of a catalytically competent conformation of the β -barrel structure. Although the amphipathic α -helix of EcPagP is equally stabilizing, the chimera is not active. One possible explanation for the dependence of HePagP activity on the presence of its native *N*-terminal extension is that the extension, which includes two pairs of tandem proline residues that disrupt α -helical structure, may trigger subtle structural rearrangements in the transmembrane β -barrel scaffold that are important for activity.

Major and minor clade PagP homologs likely share a similar catalytic mechanism since they all have strikingly conserved the two catalytic His and Ser residues in homologous positions (Figure 4.5). The catalytic Ser evaded detection when the PaPagP sequence was forced into alignment with major clade PagP homologs (Thaipisuttikul *et al.*, 2014), but its conservation became apparent once alignment was restricted to minor clade homologs (Figure 4.2). PagP enzymes are thought to function through a mechanism similar to that proposed for the carnitine acyltransferases (Jogl *et al.*, 2004; Jogl and Tong, 2003) because this mechanism is most consistent with known PagP enzymology. In our proposed mechanism for PagP, the His functions as a general base to abstract a proton from the hydroxyl group of the lipid acceptor bound at the embrasure, so it can be activated for nucleophilic attack on the carbonyl carbon of the *sn*-1-palmitoyl group in the phospholipid donor bound within the hydrocarbon ruler. The serine does not function as a nucleophile, but simply as

a hydrogen bond donor to stabilize the oxyanion in the tetrahedral transition state that forms in the ternary complex. The protonated His can then function as a general acid to donate its proton to the *sn*-1 hydroxyl group of the lysophospholipid leaving group. In major clade PagP homologs a critical Arg residue additionally functions to electrostatically stabilize the polar head group of the phospholipid donor as it docks into the hydrocarbon ruler after being laterally gated through the crenel, but this Arg is not conserved in minor clade PagP homologs. Instead, minor clade PagP homologs have a critical Tyr residue in a nearly identical location as the Arg, but it is displaced by one residue so the Tyr becomes exposed on the β -barrel exterior. The Tyr clearly cannot fulfill an analogous function as the Arg in major clade PagP homologs, but it might serve a role in gating phospholipid access through the crenel as such gating is known to be governed by a Tyr residue in EcPagP. However, the presence of a crenel structure for lateral gating of phospholipids in minor clade PagP homologs remains to be confirmed structurally.

Despite conservation of the catalytic His and Ser residues, minor clade PagP homologs palmitoylate the 3' position of lipid A instead of position 2 as is characteristic of EcPagP. However, some major clade PagP homologs from the β -Proteobacteria, namely *B. bronchiseptica* and *B. parapertussis*, have been reported to palmitoylate lipid A at the 3'-position (Hittle *et al.*, 2015; Pilione *et al.*, 2004; Preston *et al.*, 2003), further testifying that the two clades of PagP are likely derived from a common ancestor. As with PaPagP, regulated acylation at

the 3' position may be important for the lifestyle of *Halomonas. P.aeruginosa* produces a distinctly pro-inflammatory lipid A that is important for morbidity and mortality during infections (Ernst *et al.*, 2007; Ernst *et al.*, 1999). Unlike EcPagP, neither PaPagP nor HePagP transfers palmitate to the *sn*-3' OH moiety of PG, suggesting that the acquisition of this activity, along with the different lipid A regiospecificity, helps to explain the divergence of the PagP family into two separate clades.

Structures tend to be more conserved than sequences (Chothia and Lesk, 1986; Hilbert *et al.*, 1993) and we have demonstrated that structures can be aligned in spite of very low sequence identity. There are examples of divergent evolution in the catalytic triads of proteolytic enzymes, which have been adapted to serve different functions (Gerlt and Babbitt, 2001; Murzin, 1998). The case that the minor and major clades of PagP result instead from convergent evolution suffers from the shared catalytic residues, the ancestral lipid A 3'-regiospecificity, the common insertion in the T2 turn, the common stabilizing *N*-terminal extension, and the shared 8-stranded antiparallel β -barrel architecture with an interior hydrocarbon ruler. The question as to where PagP first evolved remains. The most ancient bacteria to encode PagP homologs are found in the β -Proteobacteria in both the minor and major clades. However, the minor clade clearly includes PagP homologs from *Halanaerobium* species of the Firmicutes (Figure 4.1). This interesting subclass of Gram-positive bacteria is dubbed Negativicutes because its members have a peculiar

cell wall with an LPS OM that stains Gram-negative. Whether the Negativicutes are ancestral to or derived from Gram-positive bacteria is a subject of current debate among evolutionary biologists (Cavalier-Smith, 2006; Gupta, 2011; Sutcliffe, 2010). Importantly, PagP has not been observed in α -Proteobacteria, which are ancestral to the mitochondria of eukaryotic cells. Therefore, it seems unlikely that PagP function was necessary for bacteria prior to the evolution of eukaryotic cells. PagP seems to have emerged during the subsequent establishment of bacterial interactions with eukaryotic hosts, which is consistent with the distribution of the majority of PagP homologs in both the minor and major clades among species that are known to exhibit some form of association with eukaryotic cells. Eukaryotic immune systems thus appear to be a key driving force for PagP evolution.

4.7 Acknowledgements

E. coli BKT09 and *P. aeruginosa* MB5919 Δ *pagP* were kindly provided by Dr. Pei Zhou (Duke University) and Dr. Carl Balibar (Merck Research Laboratories), respectively. We thank Dr. Radhey Gupta, who identified the CSI in his analysis of the minor clade PagP homologs. We also thank Sanchia Miller for preparing the phylogenetic tree diagram and for helpful discussion and comments on the manuscript. This work was supported by CIHR Operating Grant MOP-84329.

Chapter 5

Conclusions

This thesis addresses two subjects: PagP mediated lipid metabolism (Chapter 2) and PagP structure-function relationships (Chapter 3 and 4). The former centres on the well known *E. coli* PagP homolog, whereas the latter is based on the characterization of two recently identified homologs of a divergent clade of PagP enzymes.

5.1 PagP-catalyzed expansion of glycerophosphoglycerol phospholipids

Two years into my graduate studies, Samuel Miller's group demonstrated that PagP is a bifunctional enzyme that palmitoylates the *sn*-3'-OH moiety of phosphatidylglycerol (PG) (Dalebroux *et al.*, 2014), in addition to lipid A (endotoxin). Palmitoylation of PG reduces polarity and increases hydrophobicity and saturation of the bilayer (Dalebroux *et al.*, 2014), properties that, for lipid A, are known to contribute to resistance to cationic antimicrobial peptides (Needham and Trent, 2013). PG and lipid A compete with each other as acceptors for the palmitate chain (Dalebroux *et al.*, 2014). We know that lipid A diffuses laterally into the hydrocarbon ruler through an opening called the embrasure, flanked by prolines 28 and 50 (Khan and Bishop, 2009). NMR

studies reveal that PagP's embrasure is highly dynamic (Hwang *et al.*, 2004; Hwang *et al.*, 2002) and remarkably unselective, in that it has previously been demonstrated to recognize multiple lipid A substructures (Bishop, 2005) and various nonspecific miscible and fatty alcohols *in vitro* Khan and Bishop (2009). While we have provided detailed analysis for many aspects of PagP's multifunctionality, several molecular details are still outstanding, including, do PG and lipid A competitively bind at the embrasure? Courtesy of Dr. Adil Khan, Figure 5.1 shows that the dynamic embrasure region is also clearly responsible for the palmitoylation of phosphatidylglycerol.

Both the embrasure and crenel in *Escherichia coli* PagP display weakened transmembrane β -strand hydrogen bonding to provide lateral routes for diffusion of the palmitoyl group between the hydrocarbon ruler and outer membrane external leaflet (Khan and Bishop, 2009). The prolines flanking the PagP embrasure can be mutated to cysteines (Pro28Cys/Pro50Cys); the presence of free thiol groups in PagP leads to intramolecular disulfide bond formation, reversibly barricading the embrasure. Palmitoylation of PG and formation of BMP is impeded by intramolecular disulfide bond formation at PagP's embrasure.

The discovery of *bis*(monoacylglycero)phosphate (BMP) in *E. coli* membranes comes at a most opportune time - when strides are being made in phospholipid trafficking (Abellon-Ruiz *et al.*, 2017; Ekiert *et al.*, 2017; Isom *et al.*, 2017) and signaling (Malinverni and Silhavy, 2009), and when minor lipids

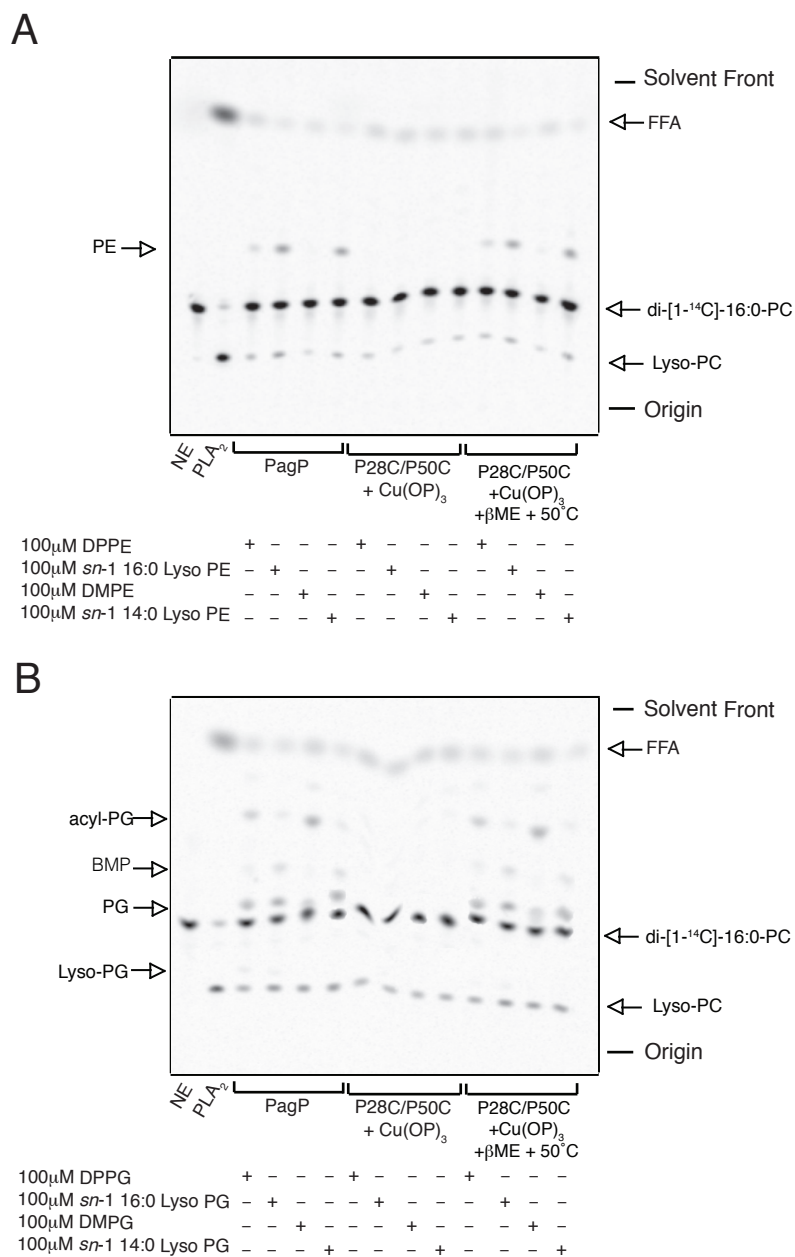


Figure 5.1 Phosphatidylglycerol binds at the embrasure of PagP. Courtest of Dr. Adil Khan A representative TLC autoradiographs of PagP phospholipase reaction supplemented with either PE, lyso-PE, PG or lyso-PG. The location of palmitate as free fatty acids (FFA) is revealed by the phospholipase A₂ (PLA₂) control. Cu²⁺-(1,10-phenanthroline)₃ [Cu(OP)₃] drives disulfide bond formation in membrane environments. Heating protein in the presence of 500 mM β ME at 50 °C for 2 h reduced the disulfide bridge A) Cold PE becomes radioactive as a result of a phospholipid exchange reaction where PE is first converted to lyso-PE by phospholipase activity. The subsequent reacylation using one of the radiolabelled palmitate of ¹⁴C-DPPC is impeded when the embrasure is reversibly baracaded by disulfide bond formation. B) Palmitoylation of PG and formation of BMP is impeded by intramolecular disulfide bond formation at the embrasure in Pro28Cys/Pro50Cys mutants.

with major roles are being reported (Dalebroux *et al.*, 2014; Sutterlin *et al.*, 2014). Our report of a novel glycerophosphoglycerol (GPG) metabolic pathway (Chapter 2) builds on Dr. Millers work, by identifying the downstream reactions after palmitoylation of PG. Dalebroux *et al.* (2014) reported the accumulation of PPG in cell membranes, the results described in Chapter 2 show that PPG is serially degraded to BMP, and then to monoacylated phosphoglycerolphosphates (Lyso-PG and Lyso-BMP). Activation of PagP in *E. coli* has been demonstrated to trigger truncation of the R3 core oligosaccharides in the cytoplasm (Smith *et al.*, 2008). However, the biological significance of the R3 truncation is not currently known. Given the physical separation between the OM and the cytoplasm, PagP most likely functions as a sensory transducer which is activated by a breach in the outer membrane permeability barrier. Efforts to discover the downstream signalling components that respond to the activated state of PagP have so far been unsuccessful. The *sn*-3' regioisomer of lyso-PG (Lyso-BMP) should be investigated for its potential as a second messenger in lipid mediated signal transduction.

5.2 The elusive *P. aeruginosa* PagP

Identification of the elusive *P. aeruginosa* PagP challenges our paradigm. We have since established that there are two clades of PagP evolved to fulfil different evolutionary functions in different bacteria. *P. aeruginosa* PagP is characteristic of a novel clade that can be characterized a lack of

primary sequence identity with major clade homologs, a His/Ser/Tyr catalytic triad, 3' lipid A regiospecificity and substrate specificity that excludes PG.

P. aeruginosa PagP produces a pro-inflammatory lipid A, distinctly different from lipid A isolated from acute infection, bronchiectasis (non-CF lung infections), or environmental isolates (Ernst *et al.*, 1999). We were able to show modification of lipid A by PaPagP contributes to this pro-inflammatory property (Chapter 3). We sought to determine whether or not the *pal343* gene was essential for virulence. We performed these experiments in a *Caenorhabditis elegans*. It has been reported recently that *P. aeruginosa* kills *C. elegans* and that many virulence factors (genes) required for maximum virulence in mouse pathogenicity are also required for maximum killing of *C. elegans* (Tan *et al.*, 1999). The toxic effects of *P. aeruginosa* are largely mediated by virulence factors. The virulence factors play an important pathological role in the colonization, the survival of the bacteria and the invasion of tissues. Figure 5.2, shows Kaplan–Meier survival curves for nematodes fed *P. aeruginosa* PAO1. To determine if the *pagP* was required for *C. elegans* virulence, we performed slow killing assays with wild-type PAO1 and a mutant in the gene encoding PagP (PAO1 Δ *pagP*). Nematodes grown on PAO1 and PAO1 Δ *pagP* have similar slow killing of *C. elegans*, indicating that the *pagP* was not required for virulence.

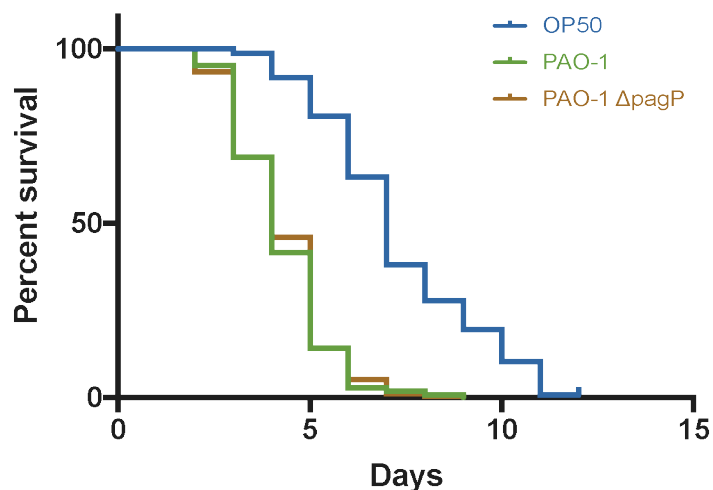


Figure 5.2. PAO-1 mediated killing of *Caenorhabditis elegans* used to model virulence. Kaplan–Meier survival curves for nematodes fed *P. aeruginosa pa1343* ($\Delta pagP$) mutants. The % survival values represent three independent experiments ($n \sim 90$) where the total number of worms equals 284. *E. coli* OP50 is the non-pathogenic food source. There is no significant difference between the wild type PAO-1 and $\Delta pa1343$ as determined by the log-rank test ($p = 0.9488$) and Gehan-Breslow-Wilcoxon test ($p = 0.9988$)

Despite having first been identified in pathogenic bacteria, the discovery of minor clade homologs forces us to consider PagP outside of the context of pathogenicity. The minor clade is largely made up of environmentally pervasive bacteria, with the exception of *Pseudomonas* and *Halomonas* which have shown potential as pathogens. Still, our understanding of the role of PagP must evolve to regard it as a part of the sensory and reactive arsenal of the OM.

5.3 PagP Structure-Function Relationships

PagP modifies lipid A in a number of Gram-negative bacteria many having distinctly different lipid A structures, giving rise to diversity in PagP lipid A regiospecificities (Bishop, 2005). Some major clade PagP homologs from the β -Proteobacteria, namely *B. bronchiseptica* and *B. parapertussis*, have been reported to palmitoylate lipid A at the 3'-position (Hittle *et al.*, 2015; Pilione *et al.*, 2004; Preston *et al.*, 2003). Sanchia Miller has also demonstrated PagP from *B. bronchiseptica* shows lipid A 3'-position regioselectivity, and two PagP homologs from the plant endophyte, *K. oxytoca* palmitoylate lipid A at the 2 and 3'-positions (Miller, unpublished). In Chapter 4, we reported the identification of *HELO_4100* as the gene encoding PagP in *Halomonas elongata*. Like PaPagP, regulated acylation at the 3' position may be important for the lifestyle of *Halomonas*. While HePagP has the same preference to palmitoylate the 3' position in lipid A, the effects of lipid A palmitoylation will

also depend on the lipid A structures displayed in *P. aeruginosa* and *H. elongata*.

The genus *Halomonas* includes bacteria favouring or tolerating high-saline and high-pH environments. *Halomonas* has only recently been recognized for its pathogenic potential in humans (Berger *et al.*, 2007; Stevens *et al.*, 2009; von Graevenitz *et al.*, 2000), capable of causing bacteremia in dialysis patients (Kim *et al.*, 2010; Stevens *et al.*, 2009). The endotoxic properties of lipopolysaccharide principally reside in the lipid A component, which is the primary immunostimulatory centre of Gram-negative bacteria. The structure of lipid A has only been reported for two species of *Halomonas*: *H. pantelleriensis* and *H. magadiensis*. *H. pantelleriensis* produces an immunostimulatory hexa-acylated lipid A (Carillo *et al.*, 2016), whereas *H. magadiensis* is reported to produce both penta- and tetra-acylated lipid A, naturally antagonistic forms of lipid A capable of inhibiting *E. coli* LPS activation of Toll-like receptor 4 expressed in human cells (Ialenti *et al.*, 2006). However, it should be duly noted that a BLAST search against all non-redundant sequences from GenBank, PDB, SwissProt, Protein Information Resource, Protein Research Foundation databases excluding environmental samples, reveals no obvious PagP homologs in either strain.

While there are currently four available structures of PagP, it may be beneficial to have an available structure of one of the divergent homologs. Our lab is currently collaborating with Dr. Peter Hwang (University of Alberta) to

obtain a structure of HePagP. It should be noted that based upon our study it is difficult to estimate how bonding interactions between the side chains on the amino acids may be affecting the tertiary structure of the protein. A solved structure would help rectify this problem. Despite these limitations, our results provide a compelling correlation of protein structure with enzymatic activity and stability.

References

Abellon-Ruiz, J., Kaptan, S.S., Basle, A., Claudi, B., Bumann, D., Kleinekathofer, U., and van den Berg, B. (2017). Structural basis for maintenance of bacterial outer membrane lipid asymmetry. *Nat Microbiol* 2, 1616-1623.

Ades, S.E., Connolly, L.E., Alba, B.M., and Gross, C.A. (1999). The *Escherichia coli* sigma(E)-dependent extracytoplasmic stress response is controlled by the regulated proteolysis of an anti-sigma factor. *Genes Dev* 13, 2449-2461.

Ahn, V.E., Lo, E.I., Engel, C.K., Chen, L., Hwang, P.M., Kay, L.E., Bishop, R.E., and Prive, G.G. (2004). A hydrocarbon ruler measures palmitate in the enzymatic acylation of endotoxin. *EMBO J* 23, 2931-2941.

Alexander, C., and Rietschel, E.T. (2001). Bacterial lipopolysaccharides and innate immunity. *J Endotoxin Res* 7, 167-202.

Altschul, S.F., Gish, W., Miller, W., Myers, E.W., and Lipman, D.J. (1990). Basic local alignment search tool. *J Mol Biol* 215, 403-410.

Anandan, A., Evans, G.L., Condic-Jurkic, K., O'Mara, M.L., John, C.M., Phillips, N.J., Jarvis, G.A., Wills, S.S., Stubbs, K.A., Moraes, I., *et al.* (2017). Structure of a lipid A phosphoethanolamine transferase suggests how conformational changes govern substrate binding. *Proc Natl Acad Sci U S A* 114, 2218-2223.

Anderson, M.S., Bull, H.G., Galloway, S.M., Kelly, T.M., Mohan, S., Radika, K., and Raetz, C.R. (1993). UDP-N-acetylglucosamine acyltransferase of *Escherichia coli*. The first step of endotoxin biosynthesis is thermodynamically unfavorable. *J Biol Chem* 268, 19858-19865.

Asikyan, M.L., Kus, J.V., and Burrows, L.L. (2008). Novel proteins that modulate type IV pilus retraction dynamics in *Pseudomonas aeruginosa*. *J Bacteriol* 190, 7022-7034.

Baba, T., Ara, T., Hasegawa, M., Takai, Y., Okumura, Y., Baba, M., Datsenko, K.A., Tomita, M., Wanner, B.L., and Mori, H. (2006). Construction of *Escherichia coli* K-12 in-frame, single-gene knockout mutants: the Keio collection. *Mol Syst Biol* 2, 2006 0008.

Babinski, K.J., Ribeiro, A.A., and Raetz, C.R. (2002). The *Escherichia coli* gene encoding the UDP-2,3-diacetylglucosamine pyrophosphatase of lipid A biosynthesis. *J Biol Chem* 277, 25937-25946.

- Bader, M.W., Sanowar, S., Daley, M.E., Schneider, A.R., Cho, U., Xu, W., Klevit, R.E., Le Moual, H., and Miller, S.I. (2005). Recognition of antimicrobial peptides by a bacterial sensor kinase. *Cell* 122, 461-472.
- Balibar, C.J., and Grabowicz, M. (2016). Mutant Alleles of lptD Increase the Permeability of *Pseudomonas aeruginosa* and Define Determinants of Intrinsic Resistance to Antibiotics. *Antimicrob Agents Chemother* 60, 845-854.
- Barchinger, S.E., and Ades, S.E. (2013). Regulated proteolysis: control of the *Escherichia coli* sigma(E)-dependent cell envelope stress response. *Subcell Biochem* 66, 129-160.
- Bechinger, B., and Lohner, K. (2006). Detergent-like actions of linear amphipathic cationic antimicrobial peptides. *Biochim Biophys Acta* 1758, 1529-1539.
- Berger, P., Barguelli, F., Raoult, D., and Drancourt, M. (2007). An outbreak of *Halomonas phocaensis* sp. nov. bacteraemia in a neonatal intensive care unit. *J Hosp Infect* 67, 79-85.
- Bishop, R.E. (2005). The lipid A palmitoyltransferase PagP: molecular mechanisms and role in bacterial pathogenesis. *Mol Microbiol* 57, 900-912.
- Bishop, R.E. (2014). Emerging roles for anionic non-bilayer phospholipids in fortifying the outer membrane permeability barrier. *J Bacteriol* 196, 3209-3213.
- Bishop, R.E., Gibbons, H.S., Guina, T., Trent, M.S., Miller, S.I., and Raetz, C.R. (2000). Transfer of palmitate from phospholipids to lipid A in outer membranes of gram-negative bacteria. *EMBO J* 19, 5071-5080.
- Bligh, E.G., and Dyer, W.J. (1959). A rapid method of total lipid extraction and purification. *Can J Biochem Physiol* 37, 911-917.
- Bogdanov, M., Dowhan, W., and Vitrac, H. (2014). Lipids and topological rules governing membrane protein assembly. *Biochim Biophys Acta* 1843, 1475-1488.
- Brady, L., Brzozowski, A.M., Derewenda, Z.S., Dodson, E., Dodson, G., Tolley, S., Turkenburg, J.P., Christiansen, L., Huges-Jensen, B., Norskov, L., et al. (1990). A serine protease triad forms the catalytic centre of a triacylglycerol lipase. *Nature* 343, 767-770.
- Braun, V. (1975). Covalent lipoprotein from the outer membrane of *Escherichia coli*. *Biochim Biophys Acta* 415, 335-377.

- Brotherus, J., Renkonen, O., Fischer, W., and Herrmann, J. (1974). Novel stereoconfiguration in lyso-bis-phosphatidic acid of cultured BHK-cells. *Chem Phys Lipids* 13, 178-182.
- Bulat, E., and Garrett, T.A. (2011). Putative *N*-acylphosphatidylethanolamine synthase from *Arabidopsis thaliana* is a lysoglycerophospholipid acyltransferase. *J Biol Chem* 286, 33819-33831.
- Carillo, S., Pieretti, G., Casillo, A., Lindner, B., Romano, I., Nicolaus, B., Parrilli, M., Giuliano, M., Cammarota, M., Lanzetta, R., *et al.* (2016). Structural characterization of the lipid A from the LPS of the haloalkaliphilic bacterium *Halomonas pantelleriensis*. *Extremophiles* 20, 687-694.
- Caroff, M., Karibian, D., Cavaillon, J.M., and Haeffner-Cavaillon, N. (2002). Structural and functional analyses of bacterial lipopolysaccharides. *Microbes Infect* 4, 915-926.
- Caroff, M., Tacken, A., and Szabo, L. (1988). Detergent-accelerated hydrolysis of bacterial endotoxins and determination of the anomeric configuration of the glycosyl phosphate present in the "isolated lipid A" fragment of the *Bordetella pertussis* endotoxin. *Carbohydr Res* 175, 273-282.
- Cavalier-Smith, T. (2006). Rooting the tree of life by transition analyses. *Biol Direct* 1, 19.
- Cheng, J., Randall, A.Z., Sweredoski, M.J., and Baldi, P. (2005). SCRATCH: a protein structure and structural feature prediction server. *Nucleic Acids Res* 33, W72-76.
- Chevallier, J., Chamoun, Z., Jiang, G., Prestwich, G., Sakai, N., Matile, S., Parton, R.G., and Gruenberg, J. (2008). Lysobisphosphatidic acid controls endosomal cholesterol levels. *J Biol Chem* 283, 27871-27880.
- Chothia, C., and Lesk, A.M. (1986). The relation between the divergence of sequence and structure in proteins. *EMBO J* 5, 823-826.
- Clementz, T., and Raetz, C.R. (1991). A gene coding for 3-deoxy-D-manno-octulosonic-acid transferase in *Escherichia coli*. Identification, mapping, cloning, and sequencing. *J Biol Chem* 266, 9687-9696.
- Costello, C.E., and Vath, J.E. (1990). Tandem mass spectrometry of glycolipids. *Methods Enzymol* 193, 738-768.

- Coughlin, R.T., Tonsager, S., and McGroarty, E.J. (1983). Quantitation of metal cations bound to membranes and extracted lipopolysaccharide of *Escherichia coli*. *Biochemistry* 22, 2002-2007.
- Cronan, J.E. (2003). Bacterial membrane lipids: where do we stand? *Annu Rev Microbiol* 57, 203-224.
- Cronan, J.E., Jr. (1968). Phospholipid alterations during growth of *Escherichia coli*. *J Bacteriol* 95, 2054-2061.
- Crowell, D.N., Anderson, M.S., and Raetz, C.R. (1986). Molecular cloning of the genes for lipid A disaccharide synthase and UDP-N-acetylglucosamine acyltransferase in *Escherichia coli*. *J Bacteriol* 168, 152-159.
- Cuesta-Seijo, J.A., Neale, C., Khan, M.A., Moktar, J., Tran, C.D., Bishop, R.E., Pomes, R., and Prive, G.G. (2010). PagP crystallized from SDS/cosolvent reveals the route for phospholipid access to the hydrocarbon ruler. *Structure* 18, 1210-1219.
- Curtis, M.A., Percival, R.S., Devine, D., Darveau, R.P., Coats, S.R., Rangarajan, M., Tarelli, E., and Marsh, P.D. (2011). Temperature-dependent modulation of *Porphyromonas gingivalis* lipid A structure and interaction with the innate host defenses. *Infect Immun* 79, 1187-1193.
- Dalebroux, Z.D., Edrozo, M.B., Pfuetzner, R.A., Ressler, S., Kulasekara, B.R., Blanc, M.P., and Miller, S.I. (2015). Delivery of cardiolipins to the *Salmonella* outer membrane is necessary for survival within host tissues and virulence. *Cell Host Microbe* 17, 441-451.
- Dalebroux, Z.D., Matamouros, S., Whittington, D., Bishop, R.E., and Miller, S.I. (2014). PhoPQ regulates acidic glycerophospholipid content of the *Salmonella Typhimurium* outer membrane. *Proc Natl Acad Sci U S A* 111, 1963-1968.
- Dasgupta, T., de Kievit, T.R., Masoud, H., Altman, E., Richards, J.C., Sadovskaya, I., Speert, D.P., and Lam, J.S. (1994). Characterization of lipopolysaccharide-deficient mutants of *Pseudomonas aeruginosa* derived from serotypes O3, O5, and O6. *Infect Immun* 62, 809-817.
- Datta, S., Costantino, N., Zhou, X., and Court, D.L. (2008). Identification and analysis of recombineering functions from Gram-negative and Gram-positive bacteria and their phages. *Proc Natl Acad Sci U S A* 105, 1626-1631.
- Davis, P.B., Drumm, M., and Konstan, M.W. (1996). Cystic fibrosis. *Am J Respir Crit Care Med* 154, 1229-1256.

- Diedrich, D.L., Stein, M.A., and Schnaitman, C.A. (1990). Associations of *Escherichia coli* K-12 OmpF trimers with rough and smooth lipopolysaccharides. *J Bacteriol* 172, 5307-5311.
- Dietmann, S., and Holm, L. (2001). Identification of homology in protein structure classification. *Nat Struct Biol* 8, 953-957.
- Doerrler, W.T., Gibbons, H.S., and Raetz, C.R. (2004). MsbA-dependent translocation of lipids across the inner membrane of *Escherichia coli*. *J Biol Chem* 279, 45102-45109.
- Dong, H., Xiang, Q., Gu, Y., Wang, Z., Paterson, N.G., Stansfeld, P.J., He, C., Zhang, Y., Wang, W., and Dong, C. (2014). Structural basis for outer membrane lipopolysaccharide insertion. *Nature* 511, 52-56.
- Dong, H., Zhang, Z., Tang, X., Paterson, N.G., and Dong, C. (2017). Structural and functional insights into the lipopolysaccharide ABC transporter LptB2FG. *Nat Commun* 8, 222.
- Dowhan, W. (1997). Molecular basis for membrane phospholipid diversity: why are there so many lipids? *Annu Rev Biochem* 66, 199-232.
- Drozdetskiy, A., Cole, C., Procter, J., and Barton, G.J. (2015). JPred4: a protein secondary structure prediction server. *Nucleic Acids Res* 43, W389-394.
- Eguchi, Y., Okada, T., Minagawa, S., Oshima, T., Mori, H., Yamamoto, K., Ishihama, A., and Utsumi, R. (2004). Signal transduction cascade between EvgA/EvgS and PhoP/PhoQ two-component systems of *Escherichia coli*. *J Bacteriol* 186, 3006-3014.
- Ekiert, D.C., Bhabha, G., Isom, G.L., Greenan, G., Ovchinnikov, S., Henderson, I.R., Cox, J.S., and Vale, R.D. (2017). Architectures of Lipid Transport Systems for the Bacterial Outer Membrane. *Cell* 169, 273-285 e217.
- El Hamidi, A., Tirsoaga, A., Novikov, A., Hussein, A., and Caroff, M. (2005). Microextraction of bacterial lipid A: easy and rapid method for mass spectrometric characterization. *J Lipid Res* 46, 1773-1778.
- Emptage, R.P., Daughtry, K.D., Pemble, C.W.t., and Raetz, C.R. (2012). Crystal structure of LpxK, the 4'-kinase of lipid A biosynthesis and atypical P-loop kinase functioning at the membrane interface. *Proc Natl Acad Sci U S A* 109, 12956-12961.

Eband, R.M., and Eband, R.F. (2011). Bacterial membrane lipids in the action of antimicrobial agents. *J Pept Sci* 17, 298-305.

Ernst, R.K., Guina, T., and Miller, S.I. (2001). *Salmonella typhimurium* outer membrane remodeling: role in resistance to host innate immunity. *Microbes Infect* 3, 1327-1334.

Ernst, R.K., Moskowitz, S.M., Emerson, J.C., Kraig, G.M., Adams, K.N., Harvey, M.D., Ramsey, B., Speert, D.P., Burns, J.L., and Miller, S.I. (2007). Unique lipid modifications in *Pseudomonas aeruginosa* isolated from the airways of patients with cystic fibrosis. *J Infect Dis* 196, 1088-1092.

Ernst, R.K., Yi, E.C., Guo, L., Lim, K.B., Burns, J.L., Hackett, M., and Miller, S.I. (1999). Specific lipopolysaccharide found in cystic fibrosis airway *Pseudomonas aeruginosa*. *Science* 286, 1561-1565.

Feist, W., Ulmer, A.J., Musehold, J., Brade, H., Kusumoto, S., and Flad, H.D. (1989). Induction of tumor necrosis factor- α release by lipopolysaccharide and defined lipopolysaccharide partial structures. *Immunobiology* 179, 293-307.

Folkesson, A., Jelsbak, L., Yang, L., Johansen, H.K., Ciofu, O., Hoiby, N., and Molin, S. (2012). Adaptation of *Pseudomonas aeruginosa* to the cystic fibrosis airway: an evolutionary perspective. *Nat Rev Microbiol* 10, 841-851.

Fu, W., Yang, F., Kang, X., Zhang, X., Li, Y., Xia, B., and Jin, C. (2007). First structure of the polymyxin resistance proteins. *Biochem Biophys Res Commun* 361, 1033-1037.

Fujimoto, Y., Shimoyama, A., Saeki, A., Kitayama, N., Kasamatsu, C., Tsutsui, H., and Fukase, K. (2013). Innate immunomodulation by lipophilic termini of lipopolysaccharide; synthesis of lipid A_s from *Porphyromonas gingivalis* and other bacteria and their immunomodulative responses. *Mol Biosyst* 9, 987-996.

Galanos, C., Hansen-Hagge, T., Lehmann, V., and Luderitz, O. (1985). Comparison of the capacity of two lipid A precursor molecules to express the local Shwartzman phenomenon. *Infect Immun* 48, 355-358.

Ganong, B.R., Leonard, J.M., and Raetz, C.R. (1980). Phosphatidic acid accumulation in the membranes of *Escherichia coli* mutants defective in CDP-diglyceride synthetase. *J Biol Chem* 255, 1623-1629.

Ganong, B.R., and Raetz, C.R. (1982). Massive accumulation of phosphatidic acid in conditionally lethal CDP-diglyceride synthetase mutants and cytidine auxotrophs of *Escherichia coli*. *J Biol Chem* 257, 389-394.

- Garcia Vescovi, E., Soncini, F.C., and Groisman, E.A. (1996). Mg²⁺ as an extracellular signal: environmental regulation of *Salmonella* virulence. *Cell* 84, 165-174.
- Garrett, T.A. (2017). Major roles for minor bacterial lipids identified by mass spectrometry. *Biochim Biophys Acta Mol Cell Biol Lipids* 1862, 1319-1324.
- Garrett, T.A., Kadmas, J.L., and Raetz, C.R. (1997). Identification of the gene encoding the *Escherichia coli* lipid A 4'-kinase. Facile phosphorylation of endotoxin analogs with recombinant LpxK. *J Biol Chem* 272, 21855-21864.
- Garrett, T.A., Kordestani, R., and Raetz, C.R. (2007). Quantification of cardiolipin by liquid chromatography-electrospray ionization mass spectrometry. *Methods Enzymol* 433, 213-230.
- Garrett, T.J., Merves, M., and Yost, R.A. (2011). Characterization of protonated phospholipids as fragile ions in quadrupole ion trap mass spectrometry. *Int J Mass Spectrom* 308, 299-306.
- Gerlt, J.A., and Babbitt, P.C. (2001). Divergent evolution of enzymatic function: mechanistically diverse superfamilies and functionally distinct suprafamilies. *Annu Rev Biochem* 70, 209-246.
- Gibbons, H.S., Lin, S., Cotter, R.J., and Raetz, C.R. (2000). Oxygen requirement for the biosynthesis of the S-2-hydroxymyristate moiety in *Salmonella typhimurium* lipid A. Function of LpxO, A new Fe²⁺/alpha-ketoglutarate-dependent dioxygenase homologue. *J Biol Chem* 275, 32940-32949.
- Gibbons, H.S., Reynolds, C.M., Guan, Z., and Raetz, C.R. (2008). An inner membrane dioxygenase that generates the 2-hydroxymyristate moiety of *Salmonella* lipid A. *Biochemistry* 47, 2814-2825.
- Golenbock, D.T., Hampton, R.Y., Qureshi, N., Takayama, K., and Raetz, C.R. (1991). Lipid A-like molecules that antagonize the effects of endotoxins on human monocytes. *J Biol Chem* 266, 19490-19498.
- Groisman, E.A. (2001). The pleiotropic two-component regulatory system PhoP-PhoQ. *J Bacteriol* 183, 1835-1842.
- Gunn, J.S., Belden, W.J., and Miller, S.I. (1998). Identification of PhoP-PhoQ activated genes within a duplicated region of the *Salmonella typhimurium* chromosome. *Microb Pathog* 25, 77-90.

- Guo, D., and Tropp, B.E. (2000). A second *Escherichia coli* protein with CL synthase activity. *Biochim Biophys Acta* 1483, 263-274.
- Guo, L., Lim, K.B., Poduje, C.M., Daniel, M., Gunn, J.S., Hackett, M., and Miller, S.I. (1998). Lipid A acylation and bacterial resistance against vertebrate antimicrobial peptides. *Cell* 95, 189-198.
- Gupta, R.S. (1998). Protein phylogenies and signature sequences: A reappraisal of evolutionary relationships among archaeobacteria, eubacteria, and eukaryotes. *Microbiol Mol Biol Rev* 62, 1435-1491.
- Gupta, R.S. (2011). Origin of diderm (Gram-negative) bacteria: antibiotic selection pressure rather than endosymbiosis likely led to the evolution of bacterial cells with two membranes. *Antonie Van Leeuwenhoek* 100, 171-182.
- Gupta, R.S., Nanda, A., and Khadka, B. (2017). Novel molecular, structural and evolutionary characteristics of the phosphoketolases from *bifidobacteria* and *Coriobacteriales*. *PLoS One* 12, e0172176.
- Gust, B., Challis, G.L., Fowler, K., Kieser, T., and Chater, K.F. (2003). PCR-targeted *Streptomyces* gene replacement identifies a protein domain needed for biosynthesis of the sesquiterpene soil odor geosmin. *Proc Natl Acad Sci U S A* 100, 1541-1546.
- Hajjar, A.M., Ernst, R.K., Tsai, J.H., Wilson, C.B., and Miller, S.I. (2002). Human Toll-like receptor 4 recognizes host-specific LPS modifications. *Nat Immunol* 3, 354-359.
- Hancock, R.E., Falla, T., and Brown, M. (1995). Cationic bactericidal peptides. *Adv Microb Physiol* 37, 135-175.
- Hardaway, K.L., and Buller, C.S. (1979). Effect of ethylenediaminetetraacetate on phospholipids and outer membrane function in *Escherichia coli*. *J Bacteriol* 137, 62-68.
- Hilbert, M., Bohm, G., and Jaenicke, R. (1993). Structural relationships of homologous proteins as a fundamental principle in homology modeling. *Proteins* 17, 138-151.
- Hiraoka, S., Matsuzaki, H., and Shibuya, I. (1993). Active increase in cardiolipin synthesis in the stationary growth phase and its physiological significance in *Escherichia coli*. *FEBS Lett* 336, 221-224.

- Hittle, L.E., Jones, J.W., Hajjar, A.M., Ernst, R.K., and Preston, A. (2015). *Bordetella parapertussis* PagP mediates the addition of two palmitates to the lipopolysaccharide lipid A. *J Bacteriol* 197, 572-580.
- Ho, H., Miu, A., Alexander, M.K., Garcia, N.K., Oh, A., Zilberleyb, I., Reichelt, M., Austin, C.D., Tam, C., Shriver, S., *et al.* (2018). Structural basis for dual-mode inhibition of the ABC transporter MsbA. *Nature* 557, 196-201.
- Horstman, A.L., Bauman, S.J., and Kuehn, M.J. (2004). Lipopolysaccharide 3-deoxy-D-manno-octulosonic acid (Kdo) core determines bacterial association of secreted toxins. *J Biol Chem* 279, 8070-8075.
- Hsu, L., Jackowski, S., and Rock, C.O. (1991). Isolation and characterization of *Escherichia coli* K-12 mutants lacking both 2-acyl-glycerophosphoethanolamine acyltransferase and acyl-acyl carrier protein synthetase activity. *J Biol Chem* 266, 13783-13788.
- Hullin-Matsuda, F., Kawasaki, K., Delton-Vandenbroucke, I., Xu, Y., Nishijima, M., Lagarde, M., Schlame, M., and Kobayashi, T. (2007). *De novo* biosynthesis of the late endosome lipid, bis(monoacylglycero)phosphate. *J Lipid Res* 48, 1997-2008.
- Hullin-Matsuda, F., Luquain-Costaz, C., Bouvier, J., and Delton-Vandenbroucke, I. (2009). Bis(monoacylglycero)phosphate, a peculiar phospholipid to control the fate of cholesterol: Implications in pathology. *Prostaglandins Leukot Essent Fatty Acids* 81, 313-324.
- Huysmans, G.H., Baldwin, S.A., Brockwell, D.J., and Radford, S.E. (2010). The transition state for folding of an outer membrane protein. *Proc Natl Acad Sci U S A* 107, 4099-4104.
- Hwang, P.M., Bishop, R.E., and Kay, L.E. (2004). The integral membrane enzyme PagP alternates between two dynamically distinct states. *Proc Natl Acad Sci U S A* 101, 9618-9623.
- Hwang, P.M., Choy, W.Y., Lo, E.I., Chen, L., Forman-Kay, J.D., Raetz, C.R., Prive, G.G., Bishop, R.E., and Kay, L.E. (2002). Solution structure and dynamics of the outer membrane enzyme PagP by NMR. *Proc Natl Acad Sci U S A* 99, 13560-13565.
- Ialenti, A., Di Meglio, P., Grassia, G., Maffia, P., Di Rosa, M., Lanzetta, R., Molinaro, A., Silipo, A., Grant, W., and Ianaro, A. (2006). A novel lipid A from *Halomonas magadiensis* inhibits enteric LPS-induced human monocyte activation. *Eur J Immunol* 36, 354-360.

- Isom, G.L., Davies, N.J., Chong, Z.S., Bryant, J.A., Jamshad, M., Sharif, M., Cunningham, A.F., Knowles, T.J., Chng, S.S., Cole, J.A., *et al.* (2017). MCE domain proteins: conserved inner membrane lipid-binding proteins required for outer membrane homeostasis. *Sci Rep* 7, 8608.
- Iyer, B.R., and Mahalakshmi, R. (2015). Residue-Dependent Thermodynamic Cost and Barrel Plasticity Balances Activity in the PhoPQ-Activated Enzyme PagP of *Salmonella typhimurium*. *Biochemistry* 54, 5712-5722.
- Iyer, B.R., and Mahalakshmi, R. (2016). Distinct Structural Elements Govern the Folding, Stability, and Catalysis in the Outer Membrane Enzyme PagP. *Biochemistry* 55, 4960-4970.
- Jaroszewski, L., Rychlewski, L., Li, Z., Li, W., and Godzik, A. (2005). FFAS03: a server for profile--profile sequence alignments. *Nucleic Acids Res* 33, W284-288.
- Jia, W., El Zoeiby, A., Petruzzello, T.N., Jayabalasingham, B., Seyedirashti, S., and Bishop, R.E. (2004). Lipid trafficking controls endotoxin acylation in outer membranes of *Escherichia coli*. *J Biol Chem* 279, 44966-44975.
- Jogl, G., Hsiao, Y.S., and Tong, L. (2004). Structure and function of carnitine acyltransferases. *Ann N Y Acad Sci* 1033, 17-29.
- Jogl, G., and Tong, L. (2003). Crystal structure of carnitine acetyltransferase and implications for the catalytic mechanism and fatty acid transport. *Cell* 112, 113-122.
- Karasawa, K., Kudo, I., Kobayashi, T., Sa-Eki, T., Inoue, K., and Nojima, S. (1985). Purification and characterization of lysophospholipase L2 of *Escherichia coli* K-12. *J Biochem* 98, 1117-1125.
- Kawasaki, K., Ernst, R.K., and Miller, S.I. (2004). 3-O-deacylation of lipid A by PagL, a PhoP/PhoQ-regulated deacylase of *Salmonella typhimurium*, modulates signaling through Toll-like receptor 4. *J Biol Chem* 279, 20044-20048.
- Kelly, T.M., Stachula, S.A., Raetz, C.R., and Anderson, M.S. (1993). The *firA* gene of *Escherichia coli* encodes UDP-3-O-(R-3-hydroxymyristoyl)-glucosamine N-acyltransferase. The third step of endotoxin biosynthesis. *J Biol Chem* 268, 19866-19874.
- Khan, M.A., and Bishop, R.E. (2009). Molecular mechanism for lateral lipid diffusion between the outer membrane external leaflet and a beta-barrel hydrocarbon ruler. *Biochemistry* 48, 9745-9756.

- Khan, M.A., Moktar, J., Mott, P.J., and Bishop, R.E. (2010a). A thiolate anion buried within the hydrocarbon ruler perturbs PagP lipid acyl chain selection. *Biochemistry* 49, 2368-2379.
- Khan, M.A., Moktar, J., Mott, P.J., Vu, M., McKie, A.H., Pinter, T., Hof, F., and Bishop, R.E. (2010b). Inscribing the perimeter of the PagP hydrocarbon ruler by site-specific chemical alkylation. *Biochemistry* 49, 9046-9057.
- Khan, M.A., Neale, C., Michaux, C., Pomes, R., Prive, G.G., Woody, R.W., and Bishop, R.E. (2007). Gauging a hydrocarbon ruler by an intrinsic exciton probe. *Biochemistry* 46, 4565-4579.
- Kim, K.K., Lee, K.C., Oh, H.M., and Lee, J.S. (2010). *Halomonas stevensii* sp. nov., *Halomonas hamiltonii* sp. nov. and *Halomonas johnsoniae* sp. nov., isolated from a renal care centre. *Int J Syst Evol Microbiol* 60, 369-377.
- Kim, S.J., Koh, D.C., Park, S.J., Cha, I.T., Park, J.W., Na, J.H., Roh, Y., Ko, K.S., Kim, K., and Rhee, S.K. (2012). Molecular analysis of spatial variation of iron-reducing bacteria in riverine alluvial aquifers of the Mankyong River. *J Microbiol* 50, 207-217.
- Kobayashi, T., Nishijima, M., Tamori, Y., Nojima, S., Seyama, Y., and Yamakawa, T. (1980). Acyl phosphatidylglycerol of *Escherichia coli*. *Biochim Biophys Acta* 620, 356-363.
- Kong, Q., Six, D.A., Liu, Q., Gu, L., Roland, K.L., Raetz, C.R., and Curtiss, R., 3rd (2011). Palmitoylation state impacts induction of innate and acquired immunity by the *Salmonella enterica* serovar typhimurium *msbB* mutant. *Infect Immun* 79, 5027-5038.
- Larkin, M.A., Blackshields, G., Brown, N.P., Chenna, R., McGettigan, P.A., McWilliam, H., Valentin, F., Wallace, I.M., Wilm, A., Lopez, R., et al. (2007). Clustal W and Clustal X version 2.0. *Bioinformatics* 23, 2947-2948.
- Lee, H., Hsu, F.F., Turk, J., and Groisman, E.A. (2004). The PmrA-regulated *pmrC* gene mediates phosphoethanolamine modification of lipid A and polymyxin resistance in *Salmonella enterica*. *J Bacteriol* 186, 4124-4133.
- Lefebvre, M.D., and Valvano, M.A. (2002). Construction and evaluation of plasmid vectors optimized for constitutive and regulated gene expression in *Burkholderia cepacia* complex isolates. *Appl Environ Microbiol* 68, 5956-5964.

- Lima, S., Guo, M.S., Chaba, R., Gross, C.A., and Sauer, R.T. (2013). Dual molecular signals mediate the bacterial response to outer-membrane stress. *Science* 340, 837-841.
- Loppnow, H., Brade, L., Brade, H., Rietschel, E.T., Kusumoto, S., Shiba, T., and Flad, H.D. (1986). Induction of human interleukin 1 by bacterial and synthetic lipid A. *Eur J Immunol* 16, 1263-1267.
- Lu, Y.H., Guan, Z., Zhao, J., and Raetz, C.R. (2011). Three phosphatidylglycerol-phosphate phosphatases in the inner membrane of *Escherichia coli*. *J Biol Chem* 286, 5506-5518.
- Lundback, A.K., van den Berg, S., Hebert, H., Berglund, H., and Eshaghi, S. (2008). Exploring the activity of tobacco etch virus protease in detergent solutions. *Anal Biochem* 382, 69-71.
- Luo, Q., Yang, X., Yu, S., Shi, H., Wang, K., Xiao, L., Zhu, G., Sun, C., Li, T., Li, D., *et al.* (2017). Structural basis for lipopolysaccharide extraction by ABC transporter LptB2FG. *Nat Struct Mol Biol* 24, 469-474.
- Makula, R.A., Torregrossa, R.E., and Isle, H.B. (1978). Identification and synthesis of acyl-phosphatidylglycerol in *Acinetobacter* sp. HO1-N. *J Bacteriol* 133, 1530-1532.
- Malinverni, J.C., and Silhavy, T.J. (2009). An ABC transport system that maintains lipid asymmetry in the gram-negative outer membrane. *Proc Natl Acad Sci U S A* 106, 8009-8014.
- McPhee, J.B., Bains, M., Winsor, G., Lewenza, S., Kwasnicka, A., Brazas, M.D., Brinkman, F.S., and Hancock, R.E. (2006). Contribution of the PhoP-PhoQ and PmrA-PmrB two-component regulatory systems to Mg²⁺-induced gene regulation in *Pseudomonas aeruginosa*. *J Bacteriol* 188, 3995-4006.
- Mi, W., Li, Y., Yoon, S.H., Ernst, R.K., Walz, T., and Liao, M. (2017). Structural basis of MsbA-mediated lipopolysaccharide transport. *Nature* 549, 233-237.
- Michaux, C., Pomroy, N.C., and Prive, G.G. (2008). Refolding SDS-denatured proteins by the addition of amphipathic cosolvents. *J Mol Biol* 375, 1477-1488.
- Miller, A.K., Brannon, M.K., Stevens, L., Johansen, H.K., Selgrade, S.E., Miller, S.I., Hoiby, N., and Moskowitz, S.M. (2011). PhoQ mutations promote lipid A modification and polymyxin resistance of *Pseudomonas aeruginosa* found in colistin-treated cystic fibrosis patients. *Antimicrob Agents Chemother* 55, 5761-5769.

- Miyazaki, C., Kuroda, M., Ohta, A., and Shibuya, I. (1985). Genetic manipulation of membrane phospholipid composition in *Escherichia coli*: *pgsA* mutants defective in phosphatidylglycerol synthesis. *Proc Natl Acad Sci U S A* 82, 7530-7534.
- Moskowitz, S.M., Brannon, M.K., Dasgupta, N., Pier, M., Sgambati, N., Miller, A.K., Selgrade, S.E., Miller, S.I., Denton, M., Conway, S.P., *et al.* (2012). PmrB mutations promote polymyxin resistance of *Pseudomonas aeruginosa* isolated from colistin-treated cystic fibrosis patients. *Antimicrob Agents Chemother* 56, 1019-1030.
- Moskowitz, S.M., and Ernst, R.K. (2010). The role of *Pseudomonas* lipopolysaccharide in cystic fibrosis airway infection. *Subcell Biochem* 53, 241-253.
- Moskowitz, S.M., Ernst, R.K., and Miller, S.I. (2004). PmrAB, a two-component regulatory system of *Pseudomonas aeruginosa* that modulates resistance to cationic antimicrobial peptides and addition of aminoarabinose to lipid A. *J Bacteriol* 186, 575-579.
- Murzin, A.G. (1998). How far divergent evolution goes in proteins. *Curr Opin Struct Biol* 8, 380-387.
- Naushad, H.S., Lee, B., and Gupta, R.S. (2014). Conserved signature indels and signature proteins as novel tools for understanding microbial phylogeny and systematics: identification of molecular signatures that are specific for the phytopathogenic genera *Dickeya*, *Pectobacterium* and *Brenneria*. *Int J Syst Evol Microbiol* 64, 366-383.
- Needham, B.D., and Trent, M.S. (2013). Fortifying the barrier: the impact of lipid A remodelling on bacterial pathogenesis. *Nat Rev Microbiol* 11, 467-481.
- Nikaido, H. (2003). Molecular basis of bacterial outer membrane permeability revisited. *Microbiol Mol Biol Rev* 67, 593-656.
- Nikaido, H., and Vaara, M. (1985). Molecular basis of bacterial outer membrane permeability. *Microbiol Rev* 49, 1-32.
- Nishihara, M., Morii, H., and Koga, Y. (1982). Bis(monoacylglycero)phosphate in alkalophilic bacteria. *J Biochem* 92, 1469-1479.
- Okuda, S., Sherman, D.J., Silhavy, T.J., Ruiz, N., and Kahne, D. (2016). Lipopolysaccharide transport and assembly at the outer membrane: the PEZ model. *Nat Rev Microbiol* 14, 337-345.

- Olsen, R.W., and Ballou, C.E. (1971). Acyl phosphatidylglycerol. A new phospholipid from *Salmonella typhimurium*. *J Biol Chem* 246, 3305-3313.
- Orskov, I., Orskov, F., Jann, B., and Jann, K. (1977). Serology, chemistry, and genetics of O and K antigens of *Escherichia coli*. *Bacteriol Rev* 41, 667-710.
- Park, B.S., Song, D.H., Kim, H.M., Choi, B.S., Lee, H., and Lee, J.O. (2009). The structural basis of lipopolysaccharide recognition by the TLR4-MD-2 complex. *Nature* 458, 1191-1195.
- Pascarella, S., and Argos, P. (1992). Analysis of insertions/deletions in protein structures. *J Mol Biol* 224, 461-471.
- Petersen, T.N., Brunak, S., von Heijne, G., and Nielsen, H. (2011). SignalP 4.0: discriminating signal peptides from transmembrane regions. *Nat Methods* 8, 785-786.
- Petrou, V.I., Herrera, C.M., Schultz, K.M., Clarke, O.B., Vendome, J., Tomasek, D., Banerjee, S., Rajashankar, K.R., Belcher Dufresne, M., Kloss, B., *et al.* (2016). Structures of aminoarabinose transferase ArnT suggest a molecular basis for lipid A glycosylation. *Science* 351, 608-612.
- Pilione, M.R., Pishko, E.J., Preston, A., Maskell, D.J., and Harvill, E.T. (2004). pagP is required for resistance to antibody-mediated complement lysis during *Bordetella bronchiseptica* respiratory infection. *Infect Immun* 72, 2837-2842.
- Poorthuis, B., and Hostetler, K.Y. (1975). Biosynthesis of bis(monoacylglyceryl)phosphate and acylphosphatidylglycerol in rat liver mitochondrial. *J Biol Chem* 250, 3297-3302.
- Preston, A., Maxim, E., Toland, E., Pishko, E.J., Harvill, E.T., Caroff, M., and Maskell, D.J. (2003). *Bordetella bronchiseptica* PagP is a Bvg-regulated lipid A palmitoyl transferase that is required for persistent colonization of the mouse respiratory tract. *Mol Microbiol* 48, 725-736.
- Preston, A., Parkhill, J., and Maskell, D.J. (2004). The bordetellae: lessons from genomics. *Nat Rev Microbiol* 2, 379-390.
- Qiao, S., Luo, Q., Zhao, Y., Zhang, X.C., and Huang, Y. (2014). Structural basis for lipopolysaccharide insertion in the bacterial outer membrane. *Nature* 511, 108-111.

- Que, N.L., Lin, S., Cotter, R.J., and Raetz, C.R. (2000). Purification and mass spectrometry of six lipid A species from the bacterial endosymbiont *Rhizobium etli*. Demonstration of a conserved distal unit and a variable proximal portion. *J Biol Chem* 275, 28006-28016.
- Qureshi, N., Takayama, K., Heller, D., and Fenselau, C. (1983). Position of ester groups in the lipid A backbone of lipopolysaccharides obtained from *Salmonella typhimurium*. *J Biol Chem* 258, 12947-12951.
- Raetz, C.R., and Dowhan, W. (1990). Biosynthesis and function of phospholipids in *Escherichia coli*. *J Biol Chem* 265, 1235-1238.
- Raetz, C.R., Purcell, S., Meyer, M.V., Qureshi, N., and Takayama, K. (1985). Isolation and characterization of eight lipid A precursors from a 3-deoxy-D-manno-octylosonic acid-deficient mutant of *Salmonella typhimurium*. *J Biol Chem* 260, 16080-16088.
- Raetz, C.R., Reynolds, C.M., Trent, M.S., and Bishop, R.E. (2007). Lipid A modification systems in gram-negative bacteria. *Annu Rev Biochem* 76, 295-329.
- Raetz, C.R., and Roderick, S.L. (1995). A left-handed parallel beta helix in the structure of UDP-N-acetylglucosamine acyltransferase. *Science* 270, 997-1000.
- Raetz, C.R., and Whitfield, C. (2002). Lipopolysaccharide endotoxins. *Annu Rev Biochem* 71, 635-700.
- Rebeil, R., Ernst, R.K., Gowen, B.B., Miller, S.I., and Hinnebusch, B.J. (2004). Variation in lipid A structure in the pathogenic *yersiniae*. *Mol Microbiol* 52, 1363-1373.
- Reynolds, C.M., Ribeiro, A.A., McGrath, S.C., Cotter, R.J., Raetz, C.R., and Trent, M.S. (2006). An outer membrane enzyme encoded by *Salmonella typhimurium* lpxR that removes the 3'-acyloxyacyl moiety of lipid A. *J Biol Chem* 281, 21974-21987.
- Robey, M., O'Connell, W., and Cianciotto, N.P. (2001). Identification of *Legionella pneumophila* rcp, a pagP-like gene that confers resistance to cationic antimicrobial peptides and promotes intracellular infection. *Infect Immun* 69, 4276-4286.
- Rost, B., Yachdav, G., and Liu, J. (2004). The PredictProtein server. *Nucleic Acids Res* 32, W321-326.

Roy, A., Kucukural, A., and Zhang, Y. (2010). I-TASSER: a unified platform for automated protein structure and function prediction. *Nat Protoc* 5, 725-738.

Roy, A., Xu, D., Poisson, J., and Zhang, Y. (2011). A protocol for computer-based protein structure and function prediction. *J Vis Exp*, e3259.

Saxena, V.P., and Wetlaufer, D.B. (1971). A new basis for interpreting the circular dichroic spectra of proteins. *Proc Natl Acad Sci U S A* 68, 969-972.

Schulz, G.E. (2002). The structure of bacterial outer membrane proteins. *Biochim Biophys Acta* 1565, 308-317.

Seeliger, D., and de Groot, B.L. (2010). Ligand docking and binding site analysis with PyMOL and Autodock/Vina. *J Comput Aided Mol Des* 24, 417-422.

Sherman, D.J., Xie, R., Taylor, R.J., George, A.H., Okuda, S., Foster, P.J., Needleman, D.J., and Kahne, D. (2018). Lipopolysaccharide is transported to the cell surface by a membrane-to-membrane protein bridge. *Science* 359, 798-801.

Silhavy, T.J., Kahne, D., and Walker, S. (2010). The bacterial cell envelope. *Cold Spring Harb Perspect Biol* 2, a000414.

Smith, A.E., Kim, S.H., Liu, F., Jia, W., Vinogradov, E., Gyles, C.L., and Bishop, R.E. (2008). PagP activation in the outer membrane triggers R3 core oligosaccharide truncation in the cytoplasm of *Escherichia coli* O157:H7. *J Biol Chem* 283, 4332-4343.

Smith, P.K., Krohn, R.I., Hermanson, G.T., Mallia, A.K., Gartner, F.H., Provenzano, M.D., Fujimoto, E.K., Goeke, N.M., Olson, B.J., and Klenk, D.C. (1985). Measurement of protein using bicinchoninic acid. *Anal Biochem* 150, 76-85.

Sohlenkamp, C., and Geiger, O. (2016). Bacterial membrane lipids: diversity in structures and pathways. *FEMS Microbiol Rev* 40, 133-159.

Somerville, J.E., Jr., Cassiano, L., Bainbridge, B., Cunningham, M.D., and Darveau, R.P. (1996). A novel *Escherichia coli* lipid A mutant that produces an antiinflammatory lipopolysaccharide. *J Clin Invest* 97, 359-365.

Sorensen, P.G., Lutkenhaus, J., Young, K., Eveland, S.S., Anderson, M.S., and Raetz, C.R. (1996). Regulation of UDP-3-O-[R-3-hydroxymyristoyl]-N-acetylglucosamine deacetylase in *Escherichia coli*. The second enzymatic step of lipid a biosynthesis. *J Biol Chem* 271, 25898-25905.

- Stenutz, R., Weintraub, A., and Widmalm, G. (2006). The structures of *Escherichia coli* O-polysaccharide antigens. *FEMS Microbiol Rev* 30, 382-403.
- Stevens, D.A., Hamilton, J.R., Johnson, N., Kim, K.K., and Lee, J.S. (2009). *Halomonas*, a newly recognized human pathogen causing infections and contamination in a dialysis center: three new species. *Medicine (Baltimore)* 88, 244-249.
- Stevenson, G., Neal, B., Liu, D., Hobbs, M., Packer, N.H., Batley, M., Redmond, J.W., Lindquist, L., and Reeves, P. (1994). Structure of the O antigen of *Escherichia coli* K-12 and the sequence of its rfb gene cluster. *J Bacteriol* 176, 4144-4156.
- Stroud, R.M., Kay, L.M., and Dickerson, R.E. (1972). The crystal and molecular structure of DIP-inhibited bovine trypsin at 2.7 Å resolution. *Cold Spring Harb Symp Quant Biol* 36, 125-140.
- Sutcliffe, I.C. (2010). A phylum level perspective on bacterial cell envelope architecture. *Trends Microbiol* 18, 464-470.
- Sutterlin, H.A., Zhang, S., and Silhavy, T.J. (2014). Accumulation of phosphatidic acid increases vancomycin resistance in *Escherichia coli*. *J Bacteriol* 196, 3214-3220.
- Takayama, K., Rothenberg, R.J., and Barbour, A.G. (1987). Absence of lipopolysaccharide in the Lyme disease spirochete, *Borrelia burgdorferi*. *Infect Immun* 55, 2311-2313.
- Tamura, K., Stecher, G., Peterson, D., Filipski, A., and Kumar, S. (2013). MEGA6: Molecular Evolutionary Genetics Analysis version 6.0. *Mol Biol Evol* 30, 2725-2729.
- Tan, B.K., Bogdanov, M., Zhao, J., Dowhan, W., Raetz, C.R., and Guan, Z. (2012). Discovery of a cardiolipin synthase utilizing phosphatidylethanolamine and phosphatidylglycerol as substrates. *Proc Natl Acad Sci U S A* 109, 16504-16509.
- Tan, M.W., Rahme, L.G., Sternberg, J.A., Tompkins, R.G., and Ausubel, F.M. (1999). *Pseudomonas aeruginosa* killing of *Caenorhabditis elegans* used to identify *P. aeruginosa* virulence factors. *Proc Natl Acad Sci U S A* 96, 2408-2413.
- Tanamoto, K., and Azumi, S. (2000). *Salmonella*-type heptaacylated lipid A is inactive and acts as an antagonist of lipopolysaccharide action on human line cells. *J Immunol* 164, 3149-3156.

Thaipisuttikul, I., Hittle, L.E., Chandra, R., Zangari, D., Dixon, C.L., Garrett, T.A., Rasko, D.A., Dasgupta, N., Moskowitz, S.M., Malmstrom, L., *et al.* (2014). A divergent *Pseudomonas aeruginosa* palmitoyltransferase essential for cystic fibrosis-specific lipid A. *Mol Microbiol* *91*, 158-174.

Thornburg, T., Miller, C., Thuren, T., King, L., and Waite, M. (1991). Glycerol reorientation during the conversion of phosphatidylglycerol to bis(monoacylglycerol)phosphate in macrophage-like RAW 264.7 cells. *J Biol Chem* *266*, 6834-6840.

Tran, A.X., Lester, M.E., Stead, C.M., Raetz, C.R., Maskell, D.J., McGrath, S.C., Cotter, R.J., and Trent, M.S. (2005). Resistance to the antimicrobial peptide polymyxin requires myristoylation of *Escherichia coli* and *Salmonella typhimurium* lipid A. *J Biol Chem* *280*, 28186-28194.

Trent, M.S. (2004). Biosynthesis, transport, and modification of lipid A. *Biochem Cell Biol* *82*, 71-86.

Trent, M.S., Ribeiro, A.A., Lin, S., Cotter, R.J., and Raetz, C.R. (2001). An inner membrane enzyme in *Salmonella* and *Escherichia coli* that transfers 4-amino-4-deoxy-L-arabinose to lipid A: induction on polymyxin-resistant mutants and role of a novel lipid-linked donor. *J Biol Chem* *276*, 43122-43131.

Trott, O., and Olson, A.J. (2010). AutoDock Vina: improving the speed and accuracy of docking with a new scoring function, efficient optimization, and multithreading. *J Comput Chem* *31*, 455-461.

Tsakagoshi, N., Kania, M.N., and Franklin, R.M. (1976). Identification of acyl phosphatidylglycerol as a minor phospholipid of *Pseudomonas* BAL-31. *Biochim Biophys Acta* *450*, 131-136.

Vogt, S.L., Evans, A.D., Guest, R.L., and Raivio, T.L. (2014). The Cpx envelope stress response regulates and is regulated by small noncoding RNAs. *J Bacteriol* *196*, 4229-4238.

von Graevenitz, A., Bowman, J., Del Notaro, C., and Ritzler, M. (2000). Human infection with *Halomonas venusta* following fish bite. *J Clin Microbiol* *38*, 3123-3124.

Whitfield, C. (2006). Biosynthesis and assembly of capsular polysaccharides in *Escherichia coli*. *Annu Rev Biochem* *75*, 39-68.

Whitfield, C., and Trent, M.S. (2014). Biosynthesis and export of bacterial lipopolysaccharides. *Annu Rev Biochem* *83*, 99-128.

- Wilkinson, S.G. (1996). Bacterial lipopolysaccharides--themes and variations. *Prog Lipid Res* 35, 283-343.
- Wyckoff, T.J., Lin, S., Cotter, R.J., Dotson, G.D., and Raetz, C.R. (1998). Hydrocarbon rulers in UDP-N-acetylglucosamine acyltransferases. *J Biol Chem* 273, 32369-32372.
- Yague, G., Segovia, M., and Valero-Guillen, P.L. (1997). Acyl phosphatidylglycerol: a major phospholipid of *Corynebacterium amycolatum*. *FEMS Microbiol Lett* 151, 125-130.
- Zhang, Y. (2008). I-TASSER server for protein 3D structure prediction. *BMC Bioinformatics* 9, 40.
- Zhou, Z., White, K.A., Polissi, A., Georgopoulos, C., and Raetz, C.R. (1998). Function of *Escherichia coli* MsbA, an essential ABC family transporter, in lipid A and phospholipid biosynthesis. *J Biol Chem* 273, 12466-12475.